

University of Bath



PHD

Low Energy Membrane Bioreactors for Decentralised Waste Water Treatment

Skouteris, George

Award date:
2010

Awarding institution:
University of Bath

[Link to publication](#)

General rights

Copyright and moral rights for the publications made accessible in the public portal are retained by the authors and/or other copyright owners and it is a condition of accessing publications that users recognise and abide by the legal requirements associated with these rights.

- Users may download and print one copy of any publication from the public portal for the purpose of private study or research.
- You may not further distribute the material or use it for any profit-making activity or commercial gain
- You may freely distribute the URL identifying the publication in the public portal ?

Take down policy

If you believe that this document breaches copyright please contact us providing details, and we will remove access to the work immediately and investigate your claim.

Download date: 13. May. 2019

**LOW ENERGY MEMBRANE BIOREACTORS FOR DECENTRALISED
WASTE WATER TREATMENT**

George S. Skouteris

A thesis submitted for the Degree of Doctor of Philosophy

University of Bath

Department of Chemical Engineering

April 2010

COPYRIGHT

Attention is drawn to the fact that copyright of this thesis rests with its author. A copy of this thesis has been supplied on condition that anyone who consults it is understood to recognise that its copyright rests with the author and they must not copy it or use material from it except as permitted by law or with the consent of the author.

This thesis may be made available for consultation within the University Library and may be photocopied or lent to other libraries for the purposes of consultation.

George S. Skouteris

ABSTRACT

This research is part of PURATREAT project, an action taken by the European Commission (EC) to investigate waste water treatment (WWT) issues in the peri-urban areas of the Middle East and North Africa (MENA) countries. The main target of this work was to develop the application of, and to determine economic viability of, membrane bioreactor (MBR) technology as an alternative to conventional activated sludge (AS) processes for municipal waste water treatment (WWT). The research particularly focused on the long-term operation of three pilot submerged MBR systems - abbreviated as MBR1, MBR2 and MBR3 -, designed and constructed by three different membrane manufacturers. All trials were performed in Tunisia, in the city of Sfax, at the North Sfax “Office National de l' Assainissement” (ONAS) WWT site. ONAS is the country’s national sanitation utility. The MBR systems were tested under different combinations of operating conditions, namely solids residence times (SRTs) and hydraulic residence times (HRTs) and conclusions regarding treated permeate quality, membrane performance and energy consumption rates are drawn.

First, the capability of the MBR systems to produce treated permeate of the appropriate quality was tested. The treated permeate had to be suitable for reuse in unrestricted irrigation in Tunisia, therefore, chemical oxygen demand (COD) concentration must be equal to or lower than 90 mg L^{-1} and it has to be free from pathogens. Two different mixed-liquor suspended solids (MLSS) concentrations were applied. Initially, the MBR systems were operated under a low MLSS concentration of about $4 - 5 \text{ g L}^{-1}$. Under this low MLSS concentration, MBR1 failed to produce treated permeate of appropriate quality whereas MBR2 and MBR3 were successful. The COD concentration removal efficiency was only 71.4 % for MBR1, but it was 88 % for MBR2 and 87.7 % for MBR3. Then, all MBR systems were operated under a higher MLSS concentration value of about $9 - 10 \text{ g L}^{-1}$. Under this MLSS concentration, all MBR systems produced treated permeate of the appropriate quality. COD concentration removal efficiency was 89.4 % for MBR1, 89.7 % for MBR2 and 90.9 % for MBR3.

Then, the membrane performance was tested. This experiment was mainly conducted when the MBR systems were operated at the high MLSS concentration of about $9 - 10$

g L⁻¹. Real/Net membrane permeate fluxes (MPFs) were increased up to values that were no longer sustainable and membrane fouling phenomena appeared to be out of control. An average maximum sustainable net membrane permeate flux (MPF) for each MBR system was then estimated. Application of this net MPF could maximise the daily production of the treated permeate and, at the same time, a reliable long-term membrane performance could be achieved. The maximum sustainable net MPF was found to be equal to 13.77 L m⁻² h⁻¹ for MBR1 and 12.81 L m⁻² h⁻¹ for MBR2. With respect to MBR3, continual membrane fouling conditions during this experiment did not allow to predict an average maximum sustainable net MPF.

Finally, it was attempted to reduce the energy consumption rates below a specific energy demand (SED) value of 3 kWh m⁻³, which is the current SED value of the full-scale conventional AS plant and, therefore, the target for this research. Initially, short-term power-analysis experiments were performed for MBR1 and MBR2. For MBR3 these experiments were not able to be conducted due to its three-phase power supply. The energy consumption rates per component were measured and SED values were calculated. At the same time, longer-term energy-analysis experiments were performed and SED values were re-calculated. By directly comparing the SED values taken by both sets of experiments, the short-term power-analysis experimental data was validated by the longer-term energy-analysis data. Finally, an Excel-based model, which was capable of predicting SED values for MBR1 and MBR2, was built. The model could predict SED values under different sets of operating conditions, *e.g.* varying SRTs/HRTs, but it was concluded that neither MBR1 nor MBR2 could produce treated permeate of the appropriate quality at SED values equal to or lower than 3 kWh m⁻³, whilst simultaneously achieving stable membrane performance. However, a modified version of MBR1 was finally able to achieve the objectives of this research. Namely production of treated permeate of the appropriate quality, at a stable long-term membrane performance, and with SED values equal to or lower than 3 kWh m⁻³.

ACKNOWLEDGEMENTS

With regard to this work, I would like to thank:

- Dr Tom Arnot, my academic supervisor, for offering me this research opportunity and helping me complete my PhD thesis, together with his continual advice and support
- The Department of Chemical Engineering at Bath University
- All the PURATREAT project partners for their help - special mention to:
 - Professor Sami Sayadi, Miss Mouna Jraou and Mr Firas Feki from “Centre de Biotechnologie de Sfax” (CBS)
 - Mr Ben Makhlouf Mohammed from North Sfax “Office National de l' Assainissement” (ONAS)
 - Dr Matthew Wade from “tz Bremerhaven”
 - ir. Harmen Zwijnenberg from the European Membrane Institute (EMI)
- The technical and administration staff of the Department of Chemical Engineering at Bath for all the help they offered to me
- Dr Tim Mays for his advice and help
- All my colleagues and friends at Bath University - special mention to Miss Kerry Anne Young for her help and support
- Dr Richard England, Dr Marianne Ellis and Dr Davide Mattia for offering me the opportunity to demonstrate laboratory courses to undergraduate Chemical Engineering students

- My family and all my friends in Greece for their support - Την οικογένειά μου κι όλους μου τους φίλους στην Ελλάδα για την υποστήριξή τους

Finally, I would like to acknowledge all the financial support, which was given to me through the PURATREAT project.

Thank you - Ευχαριστώ

George S. Skouteris

Γιώργος Σ. Σκουτέρης

Fox speaking: “It is the time you have wasted for your rose that makes your rose so important.”

“It is the time I have wasted for my rose...” said the little Prince so that he would be sure to remember.

Chapter 21, “The little Prince”, Antoine de Saint-Exupéry

TABLE OF CONTENTS

	ABSTRACT	i
	ACKNOWLEDGEMENTS	iii
	TABLE OF CONTENTS	v
	LIST OF FIGURES	x
	LIST OF TABLES	xiii
	NOMENCLATURE	xvi
CHAPTER 1	INTRODUCTION	1
1.1	Context of research	1
1.2	Description of research	2
1.3	Objectives of research	5
1.4	Structure of the PhD thesis	6
CHAPTER 2	BIOMASS SEPARATION MBRs AND RELATED THEORY	9
2.1	Biomass separation MBRs	9
2.1.1	Suspended growth aerobic AS processes and the advent of MBRs	9
2.1.2	General information on biomass separation MBRs and their characteristics	11
2.1.3	Advantages and disadvantages of the MBR processes	14
2.2	MBR biological performance	17
2.2.1	Aerobic biological oxidation	17
2.2.1.1	Microorganisms, their function and the bacterial growth pattern	17
2.2.1.2	Stoichiometry of the aerobic biological oxidation	19
2.2.2	Microbial growth kinetics	20
2.2.3	MBR mass balancing	22
2.2.3.1	Growth-limiting soluble substrate concentration mass balance	23
2.2.3.2	Mass balance for biomass concentration	25
2.2.3.3	Mass balance for DO concentration	26
2.2.4	Biomass characteristics	28
2.2.4.1	Biomass fractionation	28
2.2.4.2	EPS and SMP	28
2.2.4.3	MLSS concentrations and their relationships with the operating conditions (HRT/SRT)	30
2.2.4.4	Oxygen transfer	31
2.3	Membrane performance	34

2.3.1	Membrane fundamentals	34
2.3.2	Filtration law	36
2.3.3	Membrane fouling phenomena	37
2.3.3.1	General information: From concentration polarisation to membrane fouling	37
2.3.3.2	Membrane fouling mechanisms and forms	39
2.3.3.3	Membrane fouling progressing for constant-flux operations	41
2.3.3.4	Membrane fouling equation	43
2.3.4	Membrane fouling parameters and their interactions	43
2.3.4.1	General information	43
2.3.4.2	MLSS concentrations and mixed-liquor temperatures	45
2.3.4.3	MPF	46
2.3.4.4	Aeration	47
2.3.4.5	Sludge wasting (SRTs)	50
2.3.4.6	Application of cleanings	50
2.3.4.6	Intermittent filtration	51
2.4	MBR energy consumption	51
2.4.1	General information on MBR energy consumption	51
2.4.2	Theoretical power requirements for the air compressors used in MBR operations - Specific aeration energy demand	53
2.4.3	MBR energy demand case studies	55
CHAPTER 3	MATERIALS AND METHODS	59
3.1	PURATREAT project technologies	59
3.1.1	MBR1: EWT and COPA MBR technology/KUBOTA membranes	59
3.1.1.1	Introduction	59
3.1.1.2	KUBOTA membranes	60
3.1.2	MBR2: Weise Water Systems, GmbH and Co, KG/MicroClear filters	63
3.1.2.1	Introduction	63
3.1.2.2	MicroClear filters/The MC03 module	63
3.1.3	Martin Systems, AG/siClaro filters	65
3.1.3.1	Introduction	65
3.1.3.2	siClaro filters/The 611 module	65
3.1.3.3	Membranes: Summary	67
3.2	Description of the MBR systems	68
3.2.1	The MBR1 system	68
3.2.2	The MBR2 system	73
3.2.3	The MBR3 system	77
3.3	Characteristics of the influent waste water	81

3.4	Start-up of the plant and operating details	82
3.4.1	Start-up and operating details of MBR1	84
3.4.2	Start-up and operating details of MBR2	86
3.4.3	Start-up and operating details of MBR3	87
3.5	Analytical methods	89
3.5.1	BOD ₅ concentration measurements	89
3.5.2	COD concentration measurements	89
3.5.3	MLSS and MLVSS concentration measurements	90
3.5.4	MBR pilot trial organisation	90
CHAPTER 4	CLEAN WATER TESTS	92
4.1	Introduction	92
4.2	Clean water tests	92
4.2.1	Clean water tests for MBR1	92
4.2.2	Clean water tests for MBR2	96
4.2.3	Clean water tests for MBR3	101
4.3	Clean water data analysis	104
4.3.1	MBR1 clean water data analysis	104
4.3.2	MBR2 clean water data analysis	108
4.3.3	MBR3 clean water data analysis	112
4.4	Conclusions	114
CHAPTER 5	EFFECT OF VARIATION IN THE SRT AND THE HRT ON THE MBR PERFORMANCE	117
5.1	Introduction	117
5.2	Biomass-related data analysis	120
5.2.1	MBR1: The course of MLSS concentration	120
5.2.2	MBR2: The course of MLSS concentration	126
5.2.3	MBR3: The course of MLSS concentration	130
5.2.4	Comparisons: The course of MLSS concentration	135
5.3	Water quality issues	137
5.3.1	The course of the influent COD concentration	137
5.3.2	The courses of the effluent COD concentration/COD concentration removal efficiency	138
5.3.2.1	MBR1: The courses of the effluent COD concentration/COD concentration removal efficiency	138
5.3.2.2	MBR2: The courses of the effluent COD concentration/COD concentration removal efficiency	140
5.3.2.3	MBR3: The courses of the effluent COD concentration/COD concentration removal efficiency	141

5.3.3	Full-scale conventional AS plant: Effluent COD concentration measurements	142
5.3.4	Comparisons: The courses of the effluent COD concentration/COD concentration removal efficiency	143
5.4	MLVSS and BOD ₅ concentrations	144
5.4.1	MLVSS concentration measurements	145
5.4.2	Effluent BOD ₅ concentration measurements	147
5.5	Conclusions	147
CHAPTER 6	MEMBRANE PERFORMANCE	150
6.1	Introduction/General information	150
6.2	Mixed-liquor temperature profile	151
6.3	Membrane performance of MBR1	153
6.3.1	Introduction	153
6.3.2	Data processing	154
6.3.2.1	1 st research period: From 03-09-2008 until 02-11-2008	155
6.3.2.2	2 nd research period: From 02-11-2008 until 21-01-2009	165
6.3.2.3	3 rd research period: From 21-01-2009 until 11-04-2009	168
6.3.2.4	4 th research period: From 11-04-2009 until 14-06-2009	174
6.4	Membrane performance of MBR2	179
6.4.1	Introduction	179
6.4.2	Data Processing	180
6.4.2.1	1 st research period: From 07-11-2008 until 11-01-2009	181
6.4.2.2	2 nd research period: From 11-01-2009 until 23-03-2009	185
6.4.3.3	3 rd research period: From 23-03-2009 until 14-06-2009	194
6.5	Membrane performance of MBR3	199
6.5.1	Introduction	199
6.5.2	Data processing	200
6.5.2.1	1 st research period: From 12-09-2008 until 11-02-2009	201
6.5.2.2	2 nd research period: From 11-02-2009 until 10-05-2009	209
6.5.2.3	3 rd research period: From 10-05-2009 until 14-06-2009	213
6.6	Membrane fouling	217
6.7	Conclusions	218
CHAPTER 7	ENERGY CONSUMPTION AND MBR MODELLING	221
7.1	Introduction	221
7.2	Energy consumption analysis for MBR1	223
7.2.1	MBR1: Operating conditions during the experiments	223
7.2.2	Energy-consuming components	223
7.2.3	MBR1: Power-analysis experiments	225

7.2.4	MBR1: Energy-analysis experiments	229
7.2.4.1	MBR1: Energy-analysis experiments conducted with the aid of in-line electricity meters	229
7.2.4.2	MBR1: Energy-analysis experiments conducted with the aid of electricity meters with rotating counters	229
7.3	Energy consumption analysis for MBR2	230
7.3.1	MBR2: Operating conditions during the experiments	230
7.3.2	Energy-consuming components	231
7.3.3	MBR2: Power-analysis experiments	233
7.3.4	MBR2: Energy-analysis experiments	239
7.3.4.1	MBR2: Energy-analysis experiments conducted with the aid of in-line electricity meters	239
7.3.4.2	MBR2: Energy-analysis experiments conducted with the aid of electricity meters with rotating counters	240
7.4	Energy consumption analysis for MBR3	242
7.4.1	Operating conditions during the experiments	242
7.4.2	Energy-consuming components	243
7.4.3	MBR3: Energy-analysis experiments conducted with the aid of electricity meters with rotating counters	244
7.5	Analysis of the results	245
7.5.1	MBR energy consumption breakdown	245
7.5.2	Presentation of the SED values	250
7.6	MBR modelling	251
7.6.1	General information on the MBR modelling	251
7.6.2	Calibration/Validation of the MBR model	252
7.6.2.1	Calibration/Validation of the model for MBR1	253
7.6.2.2	Calibration/Validation of the model for MBR2	256
7.6.2.3	Calibration/Validation of the model for MBR3	258
7.6.2.4	Sample of the MBR model	260
7.6.3	Application of the MBR model: SED predictions	263
7.6.3.1	Prediction of SED values for MBR1	263
7.6.3.2	Prediction of SED values for MBR2	268
7.6.3.3	Prediction of SED values for a modified MBR1	272
7.7	Conclusions	278
CHAPTER 8	CONCLUSIONS & FUTURE WORK	280
8.1	Conclusions	280
8.2	Future work	285
8.2.1	Improvement of MBR operation	285
8.2.2	Improvement of MBR designs	287
8.2.3	Improvement of aeration	287

REFERENCES	289
APPENDIX A: P&ID DIAGRAMS FOR THE 3 MBR SYSTEMS	295

LIST OF FIGURES

Figure 2.1	A simplified flow diagram of a conventional AS process	10
Figure 2.2	MBR configurations	13
Figure 2.3	Bacterial growth curve	18
Figure 2.4	Flow diagram of a submerged MBR process	22
Figure 2.5	The membrane	34
Figure 2.6	Cross flow filtration	35
Figure 2.7	Fouling mechanisms	39
Figure 2.8	Factors affecting fouling in submerged MBRs	44
Figure 2.9	Illustrative critical curve	49
Figure 3.1	Standard KUBOTA membrane panels	61
Figure 3.2	Weise Water Systems MC03 module	64
Figure 3.3	Martin Systems siClaro 611 module	66
Figure 3.4	The MBR1 system	69
Figure 3.5	MBR1: Air diffuser	71
Figure 3.6	MBR1: Permeate line	71
Figure 3.7	Control panels	73
Figure 3.8	The MBR2 system	74
Figure 3.9	MBR2: Air diffuser	75
Figure 3.10	MBR2: Membrane unit, its housing and the diffuser	76
Figure 3.11	MBR2: Permeate line	76
Figure 3.12	The MBR3 system	78
Figure 3.13	MBR3: Membrane module, its housing and the diffusers	79
Figure 3.14	MBR3: Air diffusers	80
Figure 3.15	MBR 3: Permeate line	81
Figure 3.16	The MBR pant	83
Figure 4.1	MBR1: A schematic showing the operation	93
Figure 4.2	MBR2: A schematic showing the operation	97
Figure 4.3	MBR3: A schematic showing the operation	101
Figure 4.4	MBR1: Real permeate flow rate and pressure as provided by the pressure transducer against time	105
Figure 4.5	MBR1: Real MPF and TMP_1 against time	106
Figure 4.6	MBR1: Permeability	107
Figure 4.7	MBR2: Real permeate flow rate and pressure as provided by the pressure transducer against time	109
Figure 4.8	MBR2: Real MPF and TMP_2 against time	110
Figure 4.9	MBR2: Permeability	111
Figure 4.10	MBR3: Real permeate flow rate and pressure as provided by the	

	pressure transducer against time	112
Figure 4.11	MBR3: Real MPF and TMP ₃ against time	113
Figure 4.12	MBR3: Permeability against time	114
Figure 4.13	MPF/TMP profile when clean/waste water is filtered	115
Figure 5.1	MBR1: MLSS concentration against time	125
Figure 5.2	MBR2: MLSS concentration against time	130
Figure 5.3	MBR3: MLSS concentration against time	135
Figure 5.4	All MBRs: Average MLSS concentration against time	136
Figure 5.5	All MBRs: Influent COD concentration against time	137
Figure 5.6	MBR1: Effluent and target COD concentration and COD concentration removal efficiency against time	139
Figure 5.7	MBR2: Effluent and target COD concentration and COD concentration removal efficiency against time	140
Figure 5.8	MBR3: Effluent and target COD concentration and COD concentration removal efficiency against time	141
Figure 5.9	All MBRs: Effluent and target COD concentration against time	143
Figure 5.10	All MBRs: COD concentration removal efficiency against time	144
Figure 6.1	MBR3: Temperature of mixed-liquor within the filtration tank against time	152
Figure 6.2	MBR1: 1 st research period: Real MPF against time	157
Figure 6.3	MBR1: 1 st research period: TMP against time	158
Figure 6.4	MBR1: 1 st research period: Permeability against time	160
Figure 6.5	MBR1: Short-term flux-step test: Real MPF against time	162
Figure 6.6	MBR1: Short-term flux-step test: TMP against time	163
Figure 6.7	MBR1: Short-term flux-step test: Permeability against time	164
Figure 6.8	MBR1: 2 nd research period: Real MPF against time	165
Figure 6.9	MBR1: 2 nd research period: TMP against time	166
Figure 6.10	MBR1: 2 nd research period: Permeability against time	168
Figure 6.11	MBR1: 3 rd research period: Real MPF against time	170
Figure 6.12	MBR1: 3 rd research period: TMP against time	171
Figure 6.13	MBR1: 3 rd research period: Permeability against time	172
Figure 6.14	MBR1: 4 th research period: Real MPF against time	175
Figure 6.15	MBR1: 4 th research period: TMP against time	176
Figure 6.16	MBR1: 4 th research period: Permeability against time	178
Figure 6.17	MBR2: 1 st research period: Real MPF against time	182
Figure 6.18	MBR2: 1 st research period: TMP against time	183
Figure 6.19	MBR2: 1 st research period: Permeability against time	184
Figure 6.20	MBR2: 2 nd research period: Real MPF against time	186
Figure 6.21	MBR2: 2 nd research period: TMP against time	187
Figure 6.22	MBR2: 2 nd research period: Permeability against time	188
Figure 6.23	MBR2: Short-term flux-step test: Real MPF against time	191
Figure 6.24	MBR2: Short-term flux-step test: TMP against time	192

Figure 6.25	MBR2: Short-term flux-step test: Permeability against time	193
Figure 6.26	MBR2: 3 rd research period: Real MPF against time	195
Figure 6.27	MBR2: 3 rd research period: TMP against time	196
Figure 6.28	MBR2: 3 rd research period: Permeability against time	198
Figure 6.29	MBR3: 1 st research period: Real MPF against time	203
Figure 6.30	MBR3: 1 st research period: TMP against time	204
Figure 6.31	MBR3: 1 st research period: Permeability against time	205
Figure 6.32	MBR3: Short-term flux-step test: Real MPF against time	207
Figure 6.33	MBR3: Short-term flux-step test: TMP against time	208
Figure 6.34	MBR3: Short-term flux-step test: Permeability against time	209
Figure 6.35	MBR3: 2 nd research period: Real MPF against time	210
Figure 6.36	MBR3: 2 nd research period: TMP against time	212
Figure 6.37	MBR3: 2 nd research period: Permeability against time	213
Figure 6.38	MBR3: 3 rd research period: Real MPF against time	214
Figure 6.39	MBR3: 3 rd research period: TMP against time	215
Figure 6.40	MBR3: 3 rd research period: Permeability against time	216
Figure 6.41	MBR1: Irreversible membrane fouling	217
Figure 6.42	MBR2: Irreversible membrane fouling	217
Figure 6.43	MBR3: Irreversible membrane fouling	218
Figure 7.1	MBR1: Energy-consuming components	224
Figure 7.2	MBR2: Energy-consuming components	233
Figure 7.3	MBR3: Energy-consuming components	244
Figure 7.4	MBR1/MBR2: Energy consumption percentages with respect to MBR activities, namely baseline required by the control panels, pumping waste/treated water and MBR aeration	247
Figure 7.5	MBR1/MBR2: Energy consumption percentages per MBR component	248
Figure 7.6	MBR1: Comparison between measured and estimated MLSS concentrations	255
Figure 7.7	MBR1: Comparison between measured and estimated COD concentrations	255
Figure 7.8	MBR2: Comparison between measured and estimated MLSS concentrations	257
Figure 7.9	MBR2: Comparison between measured and estimated COD concentrations	257
Figure 7.10	MBR3: Comparison between measured and estimated MLSS concentrations	259
Figure 7.11	MBR3: Comparison between measured and estimated COD concentrations	259
Figure 7.12	MBR1: Effect of net MPFs on the SED values	264
Figure 7.13	MBR1: Effect of MLSS concentrations on the SED values	266
Figure 7.14	MBR1: Effect of MLSS concentrations and net MPFs on the SED values	267

Figure 7.15	MBR2: Effect of net MPFs on the SED values	269
Figure 7.16	MBR2: Effect of MLSS concentrations on the SED values	270
Figure 7.17	MBR2: Effect of MLSS concentrations and net MPFs on the SED values	271
Figure 7.18	Modified MBR1: Effect of net MPFs on the SED values	275
Figure 7.19	Modified MBR1: Effect of MLSS concentrations on the SED values	275
Figure 7.20	Modified MBR1: Effect of MLSS concentrations and net MPFs on the SED values	276

LIST OF TABLES

Table 2.1	Classification of membrane separation processes	35
Table 2.2	Characteristics of different membrane modules applied in MBR technology	36
Table 2.3	MBR energy demand: Case study of [Côté <i>et al.</i> , 1997]: Operating conditions	55
Table 2.4	MBR energy demand: Case study of [Ueda and Hata, 1999]: Operating conditions	56
Table 2.5	MBR energy demand: Case study of [Zang <i>et al.</i> , 2003]: Operating conditions	56
Table 2.6	MBR energy demand: Case study of [Schroebl <i>et al.</i> , 2005]: Operating conditions	57
Table 2.7	MBR energy demand: Case study of [Fan <i>et al.</i> , 2006]: Operating conditions	57
Table 3.1	KUBOTA MBR plants worldwide from 1993 until 2005	61
Table 3.2	Membrane characteristics	67
Table 3.3	Waste water characteristics	82
Table 3.4	MBR1: Start-up operating conditions	86
Table 3.5	MBR2: Start-up operating conditions	87
Table 3.6	MBR3: Start-up operating conditions	88
Table 5.1	Mass balance equations linking MLSS/MLVSS concentrations, HRTs, SRTs and COD/BOD ₅ concentrations	118
Table 5.2	MBR1: Research periods with respect to the changes of the MLSS concentration	120
Table 5.3	MBR1: Time period from 03-09-2008 until 08-12-2008: Presentation of the operating conditions	122
Table 5.4	MBR1: Time period from 09-02-2009 until 16-06-2009: Presentation of the operating conditions	124
Table 5.5	MBR2: Research periods with respect to the changes of the MLSS concentration	126
Table 5.6	MBR2: Time period from 07-11-2008 until 03-01-2009: Presentation of the operating conditions	127
Table 5.7	MBR2: Time period from 30-01-2009 until 16-06-2009: Presentation of the operating conditions	129

Table 5.8	MBR3: Research periods with respect to the changes of the MLSS concentration	131
Table 5.9	MBR3: Time period from 19-11-2008 until 03-01-2009: Presentation of the operating conditions	132
Table 5.10	MBR3: Time period from 06-02-2009 until 16-06-2009: Presentation of the operating conditions	133
Table 5.11	MBR3: Time period from 06-05-2009 until 16-06-2009: Presentation of the operating conditions	134
Table 5.12	Full-scale conventional AS plant: Average monthly COD concentrations in the effluent for year 2006	142
Table 5.13	All MBRs: Maximum, minimum and average MLVSS/MLSS percentages	145
Table 5.14	MBR1: Research periods with respect to the changes of the MLVSS concentration	145
Table 5.15	MBR2: Research periods with respect to the changes of the MLVSS concentration	146
Table 5.16	MBR3: Research periods with respect to the changes of the MLVSS concentration	146
Table 5.17	All MBRs: Maximum, minimum and average effluent BOD ₅ concentration values	147
Table 6.1	MBR1: Data processing periods	154
Table 6.2	Mass balance equations around an MBR	155
Table 6.3	MBR1: Sustainable net MPFs and their corresponding operating conditions	173
Table 6.4	MBR1: Sustainable net membrane MPFs and their corresponding operating conditions	179
Table 6.5	MBR2: Data processing periods	180
Table 6.6	MBR2: Sustainable MPF and its corresponding operating conditions.	185
Table 6.7	MBR2: Sustainable net membrane MPF and its corresponding operating conditions	189
Table 6.8	MBR2: Operating conditions during the short-term flux step test	190
Table 6.9	MBR2: Sustainable net membrane MPF and its corresponding operating conditions	199
Table 6.10	MBR3: Data processing periods	200
Table 6.11	MBR3: Operating conditions during the short-term flux-step test	206
Table 7.1	MBR1: Operating conditions during the power-analysis and energy-analysis experiments	223
Table 7.2	MBR1: Power values per component during the power-analysis experiments	225
Table 7.3	MBR1: Estimation of the runtime of Feed Pump 1 for a range of feed flow rates of the MBR1 system	227
Table 7.4	MBR1: Power values of the air blower at different air flow rates	227
Table 7.5	MBR1: Power-analysis experiments: Estimation of the overall energy consumed throughout a day	228

Table 7.6	MBR1: Power-analysis experiments: Estimation of the SED value	228
Table 7.7	MBR1: Energy-analysis experiments conducted with the aid of in-line electricity meters: Estimation of the SED value	229
Table 7.8	MBR1: Energy-analysis experiments conducted with the aid of electricity meters with rotating counters: Estimation of the SED value	230
Table 7.9	MBR2: Operating conditions during the power-analysis and energy-analysis experiments	231
Table 7.10	MBR2: Power values per component during the power-analysis experiments	234
Table 7.11	MBR2: Baseline + Suction pump: Power values under different real/net permeate flow rates	235
Table 7.12	MBR2: Estimation of the runtime of Feed Pump 1 for a range of feed flow rates of the MBR2 system	237
Table 7.13	MBR2: Power-analysis experiments: Estimation of the overall energy consumed throughout a day - Sludge pump is excluded	238
Table 7.14	MBR2: Power-analysis experiments: Estimation of the SED value - Sludge pump is excluded	238
Table 7.15	MBR2: Power-analysis experiments: Estimation of the overall energy consumed throughout a day - Sludge pump is included	239
Table 7.16	MBR2: Power-analysis experiments: Estimation of the SED value - Sludge pump is included	239
Table 7.17	MBR2: Energy-analysis experiments conducted with the aid of in-line electricity meters: Estimation of the total energy consumption rate	240
Table 7.18	MBR2: Energy-analysis experiments conducted with the aid of in-line electricity meters: Estimation of the SED value	240
Table 7.19	MBR2: Energy-analysis experiments conducted with the aid of electricity meters with rotating counters: Estimation of the total energy consumption rate	241
Table 7.20	MBR2: Energy-analysis experiments conducted with the aid of electricity meters with rotating counters: Estimation of the SED value	241
Table 7.21	MBR3: Operating conditions during the energy-analysis experiments conducted with the aid of electricity meters with rotating counters	242
Table 7.22	MBR3: Energy-analysis experiments conducted with the aid of electricity meters with rotating counters: Estimation of the total energy consumption rate	245
Table 7.23	MBR3: Energy-analysis experiments conducted with the aid of electricity meters with rotating counters: Estimation of the SED value	245
Table 7.24	MBR1/MBR2: Energy consumption percentages	246
Table 7.25	SED values	250
Table 7.26	MBR1: Estimation of best-fit kinetic/stoichiometric parameters	253

Table 7.27	MBR1: Validation of the model	254
Table 7.28	MBR2: Estimation of best-fit kinetic/stoichiometric parameters	256
Table 7.29	MBR2: Validation of the model	256
Table 7.30	MBR3: Estimation of best-fit kinetic/stoichiometric parameters	258
Table 7.31	MBR3: Validation of the model	258
Table 7.32	MBR modelling sample	260
Table 7.33	MBR1: A combination of SRTs, HRTs, net MPFs and their corresponding SED values	264
Table 7.34	MBR1: A combination of SRTs, HRTs, MLSS concentrations and their corresponding SED values	265
Table 7.35	MBR2: A combination of SRTs, HRTs, net MPFs and their corresponding SED values	268
Table 7.36	MBR2: A combination of SRTs, HRTs, MLSS concentrations and their corresponding SED values	270
Table 7.37	Modified MBR1: A combination of SRTs, HRTs, net MPFs and their corresponding SED values	273
Table 7.38	Modified MBR1: A combination of SRTs, HRTs, MLSS concentrations and their corresponding SED values	274
Table 7.39	Modified MBR1: Best-fit operating conditions regarding the objectives of this research	277

NOMENCLATURE

• Abbreviations

AS	Activated Sludge
BOD ₅	5-day Biochemical Oxygen Demand
COD	Chemical Oxygen Demand
CSTR	Continuous Stirred-tank Reactor
DO	Dissolved Oxygen
EC	European Commission
EMBRs	Extractive MBRs
EPS	Extracellular Polymeric Substances
EWT	Eimco Water Technologies
FS	Flat Sheet
FS/AN	Feed Screening/Anoxic
HF	Hollow Fibre
HRT	Hydraulic Residence Time
HRTs	Hydraulic Residence Times
MABRs	Membrane Aeration Bioreactors
MBR	Membrane Bioreactor
MBR1	Membrane Bioreactor 1
MBR2	Membrane Bioreactor 2
MBR3	Membrane Bioreactor 3

MBRs	Membrane Bioreactors
MENA	Middle East and North Africa
MF	Microfiltration
MLSS	Mixed-liquor Suspended Solids
MLVSS	Mixed-liquor Volatile Suspended Solids
MPF	Membrane Permeate Flux
MPFs	Membrane Permeate Fluxes
MST	Membrane Sewage Treatment
MT	Multitubular
NF	Nanofiltration
ONAS	Office National de l' Assainissement
PE	Population Equivalent
PID	Proportional-Integral-Derivative
RO	Reverse Osmosis
SED	Specific Energy Demand
SMP	Soluble Microbial Products
SRT	Solids Residence Time
SS	Suspended Solids
T	Tubular
TMP	Transmembrane Pressure
TOC	Total Organic Carbon
UF	Ultrafiltration
WWT	Waste Water Treatment

• **Parameters**

\bar{O}	=	Steady-state DO concentration	g m^{-3}
a	=	Coefficient	unitless
A_1	=	Membrane area for MBR1	m^2
A_2	=	Membrane area for MBR2	m^2
A_3	=	Membrane area for MBR3	m^2
A_m	=	Total membrane area	m^2
b	=	Coefficient	unitless
e	=	Efficiency of the air compressor	unitless
J	=	MPF	m s^{-1}
$J_{p,n}$	=	Net MPF	$\text{L m}^{-2} \text{h}^{-1}$
$J_{p,r}$	=	Real MPF	$\text{L m}^{-2} \text{h}^{-1}$
$J_{p,r,1}$	=	Real MPF of MBR1 at T_{cw}	$\text{L m}^{-2} \text{h}^{-1}$
$J'_{p,r,1}$	=	Temperature-corrected real MPF of MBR1 at T_{cw-ref}	$\text{L m}^{-2} \text{h}^{-1}$
$J_{p,r,2}$	=	Real MPF of MBR2	$\text{L m}^{-2} \text{h}^{-1}$
$J'_{p,r,2}$	=	Temperature-corrected real MPF of MBR1 at T_{cw-ref}	$\text{L m}^{-2} \text{h}^{-1}$
$J_{p,r,3}$	=	Real MPF of MBR1	$\text{L m}^{-2} \text{h}^{-1}$

$J'_{p,r,3}$	=	Temperature-corrected real MPF of MBR3 at T_{cw-ref}	$L m^{-2} h^{-1}$
J_{SS}	=	Steady state or terminal MPF, $m s^{-1}$	$m s^{-1}$
k	=	Maximum specific substrate utilization rate	d^{-1}
K_1	=	Permeability of MBR1 at T_{cw}	$L m^{-2} h^{-1} bar^{-1}$
K'_1	=	Temperature-corrected permeability of MBR1 at T_{cw-ref}	$L m^{-2} h^{-1} bar^{-1}$
K_2	=	Permeability of MBR2 at T_{cw}	$L m^{-2} h^{-1} bar^{-1}$
K'_2	=	Temperature-corrected permeability of MBR1 at T_{cw-ref}	$L m^{-2} h^{-1} bar^{-1}$
K_3	=	Permeability of MBR3 at T_{cw-ref}	$L m^{-2} h^{-1} bar^{-1}$
K'_3	=	Temperature-corrected permeability of MBR3 at T_{cw-ref}	$L m^{-2} h^{-1} bar^{-1}$
k_d	=	Endogenous decay co-efficient	d^{-1}
k_J	=	Constant	variable units
k_{La}	=	Liquid-phase oxygen to water mass transfer coefficient	d^{-1}
K_{La}	=	Overall liquid-phase mass transfer coefficient	d^{-1}
K_S	=	Half-velocity constant, substrate concentration at one-half the maximum specific substrate utilisation rate	$g m^{-3}$
n	=	Membrane fouling constant	unitless
n_{air}	=	Constant for air equal to 0.283	unitless
N_o	=	Rate of oxygen mass transfer	$g m^{-3} s^{-1}$
O	=	DO concentration	$g m^{-3}$
O_{SAT}	=	DO concentration in equilibrium with gas as given by Henry's law	$g m^{-3}$
O_t	=	DO concentration at time t	$g m^{-3} s^{-1}$
O_{t1}	=	DO concentration at time t_1	$g m^{-3}$
O_{t2}	=	DO concentration at time t_2	$g m^{-3}$
p_1	=	Absolute inlet pressure	atm
p_2	=	Absolute outlet pressure	atm
P_A	=	Hydraulic pressure on the permeate side of MBR2	bar
$P_{AVE,FS,1}$	=	Average pressure on the feed side of MBR1	bar
P_B	=	Hydraulic pressure on the permeate side of MBR2	bar
P_{FS}	=	Pressure on the feed side of the membranes	bar
$P_{FS,1}$	=	Pressure on the feed side of MBR1	bar
$P_{FS,2}$	=	Pressure on the feed side of MBR2	bar
$P_{FS,3}$	=	Pressure on the feed side of the membranes of MBR3	bar
P_{PS}	=	Pressure on the permeate side of the membranes	bar
$P_{PS,1}$	=	Pressure on the permeate side of MBR1	bar
$P_{PS,2}$	=	Pressure on the permeate side of MBR2	bar
$P_{PS,3}$	=	Pressure on the permeate side of MBR3	bar
$P_{sp,2}$	=	Power of suction pump of MBR2	W
$P_{TRANC,1}$	=	Instant pressure as provided by the pressure transducer of MBR1	bar
$P_{TRANC,2}$	=	Instant pressure as provided by the pressure transducer of MBR2	bar

$P_{\text{TRANC},3}$	=	Instant pressure as provided by the pressure transducer of MBR3	bar
P_w	=	Power requirement for the air blower	kW
Q_f	=	Average volumetric feed flow rate	$\text{m}^3 \text{d}^{-1}$
$Q_{f,1}$	=	Feed flow rate of MBR1 during the experiment	$\text{m}^3 \text{d}^{-1}$
$Q_{f,2}$	=	Feed flow rate of MBR2 during the experiment	$\text{m}^3 \text{d}^{-1}$
$Q_{fp,1}$	=	Designed feed flow rate of Feed Pump 1	$120 \text{m}^3 \text{d}^{-1}$
$Q_{fp,2}$	=	Designed feed flow rate of Feed Pump 2	$192 \text{m}^3 \text{d}^{-1}$
$q_o X$	=	Oxygen uptake by the cells	$\text{g m}^{-3} \text{s}^{-1}$
Q_p	=	Average volumetric permeate flow rate	$\text{m}^3 \text{d}^{-1}$
$Q_{p,r,1}$	=	Real permeate flow rate of MBR1	L h^{-1}
$Q_{p,r,2}$	=	Real permeate flow rate of MBR2	L h^{-1}
$Q_{p,r,3}$	=	Real permeate flow rate of MBR3	L h^{-1}
Q_w	=	Average volumetric waste sludge flow rate	$\text{m}^3 \text{d}^{-1}$
R	=	Engineering gas constant for air	$8.314 \text{kJ kmol}^{-1} \text{K}$
R_{ads}	=	Resistance due to pore adsorption	m^{-1}
R_f	=	Resistance due to membrane fouling	m^{-1}
r_g	=	Net biomass production rate	$\text{g m}^{-3} \text{d}^{-1}$
R_{irrev}	=	Resistance driven by the filtered volume being irreversible	m^{-1}
R_m	=	Resistance of the clean membrane	m^{-1}
R_{rev}	=	Resistance driven by the filtered volume being reversible	m^{-1}
r_{su}	=	Rate of substrate concentration change due to utilisation	$\text{g m}^{-3} \text{d}^{-1}$
S	=	Growth-limiting substrate concentration in solution	g m^{-3}
S_f	=	Growth-limiting substrate concentration in the feed	g m^{-3}
t_1	=	Time t_1	s
T_1	=	Absolute inlet temperature	K
t_2	=	Time t_2	s
T_{cw}	=	Clean water temperature during the test	$^{\circ}\text{C}$
$T_{\text{cw-ref}}$	=	Reference clean water temperature	$^{\circ}\text{C}$
t_f	=	Filtration time	min
TMP_1	=	TMP of MBR1	bar
TMP_2	=	TMP of MBR2	bar
TMP_3	=	TMP of MBR3	bar
t_r	=	Relaxation time	min
$t_{\text{run},1}$	=	Runtime of Feed Pump 1	h d^{-1}
$t_{\text{run},2}$	=	Runtime of Feed Pump 2	h d^{-1}
U_g	=	Gas superficial velocity	m s^{-1}
U_l	=	Liquid superficial velocity	m s^{-1}

V	=	Operating volume of the MBR,	m^3
W	=	Weight of flow of air	$kg\ s^{-1}$
$W_{b,m}$	=	Specific aeration power demand per unit membrane area	$kW\ m^{-2}$
$W_{b,v}$	=	Specific aeration energy demand per unit permeate volume	$kWh\ m^{-3}$
X	=	Biomass concentration	$g\ m^{-3}$
X_w	=	Biomass concentration in waste water	$g\ m^{-3}$
$Y_{X/O}$	=	Coefficient indicating biomass produced immediately upon consumption of DO	unitless
$Y_{X/S}$	=	Synthesis yield co-efficient	unitless
β	=	Exponent - usually ranges from 0.6 to 0.8	unitless
ΔP	=	Pressure difference applied across the membrane, or TMP	Pa
$\Delta \Pi$	=	Difference in the osmotic pressure across the membrane	Pa
θ	=	HRT	d
θ_C	=	SRT	d
μ	=	Viscosity of permeate	$N\ s\ m^{-2}$
μ	=	Specific biomass growth rate	d^{-1}
μ_{max}	=	Maximum specific growth rate	d^{-1}

CHAPTER 1 INTRODUCTION

1.1 Context of research

This research project took place as part of the PURATREAT project, an action taken by the European Commission (EC) to investigate waste water treatment (WWT) issues in the Middle East and North Africa (MENA) countries. The main target of the project, and also of this research, was the application and evaluation of economic viability of the membrane bioreactor (MBR) technology as an alternative to conventional activated sludge (AS) technologies in the peri-urban areas of MENA countries. The economically diverse MENA region that includes both the oil-rich economies in the Gulf and countries that are resource-scarce in relation to population, extends from Morocco in north-west Africa to Iran in south-west Asia. It specifically includes: Algeria, Bahrain, Djibouti, Egypt, Iran, Iraq, Israel, Jordan, Kuwait, Lebanon, Libya, Malta, Morocco, Oman, Qatar, Saudi Arabia, Syria, Tunisia, United Arab Emirates, West Bank and Gaza Strip and Yemen, [www.puratreat.com, 2010], [www.worldbank.org, 2010]. The PURATREAT project focused on pilot MBR trials in Tunisia.

The Mediterranean basin is one of the poorest regions in the world with respect to water resources. High urban population growth, together with an increased water consumption rate for irrigation purposes, have had an adverse effect on ground water resources, most of which are running the risk of being completely exhausted due to their over-exploitation. As limited renewable water resources are available in the area, most of the countries have already been driven to re-use their waste waters. However, waste waters in the MENA region are generally not treated efficiently, or in some cases, they are directly re-used for irrigation or sanitary purposes without any treatment at all. These waters are then serving as a carrier for diseases, as proper pathogen removal does not occur, or causing water pollution when discharged into water bodies, [www.puratreat.com, 2010].

As conventional WWT processes appear not to be too broad, MBR technology may be a promising alternative as the use of membranes produces treated water of

exceptional quality, as well as providing a real barrier against bacteria and viruses, and thus achieving good disinfection capability, [Le-Clech *et al.*, 2006], [Stephenson *et al.*, 2000]. However, most membrane bioreactors (MBRs) currently in use have relatively high running costs, *i.e.* costs relating to energy consumption. This makes their operation be under question, especially in regions where expenditure in public services can be a critical factor. Therefore, even though they win an advantage in terms of treated water quality compared to conventional WWT methods, their energy consumption in total is still higher than that for conventional AS processes, [Liao *et al.*, 2006], [www.puratreat.com, 2010].

Energy consumed by gravity-driven submerged MBRs comes from the operation of pumps and air blowers. Pumps deliver either untreated or treated water, and air blowers produce turbulent aeration, which scours the membranes to limit both concentration polarisation and membrane fouling phenomena, as well as providing proper mixing to prevent settling of biomass, together with enough oxygen for the biomass maintenance, [PURATREAT project: Deliverable 3, 2007], [Gander *et al.*, 2000]. For submerged MBRs, where gravity is not adequate for collection of the treated permeate, suction pumps have to be operated, [Ueda and Hata, 1999]. However, it is the air blowers that have been reported to be the most energy-consuming devices at percentages higher than 80 %, [Meng *et al.*, 2008], [Howell *et al.*, 2004], [Chua *et al.*, 2002], or even 90 %, [Gander *et al.*, 2000], of the overall energy consumed by submerged MBRs. This research involves an overall attempt to reduce the energy consumption values of the three pilot submerged MBR systems to values as low as possible. The research programme is described in Section 1.2.

1.2 Description of research

This research project focused on the long-term operation of three different pilot submerged MBR systems, designed and constructed by three different membrane manufacturers. The MBR systems were tested under different combinations of operating conditions and raw data regarding sludge age and treated permeate quality, together with data on membrane performance and energy consumption, was collected

All membranes tested were of flat sheet (FS) configuration so that a direct comparison could be made. Membrane bioreactor 1 (MBR1) was provided by EIMCO Water Technologies (EWT), containing KUBOTA microfiltration (MF) membranes, [www.copa.co.uk, 2010], [www.eimcotechnologies.com, 2010]. Membrane bioreactor 2 (MBR2) was purchased from Weise Water Systems GmbH and Co. It was based on the MicroClear filter technology, comprising FS membrane filters, operating in the ultrafiltration (UF) range, [www.weise-water-systems.com, 2010]. Membrane bioreactor 3 (MBR3) was supplied by Martin Systems AG. Filtration is based on UF membranes known as siClaro filters, [www.siclaro.ch, 2010]. MBR1 was a gravity-driven MBR, whereas MBR2 and MBR3 made use of suction pumps for permeate collection.

All three MBRs were shipped to Sfax, in central Tunisia, where they were assembled and installed at the North Sfax “Office National de l' Assainissement” (ONAS) waste water treatment (WWT) site. A full-scale conventional AS plant is operated at this site and ONAS is the country’s national sanitation utility. The MBRs were started-up and clean water tests were conducted. The raw data collected was real membrane permeate flow rates and gauge pressures on the permeate side of the membranes.

Membrane permeate fluxes (MPFs) and transmembrane pressure (TMP) values, together with instant permeability values, were calculated and their profiles against time were plotted. As clean water temperatures were also measured during the tests, permeability figures could be temperature-corrected at 20 °C so that a direct comparison could be made. Through these tests both the membrane performance and consequent control-related issues for all three MBR systems were investigated.

After completing the clean water tests, waste water experiments were conducted. The waste water used was that being treated by the full-scale conventional AS plant. A first issue to be explored was related to the quality of the treated effluent. The treated permeate had to be able to be re-used for unrestricted irrigation in Tunisia, so, according to the legislation, its chemical oxygen demand (COD) concentration should be equal to or lower than 90 mg L⁻¹ and the 5-day biochemical oxygen demand (BOD₅) concentration should be equal to or less than 30 mg L⁻¹, [North Sfax ONAS archives, 2006]. To investigate whether or not treated water of the appropriate quality could be produced, two lengthy experiments were conducted based on the selection of two

different mixed-liquor suspended solids (MLSS) concentrations within the MBRs. The MBR systems were first operated under a low biomass concentration of about 4 - 5 g L⁻¹, which was similar to the MLSS concentration of the full-scale conventional AS plant. In order to achieve this, the solids residence time (SRT) was adjusted to 15 d and the hydraulic residence time (HRT) was adjusted to 1.01 d. Then, as proposed by the MBR suppliers, a higher biomass concentration of about 9 - 10 g L⁻¹ was tested. Several sets of operating conditions, capable of controlling the MLSS concentration around 9 - 10 g L⁻¹, were then applied.

Another issue for investigation was related to the performance of the membranes. The average real MPFs were increased step by step up to values that were no longer sustainable and membrane fouling phenomena appeared to be out of control. For constant-flux filtration, this is indicated by an exponential increase in the TMP values. An average maximum sustainable net membrane permeate flux (MPF) for each MBR system was then estimated. Operation at this average maximum sustainable net MPF value could maximise the daily production of the treated permeate and, at the same time, a reliable long-term membrane performance could be achieved. It is worth mentioning that each MBR's average maximum sustainable net MPF was strongly related to the operating conditions of the MBR system, namely MLSS concentrations inside the MBR tanks, the temperature of the mixed-liquor and the gassing rates for membrane scouring within the MBR tanks. Finally, intermittent filtration was also tested as a measure to mitigate or retard any membrane fouling propensity, [Chua, 2002]. Both physical and chemical cleaning were applied each time the membrane fouling appeared to be out of control.

Finally, both power-analysis and energy-analysis experiments were carried out. During the short-term power-analysis experiments, the power value for each component of the MBR systems was monitored. As runtimes of all components over a day were known, an initial estimation of the daily energy consumption, both per component and per MBR system, was made for MBR1 and MBR2. However, short-term power-analysis experiments could not be performed for the MBR3 system as it had a three-phase power supply. At the same time, longer-term energy-analysis experiments were conducted by measuring the overall energy that was consumed by each MBR system over a longer time period. Then, specific energy demand (SED)

values could be estimated. By directly comparing these SED values, it was possible to check whether the short-term power-analysis experiment was validated by the longer-term energy-analysis experiment, and evaluate the MBR systems in terms of their energy demand. Finally, an Excel-based model was built, which was capable of predicting SED values by using the power values per component, as they were measured during the short-term power-analysis experiment.

The model could resolve mass balance equations, so it was capable of calculating average net MPFs, could predict MLSS concentrations and effluent COD concentrations, and finally could estimate SED values under certain sets of operating conditions, *e.g.* varying MLSS concentrations or hydraulic residence times (HRTs). Different sets of operating conditions were explored using the model until SED values equal to or lower than 3 kWh m^{-3} , which is the current SED value of the full-scale conventional AS plant, [PURATREAT project, Deliverable 16, 2009], and therefore the target value of this research, were achieved. These SED values had to coincide with a set of operating conditions that could lead to a stable long-term membrane performance and to the production of treated water of appropriate quality.

To conclude, the overall goal of this research was to identify the MBR system that could produce over a day the maximum possible quantity of treated permeate, that would also be of appropriate quality, demonstrating at the same time a reasonably stable membrane performance at the lowest energy consumption rates. It would then be able to conclude whether decentralised WWT plants based on MBR technologies could be viable in MENA countries or not.

1.3 Objectives of research

The main aim of this research was to explore whether the MBR technology would be able to be extensively applicable for the treatment of domestic sewage in the MENA region in the near future. Based on this aim, the following research objectives were then formulated.

- **Objective 1:** To demonstrate that the treated permeate, which was produced by the three MBR systems, was of appropriate quality for use in unrestricted irrigation in Tunisia.

- Objective 2: To demonstrate that the dissolved oxygen (DO) concentration within the tanks, where the aerobic biological oxidation took place, was adequate so that the aerobic bacterial cultures did not suffer from lack of oxygen.
- Objective 3: To maximise the daily production of treated permeate under defined sets of operating conditions of the MBR systems. Also, to demonstrate that during the maximization of the daily amount of the treated permeate, a stable long-term membrane performance was achieved.
- Objective 4: To obtain reasonable initial SED values and to demonstrate that they can be reduced to values equal to or lower than 3 kWh m^{-3} , which is the current SED value of the full-scale conventional AS plant, and therefore the target SED value for this research.
- Objective 5: To collect and analyse the results and to propose the MBR system, which will manage to maximise the daily production of treated permeate at a stable long-term membrane performance, to comply with the effluent requirements of this research, and to be able to lead to acceptable SED values.

1.4 Structure of the PhD thesis

This PhD thesis consists of the following chapters.

Chapter 1 Introduction

This is the introductory chapter, which includes information on the EC PURATREAT project, whose objectives are directly connected with this research. It presents the context, the general aim and the objectives of this work, as well as providing a brief description of the chapters that comprise this PhD thesis.

Chapter 2 Biomass separation MBRs and related theory

This chapter includes a review of the published literature relevant to this research. It analyses the literature so far, regarding the MBRs themselves, together with issues that are directly connected with their operation. Information on treated water quality issues, membrane performance and all the consequent membrane fouling phenomena,

together with issues related to energy consumption requirements for MBRs, supported by several energy consumption case studies, is provided.

Chapter 3 Materials and methods

This chapter focuses on the materials and methods, which were used in this research. First, it describes the membranes that were located within the MBR tanks. Then, it describes the complete pilot MBR systems and their components, and provides information about their start-up and further operational details. Finally, all methods applied in order to measure and/or calculate useful parameters are also presented, including all the analytical techniques.

Chapter 4 Clean water tests

Clean water tests are described and analysed in this chapter. The instant real MPFs, TMP values and permeability values are calculated and their profiles against time are plotted. Average real/net MPFs, together with average permeability values, are also calculated. The average permeability values are temperature-corrected at a clean water temperature equal to 20 °C and these temperature-corrected permeability values are directly compared to their corresponding values at 20 °C as provided by the membrane manufacturers. This clean water data can be used as a point of reference for any future operation of the MBRs.

Chapter 5 Effect of variation of SRT and HRT on the MBR performance

This chapter analyses the effect of variation of the operating conditions, namely the SRT and the HRT on the MBR performance. Measurements of the MLSS concentrations, together with the COD concentrations both in the influent and in the effluent, were made, and their profiles against time are plotted. Additional measurements of the mixed-liquor volatile suspended solids (MLVSS) concentrations and the influent/effluent BOD₅ concentrations were also taken. The COD removal efficiencies are finally estimated and conclusions with respect to the treated permeate quality are drawn.

Chapter 6 Membrane performance

The membrane performance is analysed in this chapter. The instant real MPFs, TMP values and permeability values are calculated and their profiles against time are plotted. Average real/net MPFs are also calculated under certain sets of operating conditions (SRTs and HRTs) and the average maximum sustainable net MPF is predicted. Hence, production of the treated permeate was maximised, and a stable long-term membrane performance was achieved. Average permeability values are also estimated and temperature-corrected at a mixed-liquor temperature equal to 20 °C. These temperature-corrected permeability values are compared to their corresponding values at 20 °C as calculated during the clean water tests so that conclusions can be made.

Chapter 7 Energy consumption and MBR modelling

This chapter is divided into two parts. The first part includes all information both on short-term power-analysis and on longer-term energy-analysis experiments, where the energy consumed by each MBR system was measured. SED values under a certain set of operating conditions for each MBR system are calculated and an initial evaluation with respect to the least cost-effective MBR system can be made. Then, the second part describes the creation, calibration, validation and application of an Excel-based MBR model that can predict SED values under different sets of operating conditions. This MBR model is able to show which MBR was most successful in achieving the objectives of this research.

Chapter 8 Conclusions/Future work

This is the final chapter the PhD thesis. Overall conclusions are made so as to check whether the objectives of this work are achieved, and which MBR system appeared to be the most-promising solution for application in the MENA region in the near future. Also, commentary on possible future work that could improve the present research, or even to introduce new experiments, is provided.

CHAPTER 2 BIOMASS SEPARATION MBRs AND RELATED THEORY

2.1 Biomass separation MBRs

2.1.1 Suspended growth aerobic AS processes and the advent of MBRs

Waste waters containing dissolved and particulate biodegradable constituents can be treated biologically, which means that the removal of all these constituents and the stabilisation of the organic matter found in these waters can be accomplished by using a variety of microorganisms, principally bacteria. These microorganisms oxidize the organic matter into simple acceptable end products and additional biomass.

The principal biological processes can be divided into two main categories: suspended growth and attached (or biofilm) growth processes. In suspended growth processes, the microorganisms are maintained in liquid suspension by applying an appropriate mixing method, whilst, in the attached growth processes, they are attached onto an inert packing material, namely rock, gravel, sand, a wide range of plastics, etc. Both suspended and attached growth processes can be operated as aerobic processes, when they occur in the presence of oxygen, or anaerobic processes, when they occur in the absence of oxygen, [Tchobanoglous *et al.*, 2004]. In this research, only suspended growth aerobic processes were applied.

The conventional activated sludge (AS) process, so-called because it involves the production of an activated mass of microorganisms, is the most common suspended growth aerobic biological process for waste water treatment (WWT). The general arrangements of an AS plant are the aeration tank and a settling tank referred to as final or secondary clarifier - frequently another clarifier for primary sedimentation is placed before the aeration tank. In the aeration tank, adequate contact time is provided for both mixing and aerating influent waste water with the microorganisms in suspension, a mixture widely known as mixed-liquor suspended solids (MLSS). In the aeration tank, the aerobic biological oxidation of organic matter takes place, [Tchobanoglous *et al.*, 2004]. More details about the biological oxidation of organic matters are given in Section 2.2.1.

The mixed-liquor then flows in the secondary clarifier where the microbial suspension is settled and thickened. The settled biomass, also known as activated sludge (AS) because active bacteria are present, is recycled back into the aeration tank so as the biodegradation of the organic matter is continued. A portion of the thickened matter is removed on a daily basis or periodically, as biomass is produced in excess, which can lead to accumulation of solids within the system. Some of these accumulated solids inescapably find their way into the final effluent treated water in the long run, deteriorating the quality, [Tchobanoglous *et al.*, 2004].

A simplified flow diagram of a conventional AS process is shown in Figure 2.1.

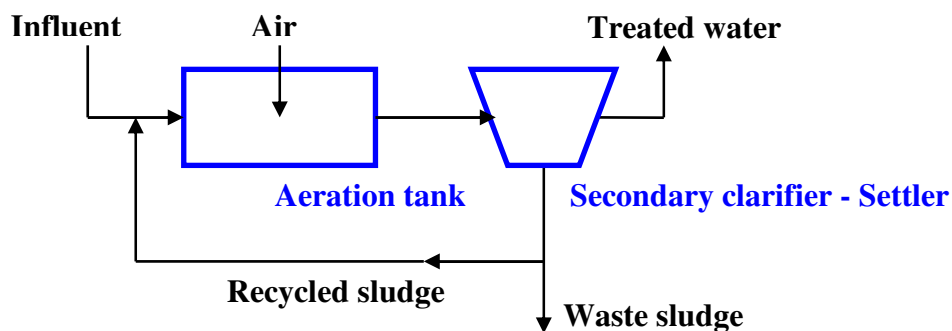


Figure 2.1 A simplified flow diagram of a conventional AS process, [Tchobanoglous *et al.*, 2004]

In the late 1960s, when microfiltration (MF) and ultrafiltration (UF) membranes became commercially available, membrane bioreactors (MBRs) were introduced as a new innovative WWT technology, [Le-Clech *et al.*, 2006]. Full-scale commercial aerobic MBRs first appeared in North America in the late 1970s, followed by Japan in the early 1980s, and finally by Europe in about the mid-1990s, [Reid, 2005]. MBRs are the main idea of this research, hence a more detailed account of them is given in the following sections.

2.1.2 General information on biomass separation MBRs and their characteristics

Despite the fact that there are three generic types of MBRs, namely biomass separation MBRs, membrane aeration bioreactors (MABRs) and extractive MBRs (EMBRs), this research only focuses on the most common type, which is the biomass separation MBRs, or simply referred to as MBRs, [Judd, 2007], [Stephenson *et al.*, 2000].

When the secondary clarifier for the separation of purified water and biomass of a conventional AS process was replaced by a membrane separation unit, MBR technology was introduced, [Lee *et al.*, 2003], [Busch *et al.*, 2007]. MBRs are then described as the combination of an AS bioreactor and a microfiltration (MF) or ultrafiltration (UF) membrane unit, [Okamura *et al.*, 2009], [Ndinisa *et al.*, 2006], [Schoeberl *et al.*, 2004], [Le-Clech *et al.*, 2003], [Stephenson *et al.*, 2000].

The original process was developed by Dorr-Oliver Inc. in the late 1960s, when the membrane sewage treatment (MST) process was introduced. This was a system that combined the traditional AS process with membrane technology for biomass-treated water separation, although it featured what would nowadays be considered as low membrane permeability values, [Judd, 2007], [Reid, 2005]. The first generation of MBRs are known as external (or re-circulated or side stream) MBRs. They consisted of cross flow operated membranes, which were installed outside the AS tank. Cross flow was applied by operating a recirculation pump, so a sludge flow velocity was generated over the membranes. The AS flow velocity provided both a high cross flow velocity for membrane cleaning and the required transmembrane pressure (TMP) values to maintain stable filtration. This method of cross flow operation required large amounts of energy, in the order of 10 kWh m^{-3} (energy consumed per unit volume of treated permeate), so these MBRs were generally considered not to be viable for application in the municipal waste water sector, [Judd, 2007], [Le-Clech *et al.*, 2006], [Van-Der-Roest *et al.*, 2006], [Yang *et al.*, 2006].

In 1989, the most important development for MBRs took place, when it was proposed for membranes to be submerged within the MBR tanks, [Yamamoto *et al.*, 1989]. This

type of submerged membrane filtration in a biological system is referred to as submerged (or immersed or integrated) MBRs. Energy consumption rates were significantly reduced due to the absence of the recirculation pump. The TMP values that were applied were considerably lower than those that were required for cross flow filtration. A cross flow over the membrane surface was provided by locating the aeration supply underneath the membrane modules, such that an up-flow was generated. The air driven cross flow both cleans the membrane surface to mitigate or retard any membrane fouling formation and provides the biomass with the required amount of oxygen for its maintenance, [Le-Clech *et al.*, 2006], [Van-Der-Roest *et al.*, 2006], [Yang *et al.*, 2006].

The introduction of submerged MBR units stimulated an exponential increase in MBR plant installations in the mid-1990s. Their economic viability practically depends on achieving good membrane permeate fluxes (MPFs) with modest energy consumption, typically lower than 1 kWh m^{-3} , [Le-Clech *et al.*, 2006]. They usually operate under lower MPFs than the side stream MBRs, so more membrane area and higher associated costs are required. On the other hand, external MBR units require less membrane area than the one required by the submerged MBRs resulting in lower capital costs and smaller footprints, [Gander *et al.*, 2000], [Stevenson *et al.*, 2000]. Also, side stream MBRs are more suitable for waste waters characterised by low filterability, [Yang *et al.*, 2006].

The two different configurations of MBRs are shown in Figure 2.2.

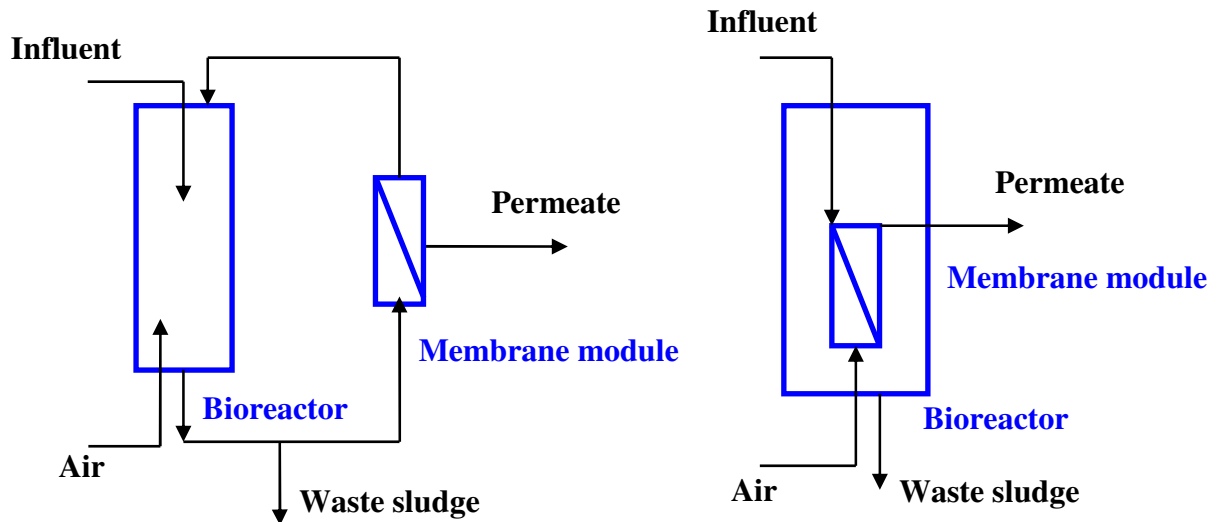


Figure 2.2 MBR configurations: Left: Side stream MBR, Right: Submerged MBR, [Gander *et al.*, 2000]

With respect to permeate collection, submerged MBRs can be either gravity-driven or suction needs to be applied. In gravity-driven systems, the available hydraulic head over the membranes provide the system with the required pressure drop so as permeate can be collected without the need for applying suction. On the other hand, when the hydraulic head within the MBR tank is not enough, a suction pump is necessitated, or otherwise filtration cannot take place, [Ueda and Hata, 1999]. In this research, MBR1 was a gravity-driven system, whereas the membranes in MBR2 and MBR3 were operated with the aid of permeate suction pumps.

Regarding the hydrodynamic operating conditions of MBR systems, the MPFs are variable from one system to the next fluctuating from $10 \text{ L m}^{-2} \text{ h}^{-1}$ to $200 \text{ L m}^{-2} \text{ h}^{-1}$. Trans-membrane pressure (TMP) values are between 10 kPa and 300 kPa. Cross flow velocities over the membrane surfaces can vary between 0.4 and 7 m s^{-1} , [Tardieu *et al.*, 1998].

MBR technology represents today in the water sector the membrane technology that grows faster, with an estimated global market of \$US 216.6 millions in 2006, an average annual growth rate of 10.9 % and an expected global market value of \$US 363 millions in 2010. Their plant sizes at the moment range between $10 \text{ m}^3 \text{ d}^{-1}$ and $50,000 \text{ m}^3 \text{ d}^{-1}$, [Guglielmi *et al.*, 2007]. [Lesjean and Huisjes, 2007], based on a

survey on the European MBR market, concluded that, between 2003 and 2005, MBR applications were characterised by a linear market growth rate including from year to year at least 50 new industrial systems and 20 municipal ones out of which 99 % of the total membrane surface was represented by submerged MBR systems. Even though their energy consumption issues are still under question, submerged MBRs seem to be viable in the WWT world market and their energy consumption rates appear to be quite competitive with those for conventional AS processes, [Guglielmi *et al.*, 2007].

2.1.3 Advantages and disadvantages of the MBR processes

MBRs have a number of advantages over the conventional AS processes, [Busch *et al.*, 2007], [Guglielmi *et al.*, 2007], [Liao *et al.*, 2006], [Ndinisa *et al.*, 2006], [Water Environmental Federation, 2006], [Schroebel *et al.*, 2005], [Arnot, 2004], [Lee *et al.*, 2003], [Zhang *et al.*, 2003], [Gander *et al.*, 2000], [Stevenson *et al.*, 2000], etc., which are as follows:

- Exceptional effluent quality

Biomass is completely retained leading to a high quality final effluent with solids concentrations less than 1 mg L⁻¹. Disinfection also occurs as a physical mechanism, and an effective separation of pathogens is provided. If additional disinfection has to be applied, MBR effluent has a minimal demand.

- Small footprint

MBRs, due to the lack of secondary clarifier, require less land than it is required by conventional AS processes. Effluent filters can also be eliminated as dispensable. Finally, as elevated MLSS concentrations are possible in MBRs, the volume of the biological tanks can be further reduced, so additional reduction in land requirements is possible.

- Robust and reliable operation

MBR systems can operate within a wide range of solids residence times (SRTs) resulting in increased flexibility and more option with respect to their optimization. Long SRTs can also help important slow-growing microorganisms such as nitrifying bacteria develop as well. In addition, MBRs can handle very high MLSS concentrations for short periods of time meaning that waste sludge can be flexibly wasted. They also offer reliable operation independent on the hydraulic and the organic loads, together with their variations. Finally, all the MBR processes are easily automated with operator requirements reduced to a minimum.

- Uncoupling of the operating conditions

In MBR processes, solids residence times (SRTs) and hydraulic residence times (HRTs) can be completely separated. This provides optimum control over the process and greater availability and flexibility in use can be achieved.

- Reduced excess sludge production

Excess sludge production is reduced - it can be approximately halved - compared to the conventional AS methods.

Despite the fact that MBRs have all these advantages, they also have some disadvantages making them unsuitable for every WWT application. These disadvantages are as follows, [Water Environmental Federation, 2006]:

- Costs

Even though the capital cost of membranes has been reduced significantly over the years, MBRs are advanced treatment processes and as such they are more expensive in terms of capital cost than conventional AS plants. Operational costs are also higher - MBR plants consume more energy than the conventional AS plants, as they have to operate air scour blowers, biological process blowers, recycle and at times permeate

suction pumps. Finally, the purchase of chemicals for membrane cleaning can add an extra operational cost, especially if the chemical usage has not been optimised.

- Limited availability of long-term data

MBRs are a relatively new technology, so a limited amount of data is available to verify properly their long-term performance. Also, issues about membrane life expectancy, as claimed by their manufacturers, are still unclear.

- Limited flow rate capacity

As MBRs are a membrane-related operation, there is a hydraulic limitation to how much water the membranes can permeate. If occasionally the flow rate requirements appear to be higher than what has been designed, alternative ways of treating waste water may have to be found.

- Increase possibility of foam formation

Operating conditions in MBRs can lead to the formation of foam, however, a careful design including foam management options can significantly help.

- System monitoring

In spite of being highly automated, MBRs have to be closely monitored in case spontaneous changes of the feed/permeate flow rates may happen.

However, the fact that they can provide effluents, whose chemical oxygen demand (COD) concentrations easily comply with the increasingly strict sanitary rules of the European Commission (EC), have made them a very promising new technology in the field of WWT processes, [Busch *et al.*, 2007].

In the next sections, the biological performance of MBRs, their membrane performance and MBR energy consumption issues are discussed.

2.2 MBR biological performance

2.2.1 Aerobic biological oxidation

2.2.1.1 Microorganisms, their function and the bacterial growth pattern

Aerobic biological oxidation is performed by a wide variety of microorganisms including mixed bacterial cultures of heterotrophic bacteria, as well as higher microorganisms, namely protozoa and metazoa, [Arnot, 2004], [Tchobanoglous *et al.*, 2004]. Together with the realisation of the aerobic biological oxidation, the aerobic heterotrophic bacteria are able to produce extracellular polymeric substances (EPS) for the formation of bioflocs, [Yang and Li, 2009], [Tchobanoglous *et al.*, 2004], [Laspidou and Rittmann, 2001]. These bioflocs, in conventional AS processes, can then be easily separated from the treated water by gravity settling, leading to a final effluent with relatively low concentrations of free bacteria and suspended solids (SS).

Protozoa, particularly ciliated protozoa, also play an important role in conventional aerobic biological treatment processes. They consume free bacteria and colloidal particulates, so they cleanse the waste stream, add weight to biofloc particles and improve their settleability, or produce and release secretions that coat and remove fine solids, like colloids, dispersed cells and particulate matter from the bulk solution to the surface of floc particles, [Gerardi, 2006], [Tchobanoglous *et al.*, 2004].

Finally, metazoa, namely rotifers and nematodes, are characterised by their capability of burrowing into bioflocs. Thus, they promote acceptable bacterial activity as dissolved oxygen (DO), substrates, and nutrients can now penetrate into the core of the bioflocs, [Gerardi, 2006]. Both protozoa and metazoa need long SRTs to grow and multiply, [Tchobanoglous *et al.*, 2004].

Figure 2.3 shows a schematic of a typical bacterial growth curve in a batch system. At time zero, only a very small population of biomass exists with both substrate and nutrients being present in excess. Substrate is consumed and four distinct growth phases develop one after the other, [Tchobanoglous *et al.*, 2004].

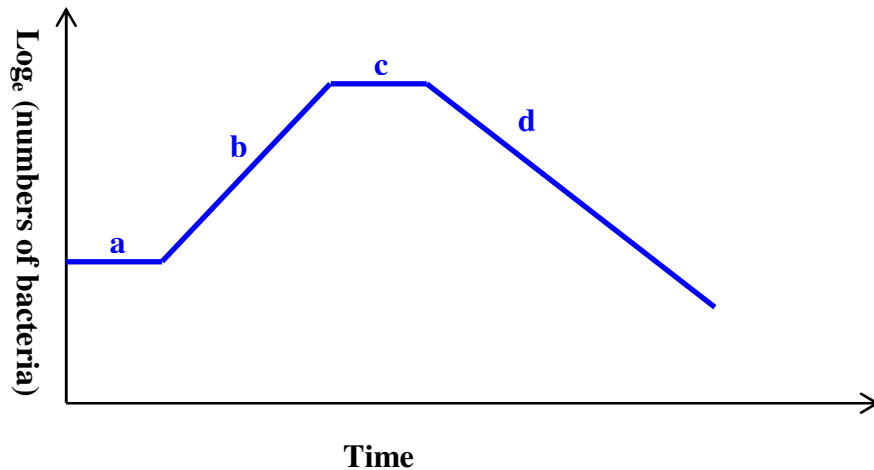


Figure 2.3 Bacterial growth curve, [Stamou and Vogiatzis, 2004]

- Phase a: The lag phase

This phase represents the time the bacteria need in order to acclimatise to the new environment, before significant cell division and biomass production occur.

- Phase b: The exponential-growth phase

During this phase, bacteria are multiplying at their maximum rate as substrate and nutrients are in excess. The biomass curve increases exponentially and the bacterial growth is only affected by the mixed-liquor temperature.

- Phase c: The stationary phase

The biomass concentration remains relatively constant with time. The bacterial growth is no longer exponential but the amount of growth is offset by the cell death.

- Phase d: The death phase

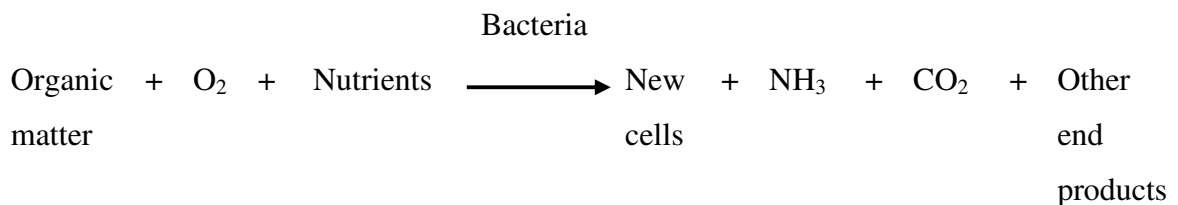
In this phase, the substrate has been consumed, so cells cannot grow but only die, with the curve often decreasing exponentially.

MBRs, as opposed to conventional AS processes, are able to be operated in the death phase, which is characterised by long SRTs, hence the production of excess sludge is greatly reduced, which is one of their advantages - see Section 2.1.3.

2.2.1.2 Stoichiometry of the aerobic biological oxidation

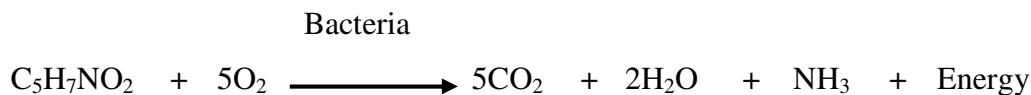
Stoichiometrically, the aerobic biological oxidation can be described by Equation 2.1 and Equation 2.2, [Arnot, 2004], [Tchobanoglous *et al.*, 2004].

• Oxidation and synthesis Equation 2.1



The organic matter can be represented as glucose (C₆H₁₂O₆) and the new cells can be represented as C₅H₇NO₂. Nutrients are nitrogen and phosphorus.

• Endogenous respiration Equation 2.2.



Because of a wide range of constituents and compounds in the waste water, the concentration of the organic matter is usually quantified in terms of chemical oxygen demand (COD), or 5-day biochemical oxygen demand (BOD₅), or total organic carbon (TOC) concentration. Similarly to the organic matter concentration, biomass concentration, regarding all microbial suspension in the process, is expressed in terms of mixed-liquor volatile suspended solids (MLVSS) concentration, which represents the volatile part of suspended solids (SS), that is to say the organic part of the bacteria, [Tchobanoglous *et al.*, 2004], [Stamou and Vogiatzis, 1994]. The total biomass concentration can also be quantified in terms of mixed-liquor suspended solids (MLSS) concentration of which MLVSS is a subset.

2.2.2 Microbial growth kinetics

The performance of the biological aerobic oxidation, as performed by heterotrophic bacteria, depends on the dynamics of two parameters, the substrate utilization rate and the biomass growth rate.

Substrate is the organic matter or nutrients that are converted during biological treatment, or that may be limiting during biological treatment, [Tchobanoglous *et al.*, 2004]. Out of the substrates in waste water, often, a single substrate exerts a dominant influence on the rate of cell growth. This substrate, which is commonly either of a carbon or of a nitrogen origin, is known as growth-limiting substrate, [Doran, 2006].

The rate at which a growth-limiting soluble substrate concentration changes due to utilisation is given by Equation 2.3. As it decreases with time due to utilisation, a negative sign is used.

$$r_{su} = -\frac{kXS}{K_s + S} \quad \text{Equation 2.3}$$

where:

r_{su}	= Rate of substrate concentration change due to utilisation	$\text{g m}^{-3} \text{d}^{-1}$
k	= Maximum specific substrate utilization rate	d^{-1}
X	= Biomass concentration	g m^{-3}
S	= Growth-limiting substrate concentration in solution	g m^{-3}
K_s	= Half-velocity constant, substrate concentration at one-half the maximum specific substrate utilisation rate	g m^{-3}

The maximum specific bacterial growth rate is defined as follows:

$$\mu_{\max} = kY_{X/S} \quad \text{Equation 2.4}$$

where:

$$\begin{aligned}\mu_{\max} &= \text{Maximum specific growth rate} && \text{d}^{-1} \\ Y_{X/S} &= \text{Synthesis yield co-efficient} && \text{unitless}\end{aligned}$$

From Equations 2.3 and 2.4, we get:

$$r_{su} = -\frac{\mu_{\max} XS}{Y_{X/S}(K_S + S)} \quad \text{Equation 2.5}$$

On the other hand, the net rate at which the biomass grows is proportional to the substrate utilisation rate via the synthesis yield coefficient, and the biomass that is present by an endogenous decay coefficient. Thus, in any culture system, the net biomass production rate, or the relationship between the biomass growth rate and the substrate utilisation rate, is given by Equation 2.6.

$$r_g = -Y_{X/S} r_{su} - k_d X \quad \text{Equation 2.6}$$

where:

$$\begin{aligned}r_g &= \text{Net biomass production rate} && \text{g m}^{-3} \text{d}^{-1} \\ k_d &= \text{Endogenous decay co-efficient} && \text{d}^{-1}\end{aligned}$$

From Equations 2.3 and 2.6, we get:

$$r_g = \frac{\mu_{\max} XS}{K_S + S} - k_d X \quad \text{Equation 2.7}$$

By dividing both sides of Equation 2.7 by the X-value, Equation 2.8 is modelled.

$$\mu = \frac{r_g}{X} = \frac{\mu_{\max} S}{(K_S + S)} - k_d \quad \text{Equation 2.8}$$

where:

μ = Specific biomass growth rate d^{-1}

Equation 2.8, which shows the relationship between the specific biomass growth rate (μ -value) and the effluent water quality (S-value), is the most important equation in microbial growth kinetics.

2.2.3 MBR mass balancing

Figure 2.4 shows the flow diagram of a submerged MBR process. The dotted line shows the system boundary. All abbreviated parameters, as shown in the flow diagram, are defined later in this section.

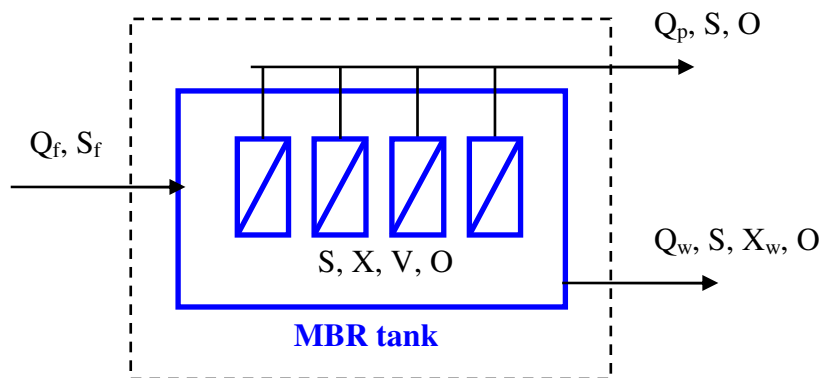


Figure 2.4 Flow diagram of a submerged MBR process, [Arnot, 2004]

It is worth mentioning that the number of membrane panels shown Figure 2.4 is illustrative only and does not affect the equations mentioned later in this section.

Any mass balance for any system is generally as follows, [Doran, 2006]:

Equation 2.9

mass	mass	mass	mass	mass
accumulated	= in	through	- out	+ generated
within	system	system	system	within
system	boundaries	boundaries	system	system

Mass balances for the calculations of the three most important biological parameters of the MBR processes, namely growth-limiting soluble substrate concentration in solution, S , biomass concentration, X , and dissolved oxygen (DO) concentration, O , are developed as follows, [Arnot, 2004]:

2.2.3.1 Growth-limiting soluble substrate concentration mass balance

This mass balance under dynamic conditions is as follows:

$$\frac{dS}{dt} = \frac{Q_f}{V} S_f - \frac{Q_p}{V} S - \frac{Q_w}{V} S - \frac{\mu X}{Y_{X/S}} \quad \text{Equation 2.10}$$

where:

Q_f	= Average volumetric feed flow rate	$\text{m}^3 \text{d}^{-1}$
V	= Operating volume of the MBR	m^3
S_f	= Growth-limiting substrate concentration in the feed	g m^{-3}
Q_p	= Average volumetric permeate flow rate	$\text{m}^3 \text{d}^{-1}$
Q_w	= Average volumetric waste sludge flow rate	$\text{m}^3 \text{d}^{-1}$

Liquid flow rates into and out of the MBR system must balance, so:

$$Q_f = Q_p + Q_w \quad \text{Equation 2.11}$$

Combining Equation 2.10 with Equation 2.11, we get:

$$\frac{dS}{dt} = \frac{Q_f}{V} (S_f - S) - \frac{\mu X}{Y_{X/S}} \quad \text{Equation 2.12}$$

When steady state is reached, the differential term may be set to zero, so:

$$\frac{dS}{dt} = 0 \quad \text{Equation 2.13}$$

By inserting Equation 2.13 into Equation 2.12 and re-arranging, we can express the mass balance at steady state:

$$\frac{Q_f}{V} (S_f - S) = \frac{\mu X}{Y_{X/S}} \quad \text{Equation 2.14}$$

For a continuous stirred-tank reactor (CSTR) operating at steady state, the hydraulic residence time (HRT), θ , is defined as follows, [Kyparissidis, 1994]:

$$\theta = \frac{V}{Q_f} \quad \text{Equation 2.15}$$

where:

$$\theta = \text{HRT} \quad \text{d}$$

By inserting Equation 2.15 into Equation 2.14 and re-arranging, we get:

$$S = S_f - \frac{X\theta\mu}{Y_{X/S}} \quad \text{Equation 2.16}$$

Finally, solving for biomass concentration, X , we get:

$$X = \frac{Y_{X/S}(S_f - S)}{\theta\mu} \quad \text{Equation 2.17}$$

Equation 2.16 predicts the treated permeate quality, and Equation 2.17 can predict the biomass concentration. From Equation 2.16 and Equation 2.17, it can be concluded that there is a direct relationship between the S-value and the X-value and practically the treated permeate quality improves each time a higher biomass concentration is applied.

2.2.3.2 Mass balance for biomass concentration

The biomass concentration in the feed, X_f , is assumed to be equal to zero, as waste water may be assumed to be free from active microorganisms. The mass balance for biomass concentration is as follows:

$$\frac{dX}{dt} = \mu X - \frac{Q_w}{V} X_w \quad \text{Equation 2.18}$$

where:

$$X_w = \text{Biomass concentration in waste water} \quad \text{g m}^{-3}$$

At steady state, the differential term becomes zero, so:

$$\frac{dX}{dt} = 0 \quad \text{Equation 2.19}$$

Also, assuming that the mixed-liquor in the MBR tank is well-mixed:

$$X = X_w \quad \text{Equation 2.20}$$

By inserting Equation 2.19 and Equation 2.20 into Equation 2.18 and re-arranging, we get the mass balance at steady state:

$$\mu X = \frac{Q_w}{V} X \quad \text{Equation 2.21}$$

As the X-value on each side of Equation 2.21 can be cancelled, Equation 2.21 is simplified as follows:

$$\mu = \frac{Q_w}{V} \quad \text{Equation 2.22}$$

The solids residence time (SRT), θ_c , based on the waste sludge flow rate, is defined as follows, [Arnot, 2004]:

$$\theta_c = \frac{V}{Q_w} \quad \text{Equation 2.23}$$

where:

$$\theta_c = \text{SRT} \quad \text{d}$$

Combining Equation 2.23 with Equation 2.22, the μ -value is expressed as follows:

$$\mu = \frac{1}{\theta_c} \quad \text{Equation 2.24}$$

Based on Equation 2.24, it can be said that if the SRT is controlled during process operation, the μ -value is also controlled.

Finally, by combining Equation 2.8 with Equation 2.24 ,we get:

$$\frac{1}{\theta_c} = \frac{\mu_{\max} S}{(K_s + S)} - k_d \quad \text{Equation 2.25}$$

Based on Equation 2.25, it can be concluded that by controlling the SRT the bacteria are forced to grow at a certain value of μ , and hence the S-value, which indicates the treated permeate quality, can be successfully regulated as well. Also, as suggested by Equation 2.25, longer SRTs are able to provide treated water of better quality.

2.2.3.3 Mass balance for DO concentration

The DO concentration in the feed, O_f , can be assumed to be equal to zero, as the waste water starts being enriched with oxygen only within the MBR tank, so there is not any useful oxygen in the feed.

The mass balance for DO concentration in a dynamic state is described as follows:

$$\frac{dO}{dt} = k_L a(O_{SAT} - O) - \frac{\mu X}{Y_{X/O}} - \frac{Q_p O}{V} - \frac{Q_w O}{V} \quad \text{Equation 2.26}$$

where:

O	= DO concentration	g m^{-3}
$k_L a$	= Liquid-phase oxygen to water mass transfer coefficient	d^{-1}
O_{SAT}	= DO concentration in equilibrium with gas as given by Henry's law	g m^{-3}
$Y_{X/O}$	= Coefficient indicating biomass produced immediately upon consumption of DO	unitless

The O_{SAT} -value can be directly derived from DO solubility tables as a function of temperature, barometric pressure, and salinity, [Tchobanoglous *et al.*, 2004].

By incorporating Equation 2.11 into Equation 2.26, we get:

$$\frac{dO}{dt} = k_L a(O_{SAT} - O) - \frac{\mu X}{Y_{X/O}} - \frac{Q_f O}{V} \quad \text{Equation 2.27}$$

When steady state is reached, we get:

$$\frac{dO}{dt} = 0 \quad \text{Equation 2.28}$$

By combining Equation 2.27 and Equation 2.28 and re-arranging, we get:

$$k_L a(O_{SAT} - O) = \frac{\mu X}{Y_{X/O}} + \frac{Q_f O}{V} \quad \text{Equation 2.29}$$

Solving Equation 2.29 for DO concentration gives:

$$O = \frac{(k_L a O_{SAT} Y_{(X/O)} - \mu X) \theta}{Y_{(X/O)} (k_L a \theta - 1)} \quad \text{Equation 2.30}$$

Through Equation 2.30, it can be checked whether the aeration system is capable of supplying enough oxygen for biomass maintenance.

2.2.4 Biomass characteristics

2.2.4.1 Biomass fractionation

Biomass is fractionated into three idealized components, namely suspended solids (SS), colloids and solutes. Solubles and colloids are defined as soluble microbial products (SMP). On the other hand, in the suspended growth processes, SS are represented by bioflocs, [Le-Clech *et al.*, 2006], [Judd, 2007], with extracellular polymeric substances (EPS) being the bonding agent for their formation, [Sheng *et al.*, 2007], [Maximova and Dahl, 2006], [Laspidou and Rittmann, 2002]. The organic compounds mentioned above are of the following sizes, [Tardieu *et al.*, 1998].

- The bioflocs contain particles ranging from 1 μm to a few hundreds of μm .
- The colloidal fraction, which contains particles from 0.001 μm to 1 μm .
- The soluble fraction, which contains compounds smaller than 0.001 μm .

Out of these fractions, in MBRs, the biological flocs typically account for 5 - 20 g L^{-1} of dry matter, whereas the soluble and colloidal fractions are limited to a few hundred mg L^{-1} of dry matter.

2.2.4.2 EPS and SMP

Extracellular polymeric substances (EPS) and soluble microbial products (SMP) are microbially produced organic materials but are not active cells, [Aquino and Stuckey, 2009], [Laspidou and Rittmann, 2002].

The EPS are organic substances (large polymeric molecules), produced by most bacteria either the microorganisms grow in suspended cultures or in biofilms. Some of their key functions are adhesion to surfaces, aggregation of bacterial cells in flocs and biofilms, stabilization of the biofilm structure, formation of a protective barrier that provides resistance to biocides or other harmful effects, retention of water, sorption of exogenous organic compounds for the accumulation of nutrients from the environment, and accumulation of enzymatic activities, such as digestion of exogenous macromolecules for nutrient acquisition. Thus, the EPS matrix allows cooperation and communication among cells in microbial aggregates and a stable, close proximity of bacteria requires that the cells should be held together by EPS, [Comte *et al.*, 2006], [Laspidou and Rittmann, 2002]. Finally, it has to be mentioned that more EPS than the usual quantities are produced when bacteria have to protect themselves against unfavourable conditions, such as the presence of toxic substances, [Sheng *et al.*, 2008]

EPS consist of different classes of organic macromolecules such as polysaccharides, proteins, nucleic acids, (phospho)lipids and other polymeric compounds, and have been found at or outside the cell surface and in the intercellular space of microbial aggregates, [Metzger *et al.*, 2007]. However, their dominant components are proteins and carbohydrates (polysaccharides), [Judd, 2007], [Jang *et al.*, 2006]. EPS, in a conventional AS system, could be found in two different forms, namely bound EPS on biofloc biomass like sheaths, capsular polymers, condensed gel, loosely bound polymers and attached organic material, and soluble EPS like soluble macromolecules, colloids and slimes, [Sponza, 2003]. In general, SMP are considered to be soluble EPS, [Metzger *et al.*, 2007], [Comte *et al.*, 2006], [Jang *et al.*, 2006].

The SMP are also microbial products, which are defined as cellular components that are released during cell lysis, diffuse through the cell membrane, are lost during synthesis, or are excreted for some purpose. They are biodegradable and are important because they usually form the majority of the effluent COD/BOD₅ concentration, for biological treatment processes, [Jarusutthirak and Amy, 2007], [Laspidou and Rittmann, 2002]. The SMP can be subdivided into substrate-utilization-associated products, which are produced directly during substrate metabolism and biomass-

associated products, which are formed from biomass, especially as part of microbial decay, [Laspidou and Rittmann, 2002].

The tendency of the microorganisms to produce EPS and SMP has a negative effect on MBR technologies because they are responsible for causing serious problems to the membranes with respect to their fouling, [Wang *et al.*, 2009], [Metzger *et al.*, 2007], [Jang *et al.*, 2007], [Tansel *et al.*, 2006], [Yamato *et al.*, 2006], [Yun *et al.*, 2006], etc., even when operation is performed under MPFs referred to as subcritical-fluxes, [Cho and Fane, 2002].

2.2.4.3 MLSS concentrations and their relationships with the operating conditions (HRT/SRT)

MLSS is an important parameter in suspended growth processes, defined as the mixture of solids resulting from combining recycled sludge with influent waste water in the bioreactor and they represent the biomass solids, [Tchobanoglous *et al.*, 2004]. The MLSS concentration impacts on the biological properties, *e.g.* the bioactivity and the microbial specification, [Judd, 2007], within the MBR tanks, the physical properties like the waste water viscosity, [Hasar *et al.*, 2004], and the oxygen transfer, [Henker *et al.*, 2009], [Germain *et al.*, 2007]. MBRs are reported to be able to maintain MLSS concentrations up to 25 g L^{-1} , [Stephenson *et al.*, 2002], even though even higher concentrations, *i.e.* 26.72 g L^{-1} , have been reported, [Mohammed *et al.*, 2008].

SRTs, in MBR operations, are usually the design parameter and their values can be easily controlled by suitably selecting the Q_w -value. The longer the SRT is, or the lower the food : microorganism (F/M) ratio is, the lower the S-value is as well, hence MBRs operated under longer SRTs stand better chances of producing effluents of appropriate quality. Long SRTs are also able to minimize excess sludge production as the microorganisms tend to grow in the endogenous respiration phase - see Phase d: the death phase of the microbial growth curve as shown in Figure 2.3. Any increase in the MLSS concentration alters the biomass characteristics and can lead to clogging of membrane channels causing membrane fouling problems, [Stamou and Vogiatzis, 1994], [Judd, 2007]. In MBRs, the SRT can vary from 2 d to infinite values, which

practically means that no sludge wasting takes place during the experiments, [Stephenson *et al.*, 2002].

Finally, regarding the HRTs, it can be said that for a given SRT, the $[X \cdot \theta]$ -product is constant. This means that if an HRT is selected, the biomass concentration is also defined and vice versa, [Stamou and Vogiatzis, 1994]. With respect to pilot MBRs treating domestic sewage, HRTs can vary from 2.7 h to 34.2 h, [Ren *et al.*, 2005].

2.2.4.4 Oxygen transfer

Oxygen transfer is the process by which oxygen is transferred from the gaseous to the liquid phase and it is a vital part in the aerobic WWT processes as their functioning depends on the availability of sufficient quantities of DO in waste water, [Tchobanoglous *et al.*, 2004]. For MBRs, the average level of DO is controlled by their air flow rates within the bioreactor tanks.

Based on the two-film theory in gas-liquid mass transfer process, the rate of mass transfer of oxygen into the waste water is given by Equation 2.31, [Tchobanoglous *et al.*, 2004], [Doran, 2006].

$$N_o = \frac{dO}{dt} = K_L a (O_{SAT} - O_t) - q_o X \quad \text{Equation 2.31}$$

where:

N_o	= Rate of oxygen mass transfer	$\text{g m}^{-3} \text{ s}^{-1}$
O_t	= DO concentration at time t	g m^{-3}
$K_L a$	= Overall liquid-phase mass transfer coefficient	s^{-1}
$q_o X$	= Oxygen uptake by the cells	$\text{g m}^{-3} \text{ s}^{-1}$

The oxygen uptake by the cells can be calculated considering the system is at steady state. At steady state, the differential term becomes zero, so we get:

$$\frac{dN_o}{dt} = 0 \quad \text{Equation 2.32}$$

Combining Equation 2.31 with Equation 2.32 and re-arranging, Equation 2.31 gives:

$$q_o X = K_L a (O_{SAT} - \bar{O}) \quad \text{Equation 2.33}$$

where:

$$\bar{O} = \text{Steady-state DO concentration } \text{g m}^{-3}$$

Because oxygen is poorly soluble in the liquid, the liquid-phase mass transfer resistance dominates and $K_L a$ is approximately equal to $k_L a$, which is the liquid-phase mass transfer coefficient, [Doran, 2006]. Combing Equation 2.31 with Equation 2.33 and substituting the $K_L a$ -value with the $k_L a$ -value, we get:

$$\frac{dO}{dt} = k_L a (\bar{O} - O_t) \quad \text{Equation 2.35}$$

Integration of Equation 2.35 between two a random times, t_1 and t_2 , leads to

$$k_L a = \frac{\ln\left(\frac{\bar{O} - O_{t1}}{\bar{O} - O_{t2}}\right)}{t_2 - t_1} \quad \text{Equation 2.36}$$

where:

$$O_{t1} = \text{DO concentration at time } t_1 \quad \text{g m}^{-3}$$

$$O_{t2} = \text{DO concentration at time } t_2 \quad \text{g m}^{-3}$$

$$t_1 = \text{Time } t_1 \quad \text{s}$$

$$t_2 = \text{Time } t_2 \quad \text{s}$$

In general, k_La -values are strongly linked with the air flow rates applied within the MBR tanks. Assuming that the liquid does not circulate, usually a power function law of the gas superficial velocity is used, [Kouakou *et al.*, 2005].

$$k_La = bU_g^\beta \quad \text{Equation 2.37}$$

where:

U_g	=	Gas superficial velocity	m s^{-1}
b	=	Coefficient	unitless
β	=	Exponent - usually ranges from 0.6 to 0.8	unitless

In case where the liquid is forced to circulate, the combined action of air and forced liquid superficial velocities on k_La is given as follows:

$$k_La = (aU_l + b)U_g^\beta \quad \text{Equation 2.38}$$

where:

U_l	=	Liquid superficial velocity	m s^{-1}
a	=	Coefficient	unitless

k_La is dramatically affected by the different air flow rates that are applied. Other parameters affecting the k_La -values are the temperature of the waste water, the level of mixing, the height of waste water over the diffuser and the waste water itself. This is usually described by a parameter known as α -factor, which represents the ratio of the waste water k_La -value over the clean water k_La -value, [Stamou and Vogiatzis, 1994]. The k_La -values in the literature may range from 0.003 s^{-1} to 0.15 s^{-1} , [Kouakou *et al.*, 2005].

2.3 Membrane performance

2.3.1 Membrane fundamentals

A membrane, as shown in Figure 2.5, can be thought of as a thin barrier between two fluids, which restricts the movement of one or more components of one or both fluids across the barrier, [Howell *et al.*, 1993]. Alternatively, a membrane is a material through which one type of substance can pass more readily than others, [Stephenson *et al.*, 2002]. The components that pass through the membrane are defined as permeate and those, which are rejected, form the retentate, [Judd, 2007].

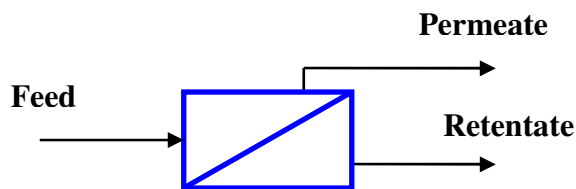


Figure 2.5 The membrane, [Judd, 2007]

Industrial membrane processes are classified according to the size range of materials that they are able to separate and the driving force used for separation, [Coulson and Richardson, 1991]. The four key membrane separation processes are reverse osmosis (RO), nanofiltration (NF), ultrafiltration (UF) and microfiltration (MF), [Judd, 2007]. In this work, only MF and UF processes were applied. Membranes used for MF or UF are usually made of polymeric materials. Most MF membranes have a symmetric pore structure and they can have porosity as high as 80 %. UF membranes have an asymmetric structure comprising a finely porous top layer on a more openly porous supporting matrix, [Coulson and Richardson, 1991].

A summary classification of membrane processes can be found in Table 2.1.

Table 2.1 Classification of membrane separation processes, [Coulson and Richardson, 1991]

Process	Driving force	Separation size range	Examples of material separated
MF	Pressure gradient	10 - 1 μm	Small particles, large colloids, microbial cells
UF	Pressure gradient	< 0.1 μm - 5 nm	Emulsions, colloids, macromolecules, proteins
NF	Pressure gradient	~ 1 nm	Dissolved salts, organics
RO	Pressure gradient	< 1 nm	Dissolved salts, small organics

Filtration, as applied in membrane processes, can be either of a dead end or of a cross flow operational mode. In dead end operations, the particle-containing fluid is pumped directly through the membrane. On the other hand, in cross flow operations, the particle-containing liquid is pumped parallel to the face of the membrane. Then, the liquid permeates through the membrane and the feed is released at the end of the membrane in a more concentrated form. Although MF can be operated either in a dead end or in a cross flow mode, UF in industry is always operated in the cross flow, [Coulson and Richardson, 1991], which is schematically depicted in Figure 2.6.

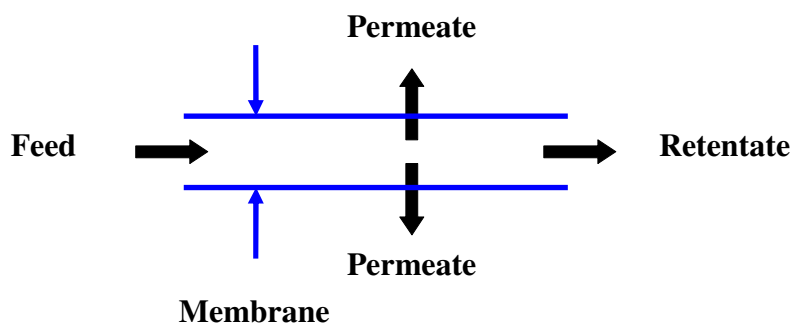


Figure 2.6 Cross flow filtration, [Coulson and Richardson, 1991]

Cross flow filtration can be operated either in a constant-TMP mode or in a constant-flux mode. In constant-TMP mode, the TMP value is maintained constant throughout the filtration run, and hence MPF decreases with time due to membrane fouling formation. Alternatively, in constant-flux mode, TMP becomes the dependent variable, hence TMP values increase with time, [Vyas *et al.*, 2002]. MBRs are routinely operated under constant-flux conditions, [Judd, 2007].

Finally, membrane equipment is usually supplied in the form of modules, [Coulson and Richardson, 1991], out of which the most common to be applied in MBR processes are tubular (T), or multi-tubular (MT), flat sheet (FS) and hollow fibre (HF). Even though only FS membranes were tested in this research, a brief summary including details about the membrane modules is given in Table 2.2.

Table 2.2 Characteristics of different membrane modules applied in MBR technology, [Judd, 2007], [Stephenson *et al.*, 2000]

Module	Cost	Turbulence promotion	Back-flushing
T (MT)	Very high	Very good	Not applicable
FS	High	Fair	Not applicable
HF	Very low	Very poor	Applicable

2.3.2 Filtration law

The standard Darcy's filtration law through which membrane permeate flux (MPF) is related to both the transmembrane pressure (TMP) value and the osmotic pressure value across the membrane is given by Equation 2.39, [Howell *et al.*, 1993]. This relationship can easily model any reduction in membrane permeate fluxes (MPFs) (or any increase in TMP values) for a constant TMP value (or MPF respectively), [Bacchin *et al.*, 2006].

$$J = \frac{|\Delta P| - |\Delta \Pi|}{(R_m + R_f)\mu} \quad \text{Equation 2.39}$$

where:

J	=	MPF	m s^{-1}
ΔP	=	Pressure difference applied across the membrane, or TMP	Pa
$\Delta \Pi$	=	Difference in the osmotic pressure across the membrane	Pa
R_m	=	Resistance of the clean membrane	m^{-1}
R_f	=	Resistance due to membrane fouling	m^{-1}
μ	=	Viscosity of permeate	N s m^{-2}

By taking membrane fouling into account, Equation 2.38 can be as follows, [Bacchin *et al.*, 2006]:

$$J = \frac{|\Delta P| - |\Delta \Pi|}{(R_m + R_{ads} + R_{rev} + R_{irrev})\mu} \quad \text{Equation 2.40}$$

where:

R_{ads}	=	Resistance due to pore adsorption	m^{-1}
R_{rev}	=	Resistance driven by the filtered volume being reversible	m^{-1}
R_{irrev}	=	Resistance driven by the filtered volume being irreversible	m^{-1}

As membrane fouling represents an import part of this research, it is described in detail in Section 2.3.3.

2.3.3 Membrane fouling phenomena

2.3.3.1 General information: From concentration polarisation to membrane fouling

Membrane fouling in MBRs is actually the major problem that impedes their fast commercialisation and affects their economic viability, [Delgado, 2007], [Zhang *et al.*, 2006]. Membrane fouling can increase both operational and maintenance costs of the membrane-based WWT process. Initially, it is responsible for deteriorating (decreasing) the membrane permeability, so it consequently increases the energy consumption costs. Then, a severely-fouled membrane must be cleaned with chemical

agents, which add an additional cost to the process, together with the fact that the disposal of these chemicals is an issue of concern, [Yamamoto *et al.*, 2006]. Membrane fouling is a general term given to the process by which a variety of species in waste water, such as bacteria, yeast, proteins, colloids, etc., increase the membrane resistance due to their build-up on the membrane surface, thereby commensurately increasing the energy demand, [Bacchin *et al.*, 2006], [Le-Clech *et al.*, 2006], [Gander *et al.*, 2000], [Stephenson *et al.*, 2000].

Initially, concentration polarisation, which is a natural consequence of the selectivity of the membrane, occurs. This phenomenon leads to an accumulation of particles or solutes in a mass transfer boundary layer adjacent to the membrane surface. As particles, together with rejected dissolved macromolecules, tend to accumulate at or near the membrane, a layer containing near-stagnant liquid is formed. This practically means that diffusion is the only mode of liquid transport in this region, a mode of transport considerably slower than convection, which takes place in the bulk liquid region. The solvent flow through the membrane is then reduced and the way with which concentration polarisation affects this value can be represented as a reduction in the effective TMP values due to an osmotic pressure difference between the filtrate and the feed solution adjacent to the membrane. Even though concentration polarisation is an inevitable phenomenon, it is reversible, [Bacchin *et al.*, 2006], [Belford *et al.*, 1994], and the application of air sparging, described later in Section 2.3.4.3, can disrupt the concentration polarisation layer, [Psoch and Schiewer, 2005]. The reversible resistance associated with the polarisation concentration layer can be expressed as a term of osmotic pressure in Equation 2.38, [Espinasse *et al.*, 2008].

When the accumulated matter at the membrane undergoes a phase transition from dispersed phase, which is controlled by concentration polarisation, to a condensed phase described as a multi-layer deposit formation, membrane fouling has already formed, [Bacchin *et al.*, 2006]. Membrane fouling, which is responsible for the increase in the TMP values in the constant-flux filtration, or for the decline in the MPF in constant-TMP operations, [Bacchin *et al.*, 2006], [Arnot *et al.*, 2000], is described in the following sections.

2.3.3.2 Membrane fouling mechanisms and forms

Both dead end and cross flow filtration proceed according to four recognised fouling mechanisms. These mechanisms are: complete pore blocking, standard pore blocking, intermediate pore blocking and cake filtration, [Wang and Tarabara, 2008], [Judd, 2007], [Le-Clech *et al.*, 2006], (see Figure 2.7). For complete blocking, it is assumed that each particle reaching the membrane blocks a membrane pore without imposing over other particles. For the standard blocking, the particles deposit within the membrane pores so that the pore volume decreases proportionally to the volume of the deposited particles, the physical cause for this is direct adsorption of the particles. When cake filtration occurs, particles depositing on the membrane do not block pores, either because the membrane is too dense and there are no pores to block, or because the pores have already been blocked by other particles and therefore, they are no more available pores. Also, the particles deposited on to the membrane surface may be larger than the membrane pore sizes. Finally, for the intermediate blocking, it is assumed that some particles deposit on other particles, which is similar to cake filtration, while other particles block membrane pores, which is similar to complete pore blocking. The pore blockage now occurs due to long-term adsorption, [Wang and Tarabara, 2008], [Le-Clech *et al.*, 2006].

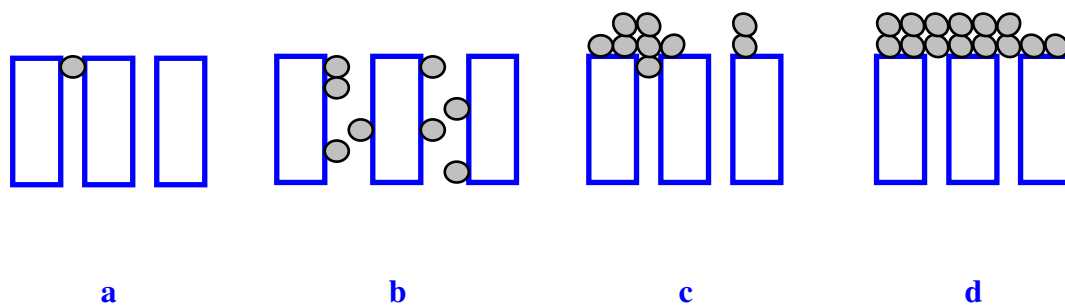


Figure 2.7 Fouling mechanisms: a: Complete blocking, b: Standard blocking, c: Intermediate blocking, d: Cake filtration, [Wang and Tarabara, 2008], [Judd, 2007], [Chua, 2003]

The matter, which can cause membrane fouling can consist of ions or molecules, macromolecules, colloids and particles, [Bacchin *et al.*, 2006]. Overall therefore, membrane fouling can take one of the following forms.

• Adsorption

A monolayer of particles or solutes can be deposited on the membrane surface when an attractive interaction between the membrane and solute or particles exists - this can take place even in the absence of MPF or under subcritical-flux conditions. Concentration polarisation can exacerbate the phenomenon if the degree of adsorption is concentration dependent. Adsorption is a rapid membrane fouling phenomenon that includes the formation of irreversible resistance and it takes place at the beginning of the operation. Its resistance can be of the same magnitude as the clean membrane resistance, [Bacchin *et al.*, 2006], [Research trends, 2002].

• Pore Blockage

Closure or partial closure of the membrane pores can also take place depending on the size of the particles, [Bacchin *et al.*, 2006].

• Deposition

Deposition of particles, growing layer by layer on the membrane surface, occurs leading to the formation of an additional resistance during filtration, [Bacchin *et al.*, 2006]. Large particles can be easily removed and the cake layer can be significantly diminished by increasing the shear over the membrane surface with the application of gas-liquid two-phase flow, [Hwang and Wu, 2008], which means that this kind of membrane fouling appears to be reversible. Bound EPS are also responsible for cake formations, [Nuengjamnong *et al.*, 2005].

• Gel formation

Gel formation appears to be a specific kind of deposit. A gel formation for specific macromolecules depends on the osmotic pressure values that can be reached and the level of concentration polarisation that can occur. It takes place when filtering macromolecules or colloids, [Wang and Waite, 2008], [Bacchin *et al.*, 2006], and occurs when the membrane undergoes a phase transition from a dispersed phase characterised by concentration polarisation to a condensed phase characterised by

multi-layer deposit, [Bacchin *et al.*, 2006]. Gel layers are considered to cause serious problems during filtration. First, it is believed that the gel layers are more resistant when being removed by shear forces as a result of their cross-linked structures. Then, regarding the gel layers, although they are of a porous structure, there is no connectivity among their pores. SMP, which are of colloidal nature, are mainly responsible for gel formations, [Wang and Waite, 2008].

Membrane fouling can be either irreversible or reversible as can be seen in Equation 2.39. Internal fouling caused by adsorption of dissolved matter into the membrane pores or by pore plugging is considered to be irreversible. Irreversible fouling can only be removed by chemical cleaning. Cake layer formation, on the other hand, is readily removable from the membranes when a physical practice like air scouring is applied, [Wu *et al.*, 2008], [Reid, 2005]. In the case of a gel layer, membrane fouling may be irreversible and only the application of a chemical regime can remove it, [Bacchin *et al.*, 2006].

2.3.3.3 Membrane fouling progressing for constant membrane flux operations

In constant-flux operations, membrane fouling is progressing through the following three stages, [Judd, 2007], [Le-Clech *et al.*, 2006], [Zhang *et al.*, 2006].

• Stage-1 membrane fouling: Initial short-term increase in TMP

First, gradual pore blocking by small particles, especially those of sizes equal to or bigger than the pore size, takes place. Also, attachment of large bioflocs on to the membrane surface happens in two stages, namely a reversible attachment of bioflocs followed by an irreversible attachment phase. This actually happens due to the EPS found around the cells, which help them stick on the surface. After a period of unstable attachment characterised by the ability of their frequent migration from the attachment site, the cells start being attached irreversibly. The imposed shear is usually able to provide an unstable environment that minimises irreversible membrane fouling but it cannot eliminate it completely. In addition, a conditioning film is being formed. Finally, an interaction between the feed and the membrane due to passive adsorption always exist so that the adhesion of EPS and other foulants can cause a

decline in the MPF value. Stage-1 membrane fouling, which can last a few hours, is characterised by adsorptive conditioning, transient biofloc interactions and pore partial blocking and closure.

- **Stage-2 membrane fouling: Long-term either linear or weakly exponential increase in TMP**

Membrane fouling is gradual and caused by products of bioactivity. The membrane surface is expected to be covered by SMP leading to an increased propensity of biomass particles and colloids to attach on the membrane surface. Also, further adsorption of material may take place leading to additional complete or partial pore blocking. As adsorption is progressing, it is possible to take place not only into the membrane pores but also on the whole surface, so biological flocs may initiate cake formation, but the membrane permeability has not been affected yet. However, the rate of EPS deposition is expected to increase when higher MPFs are applied, so the phenomenon will worsen. The high operating MPFs can then lead to significantly shorter, in terms of time, Stage-2 membrane fouling operations. Along with the fact that uneven distribution of air and liquid flow is expected within the MBR tanks, inhomogeneous membrane fouling appears.

- **Stage-3 membrane fouling: A sudden exponential TMP increase**

With regions or pores of membrane more fouled than others, MPF is expected to significantly decrease in these locations. Permeation has then to be removed to membrane areas less fouled, with local MPFs increasing, as less membrane area is now available. As local MPFs increase, they exceed the sustainable MPF value. The phenomenon is self-accelerating and soon membrane fouling is characterised by the appearance of an exponential increase in the TMP values, such that filtration cannot be maintained. This sudden rise in the TMP values can be a consequence of constant-flux operations, and is also known as the TMP jump or exponential membrane fouling.

2.3.3.4 Membrane fouling equation

For a constant-TMP cross flow filtration, the general equation that best describes the MPF decline over time due to membrane fouling is as follows, [Arnot *et al.*, 2000]:

$$\frac{dJ}{dt} = k_J (J - J_{SS}) J^{(2-n)} \quad \text{Equation 2.41}$$

where:

J_{SS}	=	Steady state or terminal MPF, m s^{-1}	m s^{-1}
k_J	=	Constant	variable units
n	=	Membrane fouling constant	unitless

Units of the k_J -value are subject to change depending on the n -value. The J_{SS} -value can be exact for moderate to long times but at early times, during which either complete or standard pore blocking may occur, it takes different values.

In addition, the n -value can only take fixed values depending on the fouling mechanism, which is occurring. These values are as follows:

n	=	2	Complete pore blocking
	=	1.5	Standard pore blocking
	=	1	Intermediate pore blocking
	=	0	Cake formation

Equation 2.41 can model all changes of the MPF due to membrane fouling formation.

2.3.4 Membrane fouling parameters and their interactions

2.3.4.1 General information

All the parameters involved in the design and operation of MBR processes can influence membrane fouling. Three major categories of factors affecting membrane

fouling are defined, namely membrane and module characteristics, feed and biomass parameters and MBR operating conditions, [Le-Clech *et al.*, 2006], [Zhang *et al.*, 2006], [Gander *et al.*, 2000].

Figure 2.8 summarises these parameters as a schematic.

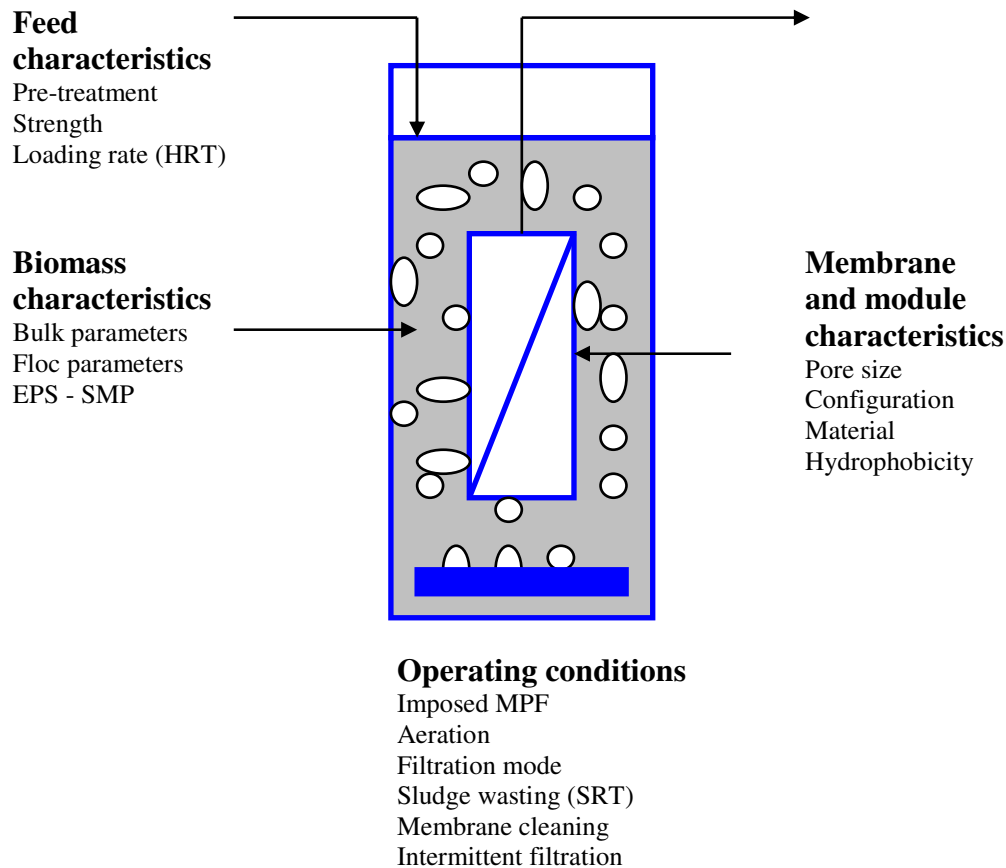


Figure 2.8 Factors affecting membrane fouling in submerged MBRs, [Le-Clech *et al.*, 2006]

While some of these factors affect membrane fouling directly, many others affect it indirectly through subsequent effects on phenomena, which may not be able to cause it, but do exacerbate it. For instance, large pore MF membranes present higher membrane fouling propensity compared to the UF membranes, as typical particle sizes are similar to the membrane pores size, so both pore blocking and their restriction are expected. Hydrophobic membranes suffer from more severe membrane fouling compared to the hydrophilic membranes due to the interactions occurring between the solutes, the microbial cells and the membrane material, [Le-Clech *et al.*, 2006].

Details about membrane fouling parameters that are more-related with this research are as follows:

2.3.4.2 MLSS concentrations and mixed-liquor temperatures

MLSS concentration is often considered to be the main foulant parameter, which has a complex interaction with membrane fouling issues, [Le-Clech *et al.*, 2006]. Assuming that all the other biomass characteristics are neglected, an increase in the MLSS concentration can have either a negative, [Chang and Kim, 2005], indicated as TMP increase or MPF decline, or positive, [Le-Clech *et al.*, 2003], or insignificant, [Hong *et al.*, 2002], effect on membrane permeability values, always depending on the range of the MLSS concentrations, which were applied during the experiments. Several research groups have tried to investigate the exact effect of the MLSS concentrations on membrane fouling, however, only controversial findings are at the moment available. In general, it can be said that there seems to be a range of MLSS concentrations consisting of values neither very low nor very high that can optimise the process in terms of membrane performance. [Rosenberger *et al.*, 2006], stated that for MLSS concentrations from 7 g L^{-1} to 14 g L^{-1} membrane fouling is not affected. In addition, any increase in the biomass concentration for MLSS concentrations below 6 g L^{-1} can have a positive effect on membrane performance, whereas any increase for MLSS concentrations above 15 g L^{-1} can have a negative effect on membrane performance, [Judd, 2007]. Finally, there seems to be a threshold of about 30 g L^{-1} above which MLSS concentrations have only negative effect on the performance of the membranes, [Judd, 2007].

It is also worth mentioning the effect of the mixed-liquor temperature on membrane fouling. Low mixed-liquor temperatures increase the MLSS viscosity. High MLSS viscosities reduce shear stresses, which are generated by the coarse bubble aeration, so that membrane scouring appears to be less effective. Less effective membrane scouring means that the membranes can become fouled more easily and more rapidly. However, there seems to be a critical MLSS concentration, between 10 g L^{-1} and 17 g L^{-1} , below which MLSS viscosity is not easily affected and remains low, [Judd, 2007].

2.3.4.3 MPF

In constant-flux operations, once membrane fouling phenomena appear, they usually self-accelerate and can eventually lead to a sharp increase in the TMP values. As membrane fouling rates may increase each time the MPF increases as well, it is more preferable for MBRs to be operated at modest MPFs, [Le-Clech *et al.*, 2006].

The initial imposed MPFs are then a crucial parameter in MBR operations. Low MPFs are followed by low treated water production rates but the increase in the TMP values is slow, leading to a long-term stability of the MBR performance before any chemical cleaning has to be applied. High imposed MPFs lead to severe membrane fouling very quickly and chemical cleaning has to be applied quite often increasing the operating cost of the operation, [Ndinisa *et al.*, 2006]. However, there is a value at which membrane fouling can become noticeable for a first time, hence the concept of critical flux is introduced - this is a convenient parameter regarding membrane fouling characterisation, [Bacchin *et al.*, 2006], [Le-Clech *et al.*, 2003].

The concept of critical-flux is widely applied to membrane operations suggesting that there is a MPF below which all species in the medium have a negligible interaction with the membrane, or no membrane fouling occurs, [Bacchin *et al.*, 2006]. MBR operation below the critical-flux can be anticipated when the TMP remains steady and does not increase with time. On the other hand, beyond this value, TMP values start to increase rapidly with time, [Pollice *et al.*, 2004]. For particles, the critical-flux can be the MPF below which no material deposits onto the membrane. For soluble species and fine colloids, it is the MPF below which the wall concentration is incapable of producing membrane fouling. For a mixed feed, the limiting critical-flux has to be defined, which is the critical-flux of the component of the lowest critical-flux, [Bacchin *et al.*, 2006], [Ndinisa *et al.*, 2006], [Cui *et al.*, 2003]. Critical-flux is a parameter strongly related to the start-up of the filtration process and is a parameter very much system specific, [Gander *et al.*, 2000].

The critical-flux at times can be very low and filtration under these circumstances can be impracticable, [Cui *et al.*, 2003], as well as filtration around the critical-flux, or even subcritical-fluxes, does not fully prevent the membrane from becoming fouled,

[Oigner *et al.*, 2004], [Schoeberl *et al.*, 2004], [Cho and Fane, 2002]. This impracticability of the critical-flux has then led to what is now considered to be a sustainable MPF. Sustainable MPFs are clearly defined MPFs, which, when applicable, it is true that some membrane fouling takes place - little or negligible increase in TMP values is recorded - but filtration only needs infrequent membrane cleaning in order to be maintained. These MPFs are then able to ensure long-term (several weeks or months) operational and economic sustainability of the process with only moderate remedial measures such as the application of intermittent filtration without any backflushing, or no remedial measures at all, [Judd, 2007], [Bacchin *et al.*, 2006], [Cui *et al.*, 2003]. As distinct membrane fouling is formed, these MPFs can no longer be defined as critical.

2.3.4.4 Aeration

Since the origin of submerged MBRs, gas bubbling has been indicated as a major strategy to introduce flow circulation and shear stress over the membrane surface, [Meng *et al.*, 2008]. Aeration used in submerged MBR system has three major roles: to provide oxygen to biomass, to maintain the AS in suspension and to mitigate membrane fouling by constant scouring of the membrane surface, [Nywening and Zhou, 2009], [PURATREAT project: Deliverable 3, 2007], [Le-Clech *et al.*, 2006]. The bubbles flowing near the membrane surface are able to introduce local shear transients and liquid flow fluctuations increasing at the same time the strength of the back transport phenomena, which are responsible for controlling membrane fouling, as well as strengthening the tangential shear forces at the membrane surface, which prohibit large particle deposition, [Le-Clech *et al.*, 2006]. However, in MF systems, the MPF decline relating to membrane fouling cannot often be fully recovered by gas sparging. This is due to the internal pore fouling, which cannot be reversed by the application of shear forces over the membrane surface, [Cui *et al.*, 2003]. This actually means that the introduction of aeration can successfully combat reversible membrane fouling like reversible cake formation on the membrane surface, but it cannot fight all the different types of membrane fouling.

Aeration takes place either by introducing air or pure oxygen into the waste water with submerged diffusers either with the installation of a diffused-air system, or by

agitating waste water mechanically so as to promote solution of air from the atmosphere into waste water, [Tchobanoglous *et al.*, 2004]. In this research, all air systems used for membrane scouring were based on the diffused-air method. Diffused-air systems, apart from the submerged diffusers, also consist of pipes, the air blowers and distributors through which the air passes. Diffusers are closely connected with the efficiency of oxygen transfer, which depends on the type of the diffusers, their size and shape, their depth of submersion and their location inside the bioreactor tanks. Diffusers can be classified as either fine or coarse bubble diffusers, with the fine ones being more efficient for oxygen transfer but the demarcation between these two categories is not clear. Finally, regarding the air blowers, they must be able to supply a wide range of air flow rates, [Tchobanoglous *et al.*, 2004].

The phenomenon that takes place within the submerged MBRs equipped with diffused-air systems is known as gas-liquid two-phase flow. Gas bubbles introduced as a second phase in a liquid volume can effectively control both concentration polarisation and subsequent membrane fouling without damaging the membranes, [Ndinisa *et al.*, 2006], [Cui *et al.*, 2003]. In submerged MBRs, the most likely gas-liquid two-phase flow patterns that occur are bubble flow and slug flow, as the air flows applied are relatively low. Bubble flow occurs when the bubble diameter is significantly smaller than the channel size, whereas slug flow occurs when flow consists of large bullet-shaped bubbles, known as Taylor bubbles, with sizes of about 60 % of the diameter of the channel width, [Cui *et al.*, 2003]. Submerged MBRs equipped with FS membranes, like FS KUBOTA membranes, are operated under slug flow conditions, which appear to be the most effective regime with respect to membrane fouling. In slug flow, large slugs alternate with liquid plugs, which may contain small dispersed bubbles, so that regions characterised by high shear stress values capable of combating membrane fouling are formed, [Ndinisa *et al.*, 2006]. In KUBOTA MBRs, membrane panels are usually located 1 m above the available coarse diffusers, as large bubbles via coalescence are able to be formed. Even though large bubbles may be more preferable than small bubbles, there seems to be an optimum large bubble size, [Ndinisa *et al.*, 2006].

As aeration can combat probable membrane fouling, some additional information about how it can be more efficient is provided. It has been found that the cake layer

removal efficiency of aeration does not increase proportionally with an increase in air flow rate, hence there seems to be an optimum air flow, beyond which any further increase in the air flow rate values appears to have very little improvement with respect to membrane fouling amelioration, [Meng *et al.*, 2007], [Ndinisa *et al.*, 2006], [Howell *et al.*, 2004].

[Liu *et al.*, 2003], and [Liu *et al.*, 2000], reported that for submerged HF membranes, cross flow velocities and air flow rates are related, and any increase in aeration flow rate automatically increases the liquid cross flow velocity, but the rate of this increase gradually decreases. Even though an air flow rate corresponds to a specific air flow rate, the cross flow velocity is a parameter system specific, which means for the same air flow rate different cross flow velocities can be attained depending on the different dimensional parameters of each MBR, [Liu *et al.*, 2000]. In the same work, it is also mentioned that, for a given MLSS concentration, a critical curve between the MPFs and the cross flow velocities exists. A few years later, in 2004, it was reported that submerged FS membranes are characterised by the same critical curves, [Howell *et al.*, 2004].

According to these critical curves, each critical cross flow velocity, or critical aeration flow rate, corresponds to a critical-flux value. So, for a critical set of data provided by the critical curve, aeration intensity must be higher than the critical aeration intensity or MPF must be lower than the critical-flux, or otherwise a cake layer starts rapidly being formed. An illustrative critical curve is shown in Figure 2.9.

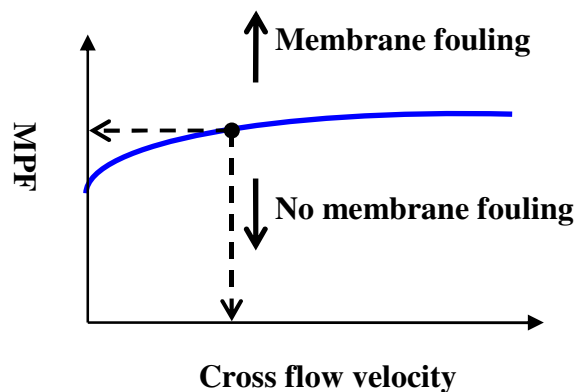


Figure 2.9 Illustrative critical curve, [Howell *et al.*, 2004], [Liu *et al.*, 2000]

In general, attention must be paid when choosing an aeration intensity value. Both high and low air flow rates can have a negative effect on membrane permeability values as in both cases membrane permeability values rapidly decline. Low air flow rates cannot remove the cake layers from the membrane surface effectively. High air flow rates, on the other hand, can significantly affect the biomass characteristics, as the microbial flocs may break due to the high shear forces, so the small-sized particles generated by this breakage can cause membrane fouling. In addition, this breakage of the bioflocs also results in the release of bound EPS, colloids and soluble components into the bulk solution leading to a rapid decrease in membrane permeability as well, [Wang *et al.*, 2009], [Meng *et al.*, 2007], [Durante *et al.*, 2006], [Van-Kaam *et al.*, 2006]. Also, too high air flow rates cannot have any significant effect on further cake diminution.

2.3.4.5 Sludge wasting (SRTs)

SRTs can affect both the state of biomass and the MLSS concentration. MBRs are usually operated at long SRTs, as the subsequent increase in MLSS concentrations is able to produce effluent of exceptional quality. However, the WWT efficiency is not linearly proportional with the MLSS concentrations, along with the fact that higher MLSS concentrations can accelerate membrane fouling, [Han *et al.*, 2005]. As SRTs can affect the physiological state of the microorganisms, membrane fouling can also be affected, as changes of the EPS and SMP concentrations occur at the same time, [Ahmed *et al.*, 2007].

2.3.4.6 Application of cleaning

Membrane cleaning can be either physical or chemical. Physical cleaning can occur either by back-flushing, which means reversal of the permeate flow for a short period of time, or membrane relaxation, during which permeation is ceased while the membrane is still being scoured by air bubbles. Chemical cleaning is performed with mineral or organic acids, caustic soda or more often with sodium hypochlorite (NaOCl), [Judd, 2007], [Gander *et al.*, 2000].

Physical cleaning is generally more rapid and demands no chemicals, so it produces no chemical waste and causes no membrane degradation, but it is less effective than chemical cleanings. Physical cleaning can remove only the solids attached to the membrane surface, so it can only cope with reversible membrane fouling. On the other hand, chemical cleaning can additionally remove more tenacious material in the residual membrane fouling range, [Judd, 2007], [Gander *et al.*, 2000].

2.3.4.6 Intermittent filtration

Intermittent filtration is a membrane cleaning technique where filtration is suspended periodically. This technique allows long-term sustainability even when a plant is operated above the critical-flux value and it is quite useful in case an MBR has to be operated with variable throughput, [Chua *et al.*, 2002]. Intermittent filtration takes place when a filtration time period is followed by a time period of membrane relaxation. Membrane fouling can be ameliorated through this technique, as deposited particles on the membrane surface can be removed when there is no filtration but there still is gas sparging, [Ndinisa *et al.*, 2006]. In addition, the longer the suspension time is, the more efficient the aeration can be with respect to membrane fouling removal, [Chua *et al.*, 2002]. Intermittent filtration can ameliorate membrane fouling problems, but it cannot eliminate them, as it cannot remove all foulants from the membrane surface but only a portion of them.

Finally, intermittent filtration has been reported as a mechanism so as the destruction of bioflocs, and all the subsequent problems, are able to be avoided, [Van-Kaam *et al.*, 2006], [Lee *et al.*, 2003].

2.4 MBR energy consumption

2.4.1 General information on MBR energy consumption

Energy consumption is a critical factor in the WWT sector, which can sometimes affect the viability of the method applied. Regarding MBRs, side stream configurations require much more energy, up to 10 kWh m⁻³, [Le-Clech *et al.*, 2006], than the conventional AS processes, and that was initially one of the main disadvantages of the

MBRs that prohibited their widely-spread application. The advent of submerged MBRs succeeded in reducing these high energy costs and today, their energy consumption rates are quite competitive with those of the traditional WWT processes, [Guglielmi *et al.*, 2007], [Industry focus, 2005].

Power requirements for side stream MBRs come from pumping waste water, recycling the retentate back into the MBR tank and aeration for the maintenance of biomass. In submerged MBRs, the energy requirements come from pumping waste water, the permeate suction, if applicable, and finally aeration for both biomass maintenance and membrane scouring. There are also two additional activities that consume remarkable amounts of energy when they take place, namely the treatment of the off-gas produced during the aerobic biological oxidation of substrates and the waste sludge disposal, [Arnot, 2004]. As these two activities are mainly connected with the treatment of by-products, they usually are not taken into account, when energy consumption rates are calculated.

Side stream configurations require more energy to operate than the submerged MBRs, as large amounts of energy are required to generate the sludge velocity across their membrane modules, and to maintain both the high cross flow velocity and the required TMP for filtration, [Stephenson *et al.*, 2002], [Van-Der-Roest *et al.*, 2002], [Gander *et al.*, 2000]. Energy consumption rates are between 2 kWh m⁻³ and 10 kWh m⁻³ for side stream MBRs and between 0.2 kWh m⁻³ and 0.4 kWh m⁻³ for submerged configurations, [Stephenson *et al.*, 2002]. In submerged MBRs, aeration is the major energy cost at percentages between 80 % and even 100 %, whereas, in side stream MBRs, it accounts only for 20 % to 50 % of the total energy cost. Submerged MBRs have no associated energy costs with respect to permeate collection unless permeate suction is applied, in such cases permeate suction accounts for up to 28 % of the total energy costs. In side stream MBRs, on the other hand, the highest energy cost comes from the use of the re-circulation pump at percentages between 60 % and 80 % of the total energy cost, [Stephenson *et al.*, 2002], [Gander *et al.*, 2000].

[Zang *et al.*, 2003], reported that the energy consumed by MBRs, in general, without providing any information about the MBR configurations, is normally between 6 kWh

m^{-3} and 8 kWh m^{-3} . Also, the energy consumed by traditional WWT methods is between 0.3 kWh m^{-3} and 0.4 kWh m^{-3} .

[Howell *et al.*, 2004], mentioned that energy consumption for submerged MBR systems is between 0.2 kWh m^{-3} and 0.4 kWh m^{-3} , indicating that more than 80 % is consumed for aeration.

[Schroebel *et al.*, 2005], reported that energy consumption rates for submerged MBRs are between 0.2 kWh m^{-3} and 2.4 kWh m^{-3} , with aeration consuming more than 80 % of the total energy.

[Liao *et al.*, 2006], reported slightly higher energy consumption rates for both side stream and submerged MBRs. It was mentioned that electricity required for municipal WWT is between 0.2 kWh m^{-3} and 0.4 kWh m^{-3} for conventional AS processes, whereas it is between 0.3 kWh m^{-3} and 0.6 kWh m^{-3} for submerged MBRs. The electricity that was consumed was only for the operation of the AS bioreactor and the secondary clarifier in the case of the conventional AS process, and only for the operation of the AS bioreactor and the membrane module in the case of the submerged MBR. It was also reported that energy requirements for side stream MBRs are between 4 kWh m^{-3} and 12 kWh m^{-3} . Finally, regarding anaerobic MBRs, the energy for filtration is between 0.25 kWh m^{-3} and 1 kWh m^{-3} for submerged configurations and between 3 kWh m^{-3} and 7.3 kWh m^{-3} for side stream MBRs.

[Ndinisa *et al.*, 2006], reported that in submerged MBRs energy consumption rates are equal to or lower than 1 kWh m^{-3} and more than 50 % of total energy is used for aeration.

2.4.2 Theoretical power requirements for the air compressors used in MBR operations - Specific aeration energy demand

The required increase in air pressure for aeration is provided by means of air compressors by applying shaft work on them. Their theoretical power requirements are as follows:

The power requirement for an air compressor for adiabatic compression is given by Equation 2.42, [Tchobanoglous et al, 2004].

$$P_w = \frac{wRT_1}{29.7n_{air}e} \left[\left(\frac{p_2}{p_1} \right)^{n_{air}} - 1 \right] \quad \text{Equation 2.42}$$

where:

P_w	=	Power requirement for the air blower	kW
w	=	Weight of flow of air	kg s ⁻¹
R	=	Engineering gas constant for air	8.314 kJ kmol ⁻¹ K
T_1	=	Absolute inlet temperature	K
p_1	=	Absolute inlet pressure	atm
p_2	=	Absolute outlet pressure	atm
n_{air}	=	Constant for air equal to 0.283	unitless
e	=	Efficiency of the air compressor	unitless

The power consumption appears to be a function of the absolute outlet pressure, which means that it is a function of the hydrostatic head provided by the depth at which the aerator is placed in the bioreactor tank.

By dividing the P_w -value with the membrane area, the specific aeration power demand per unit membrane area, $W_{b,m}$, is obtained, [Judd, 2007].

$$W_{b,m} = \frac{P_w}{A_m} \quad \text{Equation 2.43}$$

where:

$W_{b,m}$	=	Specific aeration power demand per unit membrane area	kW m ⁻²
A_m	=	Total membrane area	m ²

Finally, by dividing the P_w -value with the permeate flow rate, the specific aeration energy demand per unit permeate volume, $W_{b,v}$, is obtained, [Judd, 2007].

$$W_{b,v} = \frac{P_w}{Q_p} \quad \text{Equation 2.44}$$

where:

$W_{b,v}$ = Specific aeration energy demand per unit permeate volume kWh m⁻³

In general, by substituting the P_w -value as mentioned in Equation 2.44, with the overall power consumed by a pilot MBR plant as recorded during the operation of the MBR system, the overall specific energy demand per unit permeate volume, or simply referred to as SED, can be defined and estimated. More details about this parameter will be given in Chapter 7.

2.4.3 MBR energy demand case studies

Several researchers operated MBRs and, at the same time, they attempted to measure the energy, which was consumed by their systems. Details are as follows:

- [Côté *et al.*, 1997], operated two submerged HF MBR pilots based on ZENON membranes. Filtration, in both cases, was intermittent including back-flushing. The operating conditions of the MBRs systems are shown in Table 2.3.

Table 2.3 MBR energy demand: Case study of [Côté *et al.*, 1997]: Operating conditions

Parameters	Values		Units
	MBR1	MBR2	
MPF	35	25	L m ⁻² h ⁻¹
TMP	20	20	kPa
Air flow rate	12	8	m ³ h ⁻¹
MLSS concentration	5 - 15	5 - 15	g L ⁻¹

In both cases, the energy required for filtration was found to be 0.3 kWh m^{-3} . Of this energy, 0.02 kWh m^{-3} was consumed so as permeate was collected and 0.28 kWh m^{-3} was consumed by the air blowers.

- [Ueda and Hata, 1999], tested a gravity-driven submerged pilot MBR system based on KUBOTA membranes. The operating conditions of the MBR system are given in Table 2.4.

Table 2.4 MBR energy demand: Case study of [Ueda and Hata, 1999]: Operating conditions

Parameters	Values	Units
Average flow rate	0.47	m d^{-1}
Final TMP	15	kPa
Air flow rate	0.3	$\text{m}^3 \text{ min}^{-1}$
MLSS concentration	12.93	g L^{-1}

Based on these operating conditions, it was concluded that the average energy consumption was equal to 2.4 kWh m^{-3} .

- [Zang *et al.*, 2003], operated a low energy side stream MBR using HF membranes. The operating conditions of this MBR system are summarised in Table 2.5.

Table 2.5 MBR energy demand: Case study of [Zang *et al.*, 2003]: Operating conditions

Parameters	Pilot study	Units
Feed flow rate	10	$\text{m}^3 \text{ h}^{-1}$
Maximum TMP	1	bar
MLSS concentration	4.5 - 6	g L^{-1}

This MBR consumed approximately 2 kWh m^{-3} provided that one backflush with clean water and another one backflush with permeate were performed every day. The membrane module was responsible for consuming approximately up to 52 % of the

total energy consumed, whereas the energy consumption for aeration accounted for approximately up to 31 %.

- [Schroebel *et al.*, 2005], operated a submerged MBR using tubular (T) membranes under the operating conditions shown in Table 2.6.

Table 2.6 MBR energy demand: Case study of [Schroebel *et al.*, 2005]: Operating conditions

Parameters	Pilot study	Units
MPF	5	L m ⁻² h ⁻¹
TMP	0.2 - 0.4	bar
Aeration intensity	0.3 - 0.9	m h ⁻¹
MLSS concentration	4	g L ⁻¹

Energy requirements for both aeration and the application of suction were between 0.6 kWh m⁻³ and 2.47 kWh m⁻³ depending on the application of different combinations of suction times, backflush times and aeration intensities. Most of the energy demand was attributed to membrane aeration, whereas energy requirements for suction accounted for less than 3 % of the total energy.

- [Fan *et al.*, 2006], tested an external MBR under the operating conditions mentioned in Table 2.7.

Table 2.7 MBR energy demand: Case study of [Fan *et al.*, 2006]: Operating conditions

Parameters	Pilot study	Units
MPF	6 - 13.5	L m ⁻² h ⁻¹
TMP	2 - 9	kPa
Air flow rate	8 - 10	m ³ h ⁻¹
MLSS concentration	Bioreactor	7.3
	Membrane tank	7.71
		g L ⁻¹

Energy was consumed by the air compressor, a raw waste water pump and a permeate suction pump with the air compressor consuming most of this energy at about 85 % to 94 % of the total. MPF was initially set to $6 \text{ L m}^{-2} \text{ h}^{-1}$ with an energy consumption rate equal to 0.64 kWh m^{-3} . Then, the MPF increased, step by step, up to $13.5 \text{ L m}^{-2} \text{ h}^{-1}$ and remained stable at this value for more than five months. During that period of time, the energy consumption was reduced to 0.32 kWh m^{-3} , however, the higher MPF was subject to subsequent membrane fouling.

Having described the main issues affecting the performance of MBR systems in this literature review, and bearing in mind the objectives of the research project given in Chapter 1, the next chapter describes the materials and methods necessary to carry out the programme of work.

CHAPTER 3 MATERIALS AND METHODS

3.1 PURATREAT project technologies

The membrane bioreactor (MBR) technologies that were applied both in the PURATREAT project and in this work are described in this section.

3.1.1 MBR1: EWT and COPA MBR technology/KUBOTA membranes

3.1.1.1 Introduction

COPA is a multi-disciplinary company offering a comprehensive product range of waste water treatment (WWT) technologies and processes, together with storm water management solutions for attenuation, flow control and overflow treatment, [www.copa.ac.uk, 2010]. In a deal with KUBOTA Corporation of Tokyo, Japan, COPA acquired full rights to the KUBOTA MBR process, [Industrial News, 2004]. Today, COPA is owned by Eimco Water Technologies (EWT). EWT is the water treatment group of GVL Inc., which is a global provider of solutions in water treatment and pulp and paper production and it specialises in the design, build, operation and maintenance of solutions for the treatment and recycling both of municipal and industrial waste water, [www.copa.ac.uk, 2010], [www.eimcowatertechnologies.com, 2010].

COPA MBR technology is a membrane-based process, which produces a discharge permeate that can be re-used for toilet cisterns, wash-down, irrigation and more other applications, [www.copa.ac.uk, 2010]. The aerobic COPA MBR that is capable of treating all types of waste water for discharge and re-use applications is applicable for any population equivalent (PE) upwards of 50, and it employs simple flat sheet (FS) membrane panels, namely KUBOTA membranes, housed in stainless steel units and aerated by a coarse bubble system. It can treat a wide range of effluents. The system can successfully operate under mixed-liquor suspended solids (MLSS) concentrations in the order of 12 - 18 g L⁻¹, and as high as 20 g L⁻¹, [www.kubota-mbr.com, 2010], or even 22 g L⁻¹, [www.copa.ac.uk, 2010], producing treated water of high quality 5-day

biochemical oxygen demand (BOD₅) concentration in the effluent equal to or less than 5 mg L⁻¹, [www.copa.ac.uk, 2010]. In this research, MBR1 was built as a modification of the COPA MBR technology. Details about the membranes of this MBR system are given in Section 3.1.1.2.

3.1.1.2 KUBOTA membranes

In 1989, the Japanese Government decided to charge many of the country's corporations, including KUBOTA Corporation Environmental Plant Division, to invest both time and money in new WWT technologies that would have low footprint requirements and would produce high quality, final effluent with re-use capability. The KUBOTA submerged membrane process arose from this initiative, [Churchouse, 1997], [Churchouse and Wildgoose, 1999]. The first KUBOTA pilot plant became operational in 1989, [Churchouse, 1997], with the first commercial installation being commissioned in 1991, [Churchouse, 1997], [Kennedy and Churchouse, 2005]. It is worth noting that up to 2005 there were over 1,200 KUBOTA systems worldwide out of which 120 operating in Europe. In Europe, the first full-scale submerged MBR plant treating municipal waste water was commissioned by Wessex Water, [www.wessexwater.co.uk, 2010], in Porlock in the United Kingdom in February 1993. This plant can treat a maximum feed flow of 1,907 m³ d⁻¹ (3,800 PE), [Lesjean and Huisjes, 2007], [Kennedy and Churchouse, 2005], and it contains twenty-four KUBOTA membrane modules, with a total of 3,600 membrane panels in the plant, [Kennedy and Churchouse, 2005]. More details about KUBOTA installations are available in Table 3.1.

Table 3.1 KUBOTA MBR plants worldwide from 1993 until 2005, [Kennedy and Churchouse, 2005]

Year	Number of plants	Largest plant feed flow rate (m³ d⁻¹)
1993	4	125
1995	20	250
1997	70	800
1999	237	7,100
2002	850	12,880
2005	1200	78,000

Regarding the membrane itself, full sized KUBOTA membrane panels are fabricated from an injection moulded plastic flat plate with an ultrasonically welded chlorinated polyethylene membrane attached to each side. Each membrane panel, as shown in Figure 3.1, is double-sided, 6 mm thick, 0.4 m wide and 1 m long, with a working membrane surface of 0.8 m² and a nominal pore size of 0.4 µm. During filtration, the effective pore size is reduced due to the build-up of a bio-layer so that this effective pore size is no longer in the microfiltration (MF) range. This effective working pore size is in the ultrafiltration (UF) range, and has been estimated at about 0.01 µm, [Reid, 2005].



Figure 3.1 Standard KUBOTA membrane panels

When the membrane panels are placed into housings, a gap of approximately 7 mm is left between them so that abrasion between the panels is avoided. This space between the membrane panels is a critical factor for plants operating with FS membranes. If it is reduced, the packing density of the MBR unit or the membrane surface per land required for the installation of the plant is increased but the risk of sludge clogging between the panels is increased. On the other hand, if this spacing is increased, the risk of clogging among the panels can be avoided but a lower packing density value is achieved, [Churchouse, 1997], [Kennedy and Churchouse, 2005].

KUBOTA membrane plants are low pressure systems, the flow through the panels is of an outside-in mode and permeate is collected through a manifold either by a low pressure suction pump, or by gravity if sufficient hydraulic head exists, ideally 1 - 1.5 m of waste water. Also, in KUBOTA membrane systems, waste water is usually de-gritted and screened to 3 mm before it is pumped into the MBR. The likelihood of debris becoming stuck between the membrane panels is therefore reduced, [Churchouse, 1997], [Kennedy and Churchouse, 2005].

With regard to membrane scouring, coarse bubble aeration is used, as it meets three process requirements, which are as follows:

- It provides mixing to prevent settling of the MLSS.
- It provides air to maintain the biomass in the membrane tank.
- It creates cross flow conditions at the surface of the membrane to limit membrane fouling and reduce the frequency of cleaning.

Permeate production without coarse bubble aeration rapidly leads to detrimental membrane fouling, [PURATREAT project: Deliverable 5, 2007]. To successfully combat membrane fouling, each KUBOTA membrane panel is operated with about 10 L min⁻¹ of aeration, [Arnot, 2006-2009], [Kennedy and Churchouse, 2005].

KUBOTA Membranes Europe officially propose the use of NaOCl in order to remove irreversible membrane fouling caused by organic matter and the use of citric acid when it comes to inorganic material, [Personal communication with KUBOTA Membranes Europe, 2009].

A KUBOTA MBR was selected for the trials in Tunisia as being the most commonly used MBR system in the world, [Arnot, 2006-2009].

3.1.2 MBR2: Weise Water Systems, GmbH and Co, KG/MicroClear filters

3.1.2.1 Introduction

Weise Water Systems was founded in 2001 and is responsible for the development of the patented MicroClear filter. This filter has already been tested in various applications and it has already been installed in more than 1,000 systems around the world, [www.weise-water-systems.com, 2010]. Finally, since 2003, Weise Water has also started to develop a small membrane-based sewage treatment plant for decentralised waste water systems. In this work, MBR2 was equipped with MicroClear filters. Details of these filters are as follows:

3.1.2.2 MicroClear filters/The MC03 module

This filter is used in both private and public WWT plants, for water supply improvements, for industrial purposes, and also for producing drinking water from rain water or river water in disaster areas. Treated water quality, according to Weise Water, has a 5-day biochemical oxygen demand (BOD₅) concentration in the effluent equal to or less than 5 mg L⁻¹, or a chemical oxygen demand (COD) concentration in the effluent equal to or less than 50 mg L⁻¹. The filters are back-washable and it can be arranged in a double-decker structure. They can be used in small treatment works for 4 to 50 residents or larger plants for up to 100,000 people, being configured in units up to 525 m² each. The modules are based on robust plastic plates covered on both sides with an ultrafiltration (UF) membrane with a cut-off of 150 kDa.

In this work, the module used was the MC03, which is particularly pre-designed for small scale system applications. Its dimensions are: 207 mm long x 207 mm wide x 492 mm high. It consists of twenty-four active membranes made of polyether sulfone, placed between two protective pockets. The plate spacing is equal to 5.5 mm and the overall filter area is equal to 3.5 m². Figure 3.2 shows the MC03 module.

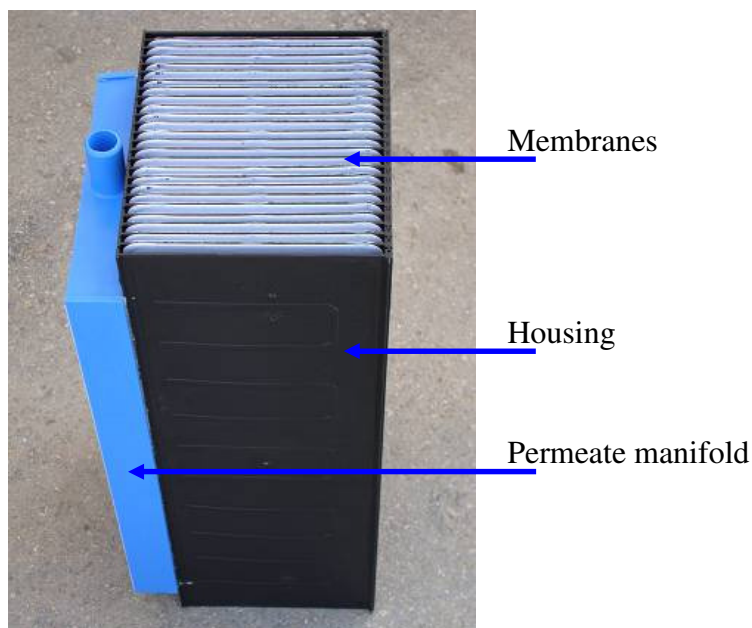


Figure 3.2 Weise Water Systems MC03 module

In terms of filtration, waste water flows from external sources through the membrane into the permeate manifold before being drawn through a treated water collector by the application of low suction pressures - the mode of filtration is intermittent. MicroClear filters, in general, are offered with their own housing and they are ready to be placed into the MBR tanks. These filters are combined with fine bubble air diffusers located underneath the membrane modules. Occasionally, they need chemical cleaning but, according to Weise Water, the application of the fine bubble aeration can limit these chemical cleanings to one or two over a year even though real membrane permeate fluxes (MPFs) up to $30 \text{ L m}^{-2} \text{ h}^{-1}$ have been applied. The MC03 module as a whole needs $6,000 \text{ L h}^{-1}$ of air with respect to membrane scouring, or otherwise permeate collection will lead to membrane fouling, and can be operated at MLSS concentrations between $6 - 12 \text{ g L}^{-1}$, [PURATREAT project, Deliverable 3, 2007], [Weise Water Systems: Main brochure, 2009], [Weise Water Systems: Product catalogue, 2009].

The Weise Water MBR was selected for this research as being new on the market and having been designed for decentralised WWT plants.

3.1.3 Martin Systems AG/siClaro filters

3.1.3.1 Introduction

Martin Systems AG has specialised for more than 10 years in the field of municipal and industrial WWT, with more than 1,000 applications around the world. Martin Systems are producing both membrane filters through their siClaro series and biological sewage treatment plants through the BMA series, [www.siclaro.ch, 2010]. MBR systems based on these filters are designed to treat only domestic sewage water, [www.siclaro.ch, 2010], [Martin Systems: Instructions for installation and operation of PURATREAT siClaro sewage treatment plant, 2008]. The siClaro filters are now described.

3.1.3.2 siClaro filters/The 611 module

The siClaro filters have a modular structure. They comprise synthetic, polymer flat sheet membrane plates, which are permanently connected to form a module with a central filtrate extraction device. The membranes operate in the ultrafiltration (UF) range, with pore sizes of less than 0.1 μm , so all substances whose particle diameters are bigger than this size including even the smallest microorganisms are excluded. Each module has a total filter area of 6.25 m^2 . The distance between the membrane plates is 6 mm. These membrane filters are operated at MLSS concentrations in the range of 3 g L^{-1} to 14 g L^{-1} , however, the optimum concentration is approximately at 10 g L^{-1} , [Martin Systems: Instructions for installation and operation of PURATREAT siClaro sewage treatment plant, 2008]. Figure 3.3 provides a photograph of the 611 module, which was used in this work.

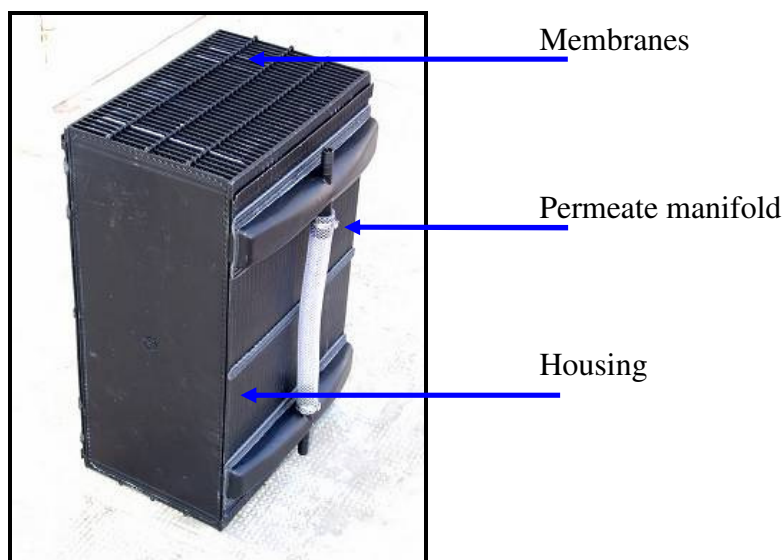


Figure 3.3 Martin Systems siClaro 611 module

Filtration is intermittent and high pressures may require longer relaxation time periods to be applied in order to control membrane fouling adequately. In general, pressures lower than 0.1 bar are defined as low pressures in these units. Sudden increases or sharp variations in the pressure differentials should also be avoided, [Martin Systems: Instructions for installation and operation of PURATREAT siClaro sewage treatment plant, 2008].

Aeration is provided at the base of the membrane module via a diffuser supplied with air from an air compressor. The default aeration rate for an effective membrane scouring is equal to $7,000 \text{ L h}^{-1}$. Chemical cleaning is also possible with these membranes and it has to be applied each time the transmembrane pressure (TMP) increase seems to be out of control. High pressure differentials have to be avoided, as they can result in membrane fouling layers growing fast on the membranes, which can inhibit filtration and more membrane cleanings may need to be applied.

Finally, during the start-up period, namely the first forty-eight hours, filtration should be limited to a maximum real membrane permeate flux (MPF) of $15 \text{ L m}^{-2} \text{ h}^{-1}$ and a transmembrane pressure (TMP) value of 0.04 bar. In these filters, optimum operating conditions are at low TMP values with satisfactory real MPFs, [Martin Systems:

Instructions for installation and operation of PURATREAT siClaro sewage treatment plant, 2008].

3.1.3.3 Membranes: Summary

Table 3.2 summarises all the technical details of the membranes, which were used for this work.

Table 3.2 Membrane characteristics, [www.weise-water-systems.com, 2010], [www.siclaro.ch, 2010], [PURATREAT Project, Deliverable 3, 2007]

Characteristics	Kubota membranes	MicroClear MC03 module	siClaro 611 module	Unit
Area per membrane or module	0.8	3.5	6.25	m ²
Number of membranes or modules	7	2	1	–
Total membrane area	5.6	7	6.25	m ²
Membrane spacing	7	5.5	6	mm
Pore size	0.4	0.05	< 0.1	µm
Material	Chlorinated polyethylene	Polyether sulfone	Polyether sulfone	–
Back-flushing	No	Yes	Yes	–
MPF relaxation	Manual	Automatic	Automatic	–
Typical MPFs	5 - 25	15 - 30	20 - 40	L m ⁻² h ⁻¹
Operating TMP values	<0.1	0.1 - 0.15	0.1	bar
RO clean water membrane permeability at 25 °C	1,110	800	700	L m ⁻² h ⁻¹ bar ⁻¹
MLSS concentration	12 - 18	6 - 12	3 - 14	g L ⁻¹
Aeration mode	Coarse bubbles	Fine bubbles	Fine bubbles	–
Aeration intensity in this research	750	1,715	1,120	L m ⁻² h ⁻¹

3.2 Description of the MBR systems

This research investigated the trial of an MBR pilot plant of the three different MBR systems. As already mentioned, the pilot plant was located in Sfax in Tunisia at North Sfax “Office National de l' Assainissement” (ONAS) site, treating local municipal waste water. Details about the three MBR systems are as follows:

3.2.1 The MBR1 system

Membrane bioreactor 1 (MBR1) was based on the use of standard KUBOTA membrane panels. Raw waste water was de-gritted and screened to 3 mm, before entering the MBR system, [Churchouse, 1997], [Kennedy and Churchouse, 2005].

MBR1, as supplied by the manufacturer, consisted of a feed screening/anoxic (FS/AN) tank, an MBR tank, all the required devices, fittings, pipes, valves, etc., and a control panel for the regulation of the operation. A photograph of the MBR1 system is shown in Figure 3.4.



Figure 3.4 The MBR1 system

- **FS/AN tank**

The FS/AN tank, as seen in Figure 3.4, is a polycarbonate plastic tank whose dimensions are 1 m long \times 1 m wide \times 1 m high leading to a total tank volume of 1 m³. This plastic tank is placed in a frame made of stainless steel to protect it against damage. It is divided in the middle in two halves, the waste water inlet side and the outlet side, by a 3 mm perforated sheet made of hard polycarbonate. This plastic sheet acts as a screen for the waste water and is held in place by an angle frame fabrication. Finally, this tank has also a drain valve located at the bottom for the periodical removal of the screenings, if required.

The outlet part of the tank usually houses a feed pump, simply called Feed Pump 1, which delivers waste water from FS/AN tank into the MBR tank. As the feed of all

three different MBR systems had to be screened before filtration, it was decided the screen provided by the FS/AN tank should be used by all three MBRs. So, the MBR2 feed pump or Feed Pump 2 and the MBR3 feed pump or Feed Pump 3 were also placed in the outlet part of the FS/AN tank.

- **MBR tank**

The MBR tank, as seen in Figure 3.4, which acts both as a biological treatment tank and also houses the membrane panels, is a cylindrical tank, which is 3 m high and 0.85 m in diameter. It comprises two vessels made of stainless steel, which adjoin with the aid of a rubber gasket, which is 5 mm thick. This tank has two outlets that control the mixed-liquor level, as well as a drain valve located at the bottom for periodical sludge wasting. In this research, a modified version of the COPA technology was used. Seven standard KUBOTA membranes were placed in a case made of stainless steel, which was then fixed within the lower vessel of the MBR tank so as any movement of the case was not possible.

Air was provided through a coarse bubble aeration line. This aeration line consisted of an air compressor, a tube diffuser, an air flowmeter for the air flow rate monitoring, all the required piping and a valve, which throttled the air back to the air compressor and was used to regulate the air flow rate value. A range of air flow rates was then able to be achieved starting from zero when the valve was fully closed, to about $5 \text{ m}^3 \text{ h}^{-1}$ when the valve was fully open. During the long-term experiment of this research, an air flow rate equal to $4.2 \text{ m}^3 \text{ h}^{-1}$ was applied - a value proposed by the membrane supplier.

The tube diffuser, shown in Figure 3.5, comprised six holes, evenly spaced and of 6 mm in diameter each, was located precisely underneath the membrane panels. The distance between the diffuser and the bottom of the tank was 6 cm and the distance between the diffuser and the bottom end of membranes was 20 cm.



Figure 3.5 MBR1: Air diffuser

Permeate came out from the membrane panels in an outside-in mode and was collected through a common manifold and a permeate line shown in Figure 3.6. The hydraulic head above the membranes, which ranged from a maximum value of 1.2 m to a minimum of 1.06 m of waste water, was able to provide gravity-driven filtration without the need for applying any suction.

The permeate line is shown Figure 3.6.

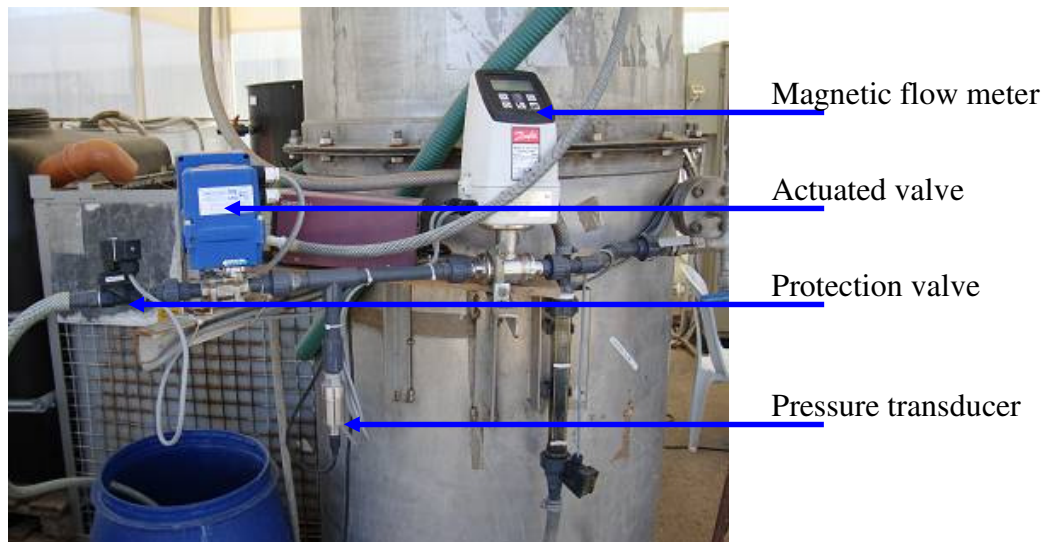


Figure 3.6 MBR1: Permeate line

The permeate line, as well as the pipes and the valves, also incorporated the following.

- A magnetic flow meter for real permeate flow rate measurements.
- A pressure transducer for measurements of the gauge pressure on the permeate side of the membranes.
- An actuated permeate valve, which regulated the permeate flow rate values, along with the aid of a proportional-integral-derivative (PID) controller, a schematic of which is provided in Appendix A.
- A (solenoid) protection valve, which was normally open to allow permeation but closed in the event of a power cut in order to stop filtration and protect membranes.

Permeate was collected in a storage tank for further use. The MBR1 system was designed for continuous filtration but some modification allowed both continuous and intermittent filtration to be tested in this research.

Waste sludge was taken from the MBR tank either automatically through the application of a sludge pump or manually through the drain valve of the tank. Finally, in this MBR system, when necessary, chemical cleaning was also applicable in-situ, as a diluted cleaning solution can be gravity fed through the permeate line directly to the membrane panels.

All switches and controls relating to the operation of this MBR system were linked to a control panel shown in Figure 3.7. This control panel also provided the MBR1 system with electricity. Feed Pump 1, the air compressor and the solenoid protection valve were able to be directly controlled by switches and their operation could be set either to a manual or to an automatic mode. The opening of the actuated valve was controlled by a PID loop so that the real permeate flow rate was regulated to the desired value. In case of a failure of the PID controller, the actuated valve can be operated manually.



Figure 3.7 Control panels

Finally, both instant values of the pressure on the permeate side of the membranes as provided by the pressure transducer, and instant real permeate flow rates as provided by the flow meter, were recorded by a data logger. This data logger was pre-programmed via a computer with the software provided so that all data could be downloaded onto this computer for further analysis.

3.2.2 The MBR2 system

Membrane bioreactor 2 (MBR2) was based on UF filters known as MC03 MicroClear AquaCell sewage treatment units provided by Weise Water Systems, GmbH and Co, KG. These units can only treat pre-treated sewage, so the waste water must have already been screened, preferably by a 2 mm screen, before starting filtration, [Weise Water offer: MicroClear AquaCell sewage treatment unit, 2007]. In this work, waste water was screened by a 3 mm screen.

The MBR2 system, as supplied by the manufacturers, comprises three tanks, along with all the required devices, fittings, pipes, valves, etc., and a control panel. Figure 3.8 shows the MBR2 system.



Figure 3.8 The MBR2 system - The control panel is in the cabinet in the back

The first tank is a pre-sedimentation tank, the second is the biological treatment tank and the third is the MBR tank, or the tank that houses the membranes. All three tanks are made of polyethylene and have the same dimensions, namely 1.4 m long \times 0.72 m wide \times 1.4 m high. The volume of each tank is about 1.1 m³.

- **The pre-sedimentation tank**

The pre-sedimentation tank aims to settle any heavy solids in the waste water and make any grease/fat float so that the waste water will be free of impurities before flowing into the biological treatment tank. It comprises an inlet, an overflow to the biological treatment tank, with a submerged pipe so that most of fat and grease is retained within this tank, and a manual drain valve located at the bottom. However, in this research, it was found that it would be more beneficial if this tank was used not only by the MBR2 system but also by the MBR1 and MBR3 systems. The pre-sedimentation tank was therefore located before the MBR1 FS/AN tank and was used as a common settling storage tank for raw waste water.

- **The biological treatment tank**

The biological treatment tank is where aerobic biological oxidation took place. Similar to the pre-sedimentation tank, it comprises an inlet, an overflow to the MBR tank and a manual drain valve. This tank was also equipped with an air compressor, whose task is to supply air for the maintenance of the biomass. The air was provided to the waste water through a plate diffuser with a membrane made of ethylene-propylene-diene M-class rubber for fine bubble aeration. Both the air compressor and the plate diffuser provided directly by the membrane supplier. Figure 3.9 shows the air diffuser.



Figure 3.9 MBR2: Air diffuser

- **The MBR tank**

The MBR tank is where the membranes are housed and filtration of the mixed-liquor takes place. In this research, two membrane units were used. The tank is also equipped with two air compressors. These air compressors provide the MBR tank with air whose main task is to scour the membrane modules and keep them clean, along with maintaining biomass active. For this reason, each air compressor is connected with a diffuser, (Figure 3.9), and each diffuser is located precisely underneath each membrane unit. The air flow rate was fixed by the manufacturers and could not be adjusted during the trial - it was equal to $6 \text{ m}^3 \text{ h}^{-1}$ per air compressor. The membrane unit with housing and the diffuser is shown in Figure 3.10.



Figure 3.10 MBR2: Membrane unit, its housing and the diffuser

Permeate came out from the membranes through a permeate withdrawal unit consisting of the following.

- A filtrate suction pump, which sucked the filtrate out of the membranes.
- A permeate pressure sensor to measure directly instant TMP values.
- A flow meter to measure instant real permeate flow rates.

This permeate line is shown in Figure 3.11.

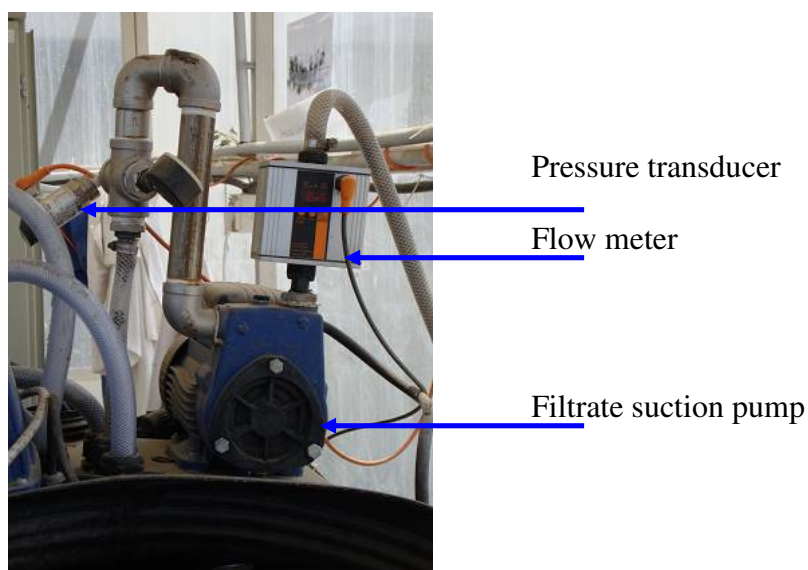


Figure 3.11 MBR2 unit: Permeate line

Permeate was drawn out of the membranes by the application of a slight negative pressure to the filtrate collector of the membrane unit via the suction pump. Filtration in these membrane units can be either continuous or intermittent. In this work, the long-term experiment was based on an intermittent filtration mode as suggested by the membrane supplier, according to which 9 min of filtration were followed by 1 min of relaxation, [Weise Water Systems: Operating and maintenance manual, 2008]. The flow rate of the permeate was regulated by adjusting the permeate pump speed in relation to the measured real permeate flow rate via a control loop.

Sludge wasting initially took place manually through the valve located at the bottom of the MBR tank. Later, a sludge pump was installed, which could remove waste sludge from the tank and was set to operate to an automatic mode. Also, a recirculation pump delivered waste water back to the biological treatment tank as appropriate.

MBR2 operation was highly automated through the use of a control panel shown in Figure 3.7, which regulated the operation of the entire MBR system. A PID controller, a schematic of which is given in Appendix A, was used. The control panel included functions for the adjustment of the operating conditions of all the components of the MBR2 system, along with the determination of each component's working hours. The programme could then be saved as software that could be downloaded and the recorded data could be analysed.

3.2.3 The MBR3 system

The membrane bioreactor 3 (MBR3) system was based on UF membranes known as 611 siClaro membrane modules provided by Martin Systems AG. These membrane filters can treat waste water, which has already been screened through a 3 mm screen before starting filtration. A photograph of the MBR3 system is shown in Figure 3.12.



Figure 3.12 The MBR3 system - The control panel is shown in Figure 3.7

The MBR3 system consists of the aeration tank, the filtration tank, and a control panel. The tanks are of the same dimensions, namely 1.8 m high and 1 m in diameter.

• The aeration tank

The aeration tank is where aerobic biological oxidation took place. Inside this tank, a recirculation pump was located so that mixed-liquor was transported into the filtration tank through a recirculation line. The recirculation line was equipped with a valve in case biomass must be removed and a valve for the adjustment of the recirculation flow rate. There is also an overflow from the filtration tank back to the aeration tank.

Air for the maintenance of the biological culture was provided by an aerator/mixer, along with a valve for regulating the aeration/mixing of the biomass. This device mixes fluids or adds gases into processes and it is capable of producing bubbles of ultra-fine size with a high performance ratio for air insertion and penetration depth, [www.jung-pumpen.de, 2010]. The valve could alter the operating conditions inside

the aeration tank, namely from aerobic conditions, when the valve was open, to anoxic conditions, when the valve was fully closed. During the start-up period and the initial phase of the MBR operation, the valve must be always open at any time so that the biomass is free to grow. Then, if necessary, the aerator/mixer can be turned off and anoxic conditions are able to be achieved. In this research, only aerobic conditions were desired, so the valve remained always open. Finally, there is also a valve located at the bottom of the tank in case the tank has to be drained, [Martin Systems: Instructions for installation and operation of PURATREAT siClaro sewage treatment plant, (2008)].

• The filtration tank

The filtration tank is where the membranes are housed and separation of mixed-liquor/treated permeate takes place. In this research, one membrane module was used. This membrane module, together with the housing and the diffusers, is shown in Figure 3.13.

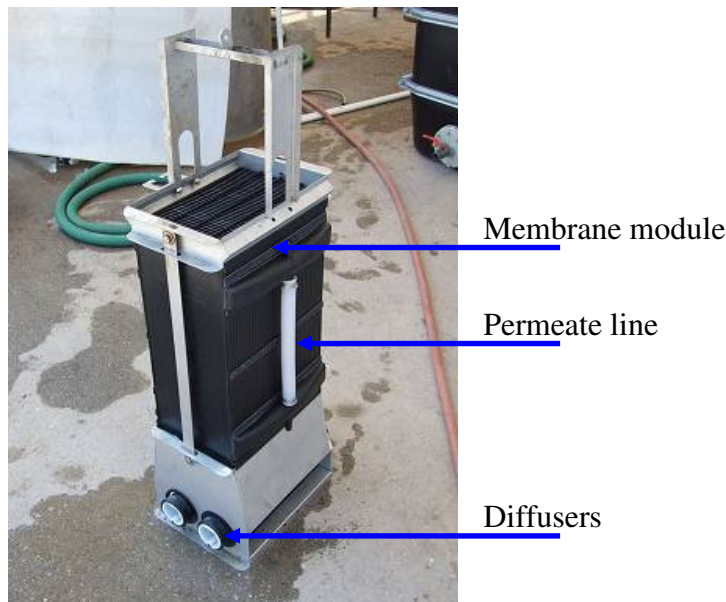


Figure 3.13 MBR3: Membrane module, its housing and the diffusers

Air, in the filtration tank, was provided through an aeration line comprising an air compressor for both scouring the membranes and for biomass maintenance, an air flow meter for the air flow rate monitoring and two fine diffusers located underneath

the filtration module. The diffusers are shown in Figure 3.14. According to the manufacturers, the air flow rate has always to be more than $6 \text{ m}^3 \text{ h}^{-1}$, regardless the real permeate flow rate, otherwise membrane fouling may occur, [Martin Systems: Instructions for installation and operation of PURATREAT siClaro sewage treatment plant, (2008)].



Figure 3.14 MBR3: Air diffusers

Permeate is withdrawn through the membranes via a central extraction device and a permeate line. This permeate line, which is shown in Figure 3.15, consisted of the following.

- A filtrate suction pump, which sucked the filtrate out of the membranes.
- A pressure transducer, which was calibrated to measure directly instant TMP values.
- A magnetic flow meter, which measured instant real permeate flow rates.

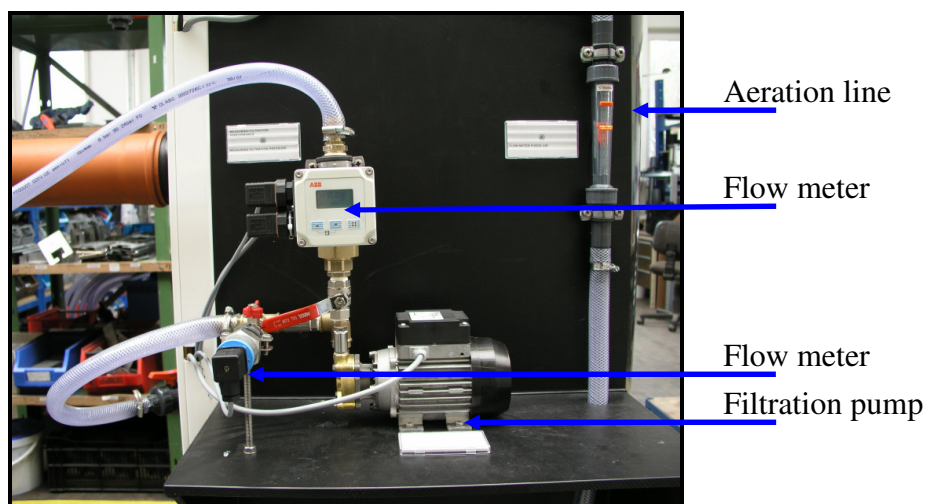


Figure 3.15 MBR 3: Permeate line - Part of the aeration line can also be seen

Permeation in this MBR system can be either continuous or intermittent by selecting a suitable filtration/relaxation cycle. In this work, intermittent filtration was selected to be applied and the long-term experiment was operated under an operational cycle of 17 min of filtration followed by 3 min of membrane relaxation. The filtrate pump speed, and hence the real permeate flow rate, were regulated by a PID control loop, a schematic of which is shown in Appendix A, via the flow meter measurements.

Surplus sludge was initially removed manually through a drain valve located at the bottom of the tank. Later, a waste pump was installed and waste sludge removed automatically on a daily basis.

The whole operation was controlled through a control panel, which is shown in Figure 3.7. All the components of the MBR unit were connected with this control panel and the operation as a whole was automated. The control panel was also equipped with a data recorder so that all data could be logged and downloaded onto a computer for further analysis.

3.3 Characteristics of the influent waste water

The waste water, which was used in this research, was the one treated by the full-scale conventional AS plant at the ONAS site. The analysis for the determination of characteristics of the waste water was carried out according to the standard methods

for the examination of water and waste water, [www.standardmethods.org, 2010]. The average values for typical physicochemical and biological characteristics of the waste water for 2006, are given in Table 3.3.

Table 3.3 Waste water characteristics, [ONAS, North Sfax, Archives, 2006]

Characteristics	Value	Unit
COD	863	mg L ⁻¹
BOD ₅	503	mg L ⁻¹
Total suspended solids (TSS)	526	mg L ⁻¹
Total volatile solids (TVS)	944	mg L ⁻¹
Chlorides	1920	mg L ⁻¹
Sulphates	910	mg L ⁻¹
Total nitrogen	N/A	mg L ⁻¹
Total phosphate	11.6	mg L ⁻¹
Fat/Grease	4.8	mg L ⁻¹
Faecal coliforms	39 × 10 ⁶	CFU* (100 ml) ⁻¹
Total coliforms	75 × 10 ⁶	CFU (100 ml) ⁻¹
Faecal streptococci	15 × 10 ⁶	CFU (100 ml) ⁻¹
Electrical conductivity	6,413	μS cm ⁻¹
pH	7.5	unitless
Average water temperature	24	°C

*CFU: Colony-forming unit

3.4 Start-up of the plant and operating details

The complete MBR pilot plant installation is shown in Figure 3.16.



Figure 3.16 The MBR pilot plant installation

Waste water was pre-treated by the “Office National de l' Assainissement” (ONAS) plant including removal of sand, fat/grease and grit and was delivered by the main feed pump to a storage tank, which was the MBR2 pre-sedimentation tank - even though this tank had been designed to be a pre-sedimentation tank by the MBR2 supplier, it actually acted as a balancing tank in this research and it was used in combined parallel with the FS/AN tank. Around the main feed pump, a mesh net was placed to protect it from becoming blocked and, at the same time, providing additional screening to waste water.

The waste water then flowed through an overflow from this balancing tank into the inlet part of the FS/AN tank. Another screening of the waste water took place, as waste water flowed from the inlet part of the FS/AN tank to the outlet part through the 3 mm perforated sheet. The operation of the main feed pump was set to an automatic mode by using a high level float switch located in the FS/AN tank, such that if the liquid level in the tank reached the maximum position, the float switch was triggered and the pump was automatically switched off.

The main feed pump's operation was also controlled by an integrated low level float switch to protect the pump against pumping air. This float switch would interrupt the main feed pump's operation in case the level of waste water in the ONAS pre-treatment basin had become lower than the level allowed by this pump. Finally, in case the liquid level in the tank would become too high, either due to human error in manual mode operation, or because the float switch within the FS/AN tank was not tripped during operation in automatic mode, a mechanical overflow allowed overspill from the FS/AN tank back into the waste water storage basin so that flooding was avoided.

The three MBR feed pumps were placed in the second half of the FS/AN tank, so feed waste water was distributed to the three different MBR units from the same source.

3.4.1 Start-up and operating details of MBR1

Feed Pump 1 delivered waste water from the outlet part of the FS/AN tank to the MBR tank of the MBR1 system. The operation was set to an automatic mode by using level float switches. This MBR tank was then equipped with two float switches at the high and low levels. When the liquid level reached the minimum height due to filtration, the low level float switch was triggered so that Feed Pump 1 had to start delivering waste water into the MBR tank. As the waste water level increased, it reached the maximum position, controlled by the high level float switch, which was then tripped and Feed Pump 1 had to stop delivering waste water into the MBR tank. Finally, in the unlikely event the high level float switch was not tripped, waste water could be channelled to the ONAS pre-treated waste water basin through two overflows. Also, the drain valve at the bottom of the tank had to be always closed unless sludge wasting was taking place.

The air blower was set to an automatic mode and coarse bubble aeration was continuously provided in the activated sludge (AS) through the diffuser located underneath the membrane panels. A valve could throttle the air flow from the air compressor. By adjusting the opening of this valve, the selected air flow rate could be achieved. The air flow rate was monitored by an air flow meter.

The real permeate flow rate was then regulated - details about the difference between the real and the net permeate flow rates/MPFs are given later in Chapter 6. This occurred through the actuated permeate valve, which was controlled by a PID controller. The PID controller was able to adjust the opening of the actuated valve to a certain place so that the selected permeate flow rate was obtained. Instant real permeate flow rates were monitored by a magnetic flow meter and recorded by a data logger. The PID control loop needs occasionally re-tuning. The option of operating the actuated valve manually without the need for using the PID controller is also possible.

Permeate was continuously pushed through the membranes to the permeate outlet. Instant pressure values on the permeate side of the membranes were monitored by a pressure transducer and were recorded by a data logger. Instant pressure values on the feed side of the membranes could not be recorded and an average value based on the minimum and the maximum hydraulic heads was accepted. Both instant real MPFs and instant TMP values were then estimated.

Even though this MBR system had been designed to operate continuously, during the long-term experiment, intermittent filtration tested over a period of a few months. A 19/1 min/min filtration/relaxation cycle was chosen and a timer was set so as the selected cycle could be applied. During the relaxation time period, the solenoid valve was forced to close so that the permeate flow was blocked. However, it was found that the application of intermittent filtration was not a good practice because it caused anomalies to the operation of the PID controller as it was trying to maintain the real permeate flow rate. Intermittent filtration was then discontinued and the membranes were operated in continuous mode.

The MBR1 system was started-up with a solids residence time (SRT) set to 15 d and a hydraulic residence time (HRT) set to 1.01 d in order to control the MLSS concentration at about 4 - 5 g L⁻¹. All the initial operating conditions of the MBR1 system are summarised in Table 3.4.

Table 3.4 MBR1: Start-up operating conditions

Parameter	Value	Unit
HRT	1.01	d
SRT	15	d
Average net MPF	9.47	L min ⁻¹
MLSS concentration	4 - 5	g L ⁻¹
Air flow rate: Membrane scouring + Biomass maintenance (MBR tank)	4,200	L h ⁻¹
Initial mixed-liquor temperature	31	°C

3.4.2 Start-up and operating details of MBR2

Feed Pump 2 delivered waste water from the outlet part of the FS/AN tank into the biological treatment tank of the MBR2 system. The biological treatment tank was filled with waste water, which then flowed into the MBR tank through an overflow. Due to the overflow, the liquid level in both tanks was constant all the time. The filtration process was automated through a control panel by means of two float switches located in the MBR tank, which controlled Feed Pump 2. The operation of these two float switches was similar to the operation described in Section 3.3.1 regarding the operation of Feed Pump 1.

Both the air blower in the biological treatment tank and the air blowers in the MBR tank were set to an automatic mode and fine bubble aeration was provided in both tanks. The air flow rate was automatically controlled through the control panel and was fixed according to the manufacturer's instructions. The air blower, which provided air within the biological treatment tank, was set to operate intermittently based on a 5/5 min/min on/off operational cycle, but the air blowers, which provided air within the MBR tank mainly for membrane scouring, operated continuously.

The real permeate flow rate was regulated through the control panel. As intermittent permeation was applied, the suction pump was operated in cycles, and a 9/1 min/min filtration/relaxation cycle was applied. Instant real permeate flow rate values were measured by a flow meter and recorded via software provided by the manufacturers.

At the same time, a pressure transducer was measuring the pressure values on the permeate side. The pressure readings were recorded with the aid software and were possible to be downloaded onto a computer for further analysis. The pressure on the feed side of the membranes could not be measured and an average value had to be accepted. Finally, based on the raw data, instant real MPFs and instant TMP values were calculated.

The initial operating conditions are now summarised in Table 3.5.

Table 3.5 MBR2: Start-up operating conditions

Parameter	Value	Unit
HRT	1.01	d
SRT	15	d
Average net MPF	11.12	L min ⁻¹
MLSS concentration	4 - 5	g L ⁻¹
Air flow rate: Biomass maintenance (Biological treatment tank)	6,000	L h ⁻¹
Air flow rate: Membrane scouring + Biomass maintenance (MBR tank)	12,000	L h ⁻¹
Initial mixed-liquor temperature	31	°C

3.4.3 Start-up and operating details of MBR3

Feed Pump 3 delivered waste water from the outlet part of the FS/AN tank to the aeration tank of the MBR3 system. The tank was filled with waste water, which then flowed to the filtration tank with the aid of the recirculation pump, which was switched on all the time. Waste water could flow from the filtration tank back to the aeration tank through an overflow, maintaining the liquid level above the membranes at a constant value. The operation could be set either to a manual mode or to an automatic one through a control panel. In this research, the automatic mode was selected. For this reason, two float switches at low and high levels were placed in the filtration tank controlling the operation of Feed Pump 3.

The fine bubble air flow rate in both tanks was automatically controlled through a control panel. The aeration/mixing device in the aeration tank was set to operate in cycles, meaning 3/3 min/min filtration/relaxation at its maximum value, as the valve that could control the air flow rate was fully open during the long-term experiment. The air compressor in the filtration tank was set to operate continuously. A range of air flow rates in the filtration tank were able to be selected via the control panel and, at any time, these air flow rates were able to be observed through the use of a rotameter.

The real permeate flow rate was also regulated through the control panel. Intermittent filtration was applied with a filtration/relaxation cycle of 17/3 min/min. A flow meter recorded the real permeate flow rate values all the time and a pressure transducer located on the permeate side was calibrated to measure TMP values. Both instant real permeate flow rates and instant TMP values were recorded and downloaded onto a computer. Then, instant real MPFs were calculated.

The start-up operating conditions for this MBR system are shown in Table 3.6. As seen in Table 3.6, the selected SRT/HRT values were the same with the values for the MBR1 and MBR2 systems, so, as expected, they led to a similar MLSS concentration.

Table 3.6 MBR3: Start-up operating conditions

Parameter	Value	Unit
HRT	1.01	d
SRT	15	d
Average net MPF	13.58	L min ⁻¹
MLSS concentration	4 - 5	g L ⁻¹
Air flow rate: Biomass maintenance (Aeration tank)	N/A	L h ⁻¹
Air flow rate: Membrane scouring + Biomass maintenance (Filtration tank)	7,300	L h ⁻¹
Initial mixed-liquor temperature	31	°C

3.5 Analytical methods

3.5.1 BOD₅ concentration measurements

The BOD₅ concentration for all MBR systems was estimated with the aid of the WTW OxiTop control system, [www.wtw.com, 2010]. The general measuring principle of the system is manometric based on pressure measurements in a closed system. The BOD₅ bottles are filled with assigned amounts of water (depending on the BOD₅ measuring range), which are then seeded with a diluted sample of microorganisms from the mixed-liquor whose BOD₅ concentration has to be measured. The bottles are placed on an inductive stirring system where good mixing is provided and then incubated at a temperature of 20 ± 0.5 °C for 5 days. The bacteria consume oxygen in this closed system and release carbon dioxide. The carbon dioxide produced is absorbed by a sodium hydroxide pellet in a rubber quiver above the headspace of the bottle. As carbon dioxide is absorbed, the pressure in the bottle drops. This change of the pressure is then detected and stored by a piezoelectric measuring head. The data is finally transferred to a controller via infra-red transmission and BOD₅ values can directly be read. With the aid of a computing environment, all this information can be downloaded for further use and analysis, [Sim, 2003]. All BOD₅ concentrations regarding the influent of the MBR plant and the effluents of all three MBR systems were measured on a regular basis during the long-term experiments. Each BOD₅ value was the average from three samples and the accuracy of the measurements was in the range of ± 0.1 mg L⁻¹.

3.5.2 COD concentration measurements

COD concentrations for all three MBR systems were measured with the Hach's United States Environmental Protection Agency approved COD method, [www.hach.com, 2010]. This method's pre-measured ready-to-use reagents are a dichromate standard solution, sulphuric acid and a strong oxidant with a silver compound added as a catalyst to promote the oxidation of the resistant organic compounds. Mercuric sulphate is also added to reduce any interference caused by the oxidation of chloride ions by the dichromate potassium. The digestion takes place within the Hach's COD reactor at a temperature of 150 °C. The reagent phial necks

and caps only reach a temperature of about 85 °C because they are outside the reactor. This temperature difference is then able to produce proper refluxing within the phial. After 2 hr of digestion, the COD concentration value can be recorded using the Hach DR/890 colorimeter, [Sim, 2003]. COD concentrations were measured for the influent of the MBR plant and for each MBR's effluent, and their accuracy was in the range of $\pm 0.1 \text{ mg L}^{-1}$. Values presented are the average of from three samples at each point.

3.5.3 MLSS and MLVSS concentration measurements

MLSS and MLVSS concentration measurements for all three MBR systems were made with the aid of standard methods for the examination of water and waste water - 2540E for fixed and volatile solids ignited at 550 °C, [www.standarrdmethods.org, 2010]. A glass beaker was dried in a furnace at a temperature of $550 \pm 50 \text{ °C}$ for 2 hours to dispose of any volatile compounds. Then, the beaker was allowed to cool in a desiccator and it was weighed. An assigned amount of activated sludge (AS) was then placed onto the dehydrated beaker. The beaker was placed into an oven and dried at temperatures between 103 °C and 105 °C. The difference between the weight of the beaker after drying and the weight of the beaker when it was empty provides the MLSS concentration, which can be expressed in g L^{-1} . Next, the residue in the beaker was dried in a furnace at $550 \pm 50 \text{ °C}$ for 2 hours. It was left to cool down and it was weighed. The difference of the weight of the beaker after drying in the oven and the weight of the beaker after drying in the furnace provides the MLVSS concentration, which is usually expressed in g L^{-1} , [Sim, 2003]. By taking AS samples from all MBR units, both the MLSS concentration and the MLVSS concentration within the MBR tanks were able to be measured. The accuracy of the measurements was for both MLSS and MLVSS concentrations in the range of $\pm 0.001 \text{ g L}^{-1}$. Values presented are the average from three samples.

3.5.4 MBR pilot trial organisation

The pilot trials of the three MBR systems were conducted in Tunisia, on the North Sfax ONAS WWT works. Day-to-day operation of the MBR systems and routine water quality/microbiological analysis were conducted by staff from "Centre de Biotechnologie de Sfax" (CBS) and also staff from ONAS, both services are located

in the city of Sfax. The data covering MBR mixed-liquor temperatures, MPFs, and TMP values was collected routinely via data-loggers, was compiled into spreadsheets, and shared electronically with the PURATREAT project partners.

The role of staff at Bath was to procure the MBR systems, to define the operating conditions that were being tested on the ground in Sfax, to co-ordinate and conduct the energy consumption experiments and to do the engineering analysis of the results. This included membrane performance analysis, mass balancing and biological modelling, and analysis of the SED values.

During the pilot trials, a series of visits were made to Sfax in order to conduct experiments, collect and discuss results, and to ensure that the experimental protocols were being followed correctly. The main focus of this thesis is the engineering analysis and modelling of the performance of the three MBR systems, including recommendations about the most appropriate MBR system in terms of treated water quality, membrane performance and energy costs.

The next chapter describes the clean water tests that were conducted prior to the treatment of waste water by the MBR systems.

CHAPTER 4 CLEAN WATER TESTS

4.1 Introduction

Clean water tests were run with either new membrane panels/units or membrane panels/units following chemical cleaning using tap water from the domestic water supply system at the North Sfax “Office National de l' Assainissement” (ONAS) site. The water temperature, which was indicated by the thermocouple located in the membrane bioreactor 3 (MBR3) system, was 34 °C and it was accepted to be the water temperature for all three membrane bioreactor (MBR) systems during the tests. Clean water tests are usually performed before conducting waste water experiments mainly for two reasons. First, the raw data that is collected help understand how bad the membrane fouling can be when clean water is replaced by waste water - clean water is accepted not to be subject to any membrane fouling. Also, it can be seen how effective the physical/chemical cleanings can be in terms of removing both reversible and irreversible membrane fouling.

4.2 Clean water tests

4.2.1 Clean water tests for MBR1

Clean water tests for the membrane bioreactor 1 (MBR1) system, as shown in Figure 3.4, were run with new membrane panels. The MBR tank was intermittently filled with clean water whose height varied from a maximum of 2.5 m (a high level float switch was triggered) to a minimum of 2.36 m (a low level float switch was then triggered). The level of the water within the MBR tank decreased due to continuous permeate removal, and it rose each time the feed pump was operated.

As the top parts of the membranes were located 1.3 m from the bottom of the MBR tank, the total hydraulic head above the membranes varied from a maximum of 1.2 m to a minimum of 1.06 m of water. These two water level values corresponded to gauge hydraulic head pressure values, which varied from a maximum of 0.118 bar to a minimum of 0.104 bar, [Brodkey and Hershey, 1990]. As the changes of the

hydraulic head pressure, also known as pressure on the feed side of the membranes, could not be recorded, an average value equal to 0.111 bar was calculated and used. On the other hand, the pressure on the permeate side of the membranes was continuously measured by a pressure transducer. Figure 4.1 shows the MBR1 system.

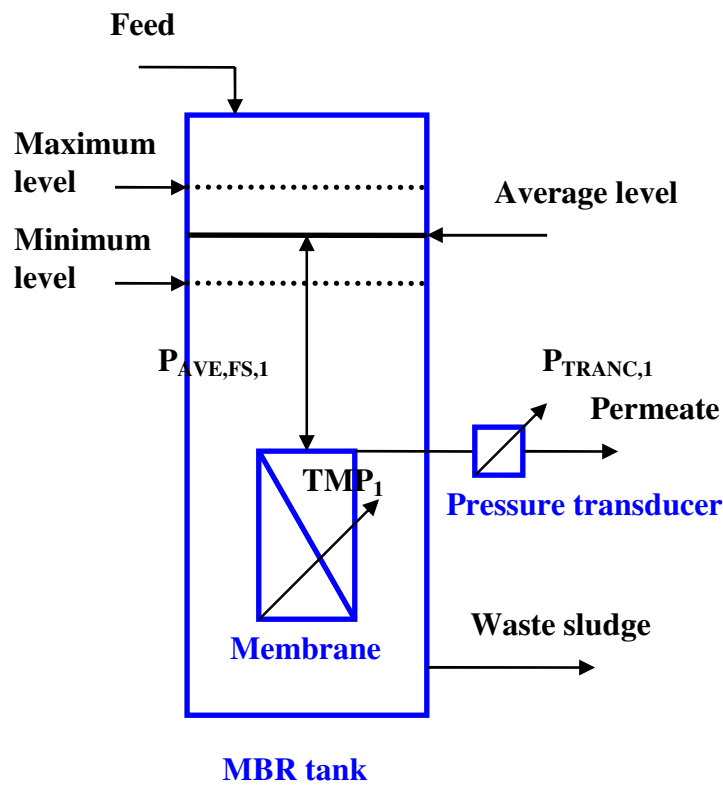


Figure 4.1 A schematic showing the operation of MBR1

Permeation was continuous with no membrane relaxation. During the tests, the real permeate flow rate was stepped up and down by making adjustments to the set-point of the permeate flow controller over intervals of time. In general, real permeate flow rates are the rate values as provided by the flow meter. More details about the difference between real/net permeate flow rates, and real/net membrane permeate fluxes (MPFs), will be given later in Chapter 6. However, the real and the net values are different only when intermittent filtration is applied, which was not the case for the MBR1 system so far. The resulting real flow rates of permeate and pressure values on the permeate side of the membranes were recorded by a data logger. Based on the raw data, real membrane permeate fluxes (MPFs) and transmembrane pressure (TMP) values of the system were calculated. Based on these estimates, the membrane

permeability value was also calculated and temperature-corrected at a reference temperature of 20 °C. This average temperature-corrected permeability value was directly compared with the clean water membrane permeability as provided by the membrane manufacturer. The real membrane permeate flux (MPF), the transmembrane pressure (TMP) and the membrane permeability are defined as follows, [Judd, 2007]:

• **Real MPF**

The real MPF of MBR1, $J_{p,r,1}$, at a clean water temperature, T_{cw} , - temperature during the test -, is given by Equation 4.1.

$$J_{p,r,1} = \frac{Q_{p,r,1}}{A_1} \quad \text{Equation 4.1}$$

where:

$$\begin{aligned} J_{p,r,1} &= \text{Real MPF of MBR1 at } T_{cw} && \text{L m}^{-2} \text{ h}^{-1} \\ Q_{p,r,1} &= \text{Real permeate flow rate of MBR1} && \text{L h}^{-1} \\ A_1 &= \text{Membrane area for MBR1} && \text{m}^2 \\ T_{cw} &= \text{Clean water temperature} && \text{°C} \end{aligned}$$

If necessary, the real MPF can be temperature-corrected at a reference clean water temperature, T_{cw-ref} , usually equal to 20 °C. This temperature-corrected real MPF is calculated with the aid of Equation 4.2, [Judd, 2007].

$$J'_{p,r,1} = \frac{J_{p,r,1}}{1.025^{(T_{cw}-T_{cw-ref})}} \quad \text{Equation 4.2}$$

where:

$$\begin{aligned} J'_{p,r,1} &= \text{Temperature-corrected real MPF of MBR1 at } T_{cw-ref} && \text{L m}^{-2} \text{ h}^{-1} \\ T_{cw-ref} &= \text{Reference clean water temperature} && \text{°C} \end{aligned}$$

• **TMP**

In general, TMP in all membrane-based processes is defined as follows:

$$TMP = P_{FS} - P_{PS} \quad \text{Equation 4.3}$$

where:

P_{FS} = Pressure on the feed side of the membranes bar

P_{PS} = Pressure on the permeate side of the membranes bar

For MBR1, we get:

$$TMP_1 = P_{FS,1} - P_{PS,1} \quad \text{Equation 4.4}$$

TMP_1 = TMP of MBR1, bar bar

$P_{FS,1}$ = Pressure on the feed side of MBR1 bar

$P_{PS,1}$ = Pressure on the permeate side of MBR1 bar

The pressure value on the feed side of MBR1 could not be recorded, so an average value between the maximum and the minimum was accepted. The pressure value on the permeate side of MBR1 was directly measured by a pressure transducer. Based on these comments, Equation 4.4 can then be modified as follows:

$$TMP_1 = P_{AVE,FS,1} - P_{TRANC,1} \quad \text{Equation 4.5}$$

where:

$P_{AVE,FS,1}$ = Average pressure on the feed side of MBR1 bar

$P_{TRANC,1}$ = Instant pressure as provided by the pressure transducer of MBR1 bar

• Permeability

Permeability of MBR1, K_1 , at a clean water temperature, T_{cw} , is estimated through Equation 4.6.

$$K_1 = \frac{J_{p,r,1}}{TMP_1} \quad \text{Equation 4.6}$$

where:

$$K_1 = \text{Permeability of MBR1 at } T_{cw} \quad \text{L m}^{-2} \text{ h}^{-1} \text{ bar}^{-1}$$

Then, if necessary, permeability of MBR1, K_1 , can be temperature-corrected at the reference temperature, T_{cw-ref} , as follows:

$$K'_1 = \frac{J'_{p,r,1}}{TMP_1} \quad \text{Equation 4.7}$$

where:

$$K'_1 = \text{Temperature-corrected permeability of MBR1 at } T_{cw-ref} \quad \text{L m}^{-2} \text{ h}^{-1} \text{ bar}^{-1}$$

4.2.2 Clean water tests for MBR2

Clean water tests for membrane bioreactor 2 (MBR2), as shown in Figure 3.8, were run with membrane units following chemical cleaning. The available hydraulic head above the membranes in MBR2, which was on average equal to 0.25 m, or 0.024 bar, was not enough to operate MBR2 gravitationally, hence permeate suction was applied, or otherwise filtration could not occur. This required pressure drop through the membrane was provided by operating a suction pump. At the same time, a pressure transducer measured pressure values on the permeate side of the membranes.

The real permeate flow rate was controlled by adjusting the set-point of the permeate flow controller. Filtration, during this experiment, was intermittent with a filtration/relaxation cycle equal to 9/1 min/min on/off. All the raw data including real permeate flow rates and pressure values on the permeate side of the membranes were recorded by a data logger and downloaded onto a computer. The permeate flow rates were provided by the flow meter. The real permeate flow rate values were then adjusted so as to calculate real MPFs.

The operation of MBR2 is shown in Figure 4.2. More details about the pressures exerted on the system, as shown in Figure 4.2, will follow in this section.

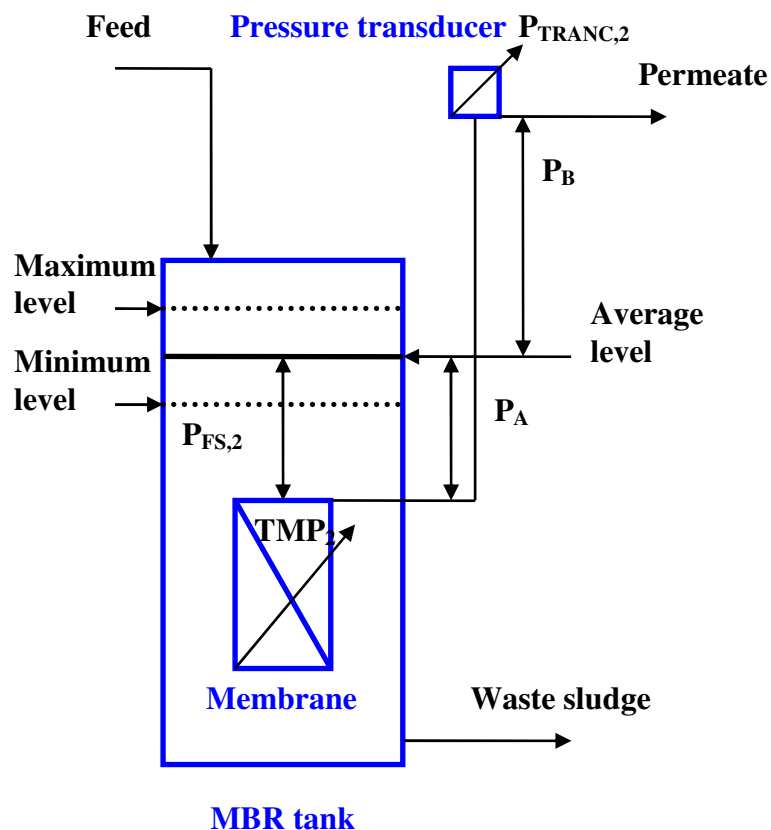


Figure 4.2 A schematic showing the operation of MBR2

Real MPFs and TMP values of the MBR system were calculated. Based on these estimates the membrane permeability value of the MBR2 system was also calculated, and was temperature-corrected at the reference clean water temperature of 20 °C. This average temperature-corrected permeability value was compared with the clean water

membrane permeability value as provided by the membrane manufacturer. In order to do these calculations, the following expressions were used, [Judd, 2007].

• Real MPF

The real MPF of MBR2, $J_{p,2}$, at a clean water temperature, T_{cw} , is given by Equation 4.8.

$$J_{p,r,2} = \frac{Q_{p,r,2}}{A_2} \quad \text{Equation 4.8}$$

where:

$$\begin{aligned} J_{p,r,2} &= \text{Real MPF of MBR2} && \text{L m}^{-2} \text{ h}^{-1} \\ Q_{p,r,2} &= \text{Real permeate flow rate of MBR2} && \text{L h}^{-1} \\ A_2 &= \text{Membrane area for MBR2} && \text{m}^2 \end{aligned}$$

A temperature-corrected real MPF at the reference clean water temperature, T_{cw-ref} , of 20 °C, is calculated through Equation 4.9, [Judd, 2007].

$$J'_{p,r,2} = \frac{J_{p,r,2}}{1.025^{(T_{cw} - T_{cw-ref})}} \quad \text{Equation 4.9}$$

where:

$$J'_{p,r,2} = \text{Temperature-corrected real MPF of MBR1 at } T_{cw-ref} \quad \text{L m}^{-2} \text{ h}^{-1}$$

• TMP

This time, it was the application of some negative pressure by means of the operation of a suction pump that helped collect treated permeate at the end of the permeate line. Also, the relative position of the pressure transducer compared to the top part of the

membranes introduced some additional hydraulic pressure on the permeate side of the membranes, as shown in Figure 4.2.

The TMP_2 is accepted to be as follows:

$$TMP_2 = P_{FS,2} - P_{PS,2} \quad \text{Equation 4.10}$$

TMP_2	=	TMP of MBR2	bar
$P_{FS,2}$	=	Pressure on the feed side of MBR2	bar
$P_{PS,2}$	=	Pressure on the permeate side of MBR2	bar

As operation was intermittent, two different cases with respect to TMP ought to be analysed - the first case is when membranes were filtering and the other one is when membrane relaxation was applied.

During filtration, the pressure on the permeate side of membranes was given by the indication of the pressure transducer, along with an additional hydraulic pressure due to the fact that some water was always trapped in the pipe line, which connected the top part of the membranes with the pressure transducer. This additional hydraulic pressure was divided into two pressures values, pressure P_A and pressure P_B , as it was easier to do calculations with respect to TMP_2 , (Figure 4.2). By taking into account these pressure values, we get:

$$P_{PS,2} = P_{TRANC,2} + P_A + P_B \quad \text{Equation 4.11}$$

$P_{PS,2}$	=	Pressure on the permeate side of MBR2	bar
$P_{TRANC,2}$	=	Instant pressure as provided by the pressure transducer of MBR2	bar
P_A	=	Hydraulic pressure on the permeate side of MBR2	bar
P_B	=	Hydraulic pressure on the permeate side of MBR2	bar

Observing Figure 4.2, we get:

$$P_{FS,2} = P_A \quad \text{Equation 4.12}$$

Inserting Equation 4.11 and Equation 4.12 into Equation 4.10, we get:

$$TMP_2 = -P_{TRANC,2} - P_B \quad \text{Equation 4.13}$$

Through Equation 4.13, the true TMP_2 values during filtration can be estimated.

During relaxation, on the other hand, it was noticed that the pressure transducer was always recording a negative pressure value equal to P_B . Based on this, it can be said that Equation 4.13 can be applied again as it leads to TMP_2 values of zero, which is what is expected when membrane relaxation occurs. The hydraulic pressure P_A during relaxation of the membranes must not to be taken into account as pressure P_A and the pressure on the feed side of the membranes can cancel, hence it did not exert any additional hydraulic force on the piping system.

Through Equation 4.13, the true TMP_2 can be calculated both during filtration and during membrane relaxation.

• Permeability

Permeability of MBR2, K_2 , at a clean water temperature, T_{cw} , is estimated through Equation 4.14.

$$K_2 = \frac{J_{p,r,2}}{TMP_2} \quad \text{Equation 4.14}$$

where:

$$K_2 = \text{Permeability of MBR2 at } T_{cw} \quad \text{L m}^{-2} \text{ h}^{-1} \text{ bar}^{-1}$$

Then, if necessary, permeability of MBR2, K_2 , can be temperature-corrected at the reference temperature, T_{cw-ref} , as follows:

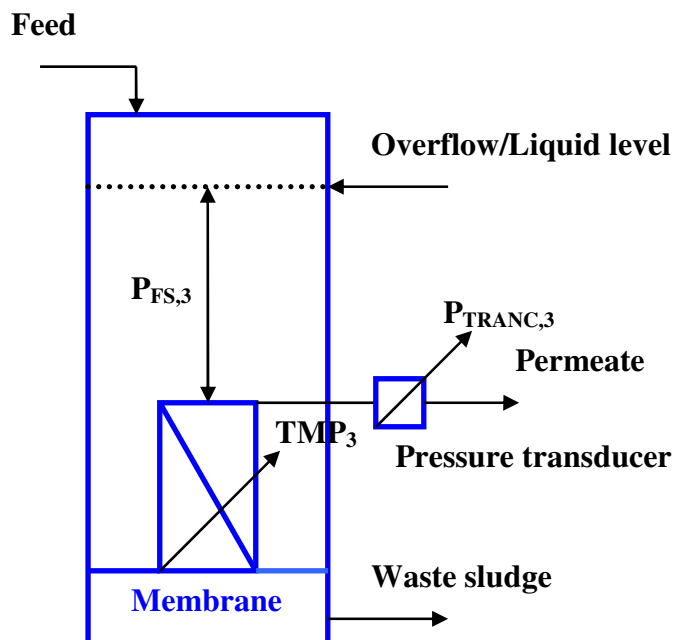
$$K'_2 = \frac{J'_{r,p,1}}{TMP_1} \quad \text{Equation 4.15}$$

where:

$$K'_2 = \text{Temperature-corrected permeability of MBR1 at } T_{\text{cw-ref}} \quad \text{L m}^{-2} \text{ h}^{-1} \text{ bar}^{-1}$$

4.2.3 Clean water tests for MBR3

Clean water tests for MBR3 were run with a membrane filter following chemical cleaning. Under normal operating conditions, the membrane filter has to be sitting at the bottom of the filtration tank allowing a liquid height above the top part of the membranes of 0.7 m, or a constant pressure on the feed side of the membranes of 0.069 bar - the liquid height over the membranes remained constant due to an overflow delivering waste water back to the aeration tank. This is illustrated in Figure 4.3.



MBR3: Aeration tank

Figure 4.3 A schematic showing the operation of MBR3

During these initial tests, the membrane module was tending to float near the liquid surface instead of sitting at the bottom of the aeration tank. The hydraulic head above the membranes was significantly reduced to 0.075 m resulting in a low pressure on the feed side of the membranes, which was 0.007 bar. This tendency of the membrane module to float could have been caused due to some trapped air in the spaces between the membrane panels. However, it was initially assumed that these technical conditions would not be a critical issue during the clean water tests, hence all tests were performed under a pressure value on the feed side of the membranes equal to 0.007 bar.

During MBR3 operation, flux-steps were not performed as the MBR system was run at the default real permeate flow rate of 100 L h⁻¹ suggested by the manufacturers. During the tests, filtration was intermittent, and a selected filtration/permeation cycle of 17/3 min/min on/off was selected. All permeate flow rates/MPFs with respect to this test are real values. The resulting real permeate flow rates and the pressure values on the permeate side of the membranes were recorded by a data logger. For clean water testing, flux-step tests could be avoided, but it is worth mentioning that when biomass was being filtered a wider range of real permeate flow rates had to be applied.

The real MPF, the TMP and the permeability, along with the temperature-corrected real MPF and temperature-corrected permeability, were calculated. The equations used for these calculations are as follows:

• **Real MPF**

The real MPF, $J_{p,3}$, at a temperature T_{cw} is given by Equation 4.16.

$$J_{p,r,3} = \frac{Q_{p,r,3}}{A_3} \quad \text{Equation 4.16}$$

$J_{p,r,3}$	= Real MPF of MBR1	$L m^{-2} h^{-1}$
$Q_{p,r,3}$	= Real permeate flow rate of MBR3	$L h^{-1}$
A_3	= Membrane area for MBR3	m^2

Real MPF can also be temperature-corrected at the reference temperature, $T_{\text{cw-ref}}$, of 20 °C are as follows, (Equation 4.17, [Judd, 2007]):

$$J'_{p,r,3} = \frac{J_{p,3}}{1.025^{(T_{\text{cw}} - T_{\text{cw-ref}})}} \quad \text{Equation 4.17}$$

where:

$$J'_{p,r,3} = \text{Real MPF of MBR3 at } T_{\text{cw-ref}} \quad \text{L m}^{-2} \text{ h}^{-1}$$

• TMP

The TMP_3 is given by Equation 4.18.

$$\text{TMP}_3 = P_{\text{FS},3} - P_{\text{PS},3} \quad \text{Equation 4.18}$$

where:

$$\text{TMP}_3 = \text{TMP of MBR3} \quad \text{bar}$$

$$P_{\text{FS},3} = \text{Pressure on the feed side of the membranes of MBR3} \quad \text{bar}$$

$$P_{\text{PS},3} = \text{Pressure on the permeate side of the membranes of MBR3} \quad \text{bar}$$

As the membrane module was designed to be sitting at the bottom of the aeration tank and the liquid level above the top part of the membranes was successfully controlled, the $P_{\text{FS},3}$ -value remained constant. Taking advantage of this constant pressure on the feed side of the membranes, the membrane manufacturer calibrated the pressure transducer so that it could read directly TMP_3 values - an offset pressure value had been used.

So, it finally the TMP_3 is given by Equation 4.19.

$$\text{TMP}_3 = -P_{\text{TRANC},3} \quad \text{Equation 4.19}$$

where:

$P_{\text{TRANC},3}$ = Instant pressure as provided by the pressure transducer of MBR3 bar

Equation 4.19 can be used both during filtration and during membrane relaxation. However, during the clean water tests, the tendency of the module to float did lead to questionable TMP_3 values to be recorded, as the pressure on the feed side was of the membranes was different to the offset of the pressure transducer. However, even if the TMP_3 values that were recorded were correct or not, some general comments can still be made.

• Permeability

The permeability, K_3 , at a temperature T_{cw} , along with the temperature-corrected value at the reference temperature, $T_{\text{cw-ref}}$, of 20 °C are as follows, (Equation 4.20 and Equation 4.21 respectively):

$$K_3 = \frac{J_{p,r,3}}{TMP_3} \quad \text{Equation 4.20}$$

$$K'_3 = \frac{J'_{p,r,3}}{TMP_3} \quad \text{Equation 4.21}$$

where:

K_3 = Permeability of MBR3 at $T_{\text{cw-ref}}$ $\text{L m}^{-2} \text{h}^{-1} \text{bar}^{-1}$

K'_3 = Temperature-corrected permeability of MBR3 at $T_{\text{cw-ref}}$ $\text{L m}^{-2} \text{h}^{-1} \text{bar}^{-1}$

4.3 Clean water data analysis

4.3.1 MBR1 clean water data analysis

The raw data is plotted against time and it is shown in Figure 4.4.

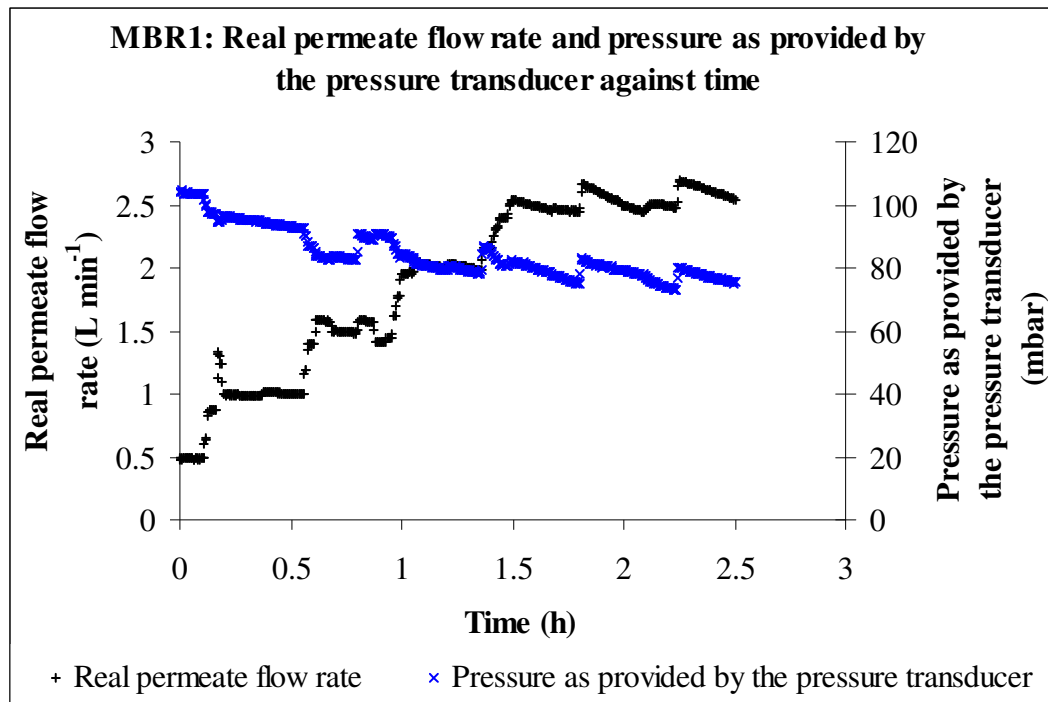


Figure 4.4 MBR1: Real permeate flow rate, $Q_{p,r,1}$, and pressure as provided by the pressure transducer, $P_{TRANC,1}$, at a clean water temperature, $T_{cw} = 34\text{ }^{\circ}\text{C}$, against time

As seen in Figure 4.4, quite good control of the lower real permeate flow rates was achieved, but at higher values of the permeate flow proportional-integral-derivative (PID) controller operated less effectively leading to more variation around the selected flow rate set-points. It can also be seen that the general trend of the pressure values as provided by the pressure transducer was decreasing over time. As permeate was flowing from the tank and operation of the feed pump was intermittent, the water level in the MBR tank reduced, resulting in a reduction in the pressure on the feed side of the membranes. As long as the pressure on the feed side of the membranes reduced and the real permeate flow rate remained practically constant, the pressure on the permeate side of the membranes had to reduce, which is shown in Figure 4.4.

Real MPFs and TMP_1 values can be calculated and are shown in Figure 4.5.

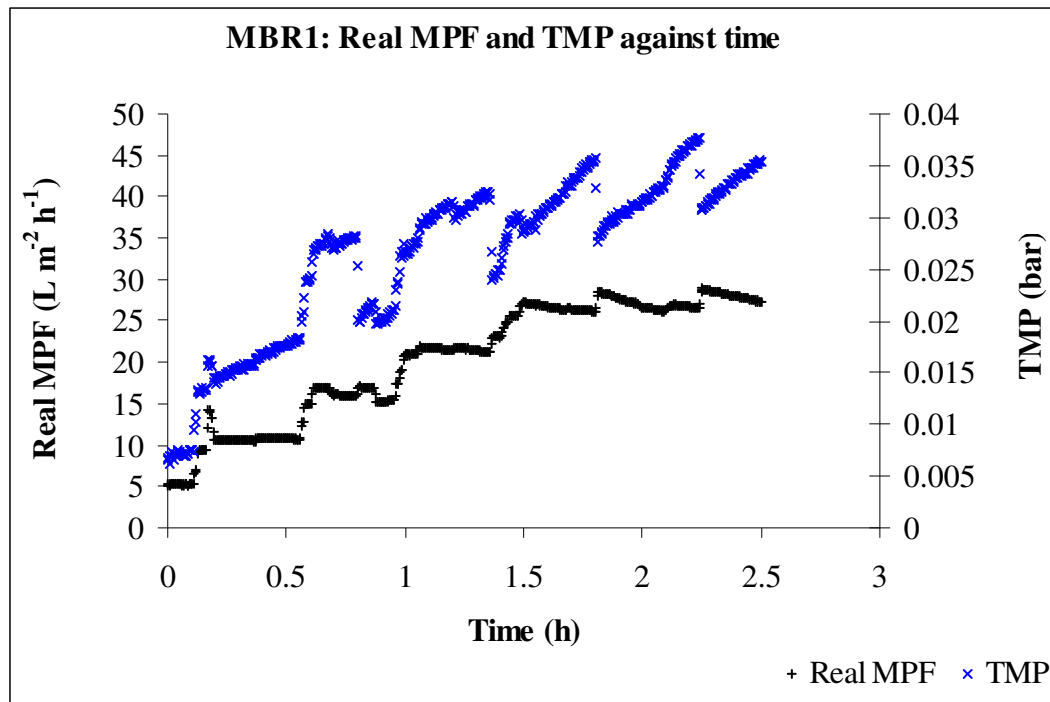


Figure 4.5 MBR1: Real MPF, $J_{p,r,1}$, and TMP_1 at a clean water temperature, $T_{cw} = 34\text{ }^{\circ}\text{C}$, against time

As seen in Figure 4.5, the membrane was operated at a range of real MPFs, from about $5\text{ L m}^{-2}\text{ h}^{-1}$ to about $30\text{ L m}^{-2}\text{ h}^{-1}$. For short-term operations and regarding the TMP values a “saw-tooth”-like phenomenon occurred. The “saw-tooth” phenomenon came from the fact that the clean water level in the MBR tank was not constant during operation, but it fluctuated between a maximum and a minimum. These changes of liquid level corresponded to changes of the pressure on the feed side of the membranes. However, the instant pressure values on the feed side of the membranes could not be measured, so a constant average value was calculated. The combination of the average pressure value on the feed side of the membranes with the real instant pressure values on the permeate values of the membranes led to the estimation of slightly distorted TMP_1 values, hence the “saw-tooth” phenomenon. In fact, as the pressure on both sides behaves in a similar way, the TMP_1 profile in reality has to be smoother than those calculation artefacts shown in calculation in Figure 4.5. During clean water tests, no membrane fouling occurs, [Bacchin *et al.*, 2006], and therefore, the true value of the TMP would be constant with time, for each of the real MPFs that were tested.

For short-term clean water experiments, the “saw-tooth” effect can be accepted, however, when conducting short-term waste water experiments, better estimates of the pressure on the feed side of the membranes must be obtained. As short-term waste water tests are usually performed in order to predict possible sustainable real/net MPFs, the TMP values must only be affected by the extent of membrane fouling rather than artefacts in calculations. As long as the pressure on the feed side of MBR1 could not be measured, the problem would be able to be resolved by maintaining the liquid level in the MBR tank at a constant value, removing the “saw-tooth” effect. This was achieved by switching the feed pump off and recycling permeate into the MBR tank using another pump. The biology in the MBR tank was not affected as recycling treated water back in the tank lasted only for a short period of time.

By plotting TMP_1 values against real MPF values, we get Figure 4.6.

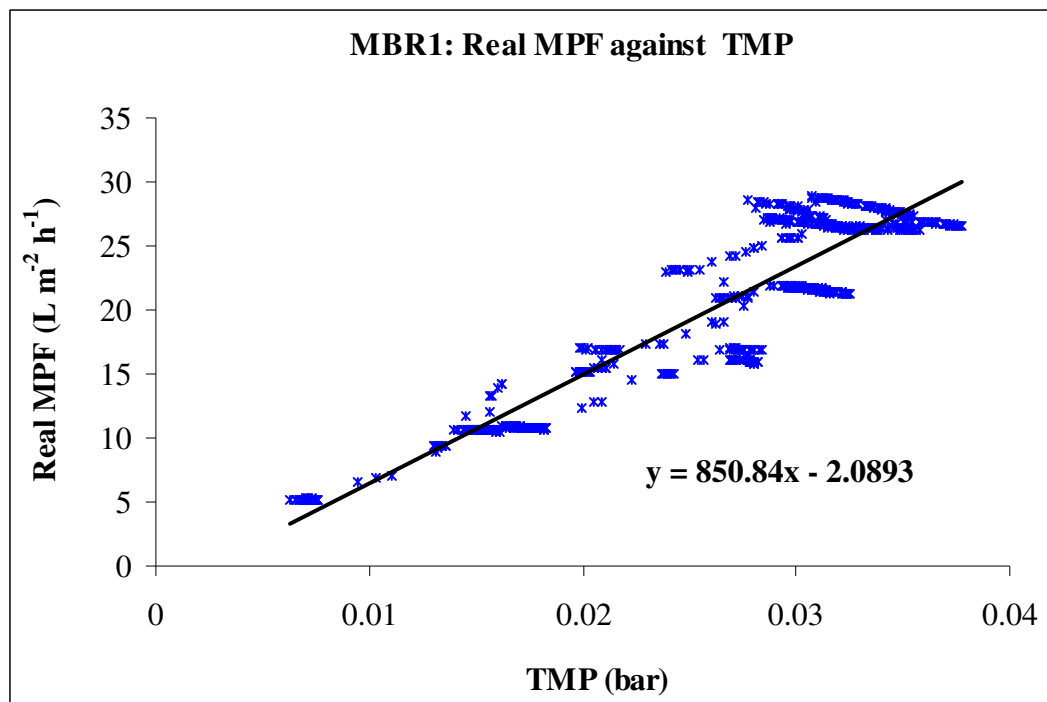


Figure 4.6 MBR1: Permeability at a clean water temperature, $T_{wc} = 34\text{ }^{\circ}\text{C}$

As seen in Figure 4.6, there are clusters of data points around the real MPFs that were tested during the tests, mainly due to the “saw-tooth” artefact. Also, the fact that the real MPF was not perfectly controlled by the PID controller led to some additional scatter. Despite the increased scatter, the regression line showed that a good linear

relationship between the TMP_1 values and the real MPFs can be obtained. The gradient of this line represents the permeability value, which is roughly equal to $850 \text{ L m}^{-2} \text{ h}^{-2} \text{ bar}^{-1}$ at $T_{cw} = 34 \text{ }^\circ\text{C}$.

The permeability value provided by the membrane manufacturer at $T_{cw} = 25 \text{ }^\circ\text{C}$ for reverse osmosis (RO) clean water is equal to $1,110 \text{ L m}^{-2} \text{ h}^{-1} \text{ bar}^{-1}$, [PURATREAT, Deliverable 6, 2009]. Both this membrane permeability value and the permeability value that was found during the tests were temperature-corrected at a T_{cw-ref} of $20 \text{ }^\circ\text{C}$. Through Equation 4.7, the temperature-corrected value for the permeability value from the clean water tests was found to be equal to $610 \text{ L m}^{-2} \text{ h}^{-1} \text{ bar}^{-1}$, whereas the temperature-corrected permeability value, as provided by the manufacturers, was found to be equal to $977 \text{ L m}^{-2} \text{ h}^{-1} \text{ bar}^{-1}$. Even though there seems to be a significant difference between the two values, it should be noted that the value provided by the manufacturer is for RO clean water, whereas the actual clean water tests were run with tap water from the domestic water supply system at the ONAS site. As the quality of water that was used during the clean water tests will not be as good as RO clean water, it is expected that the temperature-corrected permeability value for the clean water tests would be lower than the temperature-corrected permeability value provided by the membrane supplier. To conclude, both membrane permeability values are in the same range of values, and it can be assumed that the clean water tests were validated.

4.3.2 MBR2 clean water data analysis

All raw data collected during the tests is shown in Figure 4.7. In order to clarify the results, the data points during the membrane relaxation have been removed, although some of the scatter points in this figure are still a consequence of the filtration/relaxation cycle.

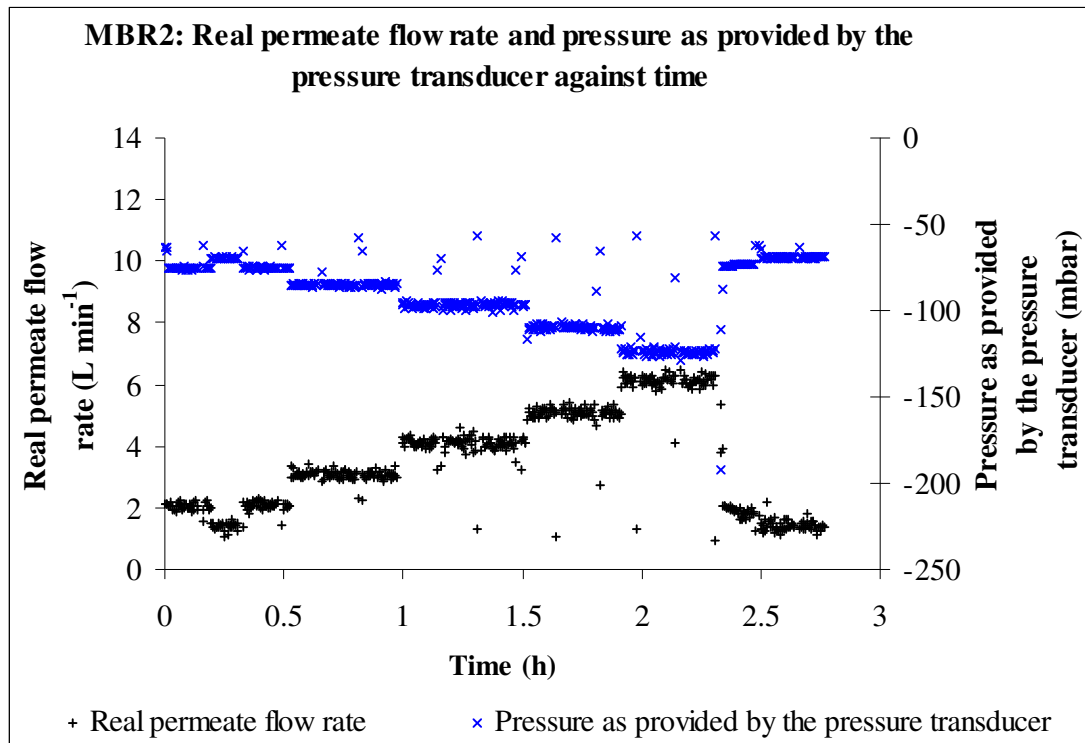


Figure 4.7 MBR2: Real permeate flow rate, $Q_{p,r,2}$, and pressure as provided by the pressure transducer, $P_{2,TRANC}$, at a clean water temperature $T_{cw} = 34\text{ }^{\circ}\text{C}$ against time

As seen in Figure 4.7, the real permeate flow rates were controlled satisfactorily during the tests. Each time the real permeate flow rate increased, the suction pressure values became more negative, or lower vacuums needed to be applied in order to maintain filtration, which is what was expected to happen.

Real MPFs and TMP values were also calculated and they are plotted against time, (Figure 4.8).

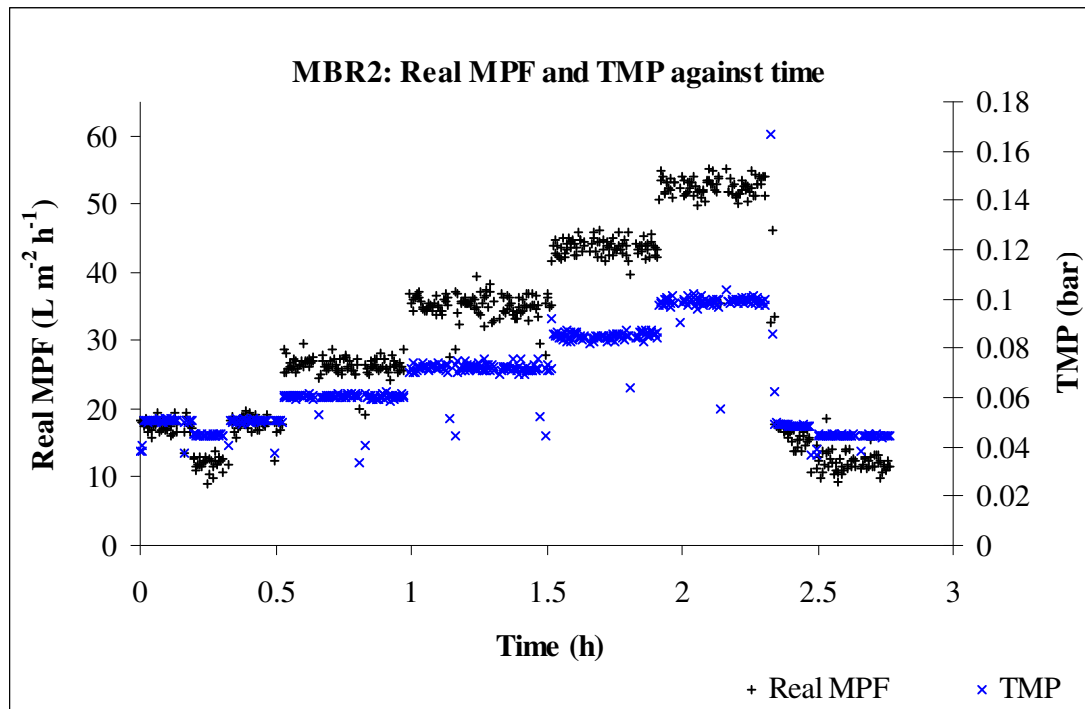


Figure 4.8 MBR2: Real MPF, $J_{p,r,2}$, and TMP_2 at a clean water temperature, $T_{cw} = 34\text{ }^{\circ}\text{C}$, against time

Figure 4.8 shows that during the clean water tests, good control of both the real MPFs and the TMP_2 values was achieved. The real MPF values ranged from a value of about $10\text{ L m}^{-2}\text{ h}^{-1}$ up to a value of about $55\text{ L m}^{-2}\text{ h}^{-1}$ and the corresponding TMP_2 values varied between 0.045 bar and 0.1 bar. Also, as expected, each time the real MPF increased, the TMP_2 values also increased. The spikes in the data in both Figure 4.7 and Figure 4.8 indicate anomalies being caused by the application of intermittent filtration.

Finally, the membrane permeability was estimated by plotting real MPFs against their corresponding TMP_2 values, (Figure 4.9).

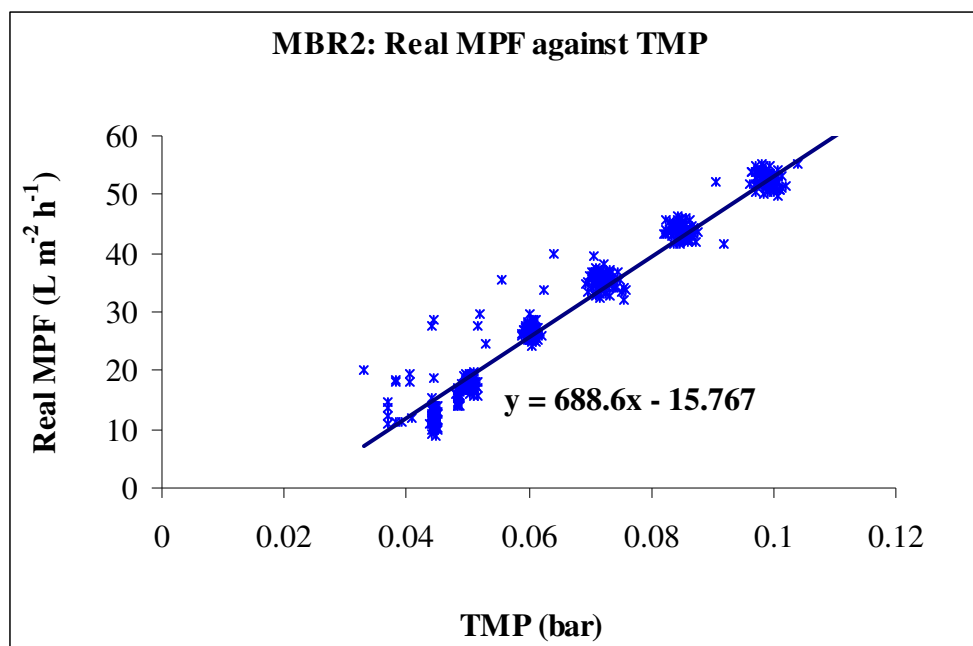


Figure 4.9 MBR2: Permeability at a clean water temperature, $T_{cw} = 34$ °C

As seen in Figure 4.9, there are clusters of data values around the real MPFs with the scatter being due to the effect of the flow controller on the flow rate values as well as the intervals of the membrane relaxation. Adding a regression line, it can be concluded that there is a linear relationship between the real MPFs that were tested and their corresponding TMP_2 values. The gradient of the line represents the membrane permeability value, which was roughly equal to $689 \text{ L m}^{-2} \text{ h}^{-2} \text{ bar}^{-1}$ at $T_{cw} = 34$ °C. The manufacturer of the membranes has provided a value of $800 \text{ L m}^{-2} \text{ bar}^{-1}$ at $T_{cw} = 25$ °C, [PURATREAT, Deliverable 6, 2009]. Both permeability values were temperature-corrected at $T_{cw-ref} = 20$ °C by using Equation 4.15. The temperature-corrected permeability values at $T_{cw-ref} = 20$ °C are $494 \text{ L m}^{-2} \text{ h}^{-2} \text{ bar}^{-1}$ for the value from the clean water tests, and $710 \text{ L m}^{-2} \text{ h}^{-2} \text{ bar}^{-1}$ for the value that was provided by the equipment supplier. The difference between these two permeability values is attributed to the poor quality of the tap water that was used during the tests, which can lead to significantly reduced membrane permeability values. This effect would be more severe for MBR2, which utilises ultrafiltration (UF) membranes, compared to MBR1 with microfilters.

4.3.3 MBR3 clean water data analysis

The raw data that was collected during the tests is presented in Figure 4.10. It is worth mentioning that the scatter data resulting from the relaxation periods have been removed from the following figures in order to clarify the real MPFs, the TMP_3 and their relationship.

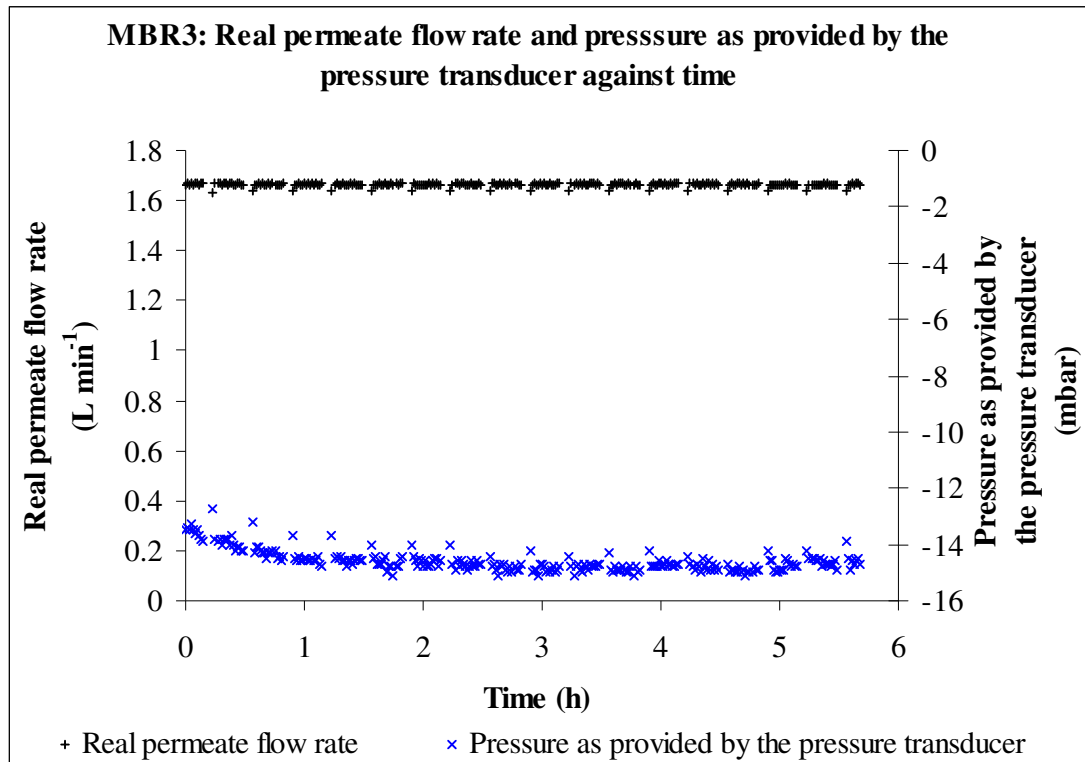


Figure 4.10 MBR3: Real permeate flow rate, $Q_{p,r,3}$, and pressure as provided by the pressure transducer, $P_{TRANC,3}$, at a clean water temperature, $T_{cw} = 34\text{ }^{\circ}\text{C}$ against time

Figure 4.10 shows that good control around the selected real permeate flow rate of 100 L h^{-1} was achieved. The pressure initially became gradually more negative before stabilising at a constant value. This means that the TMP_3 values have to slightly increase before they stabilise at a constant value. This might have occurred due to the fact that it takes some time for the membranes to become acclimatised to their operating conditions. As these membranes had recently been cleaned perhaps the early change corresponded to removal of trapped air from the membranes.

Figure 4.11 shows the real MPF and TMP_3 values.

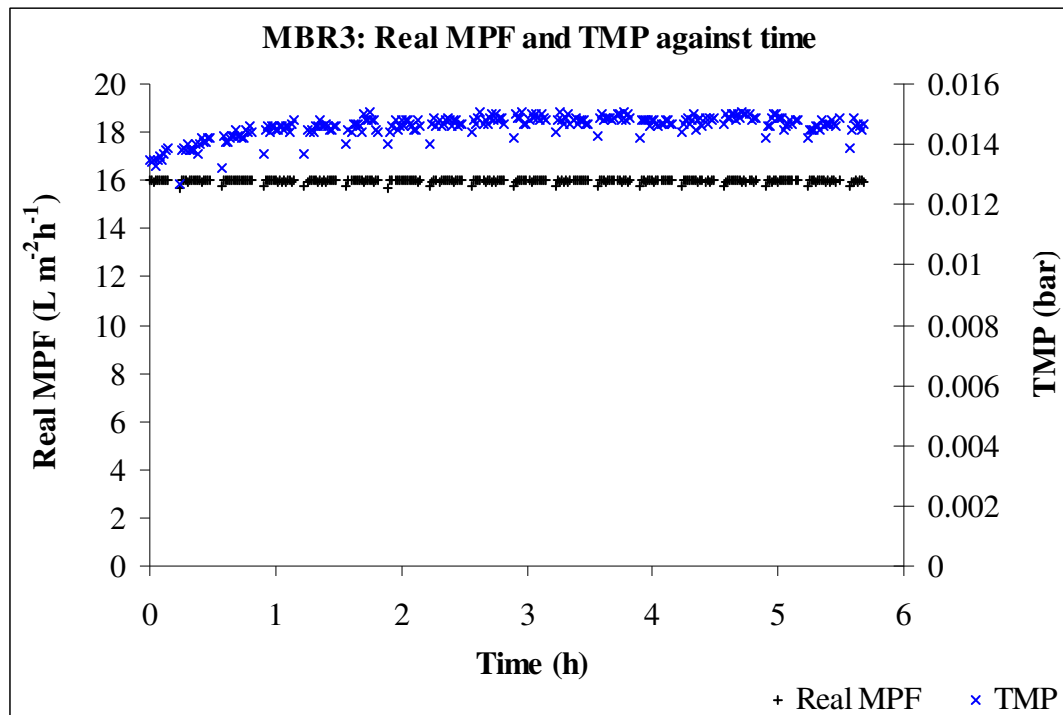


Figure 4.11 MBR3: Real MPF, $J_{p,r,3}$, and TMP_3 a clean water temperature $T_{cw} = 34$ °C against time

The real MPF was well-controlled, always remaining constant at the selected value, which was roughly equal to $16 L m^{-2} h^{-1}$. The TMP_3 slightly increased before stabilising at a value of about 0.015 bar. The spikes in Figure 4.10 and Figure 4.11 are due to the fact that filtration was intermittent.

Figure 4.12 shows membrane permeability against time. When plotting this figure, it was decided to remove the permeability values during the initial short period of time, which was characterised by changing TMP conditions.

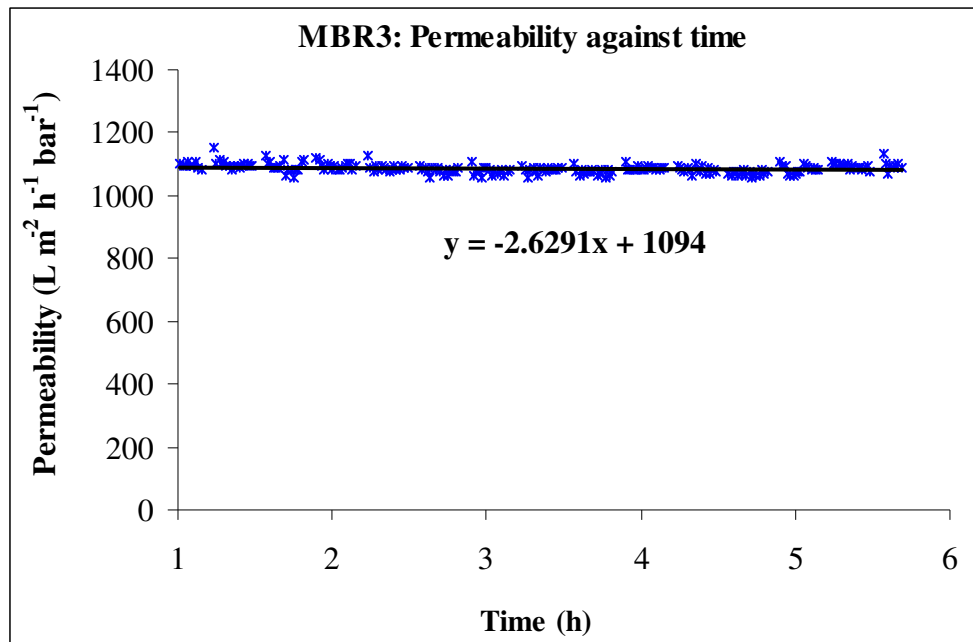


Figure 4.12 MBR3: Permeability, K_3 , at a clean water temperature $T_{cw} = 34$ °C against time

Figure 4.12 shows that the membrane permeability value was roughly equal to $1094 \text{ L m}^{-2} \text{ h}^{-1} \text{ bar}^{-1}$ at $T_{cw} = 34$ °C. The RO clean water permeability value that was provided by the membrane manufacturer at 25 °C was $700 \text{ L m}^{-2} \text{ h}^{-1} \text{ bar}^{-1}$ at 25 °C. By temperature-correcting these two values at $T_{cw-ref} = 20$ °C through Equation 4.21, the temperature-corrected permeability value with respect to the clean water tests was equal to $785 \text{ L m}^{-2} \text{ h}^{-1} \text{ bar}^{-1}$, and the temperature-corrected permeability value as provided by the manufacturers was equal to $619 \text{ L m}^{-2} \text{ h}^{-1} \text{ bar}^{-1}$. It should be expected that the value from the manufacturer would have been higher than that from the test on site as the water used by the manufacturer was of better quality than that which was used during the clean tests. The difference can be explained by the fact that the default calibration of the pressure transducer could not cope with a floating membrane module, such that the estimated TMP value during the on site test was incorrect.

4.4 Conclusions

Short-term clean water tests were performed and, as an overall conclusion, it can be said that membrane performance was obtained as expected. Regarding MBRs, clean water tests are usually performed before they are operated with waste water. In

general, a MPF/TMP profile relating to clean water tests is as follows, [Bacchin *et al.*, 2006]:

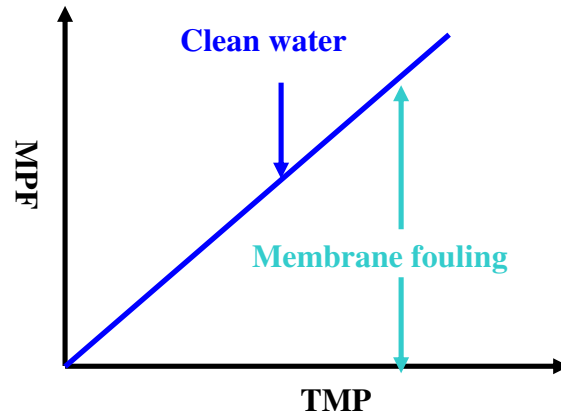


Figure 4.13 MPF/TMP profile when clean/waste water is filtered, [Bacchin *et al.*, 2006]

As seen in Figure 4.13, the values of the TMP are constant with time, always at a different value depending on the real/net MPF that is being tested. Also, the gradient of the straight line is the permeability of the membrane, which is reversely proportional to the resistance applied against filtration. When filtering clean water, the permeability is always constant and system-specific and it obtains its maximum value. Clean water tests can provide a baseline, with respect to membrane performance. When clean water is replaced by waste water, MBRs operate in the membrane fouling area, as seen in Figure 4.13. This happens due to the fact that membrane fouling phenomena decrease the membrane permeability. Clean water data can then be used as a point of reference for any future operation of the MBRs in order to evaluate membrane fouling. Also, the efficiency of the physical/chemical cleanings against reversible/irreversible membrane fouling can be calculated.

Regarding MBR1 and MBR2, the flux-step tests that were applied were successful leading to good control of both real MPFs and TMP values. Permeability values were found to be lower than expected when compared with the values that were provided by the membrane manufacturers. This can be attributed to the fact that the manufacturers used RO water when conducting their tests, whereas local tap water was used at the ONAS site when the clean tests were performed.

On the other hand, clean water tests with regard to MBR3 operation led to a membrane permeability value higher than the one that was provided by the membrane manufacturer. This was caused due to the pressure transducer and its default calibration. Also, it was only one value of real MPF that was tested and not a number of real MPFs, which can also affect the validity of the membrane permeability.

In Chapter 5 and Chapter 6, clean water was replaced with waste water and the MBRs were operated under real conditions applied to any WWT plant. Chapter 5, which follows, particularly analyses the effect of different sets of solids residence times (SRTs) and hydraulic residence times (HRTs), and helps conclude whether or not treated permeate of the appropriate quality was produced by the three MBR systems.

CHAPTER 5 EFFECT OFF VARIATION IN THE SRT AND THE HRT ON THE MBR PERFORMANCE

5.1 Introduction

This chapter describes the performance of the three membrane bioreactor (MBR) systems and analyses the changes of the mixed-liquor suspended solids (MLSS) concentrations during the long-term experiments, together with the changes of the influent/effluent chemical oxygen demand (COD) concentrations. The MLSS concentrations represent the biomass changes within the MBR tanks and the effluent COD concentrations represent the quality of the treated permeate, thus, it can be seen whether the membrane bioreactors (MBRs) succeeded in producing treated permeate of the appropriate quality or not. In this research, the produced treated permeate is intended for reuse in unrestricted irrigation in Tunisia - the COD concentration values in the effluent should be equal to or lower than 90 mg L^{-1} according to the Tunisian standard.

The inoculum sludge was taken from the full-scale waste water treatment (WWT) plant at the North Sfax “Office National de l' Assainissement” (ONAS) site - a plant operating a conventional activated sludge (AS) process. Samples of mixed-liquor from all MBR systems were taken on a regular basis in order to measure both the MLSS concentrations within the MBR tanks and the influent/effluent COD concentration values. The operating conditions, namely solids residence times (SRTs) and hydraulic residence times (HRTs) that were applied corresponded either to an MLSS concentration of about $4 - 5 \text{ g L}^{-1}$ or to an MLSS concentration of about $9 - 10 \text{ g L}^{-1}$. The low MLSS concentration value of $4 - 5 \text{ g L}^{-1}$ was selected because it is the normal operating value for the full-scale conventional AS plant at the ONAS site. The higher MLSS concentration value of $9 - 10 \text{ g L}^{-1}$ was selected after taking into account suggestions from the MBR manufacturers about the optimum MLSS concentrations within the MBR tanks.

Based on the measured MLSS/effluent COD concentrations, direct comparisons with respect to the biological performance both among the MBRs and between the MBRs

and the full-scale conventional AS plant were made. The instant COD concentration values in the feed were identical for all three MBRs and the conventional AS plant.

In addition to the MLSS and the influent/effluent COD concentrations, the mixed-liquor volatile suspended solids (MLVSS) and the influent/effluent 5-day biochemical oxygen demand (BOD₅) concentrations were also measured but these measurements were not taken on such a regular basis for practical reasons. Whilst these values will not be used to describe the biological performance of the MBR systems, it is good practice to measure both COD and BOD₅ concentrations before discharging treated water into water bodies. As the SRTs and the HRTs were both successfully regulated during the long-term experiment, and the MLSS or MLVSS and the COD or BOD₅ concentrations were measured, a model based on an Excel spreadsheet was successfully calibrated and validated so as to predict the kinetic and stoichiometric parameters, that is to say K_S , k (μ_{\max}), k_d , and $Y_{X/S}$ for each MBR system. Details about the model will be given in Chapter 7.

A brief summary regarding the most important mass balance equations used in this chapter is provided in Table 5.1. All the parameters mentioned in Table 5.1 are defined in detail in Chapter 2.

Table 5.1 Mass balance equations linking MLSS/MLVSS concentrations, HRTs, SRTs and COD/BOD₅ concentrations

Equation	Equation number as given in Chapter 2
$Q_f = Q_p + Q_w$	2.11
$\theta = \frac{V}{Q_f}$	2.15
$S = S_f - \frac{X\theta\mu}{Y_{X/S}}$	2.16
$X = \frac{Y_{X/S}(S_f - S)}{\theta\mu}$	2.17
$\theta_c = \frac{V}{Q_w}$	2.23
$\mu = \frac{1}{\theta_c}$	2.24
$\mu = \frac{1}{\theta_c} = \frac{\mu_{\max} S}{(K_S + S)} - k_d$	2.25

The equations shown in Table 5.1 describe the relationship between the MLSS concentrations, X , the COD concentrations both in the feed, S_f , and in the permeate, S , the SRTs, θ_C , and the HRTs, θ . Some commentary is as follows:

The sludge age (solids residence time (SRT)) is the parameter, which is usually regulated, as shown in Equation 2.23, by simply adjusting the sludge wasting rate, Q_w , to a constant value for a constant operating volume, V . In some MBRs, like MBR1 and MBR2, it is common for the operating volume to be subject to small changes during filtration. However, these changes of the operating volume are normally very small and a satisfactory average value is accepted. The SRT is capable of regulating the specific biomass growth rate, μ , - these two values are reversely proportional as can be seen in Equation 2.24. Bacteria are then forced to grow to a specific μ -value. As the COD concentration in the effluent, S , is a consequence of the μ -value, the S -value can also be regulated as long as the kinetic parameters μ_{max} , K_S and k_d , which are defined in Section 2.2.2, are constant.

The biomass within the MBR tanks has to be controlled so that the effluent COD concentration (or BOD₅ concentration), S , satisfies a target value depending on further uses of treated water, *i.e.* unrestricted irrigation, direct discharge into rivers/lakes, etc. In this research, the S -value had to be regulated so that the treated water could be re-used for unrestricted irrigation in Tunisia, - effluent COD concentrations must be equal to or lower than 90 mg L⁻¹, or BOD₅ concentrations must be equal to or lower than 30 mg L⁻¹, [North Sfax ONAS archives, 2009].

The hydraulic residence time (HRT), θ , can also be easily fixed at a selected value by simply regulating the feed flow rate, Q_f , or by regulating the sludge wasting rate, Q_w , and the permeate flow rate, Q_p , both of which are possible and subject only to small fluctuations as seen in Equation 2.11 and Equation 2.15. As seen in Equation 2.17, the X -value is a function of θ , μ (θ_C), S and S_f , assuming that the stoichiometric parameter $Y_{X/S}$ remains constant. Then, the MLSS concentration, X , is controlled. The only problem is that the feed concentration is not constant, so the S_f -value, which represents the influent COD concentration, always changes. As it is impossible to control this parameter, MLSS concentrations may slightly vary - this is not untypical for WWT plants. However, the profile of the S_f -value over time is not subject to

extreme changes and the X-value can be satisfactorily controlled. If a big increase in the S_f -value occurs, or if a big decrease in the S_f -value happens, the instant MLSS concentrations will also change. The effect of the variation in the operating conditions regarding the performance of each MBR system is analysed in the following sections.

5.2 Biomass-related data analysis

Measurements of the MLSS concentrations for each MBR system are now provided. The time periods, as defined in this section, are based on the days the waste water samples were collected.

5.2.1 MBR1: The course of MLSS concentration

Measurements of biomass concentrations were taken for about 9.5 months, from start of September 2008 until mid-June 2009. The whole experiment can be divided into four research time periods. These time periods are summarised in Table 5.2, and will allow determination of the changes of the MLSS concentrations within membrane bioreactor 1 (MBR1).

Table 5.2 MBR1: Research periods with respect to the changes of the MLSS concentration

Time period (dates)	Average MLSS concentration (g L^{-1})	+/- Variation of the average MLSS concentration	
		- From maximum value	+ From minimum value
1. 03-09-2008 until 06-12-2008	4.643	-1.461	+1.467
2. 07-12-2008 until 24-01-2009	No measurements	N/A	N/A
3. 25-01-2009 until 08-02-2009	Transition period 4.643 to 9.658	N/A	N/A
4. 09-02-2009 until 16-06-2009	9.658	-3.052	+2.808

The +/- variation simply represents the numerical difference, which was estimated when the average MLSS concentration value was subtracted from the maximum or

the minimum MLSS concentration value. These values define the range of the MLSS concentrations that were measured during the long-term experiment.

1. Time period from 03-09-2008 until 06-12-2008

During this time period, the MLSS concentration was controlled around 4 - 5 g L⁻¹. MBR1 was seeded with inoculum sludge of an initial MLSS concentration value of 5.4 g L⁻¹. Sludge started being wasted manually immediately after the inoculation, once a day or a few times a week, in order to fix the initial SRT at 15 d. The initial HRT value was fixed at 1.01 d by properly adjusting the real permeate flow rate. The values of these operating conditions could increase but they can still maintain the MLSS concentration at the selected value of about 4 - 5 g L⁻¹. It is worth mentioning that any time the real permeate flow rate, or the real membrane permeate flux (MPF), need to be adjusted to a new value, the HRT is subject to change. In order to successfully control the MLSS concentrations around the selected value, the SRT has to be slightly adjusted as well. In addition, both the SRT and the HRT are subject to instant small changes due to the fact that both the sludge wasting rate and the feed flow rate fluctuate no matter how properly they have been controlled. Sludge wasting did not take place automatically but manually, along with the fact that it was not a continuous process. With regard to the feed flow rate, as long as both the real permeate flow rate, whose values used to fluctuate around the selected set-point, and the sludge wasting rate were not constant, the instant feed flow rate was also subject to small changes. However, despite these changes the average SRT and the average HRT values are assumed not to be affected.

All operating conditions applied during this research period are shown in Table 5.3. During this research period, only one set of SRT/HRT was applied, namely [SRT, HRT]: [15 d, 1.01 d]. Filtration was continuous, so during this research period both net and real permeate flow rates/membrane permeate fluxes (MPFs) were identical. Details about the difference between real and net MPFs during intermittent filtration, where appropriate, are available in Chapter 6. All real/net permeate flow rates that were used to in order fix the SRT and the HRT at the selected values were calculated with the aid of the Excel-based model.

Table 5.3 MBR1: Time period from 03-09-2008 until 08-12-2008: Presentation of the operating conditions

Parameter	Data	Unit
Operating volume	1.38	m ³
Feed flow rate	1.365	m ³ d ⁻¹
HRT	1.01	d
Sludge wasting rate	0.092	m ³ d ⁻¹
SRT	15	d
Net permeate flow rate	1.273	m ³ d ⁻¹
Net MPF	9.47	L m ⁻² h ⁻¹
MLSS concentration	4.643	g L ⁻¹
Filtration	Continuous	–

During this research time period, the MLSS concentrations were fluctuated from a maximum of 6.104 g L⁻¹ to a minimum of 3.176 g L⁻¹, mainly due to fluctuation in concentration of the organic matter in the feed. An average value of 4.643 g L⁻¹ was estimated and it was accepted to be the biomass concentration during this time period.

On 07-12-2008, MBR1 operation was forced to be suspended as unstable membrane performance was observed. A failure in the air pipe line led to serious membrane fouling formation and although aeration was immediately restored the MBR continued to suffer from membrane fouling. The MBR system was shut down and chemical cleaning was applied. The biomass was maintained in another tank with aeration for a short period of time and some additional MLSS concentration measurements were taken - until 06-12-2008. On 06-12-2008 the MLSS concentration was measured and it was found that it had been reduced to a value of 3.781 g L⁻¹. It was then decided to stop maintaining the biomass and to re-seed the MBR1 system with new biomass when it was re-started.

2. Time period from 07-12-2008 until 24-01-2009

During this time period, no MLSS concentration measurements were taken, as the MBR1 operation was suspended.

3. Time period from 25-01-2009 until 08-02-2009

The MBR system was re-started and having been re-seeded with biomass, of an initial concentration of 5.4 g L^{-1} . The biomass was left to establish and increase. Initially biomass was not wasted so as to speed up the growth of bacteria. Then, the SRT was adjusted to 30 d with biomass being wasted once a day or a few times a week, and the HRT was adjusted to 1.01 d. This set of operating conditions resulted in an increase of the biomass concentration up to about $9 - 10 \text{ g L}^{-1}$, which was the new selected MLSS concentration value. At the end of this time period, the MLSS concentration had reached a value of 9.48 g L^{-1} .

4. Time period from 09-02-2009 until 16-06-2009

During this research period, the MLSS concentration was controlled to $9 - 10 \text{ g L}^{-1}$. Sludge was still wasted on a regular basis, once a day or a few times over a week. Initially, the SRT was still equal to 30 d and the HRT was equal to 1.01 d. However, during this time period, the operating conditions were continuously altered, as different real/net MPFs had to be tested - this is connected with the membrane performance analysis, which is described and analysed in Chapter 6. The combinations of the selected SRTs/HRTs were able to successfully control the MLSS concentration around the selected value of $9 - 10 \text{ g L}^{-1}$. Each time a new shorter HRT was selected to be applied in order to increase the average net MPF, the SRT value had to be respectively adjusted, or otherwise the MLSS concentration would not be able to be successfully controlled. This can be explained as follows: The product $[X \cdot \theta]$ is always constant, so each time the HRT value decreases the MLSS concentration is subject to increase. However, by reducing the SRT the MLSS concentration could be maintained at around the selected value.

The sets of SRT/HRT values that were applied during this research period are shown in Table 5.3, together with their corresponding operating conditions. It is also worth mentioning that during this time period an attempt to operate an intermittent MBR process with a filtration/relaxation cycle equal to 19/1 min/min on/off was made. The intermittent filtration started on 28-02-2009 and finished on 16-04-2009. This has

been taken into account when Table 5.4 was produced. More details about the intermittent MBR1 operation will be given in Section 6.3.2.3.

Table 5.4 MBR1: Time period from 09-02-2009 until 16-06-2009: Presentation of the operating conditions

Parameter	Sets of data					Unit
	1 st	2 nd	3 rd	4 th	5 th	
Time period	09-02-2009 until 17-02-2009	18-02-2009 until 23-04-2009	24-04-2009 until 05-05-2009	06-05-2009 until 07-06-2009	08-06-2009 until 16-06-2009	date
Operating volume	1.38	1.38	1.38	1.38	1.38	m ³
Feed flow rate	1.365	1.515	1.651	1.79	1.914	m ³ d ⁻¹
HRT	1.01	0.91	0.835	0.77	0.72	d
Sludge wasting rate	0.046	0.048	0.054	0.059	0.063	m ³ d ⁻¹
SRT	30	29	25.5	23.5	21.8	d
Net permeate flow rate	1.319	1.467	1.596	1.731	1.851	m ³ d ⁻¹
Net MPF	9.81	10.92	11.88	12.88	13.77	L m ⁻² h ⁻¹
MLSS concentration	9.528	10.168	9.013	8.846	9.259	g L ⁻¹
Filtration	Continuous	Continuous	Intermittent (19/1)	Continuous	Continuous	min on/min off

During this time period, the MLSS concentration fluctuated from a maximum value of 12.71 g L⁻¹ to a minimum value of 6.85 g L⁻¹. This was a consequence of the fluctuations of the COD values in the feed. Table 5.4 shows the average MLSS concentration values as they were calculated for each pair of SRT/HRT. Also, an average MLSS concentration was calculated for the whole time period and it was found to be equal to 9.658 g L⁻¹, which indicates that good control of the MLSS concentration around the selected value was achieved.

The course of the MLSS concentration against time is shown in Figure 5.1.

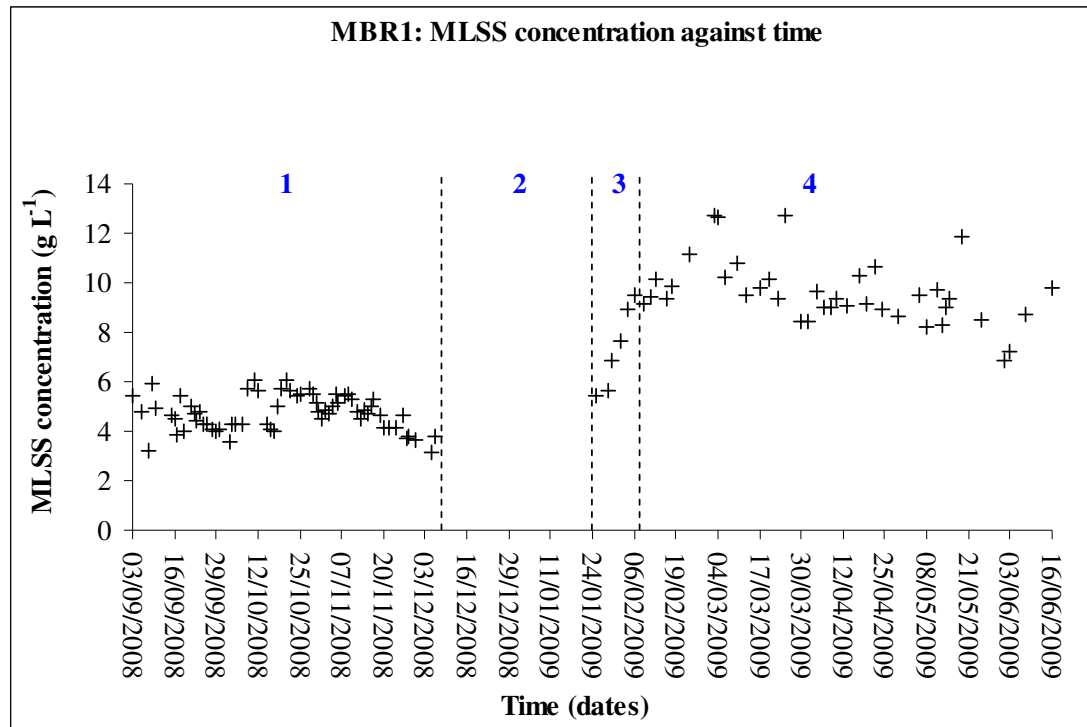


Figure 5.1 MBR1: MLSS concentration against time - **1.** From 03-09-2008 until 06-12-2008: Average MLSS concentration, $X_{MLSS} = 4.643 \text{ g L}^{-1}$, SRT, $\theta_C = 15 \text{ d}$, HRT = 1.01 d. From now on only the symbols of the parameters will be used. **4.** From 09-02-2009 until 17-02-2009: $X_{MLSS} = 9.528 \text{ g L}^{-1}$, $\theta_C = 30 \text{ d}$, $\theta = 1.01 \text{ d}$, From 18-02-2009 until 23-04-2009: $X_{MLSS} = 10.168 \text{ g L}^{-1}$, $\theta_C = 29 \text{ d}$, $\theta = 0.91 \text{ d}$, From 24-04-2009 until 05-05-2009: $X_{MLSS} = 9.013 \text{ g L}^{-1}$, $\theta_C = 25.5 \text{ d}$, $\theta = 0.835 \text{ d}$, From 06-05-2009 until 07-06-2009: $X_{MLSS} = 8.846 \text{ g L}^{-1}$, $\theta_C = 23.5 \text{ d}$, $\theta = 0.77 \text{ d}$, From 08-06-2009 until 16-06-2009: $X_{MLSS} = 9.259 \text{ g L}^{-1}$, $\theta_C = 21.8 \text{ d}$, $\theta = 0.72 \text{ d}$, (**2.** MBR1 was not operational, **3.** Transition period)

As seen in Figure 5.1, quite good control of the biomass concentration was achieved both for the low and the higher biomass concentration set-points. Some fluctuation appears and this can be attributed to the fact that sludge wasting was not a continuous process but it took place manually once a day, or a few times a week. This could lead to measurements that were affected by the time during which the mixed-liquor sample was collected. Collection of the sample just before or just after sludge wasting can lead to two different MLSS concentrations. In addition, as long as sludge is removed manually from the MBR tank, the amount of sludge, which was removed, could also be subject to human error. However, the most possible explanation is that these

fluctuations were very likely to be due to variation in the feed waste water composition, or the S_f -value, a parameter that was impossible to control. To conclude, it can be said that MBR1 was operated well around the two different MLSS values, and the scatter in the data was not untypical for a WWT plant.

5.2.2 MBR2: The course of MLSS concentration

Even though the membrane bioreactor 2 (MBR2) system was operational from 02-09-2008, very few biological measurements were taken before 07-11-2008. During this time period, a number of operational teething problems were addressed via minor modifications to the equipment. MBR2 was successfully re-started on 07-11-2008 and the system operated as it should. Filtration, during the long-term experiment, was intermittent with a filtration/relaxation cycle equal to 9/1 min/min on/off, so all permeate flow rates/MPFs, which will be mentioned in this section, are net values.

With regard to the changes of the MLSS concentrations, measurements were taken for about 7.5 months, from start of November 2008 until mid-June 2009, and this time period can be divided into three shorter time periods, which will allow better determining all changes of the MLSS concentration values. Samples of the mixed-liquor were taken from the biological tank of the MBR system. The time periods are summarised in Table 5.5.

Table 5.5 MBR2: Research periods with respect to the changes of the MLSS concentration

Time period (dates)	Average MLSS concentration (g L ⁻¹)	+/- Variation of the average MLSS concentration	
		- From maximum value	+ From minimum value
1. 07-11-2008 until 03-01-2009	4.592	-0.958	+2.092
2. 04-01-2009 until 29-01-2009	Transition period 4.592 to 9.523	N/A	N/A
3. 30-01-2009 until 16-06-2009	9.523	-1.567	+1.553

1. Time period from 07-11-2008 until 03-01-2009

Upon start-up, the MBR2 system was seeded with biomass of 4.292 g L^{-1} . Sludge was wasted manually immediately after the inoculation once a day, or, at least, a few times over a week. The SRT value was set to 15 d and the HRT was set to 1.01 d, a combination of operating conditions that should maintain the biomass concentration at about $4 - 5 \text{ g L}^{-1}$.

Table 5.6 shows the operating conditions that were applied during this time period.

Table 5.6 MBR2: Time period from 07-11-2008 until 03-01-2009: Presentation of the operating conditions

Parameter	Data	Unit
Operating volume	2.02	m^3
Feed flow rate	2.002	$\text{m}^3 \text{ d}^{-1}$
HRT	1.01	d
Sludge wasting rate	0.135	$\text{m}^3 \text{ d}^{-1}$
SRT	15	d
Net permeate flow rate	1.867	$\text{m}^3 \text{ d}^{-1}$
Net MPF	11.12	$\text{L m}^{-2} \text{ h}^{-1}$
MLSS concentration	4.592	g L^{-1}
Filtration	Intermittent (9/1)	min on/min off

Measurements of the MLSS concentrations, which fluctuated from a maximum value of 5.55 g L^{-1} to a minimum value of 2.5 g L^{-1} , were taken. These fluctuations are mainly attributed to the variation in the composition of the feed. However, an average value of 4.592 g L^{-1} can be estimated showing that the MLSS concentration was successfully controlled around the selected set-point of about $4 - 5 \text{ g L}^{-1}$.

2. Time period from 04-01-2009 until 29-01-2009

During this transition time period, biomass was allowed to grow in order to reach higher values in the range of 9 - 10 g L⁻¹. The SRT was set to 30 d and the HRT was set to 1.01 d, a set of operating conditions that can successfully stabilise the MLSS concentration at about 9 - 10 g L⁻¹.

3. Time period from 30-01-2009 until 16-06-2009

Biomass was still wasted but this time sludge wasting occurred automatically as a sludge pump had been connected with the MBR2 system in the mean time. However, the operation of the pump was not continuous and sludge was wasted a few times a day. Initially, the SRT was still equal to 30 d and the HRT was still equal to 1.01 d. As the membrane performance had also to be tested during this time period, different real/net MPFs had to be applied. Different real/net MPFs indicate different HRTs, so the SRTs had also to be adjusted. The sets of SRTs/HRTs, which were applied during this time period, together with the rest of the operating conditions, are shown in Table 5.7.

Table 5.7 MBR2: Time period from 30-01-2009 until 16-06-2009: Presentation of the operating conditions

Parameter	Sets of data			Unit
	1 st	2 nd	3 rd	
Time Period	30-01-2009 until 07-04-2009	08-04-2009 until 28-04-2009	29-04-2009 until 16-06-2008	date
Operating volume	2.02	2.02	2.02	m ³
Feed flow rate	2.002	2.222	2.422	m ³ d ⁻¹
HRT	1.01	0.91	0.835	d
Sludge wasting rate	0.067	0.07	0.079	m ³ d ⁻¹
SRT	30	29	25.5	d
Net permeate flow rate	1.935	2.153	2.343	m ³ d ⁻¹
Net MPF	11.52	12.81	13.94	L m ⁻² h ⁻¹
Average MLSS concentration	9.687	9.206	9.379	g L ⁻¹
Filtration	Intermittent (9/1)	Intermittent (9/1)	Intermittent (9/1)	min on/min off

The average MLSS concentration during this time period was found to be equal to 9.424 g L⁻¹. The maximum MLSS concentration value that was recorded was equal to 11.09 g L⁻¹ and a minimum value was equal to 7.97 g L⁻¹. In addition, in Table 5.7 there are also shown the average MLSS concentrations for each specific set of SRT/HRT. The operation of an automatic sludge pump did not succeed in providing a smoother profile regarding the biomass concentrations and some scatter appeared again. As long as excess sludge was not wasted continuously, this scatter was inevitable. However, it was the unstable concentration of the feed stream that mainly caused the fluctuations in the MLSS concentration measurements. Despite the fluctuations, the average MLSS concentration of 9.424 g L⁻¹ showed that, in general, the MLSS concentration was controlled as required.

The course of MLSS concentration against time is shown in Figure 5.2.

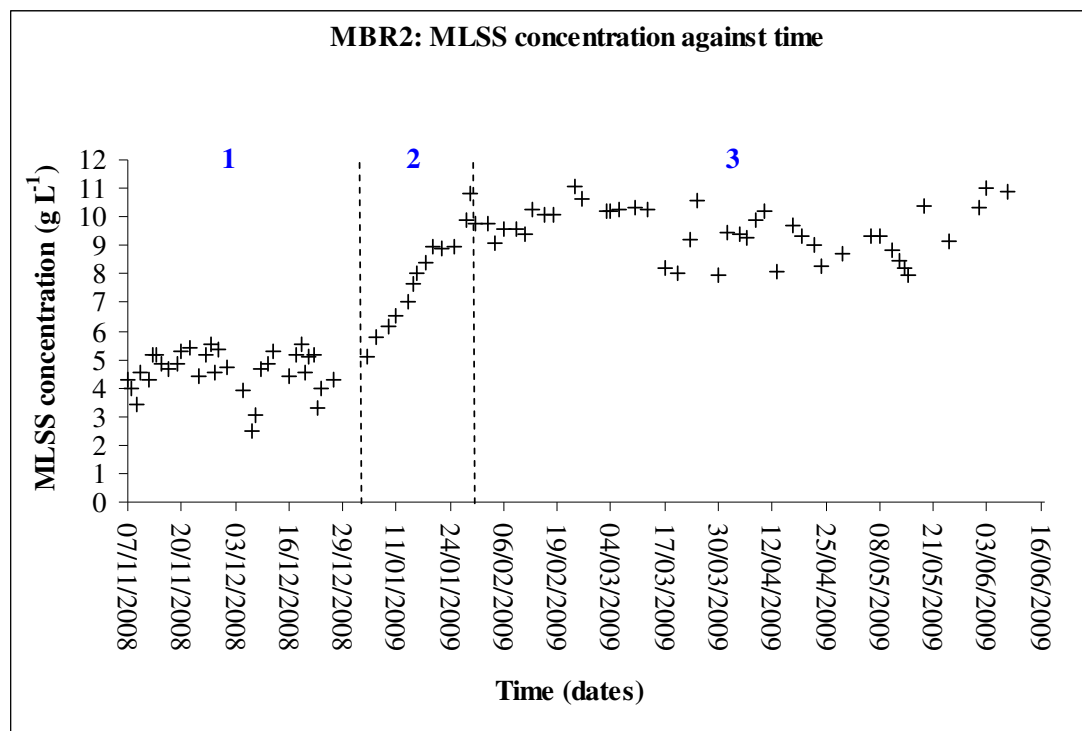


Figure 5.2 MBR2: MLSS concentration against time - **1.** From 07-11-2008 until 03-01-2009: $X_{MLSS} = 4.592 \text{ g L}^{-1}$, $\theta_C = 15 \text{ d}$, $\theta = 1.01 \text{ d}$, **3.** From 30-01-2009 until 07-04-2009: $X_{MLSS} = 9.687 \text{ g L}^{-1}$, $\theta_C = 30 \text{ d}$, $\theta = 1.01 \text{ d}$, From 08-04-2009 until 28-04-2009: $X_{MLSS} = 9.206 \text{ g L}^{-1}$, $\theta_C = 29 \text{ d}$, $\theta = 0.91 \text{ d}$, From 29-04-2009 until 16-06-2009: $X_{MLSS} = 9.379 \text{ g L}^{-1}$, $\theta_C = 25.5 \text{ d}$, $\theta = 0.835 \text{ d}$, **(2.** Transition period)

5.2.3 MBR3: The course of MLSS concentration

Membrane bioreactor 3 (MBR3) started-up on 02-09-2008 but an operational problem appeared, as the membrane module kept floating near the surface rather than sitting at the bottom of the filtration tank. The membrane module became fouled very quickly and, on 11-10-2008, the operation was suspended to avoid the risk of seriously damaging the membranes. During this period of time, very few measurements in terms of the biology were taken. MBR3 was re-started on 10-11-2008, with the membrane module fixed to the bottom of the filtration tank. Biological measurements started being continually taken from 19-11-2008 until 16-06-2009. As with MBR1 and MBR2, MBR3 was initially operated under a low MLSS concentration of about 4 - 5 g L^{-1} , which was later increased to a value of about 9 - 10 g L^{-1} . Filtration was intermittent with an applied filtration/relaxation cycle equal to 17/3 min/min on/off. All permeate flow rates/MPFs mentioned in this section are net values.

With regard to the changes of the MLSS concentrations, four time periods can be defined and are summarised in Table 5.8.

Table 5.8 MBR3: Research periods with respect to the changes of the MLSS concentration

Time period (dates)	Average MLSS concentration (g L^{-1})	+/- Variation of the average MLSS concentration	
		- From maximum value	+ From minimum value
1. 19-11-2008 until 03-01-2009	4.033	-1.908	+1.263
2. 04-01-2009 until 05-02-2009	Transition period 4.033 to 9.043	N/A	N/A
3. 06-02-2009 until 05-05-2009	9.043	-2.637	+2.923
4. 06-05-2009 until 16-06-2009	5.043	-2.267	+2.09

1. Time period from 11-11-2008 until 03-01-2009

MBR3 was inoculated with sludge of 4.05 g L^{-1} . As the concentration of the sludge was already around the selected value of about $4 - 5 \text{ mg L}^{-1}$, sludge was manually wasted immediately after the inoculation. The SRT was adjusted to 15 d and the HRT was adjusted to 1.01 d, a pair of operating conditions that can control the MLSS concentration around $4 - 5 \text{ g L}^{-1}$. The operating conditions during this time period are presented in Table 5.9.

Table 5.9 MBR3: Time period from 19-11-2008 until 03-01-2009: Presentation of the operating conditions

Parameter	Data	Unit
Operating volume	2.21	m ³
Feed flow rate	2.184	m ³ d ⁻¹
HRT	1.01	d
Sludge wasting rate	0.147	m ³ d ⁻¹
SRT	15	m
Net permeate flow rate	2.037	m ³ d ⁻¹
Net MPF	13.58	L m ⁻² h ⁻¹
MLSS concentration	4.033	g L ⁻¹
Filtration	Intermittent (17/3)	min on/min off

Based on Table 5.9, an average MLSS concentration of 4.033 g L⁻¹ was calculated - during this time period, the MLSS concentration fluctuated from a minimum value of 2.77 g L⁻¹ to a maximum value of 5.941 g L⁻¹, mainly due to the changes of the concentration of the organic matter in the feed. However, the average MLSS concentration value indicates that the MLSS concentration was well-controlled.

2. Time period from 04-01-2009 until 05-02-2009

This is the transition time period, during which biomass concentration was increased from a low value to the higher selected value of about 9 - 10 g L⁻¹. The SRT was fixed at 30 d and the HRT was fixed at 1.01 d, and biomass was left to spontaneously increase. The selected operating conditions were able to both increase and stabilise the biomass concentration around the selected value of 9 - 10 g L⁻¹.

3. Time period from 06-02-2009 until 05-05-2009

During this time period, the biomass concentration had stabilised around 9 - 10 g L⁻¹. Sludge wasting was performed with the aid of a sludge pump, which had been newly

installed, so excess sludge was wasted a few times over a day. The operating conditions that were applied are given in Table 5.10.

Table 5.10 MBR3: Time period from 06-02-2009 until 16-06-2009: Presentation of the operating conditions

Parameter	Sets of data			Unit
	1 st	2 nd	3 rd	
Time Period	06-02-2009 until 07-04-2009	08-04-2009 until 25-04-2009	26-04-2009 until 05-05-2009	date
Operating volume	2.21	2.21	2.21	m ³
Feed flow rate	2.184	2.424	2.642	m ³ d ⁻¹
HRT	1.01	0.91	0.835	d
Sludge wasting rate	0.074	0.076	0.087	m ³ d ⁻¹
SRT	30	29	25.5	d
Net permeate flow rate	2.11	2.348	2.555	m ³ d ⁻¹
Net MPF	14.07	15.65	17.04	L m ⁻² h ⁻¹
MLSS concentration	9.151	8.793	8.53	g L ⁻¹
Filtration	Intermittent (17/3)	Intermittent (17/3)	Intermittent (17/3)	min on/min off

MLSS concentration values fluctuated from a maximum value of 11.68 g L⁻¹ to a minimum value of 6.12 g L⁻¹. As already known, the changes of the concentration in the feed can affect the MLSS concentration measurements. With respect to MBR3 and its continual membrane fouling conditions, the repetitive application of chemical cleaning might have also affected the biomass concentration. However, a quite good average MLSS concentration of 9.043 g L⁻¹ can be calculated and the MLSS concentration was successfully controlled around the required value.

4. Time period from 06-05-2009 until 16-06-2009

Due to the serious membrane fouling problems of the MBR3 system, it was decided to reduce the MLSS concentration back to the initial value of about 4 - 5 g L⁻¹. The SRT was reduced to 12 d and the HRT remained at 0.835 d - this set of operating conditions reduced the MLSS concentration to a value of about 4 - 5 g L⁻¹ and stabilised it. The operating conditions regarding this time period are shown in Table 5.11.

Table 5.11 MBR3: Time period from 06-05-2009 until 16-06-2009: Presentation of the operating conditions

Parameter	Data	Unit
Operating volume	2.21	m ³
Feed flow rate	2.865	m ³ d ⁻¹
HRT	0.77	d
Sludge wasting rate	0.184	m ³ d ⁻¹
SRT	12	d
Net permeate flow rate	2.681	m ³ d ⁻¹
Net MPF	17.87	L m ⁻² h ⁻¹
MLSS concentration	5.043	g L ⁻¹
Filtration	Intermittent (17/3)	min on/min off

The maximum MLSS concentration value that was measured during this time period was equal to 7.31 g L⁻¹ and the minimum value was equal to 3.34 g L⁻¹. An average MLSS concentration was calculated and it was found to be equal to 5.043 g L⁻¹, which is a little increased but it is still in the correct range of values.

The course of MLSS concentration against time is shown in Figure 5.3.

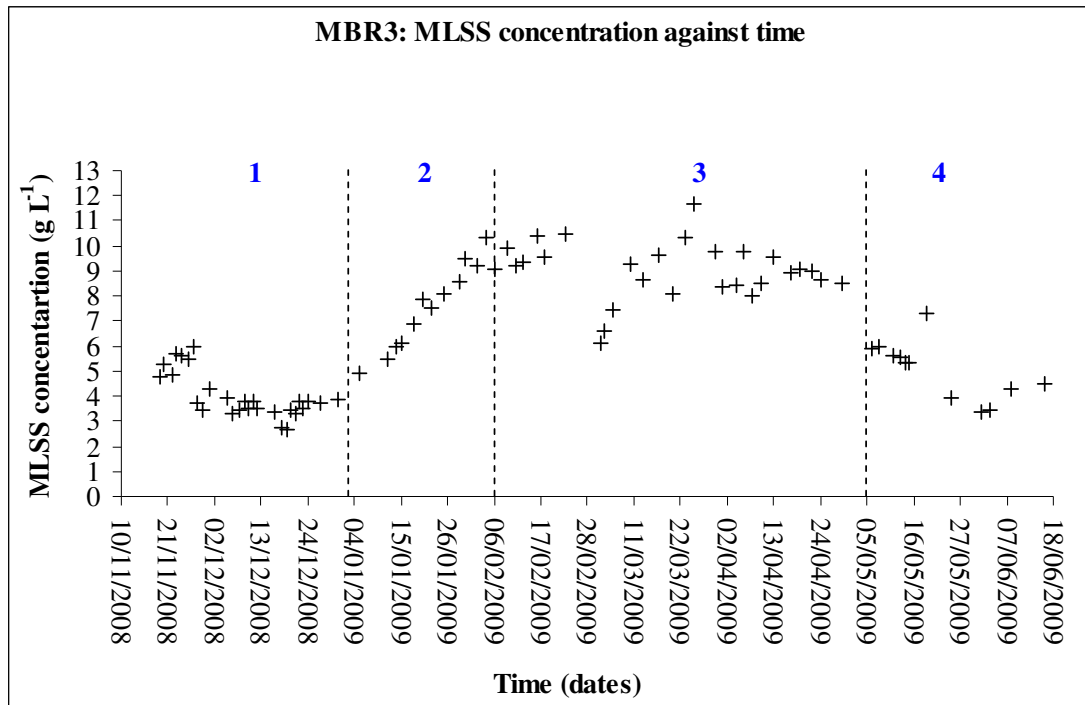


Figure 5.3 MBR3: MLSS concentration against time - **1.** From 19-11-2008 until 03-01-2009: $X_{MLSS} = 4.033 \text{ g L}^{-1}$, $\theta_C = 15 \text{ d}$, $\theta = 1.01 \text{ d}$, **3.** From 06-02-2009 until 07-04-2009: $X_{MLSS} = 9.151 \text{ g L}^{-1}$, $\theta_C = 30 \text{ d}$, $\theta = 1.01 \text{ d}$, From 08-04-2009 until 25-04-2009: $X_{MLSS} = 8.793 \text{ g L}^{-1}$, $\theta_C = 30 \text{ d}$, $\theta = 1.01 \text{ d}$, From 26-04-2009 until 05-05-2009: $X_{MLSS} = 8.53 \text{ g L}^{-1}$, $\theta_C = 25.5 \text{ d}$, $\theta = 0.835 \text{ d}$, **4.** From 06-05-2009 until 16-06-2009: $X_{MLSS} = 5.043 \text{ g L}^{-1}$, $\theta_C = 12 \text{ d}$, $\theta = 0.835 \text{ d}$, (**2.** Transition period)

As seen in Figure 5.3, the biomass concentration was satisfactorily controlled around the selected MLSS concentration set-points. Regarding the fluctuations in the MLSS concentration, apart from the changes of the feed concentration, they may also be attributed to the fact that MBR3 was experienced serious membrane fouling problems during the long-term experiment. As membranes had then to be chemically cleaned, this disturbance might have affected the biological culture too.

5.2.4 Comparisons: The course of MLSS concentration

Figure 5.4 shows the changes of MLSS concentrations of all the MBR systems.

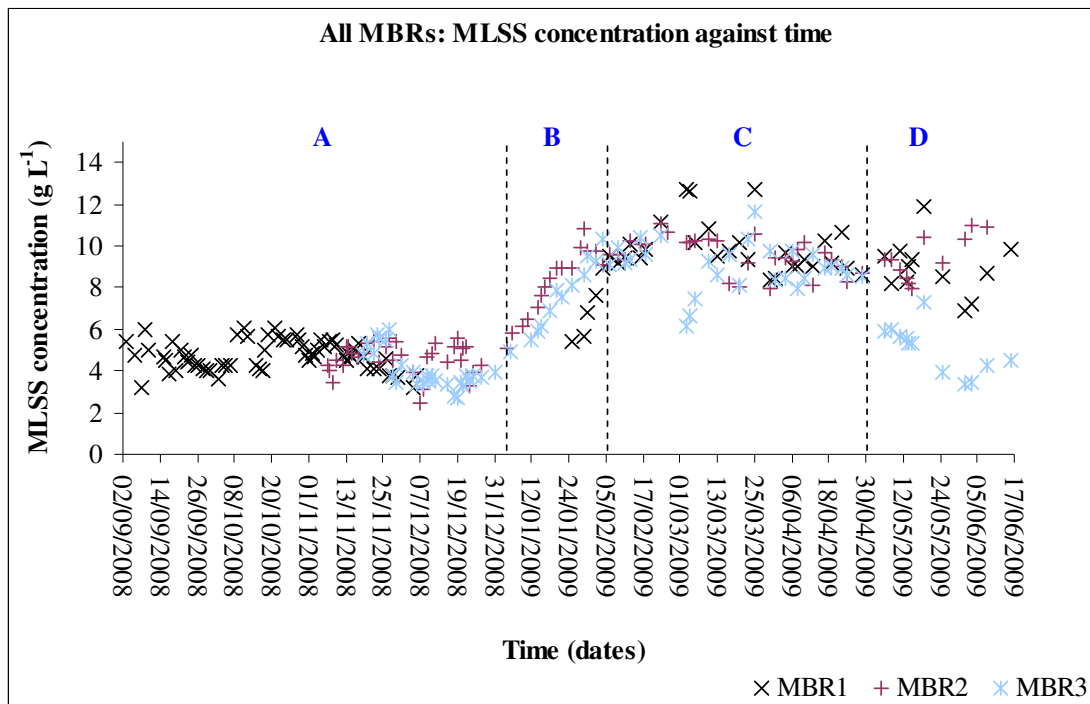


Figure 5.4 All MBRs: Average MLSS concentration against time - **MBR1: A:** From 03-09-2008 until 06-12-2008: $X_{MLSS} = 4.643 \text{ g L}^{-1}$, **C/D:** From 09-02-2009 until 16-06-2009: $X_{MLSS} = 9.658 \text{ g L}^{-1}$, **MBR2: A:** From 07-11-2008 until 03-01-2009: $X_{MLSS} = 4.592 \text{ g L}^{-1}$, **C/D:** From 30-01-2009 until 16-06-2009: $X_{MLSS} = 9.523 \text{ g L}^{-1}$, **MBR3: A:** From 19-11-2008 until 03-01-2009: $X_{MLSS} = 4.033 \text{ g L}^{-1}$, **C:** From 06-02-2009 until 05-05-2009: $X_{MLSS} = 9.043 \text{ g L}^{-1}$, **D:** From 06-05-2009 until 16-06-2009: $X_{MLSS} = 5.043 \text{ g L}^{-1}$, (**B:** Transition period)

As seen in Figure 5.4, it can be concluded that all MBRs are characterised by similar MLSS concentration profiles, which means that the biomass was equally controlled in all the tanks. Scatter in the low MLSS concentration was less significant than that at the higher MLSS concentration, meaning that biomass was better controlled at low MLSS concentrations. This can be attributed to membrane fouling, which took place more frequently at higher MLSS concentrations. Even though membrane fouling itself cannot affect the biomass concentration, the interruption of aeration, which occasionally took place in the MBR tanks, along with the application of chemical cleaning did affect the biomass. Also, fluctuations in general, regarding both low and high MLSS concentrations, are due to the variation in the feed composition, a parameter, which is impossible to be regulated when real municipal waste waters have to be treated.

5.3 Water quality issues

Measurements for the determination of feed water and treated water quality regarding all three pilot MBRs and the full-scale conventional AS plant were taken. Treated water quality was one of the main issues in this research - for its determination the effluent COD concentration values were measured. Effluent COD concentrations ought to comply with the Tunisian standards for unrestricted irrigation, or COD concentrations must be equal to or lower than 90 mg L^{-1} , [North Sfax ONAS archives, 2009].

5.3.1 The course of the influent COD concentration

The changes of the COD concentration in the feed with respect to all three MBR systems against time are shown in Figure 5.5.

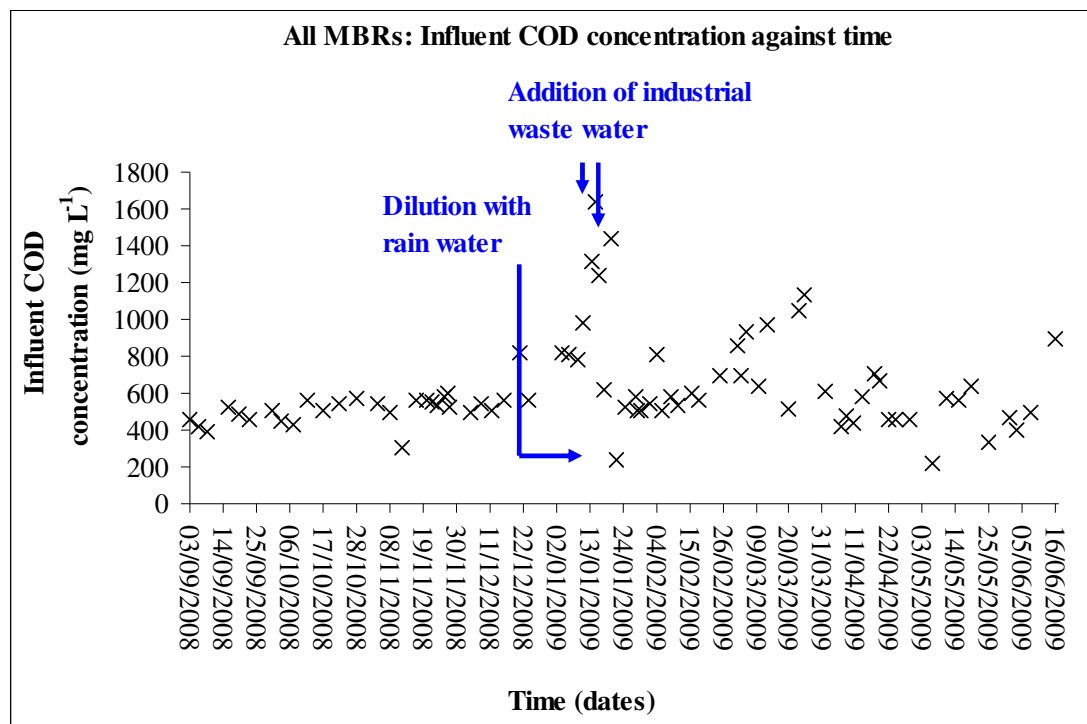


Figure 5.5 All MBRs: Influent COD concentration against time

As seen in Figure 5.5, the COD concentrations in the feed remained most of the time between 400 and 600 mg L^{-1} , but a few significant decreases/increases in these values

also appeared. These significant changes, which are shown in Figure 5.5, can be explained as follows:

The increase in the COD concentration values was mainly due to the fact that the municipal waste water was quite often contaminated by industrial waste water, which had been discharged into the domestic sewage before reaching the ONAS site. The problem reaches a maximum between mid-December and end of January when waste water from olive oil mills is mixed with the municipal waste water. During that time period, COD concentrations increased to values between 1,450 mg L⁻¹ and 1,650 mg L⁻¹. These discharges of industrial waste water are a long-lasting problem and these fluctuations of the influent COD concentrations are inevitable.

The low values of about 250 mg L⁻¹, on the other hand, came from the fact that the waste water was diluted with rain water, which gets into the sewer system via road drains, hence dilution of the municipal waste water occurs. It is worth mentioning that this phenomenon is rare, as the annual rainfall in the region of Sfax is very low, with values ranging from a total zero in June / July to a maximum of a little more than 30 mm in October/November, [www.bbc.co.uk/weather/world/city_guides, 2010]. These fluctuations in the composition of the feed waste water would contribute to the variation in the MLSS concentration as described in Section 5.2.

5.3.2 The courses of the effluent COD concentration/COD concentration removal efficiency

5.3.2.1 MBR1: The courses of the effluent COD concentration/COD concentration removal efficiency

Both MBR1 effluent COD concentration values and the COD concentration removal efficiency are shown in Figure 5.6.

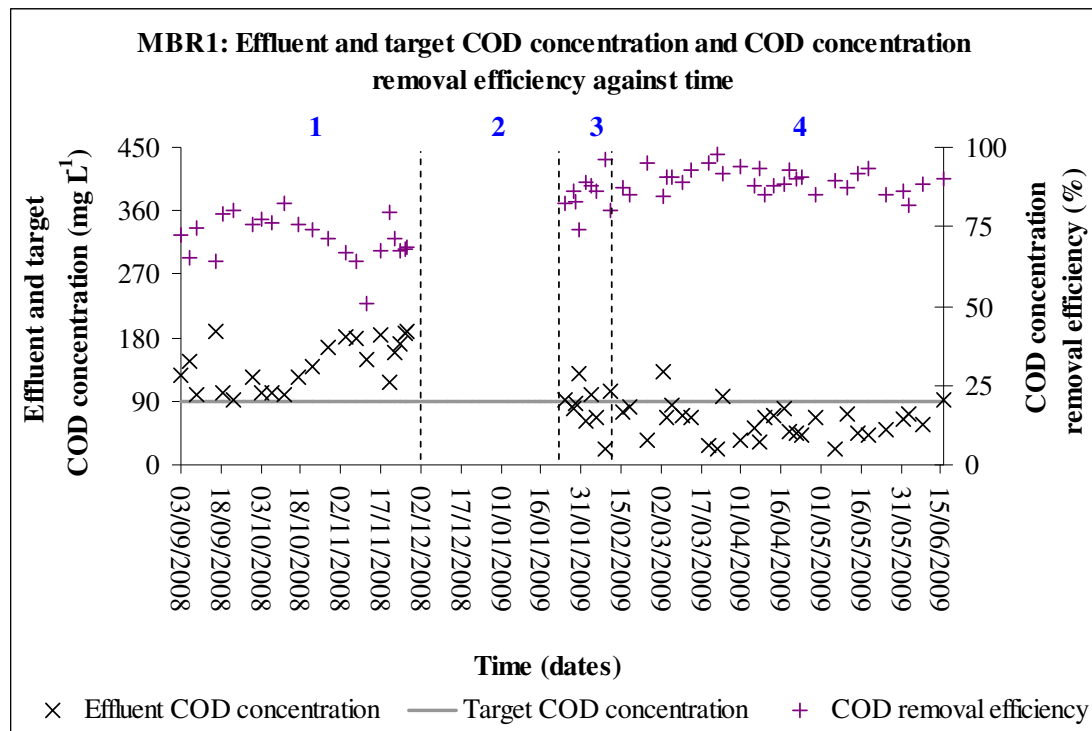


Figure 5.6 MBR 1: Effluent and target COD concentration and COD concentration removal efficiency against time: **1:** From 03-09-2008 until 06-12-2008; $X_{MLSS} = 4.643 \text{ g L}^{-1}$, **4:** From 09-02-2009 until 16-06-2009; $X_{MLSS} = 9.658 \text{ g L}^{-1}$, (**2:** MBR1 was not operational, **3.** Transition period)

As seen in Figure 5.6, when biomass concentration was stabilised at the low average MLSS concentration of 4.643 g L^{-1} , the treated permeate that was produced was not suitable for unrestricted irrigation in Tunisia, as the majority of the effluent COD concentration values were higher than the target COD concentration value. The COD concentration removal efficiency was also low as an average value of 71.4 % was calculated. On the other hand, when the average MLSS concentration increased to a value of 9.658 g L^{-1} , most of the effluent COD concentrations that were measured were lower than 90 mg L^{-1} , so treated permeate of the appropriate quality was produced. This is expected as treated water quality improves when the MLSS concentration increases. The new COD concentration removal efficiency increased to 89.4 %. However, it has to be stressed that the MBR1 system is designed to operate at MLSS concentrations in the range of $9 - 10 \text{ g L}^{-1}$ or higher, so MBR operation at MLSS concentrations as low as $4 - 5 \text{ g L}^{-1}$, used in this case to compare with the conventional AS, are not suggested, [Churchouse, 1997], [Kennedy and Churchouse, 2005].

5.3.2.2 MBR2: The courses of the effluent COD concentration/COD concentration removal efficiency

Figure 5.7 showing the profile of the effluent COD concentration against time and the profile of the COD concentration removal efficiency against time is plotted.

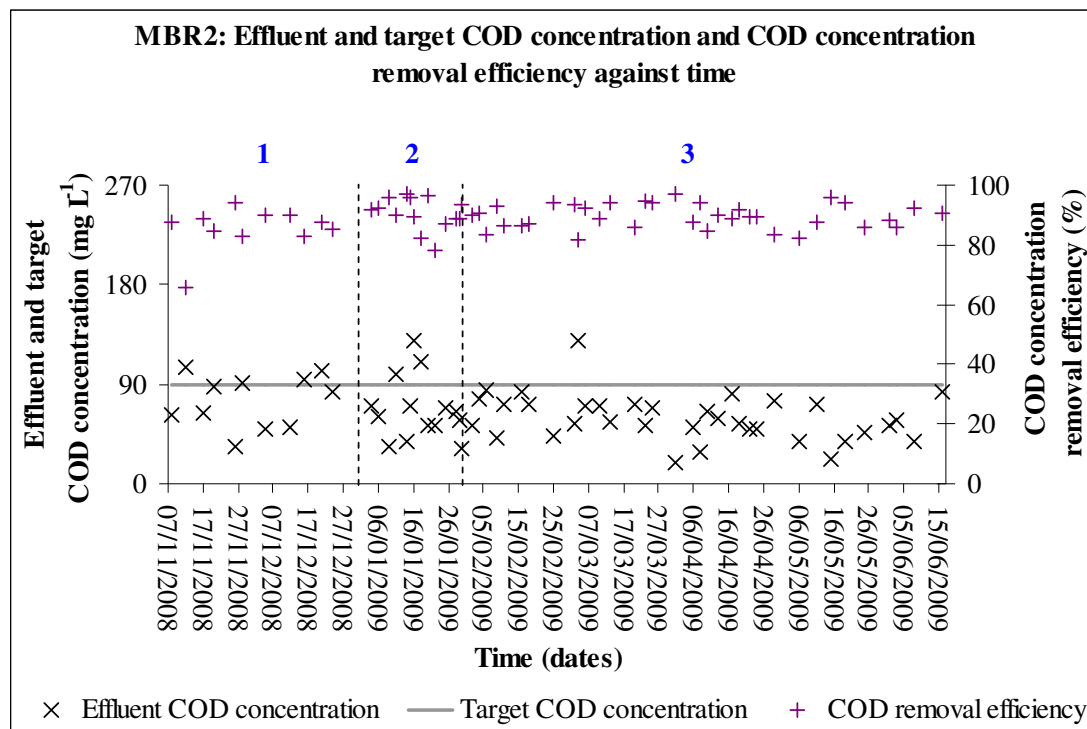


Figure 5.7 MBR2: Effluent and target COD concentration and COD concentration removal efficiency against time - **1:** From 07-11-2008 until 03-01-2009; $X_{MLSS} = 4.592 \text{ g L}^{-1}$, **3:** From 06-06-2009 until 16-06-2009; $X_{MLSS} = 9.523 \text{ g L}^{-1}$, (**2:** Transition period)

As seen in Figure 5.7, the MBR2 system produced treated water of the appropriate quality at both low and at higher MLSS concentrations. The average COD concentration removal efficiency was 88 % at an average MLSS concentration of about 4.592 g L^{-1} and 89.7 % at an average MLSS concentration of about 9.523 g L^{-1} . The fact that the MBR2 system managed to produce treated permeate of appropriate quality both at low and high MLSS concentrations comes from the fact that MBR2 was designed to operate successfully to MLSS concentrations lower than 12 g L^{-1} . [Weise Water Systems: Operating and maintenance manual, (2008)]. Also, it should be remembered that MBR2 was equipped with ultrafiltration (UF) membranes,

whereas MBR1 was equipped with microfiltration (MF) membranes. As UF can technically remove more colloidal and high-molecular weight organic compounds than MF, [Kim *et al.*, 2008], UF membranes are more effective under low MLSS concentrations.

5.3.2.3. MBR3: The courses of the effluent COD concentration/COD concentration removal efficiency

Figure 5.8 shows both the effluent COD concentration profile against time and the COD removal efficiency profile against time.

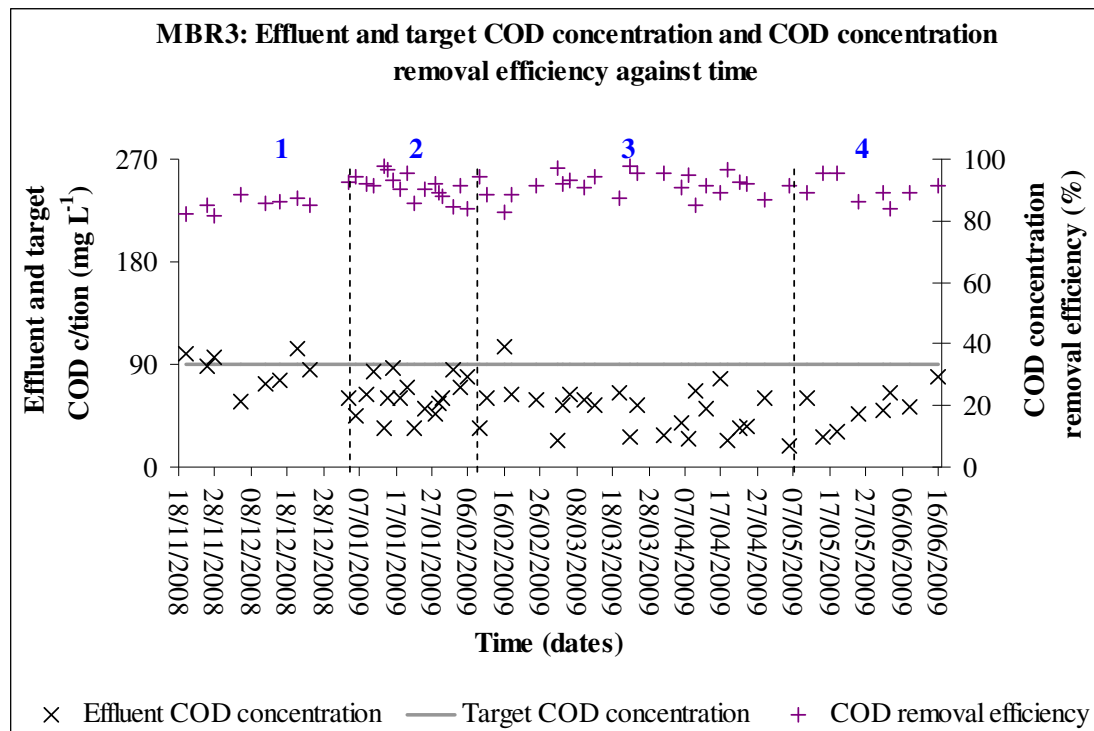


Figure 5.8 MBR3: Effluent and target COD concentration and COD concentration removal efficiency against time - **1.** From 19-11-2008 until 03-01-2009: $X_{MLSS} = 4.033 \text{ g L}^{-1}$, **3.** From 06-02-2009 until 05-05-2009: $X_{MLSS} = 9.043 \text{ g L}^{-1}$, **4.** From 06-05-2009 until 16-06-2009: $X_{MLSS} = 5.043 \text{ g L}^{-1}$, (**2:** Transition period)

As seen in Figure 5.8, MBR3 produced treated water of the appropriate quality for the whole range of the tested MLSS concentrations. The average COD concentration removal efficiency was equal to 87.7 % at the low MLSS concentration and equal to 90.9 % at the higher MLSS concentration.

MBR3 also had UF membranes, which appear to be more effective when lower MLSS concentrations are applied. Also, MBR3 was designed to operate at MLSS concentrations between 3 g L^{-1} and 14 g L^{-1} , which means that water of the appropriate quality could be produced all the time during the long-term experiment according to the manufacturer's guidelines. However, the optimum MLSS concentration is at about 10 mg L^{-1} [Martin Systems: Instructions for installation and operation of PURATREAT siClaro sewage treatment plant, 2008], so a more reliable MBR operation may be achieved at the high MLSS concentration.

5.3.3 Full-scale conventional AS plant: Effluent COD concentration measurements

According to data with regard to average COD values in the effluent of the full-scale conventional AS plant, which was collected during 2006, the full-scale conventional AS plant fails most of the time to produce treated water capable of being used for unrestricted irrigation in Tunisia. Table 5.12 shows this data.

Table 5.12 Full-scale conventional AS plant: Average monthly COD concentrations in the effluent for year 2006

Month	Average effluent COD concentration (mg L^{-1})
January	123
February	107
March	124
April	137
May	110
June	134
July	116
August	60
September	60
October	72
November	77
December	223

Assuming that each year the waste water that is treated is of similar composition, it can be concluded that the conventional AS plant most of the time failed to produce waste water of the appropriate quality.

5.3.4 Comparisons: The courses of the effluent COD concentration/COD concentration removal efficiency

Comparisons, with respect to the quality of the treated permeate that was produced by all three MBRs, are made in this section. Figure 5.9 and Figure 5.10 show the course of the effluent COD concentration against time and the COD concentration removal efficiency against time respectively.

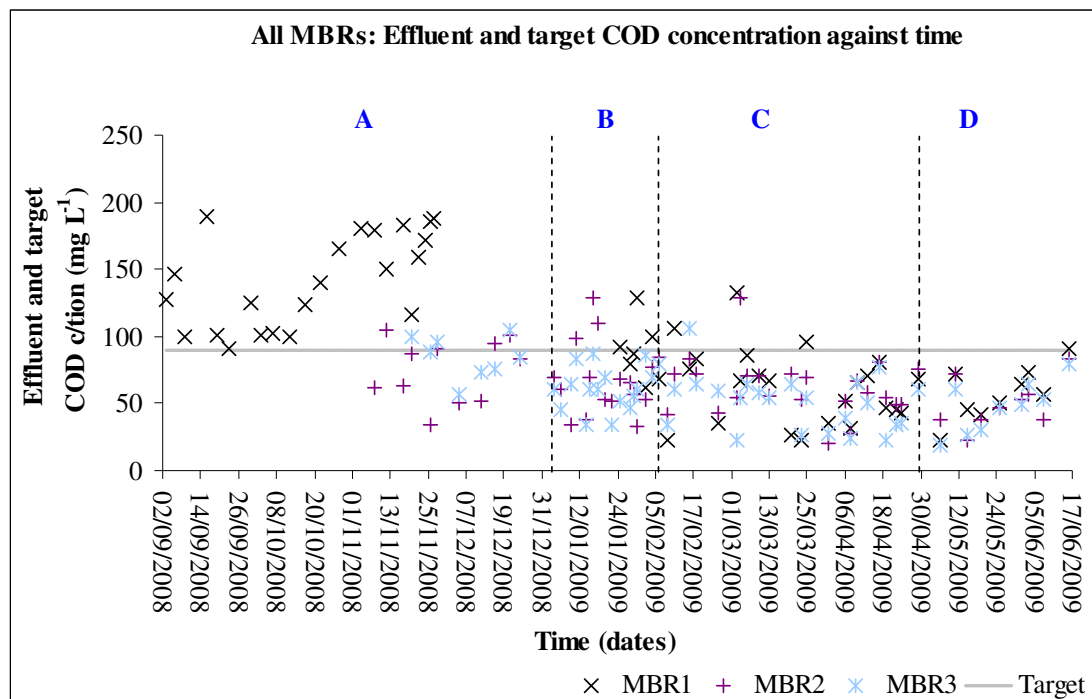


Figure 5.9 All MBRs: Effluent and target COD concentration against time - **MBR1: A:** From 03-09-2008 until 06-12-2008: $X_{MLSS} = 4.643 \text{ g L}^{-1}$, **C/D:** From 09-02-2009 until 16-06-2009: $X_{MLSS} = 9.658 \text{ g L}^{-1}$, **MBR2: A:** From 07-11-2008 until 03-01-2009: $X_{MLSS} = 4.592 \text{ g L}^{-1}$, **C/D:** From 30-01-2009 until 16-06-2009: $X_{MLSS} = 9.523 \text{ g L}^{-1}$, **MBR3: A:** From 19-11-2008 until 03-01-2009: $X_{MLSS} = 4.033 \text{ g L}^{-1}$, **C:** From 06-02-2009 until 05-05-2009: $X_{MLSS} = 9.043 \text{ g L}^{-1}$, **D:** From 06-05-2009 until 16-06-2009: $X_{MLSS} = 5.043 \text{ g L}^{-1}$, (**B:** Transition period)

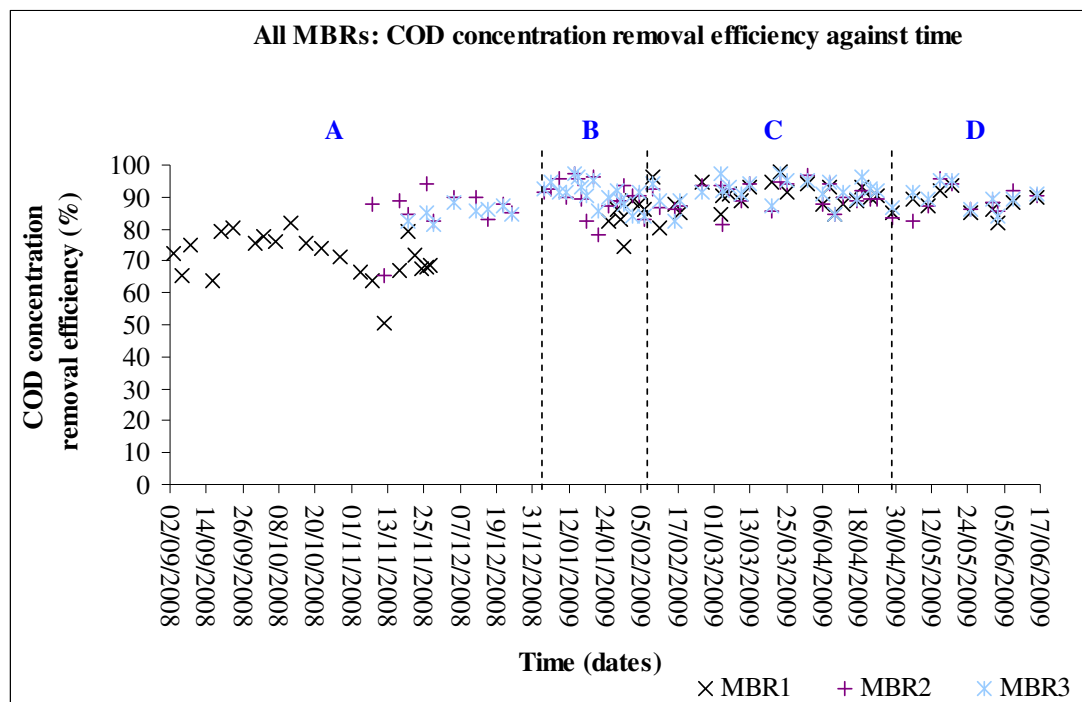


Figure 5.10 All MBRs: COD concentration removal efficiency against time -
MBR1: A: From 03-09-2008 until 06-12-2008: $X_{MLSS} = 4.643 \text{ g L}^{-1}$,
C/D: From 09-02-2009 until 16-06-2009: $X_{MLSS} = 9.658 \text{ g L}^{-1}$,
MBR2: A: From 07-11-2008 until 03-01-2009: $X_{MLSS} = 4.592 \text{ g L}^{-1}$,
C/D: From 30-01-2009 until 16-06-2009: $X_{MLSS} = 9.523 \text{ g L}^{-1}$,
MBR3: A: From 19-11-2008 until 03-01-2009: $X_{MLSS} = 4.033 \text{ g L}^{-1}$,
C: From 06-02-2009 until 05-05-2009: $X_{MLSS} = 9.043 \text{ g L}^{-1}$, **D:** From
06-05-2009 until 16-06-2009: $X_{MLSS} = 5.043 \text{ g L}^{-1}$, (**B:** Transition
period)

As already mentioned, at low MLSS concentrations ($4 - 5 \text{ g L}^{-1}$), the MBR1 system did not produce treated permeate of appropriate quality whereas at high MLSS concentration ($9 - 10 \text{ g L}^{-1}$) all MBR systems managed to do so. However, MBR1 was not designed to operate at biomass concentrations lower than 10 g L^{-1} .

5.4 MLVSS and BOD₅ concentrations

During the long-term experiments, MLVSS concentrations (biomass-related data) and BOD₅ concentrations (water quality issues) regarding all three MBRs were additionally measured. Despite the fact that very few measurements were taken, the values that were measured made good sense in comparison to published values, [Tchobanoglous *et al.*, 2004].

5.4.1 MLVSS concentration measurements

MLVSS measurements were taken occasionally. The average percentage, which shows the amount of the MLVSS out of the total MLSS, is shown in Table 5.13.

Table 5.13 All MBRs: Maximum, minimum and average MLVSS/MLSS percentages

MBR	MLVSS/MLSS percentage (%)		
	Minimum	Maximum	Average
MBR1	65.0	72.0	69.6
MBR2	69.5	72.4	69.8
MBR3	68.3	74.2	71.4
All MBRs	-	-	70.3

As seen in Table 5.12, the average MLVSS/MLSS percentage was calculated to be equal to 70.3 %. Based on this percentage, MLVSS concentrations for each MBR system during the long-term experiment are as follows:

• MBR1

Table 5.14 presents the average MLVSS concentrations within the MBR tank of the MBR1 system during the time periods as defined in Section 5.2.1. The operating conditions are as given in Section 5.2.1.

Table 5.14 MBR1: Research periods with respect to the changes of the MLVSS concentration

Time period (dates)	Average MLVSS concentration (g L^{-1})
1. 03-09-2008 until 06-12-2008	3.264
2. 07-12-2008 until 24-01-2009	Operation suspended
3. 25-01-2009 until 08-02-2009	3.264 to 6.79
4. 09-02-2009 until 16-06-2009	6.79

• **MBR2**

Table 5.15 shows the average MLVSS concentrations within the MBR tank of the MBR2 system during the time periods as defined in Section 5.2.2. The operating conditions are as given in Section 5.2.2.

Table 5.15 MBR2: Research periods with respect to the changes of the MLVSS concentration

Time period (dates)	Average MLVSS concentration (g L⁻¹)
1. 07-11-2008 until 03-01-2009	3.228
2. 04-01-2009 until 29-01-2009	3.228 to 6.695
3. 30-01-2009 until 16-06-2009	6.695

• **MBR3**

Table 5.16 presents the average MLVSS concentrations within the filtration tank of the MBR3 system during the time periods as defined in Section 5.2.3. The operating conditions are as given in Section 5.2.3.

Table 5.16 MBR3: Research periods with respect to the changes of the MLVSS concentration

Time period (dates)	Average MLVSS concentration (g L⁻¹)
1. 19-11-2008 until 03-01-2009	2.835
2. 04-01-2009 until 05-02-2009	2.835 to 6.357
3. 06-02-2009 until 05-05-2009	6.357
4. 06-05-2009 until 16-06-2009	3.545

5.4.2 Effluent BOD₅ concentration measurements

With respect to the effluent BOD₅ concentrations, very few measurements, and only at the high MLSS concentration, were taken due to both practical and resource limitations on the site. Minimum, average and maximum BOD₅ concentration values in the effluent are given Table 5.17.

Table 5.17 All MBRs: Maximum, minimum and average effluent BOD₅ concentration values

MBR system	BOD ₅ concentration values (mg L ⁻¹)		
	Minimum value	Average value	Maximum value
MBR1	5	7	10
MBR2	5	6	10
MBR3	5	7	10

As shown in Table 5.17, all BOD₅ concentration values in the effluent at high MLSS concentrations comply with the target BOD₅ concentration value for unrestricted irrigation in Tunisia - the target value is 30 mg L⁻¹, [North Sfax ONAS archives, 2006]. To conclude, both effluent COD and effluent BOD₅ concentration values showed that at the high MLSS concentration of about 9 - 10 g L⁻¹, successfully treated permeate can be produced regardless the MBR system/membranes that were used.

5.5 Conclusions

In this chapter, the performance of the three MBR systems was tested. The MBR systems were operated under two different MLSS concentrations, which were successfully controlled by applying suitable sets of operating conditions, namely SRTs and HRTs, so that the treated permeate quality can be explored. The MLSS concentrations that were tested were:

- 4 - 5 g L⁻¹: This MLSS concentration value is similar to the MLSS concentration value of the full-scale conventional AS plant, and

- 9 - 10 g L⁻¹: This is the MLSS concentration value, under which, according to the membrane suppliers, all three MBR systems can successfully operate without confronting any serious membrane fouling problems.

The SRTs/HRTs that were applied during the long-term experiments were able to stabilise and maintain the MLSS concentration within the MBR tanks at the selected values. Direct comparisons among the MBRs and between the MBRs and the full-scale conventional AS plant with respect to their capability of producing treated water of the appropriate quality were made.

- **Low MLSS concentration: 4 - 5 g L⁻¹**

At low MLSS concentration values, MBR2 and MBR3 managed to produce treated water of appropriate quality, whereas MBR1 did not succeed in doing so. MBR1 was not designed to operate under these low MLSS concentrations but preferably at MLSS concentrations of about 10 g L⁻¹ or even higher need to be applied. On the other hand, MBR2 was designed to operate at MLSS concentrations lower than 12 g L⁻¹ and MBR3 can operate at MLSS concentrations in the range of 3 - 14 g L⁻¹, so they both were able to produce treated permeate at low MLSS concentrations. Also, the fact that MBR2 and MBR3 had UF membranes, whereas MBR1 had MF membranes, might have helped MBR2 and MBR3 produce treated water of better quality than MBR1. This can be attributed to the fact that UF membranes are able to technically reject more organic material compared to the MF membranes regardless of the MLSS concentration values. Finally, it is worth mentioning that the full-scale AS plant did not manage to produce treated water of the appropriate quality as concluded through this research.

Regarding the COD removal efficiencies, they were found to be equal to 71.4 % for MBR1, 88 % for MBR2 and 87.7 % for MBR3. MBR2 and MBR3 had nearly the same COD removal efficiency because of the similarities between their membranes, whereas MBR1 had a lower COD removal efficiency.

- **High MLSS concentration: 9 - 10 g L⁻¹**

At higher MLSS concentrations, all MBR units managed to produce treated water of the appropriate quality. MBRs, in general, can operate at elevated MLSS concentrations, or longer sludge ages, compared to conventional AS processes, and this is one of their advantages. As higher MLSS concentrations can produce treated water of better quality, [Stamou and Vogiatzis, 1994], these higher MLSS concentrations are usually more desirable.

The COD concentration removal efficiencies were quite higher this time, namely 89.4 % for MBR1, 89.7 % for MBR2 and 90.9 % for MBR3 indicating that about 90 % of the organic matter was successfully consumed by the microorganisms.

Theoretically, infinite SRTs can be applied. Practically, this is not possible, as long SRTs affect the stability of the membrane performance, as well as after threshold SRT treated permeate quality stops improving. The stability of the membrane performance throughout the long-term experiments will now be described in detail in Chapter 6.

CHAPTER 6 MEMBRANE PERFORMANCE

6.1 Introduction/General information

The membrane performance of all three membrane bioreactors (MBRs) operating with raw waste water feed is described in this chapter. Membrane fouling, a phenomenon, which is related to a number of different parameters, such as mixed-liquor suspended solids (MLSS) concentrations, gassing rates for membrane scouring and the mixed-liquor temperature, together with hydrodynamic parameters like the imposed real/net membrane permeate fluxes (MPFs) and their consequent transmembrane pressure (TMP) values, will be explored. For constant-flux membrane bioreactor (MBR) operations, as already mentioned in Section 2.3.1, membrane fouling might have already occurred when a continuous increase in the TMP values starts taking place.

The aim of this chapter is to predict sets of operating conditions capable of leading to a stable long-term membrane performance with negligible or little membrane fouling taking place. During the long-term experiment, real/net MPFs will be increased up to values, which will no longer appear to be sustainable. This will help define the maximum average sustainable net membrane permeate flux (MPF) at a certain set of operating conditions, maximising at the same time the amount of the treated permeate, which is produced over a day. As the production of the treated water increases, the energy consumed per unit volume of treated permeate, or the specific energy demand (SED) value, becomes lower - this will be analysed in Chapter 7.

Regarding the operating conditions, the air flow rate for both membrane scouring and biomass maintenance for each MBR system remained constant during the long-term experiments and the values that were selected were those suggested by the MBR manufacturers. For the membrane bioreactor 1 (MBR1) system, the applied air flow rate for both membrane scouring and biomass maintenance was equal to $4,200 \text{ L h}^{-1}$, for the membrane bioreactor 2 (MBR2) system it was equal to $12,000 \text{ L h}^{-1}$ and finally for the membrane bioreactor 3 (MBR3) system it was equal to $7,300 \text{ L h}^{-1}$. The air flow rates for biomass maintenance within the biological treatment tank of the

MBR2 system and the aeration tank of the MBR3 system were also the default values suggested by the membrane manufacturers. In general, active biomass was maintained in all five tanks where the aerobic biological oxidation took place, as there was always active consumption of the substrates. With respect to MLSS concentrations, even though a detailed account has already been given in Chapter 5, it is worth re-mentioning that two different MLSS concentrations were tested, namely a low value of about 4 - 5 g L⁻¹ and a high value of about 9 - 10 g L⁻¹. Finally, with regard to the operating temperature of the mixed-liquors, a detailed analysis is provided in Section 6.2.

The raw data, which was collected during this experiment, was real permeate flow rates as measured by the flow meters and recorded by the data loggers, and pressure values as measured by the installed pressure transducers on the permeate side of the membranes and recorded by the data loggers. This data was respectively changed into average real/net MPFs and TMP values. Average permeability values were also calculated and, if necessary, they were temperature-corrected to a reference temperature of 20 °C so that a direct comparison could be made between the permeability values for the three MBRs at different MLSS concentrations.

6.2 Mixed-liquor temperature profile

In this research, only the instant mixed-liquor temperature values within the filtration tank of the MBR3 system could be measured, however, it can logically be assumed that the temperatures of the mixed-liquors for MBR1 and MBR2 were similar to the that one for MBR3, as all three systems were receiving the same raw feed water and operating in the same location. The temperature profile against time is given in Figure 6.1, providing temperature values from about mid-September to about mid-June. The gap in the data corresponds to the time during which the operation of MBR3 was suspended, so mixed-liquor temperatures could not be recorded.

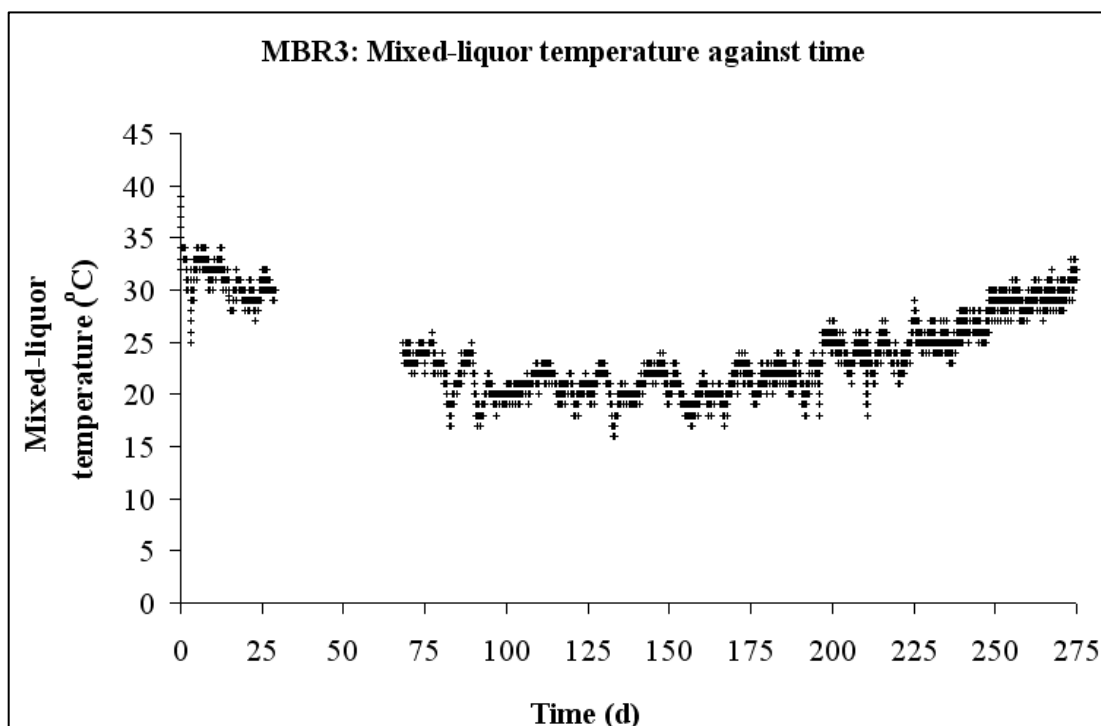


Figure 6.1 MBR3: Temperature of mixed-liquor within the filtration tank against time

As seen in Figure 6.1, the mixed-liquor temperature for MBR3 underwent changes from relatively high values of 35 °C to quite low values of 16 °C, essentially depending on the ambient seasonal conditions. Immediately after the beginning of the long-term experiment the temperature started to decrease. On Day 29, 11-10-2008, the temperature had reached a value equal to 30 °C. After that day operation of MBR3 was interrupted and no more temperature values were recorded until MBR3 was re-started, on Day 68, 19-11-2008. After Day 68, 19-11-2008, and until Day 197, 28-03-2009, *i.e.* during the winter months, the temperature remained in the same range of values. A useful average value was then estimated and it was found to be equal to 21.2 °C. After Day 197, 28-03-2009, and until the end of the long-term experiment on Day 275, 14-06-2009, the mixed-liquor temperature increased from the average value of 21.2 °C to a maximum of 33 °C. As with the winter months, the mixed-liquor temperature possibly also stabilises during the summer months, but this can only be anticipated as MBR3 was shut-down on Day 275, 14-06-2009.

As seen in Figure 6.1, mixed-liquor temperatures significantly fluctuated during the long-term experiments. These temperature changes need to be taken into account as

they can affect the viscosity of the mixed-liquor, and, as already known, this viscosity seriously affects the membrane performance, [Judd, 2007]. It is necessary to clarify whether changes of the biomass viscosity were caused due to changes of the MLSS concentration or by changes of the temperature of the mixed-liquor, and thence whether these changes of the activated sludge (AS) viscosity affected the membrane performance or not.

Finally, even though temperature changes over seasons is a natural phenomenon and it affected all three MBR systems in the same way, it would be better to temperature-correct the membrane permeability values at 20 °C, as more reliable direct comparisons could be made, and any significant error relating to temperature differences can be avoided.

6.3 Membrane performance of MBR1

6.3.1 Introduction

The MBR1 long-term experiment was run from Day 1, 03-09-2008, until Day 284, 14-06-2009, and raw data was continuously recorded during this time period. The initial air flow rate within the MBR tank, both for membrane scouring and for biomass maintenance, was set to 4,200 L h⁻¹ following the manufacturer's guidelines. According to the membrane supplier, each membrane panel needs 10 L min⁻¹ of air, [Arnot, 2006-2009], or 600 L h⁻¹, so the seven panels located inside MBR1 needed 4,200 L h⁻¹.

In the MBR1 system, cross flow filtration was applied due to the gassing and it was operated in a constant-flux mode. In constant-flux processes, real/net MPF remains constant and it is the changes of the TMP values that are recorded as the time elapses. As long as the MBR was operated under nearly-constant MLSS concentrations, any increase in the TMP values during the long-term experiment could imply that membrane fouling was taking place.

6.3.2 Data processing

The experimental time period was divided into four data processing periods in order to allow a clearer presentation of the results. This data processing time periods are summarised in Table 6.1.

Table 6.1 MBR1: Data processing periods

Research time periods (dates)	Number of days
03-09-2008 until 02-11-2008	1 to 60
02-11-2008 until 21-01-2009	60 to 140
21-01-2009 until 11-04-2009	140 to 220
11-04-2009 until 14-06-2009	220 to 284

Initially, the expected real/net MPFs for each set of operating conditions were calculated - details are provided in Section 6.3.2.1. Then, based on the raw data, instant real MRFs, TMP values and permeability values were estimated with the aid of Equations 4.1, 4.5 and 4.6. Figures of instant real MPFs, TMP and permeability values against time were plotted. By directly comparing the expected real MPF with the instant real MPF values it could be concluded whether the expected real MPF for a given set of solids residence time (SRT)/hydraulic residence time (HRT) was satisfactorily controlled or not. Average TMP values and membrane permeability values were also calculated directly from the figures, however, scatter, which was always present, made it difficult to work with the raw values at times. The calculated average values lead to reliable analyses with regard to membrane performance. Finally, average temperature-corrected permeability values at 20 °C were also estimated through Equation 4.7. Temperature-corrected permeability values can be used to make accurate direct comparisons among the three MBR systems and their corresponding membrane performances.

6.3.2.1 1st research period: From 03-09-2008 until 02-11-2008

• Long-term experiment

The 1st research period started on Day 1, 03-09-2008, and ended on Day 60, 02-11-2008. During this time period, the SRT was set to 15 d and the HRT was set to 1.01 d. Average MLSS concentration was calculated to be equal to 4.643 g L⁻¹. However, if necessary, the real time MLSS concentration values will be taken into consideration, especially in case that a dramatic change in the real MPF/TMP profiles had occurred. The net MPF was calculated to be equal to 9.47 L m⁻² h⁻¹ (real MPF: 9.47 L m⁻² h⁻¹). For these calculations, the equations listed in Table 6.2, together with Equations 6.1 and 6.2, were used.

The net MPF, which corresponds to a certain set of operating conditions, is calculated with the aid of the mass balance equations, as they are presented in Section 2.2.3 and summarised in Table 6.2, together with the aid of Equation 6.1.

Table 6.2 Mass balance equations around an MBR

Equation	Equation number as given in Chapter 2
$\theta_c = \frac{V}{Q_w}$	2.23
$\theta = \frac{V}{Q_F}$	2.15
$Q_{p,n} = Q_f - Q_w$	2.11 - slightly adjusted

where:

$$Q_{p,n} = \text{Net permeate flow rate} \quad \text{L h}^{-1}$$

The average net MPF is then defined as follows:

$$J_{p,n} = \frac{Q_{p,n}}{A_m} \quad \text{Equation 6.1}$$

where:

$$J_{p,n} = \text{Net MPF} \quad \text{L m}^{-2} \text{h}^{-1}$$

Finally, the relationship that combines both real and net MPFs is as follows:

$$J_{p,n} = J_{p,r} \frac{t_f}{t_f + t_r} \quad \text{Equation 6.2}$$

where:

$$J_{p,r} = \text{Real MPF} \quad \text{L m}^{-2} \text{h}^{-1}$$

$$t_f = \text{Filtration time} \quad \text{min}$$

$$t_r = \text{Relaxation time} \quad \text{min}$$

Equations 6.1 and 6.2 can be applied to all three MBR systems.

The difference between the real and the net permeate flow rates/MPFs is now explained. When filtration is continuous, these two permeate flow rate values are identical - so are the MPF values. However, once intermittent filtration is applied, these two permeate flow rate values are different. During filtration the real permeate flow rate represents the permeate flow rate value as provided by the flow meter. During relaxation the real permeate flow rate is always equal to zero - again this value is provided by the flow meter. In this work, instant real permeate flow rates were recorded by the data loggers during the long-term experiments. On the other hand, the net permeate flow rate/MPF is an average value, which is calculated by the mass balance equations. The net permeate flow rates/MPFs are always lower than the real permeate flow rate/MPFs as estimated during the filtration time period.

The average temperature of the mixed-liquor during this period of time was estimated at 27.5 °C. This average temperature was estimated by assuming some of the temperature values during the time the operation of the MBR3 system was suspended and mixed-liquor temperature values could not be recorded. When MBR3 was re-started, real mixed-liquor temperature data values were used.

Figure 6.2, showing the course of the real MPF over time is plotted.

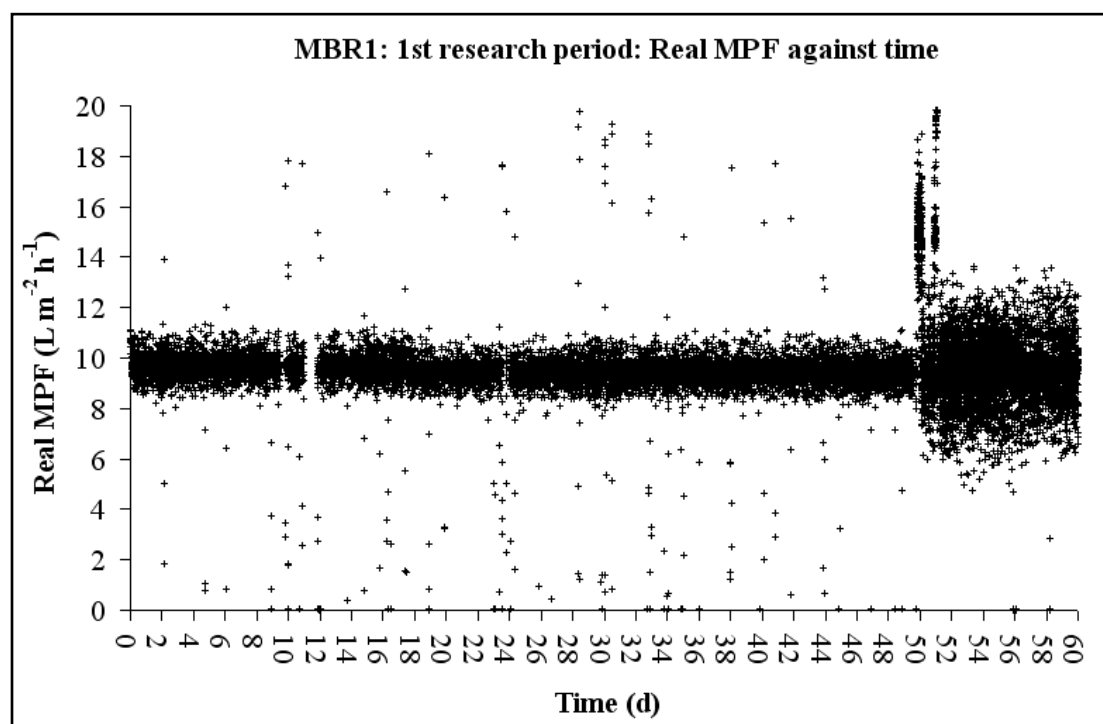


Figure 6.2 MBR1: 1st research period: Real MPF against time: From Day 1 until Day 60: SRT, $\theta_C = 15$ d, HRT, $\theta = 1.01$ d, Average MLSS concentration, $X_{MLSS} = 4.643$ g L⁻¹, Mixed-liquor temperature, $T_{ML} = 27.5$ °C, Air flow rate for membrane scouring, $Q_{AIR, MS} = 4,200$ L h⁻¹. From now on only symbols for the above-mentioned parameters will be used with respect to the figures of this chapter

The corresponding real/net MPF of 9.47 L m⁻² h⁻¹ was quite well-controlled. As seen in Figure 6.2, from Day 1, 03-09-2008, until Day 50, 23-10-2008, better control of the instant real MPFs took place as less scatter appeared. During this period of time, measurements of real MPFs were collected every 5 min. On Day 50, 23-10-2008, a short-term flux-step test was performed and this will be described in later in this section. After the completion of the short-term flux-step test, the real permeate flow

rate was reset to its initial value. The recording time was changed from 5 min to 1 min. The change of the sampling time led to more scatter as at the shorter sampling time of 1 min reduced data filtering took place. It is also worth mentioning that some gaps in Figure 6.2 are due to power cuts which occurred during this research period. These power cuts seemed not to have affected the stability of the real MPF, demonstrating some robustness in the system. The TMP values against time are shown in Figure 6.3.

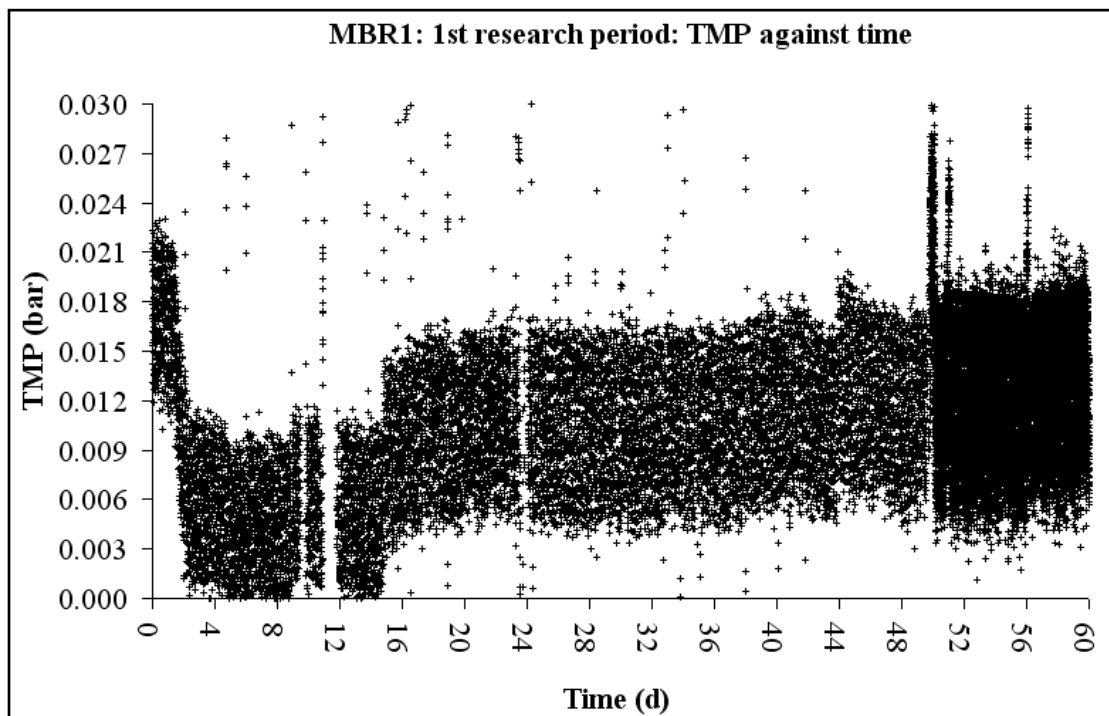


Figure 6.3 MBR1: 1st research period: TMP against time: From Day 1 until Day 60; $\theta_C = 15$ d, $\theta = 1.01$ d, $X_{MLSS} = 4.643$ g L⁻¹, $T_{ML} = 27.5$ °C, $Q_{AIR, MS} = 4,200$ L h⁻¹

Figure 6.3 can be divided into two distinct regions, the 1st region before Day 15, 18-09-2008, and the 2nd region after that day. During the first 15 days (1st region), the TMP profile against time appears to be quite different to that after Day 15, 18-09-2008, (2nd region). This could be attributed to the fact that as membranes came into contact with the mixed-liquor for the first time, they did not become immediately acclimatised to the new operating conditions. However, biomass concentration appeared to be well-controlled during this research period and some fluctuation with

regard to the measured values may be well-related only to the unavoidable changes of the feed concentration.

During the time period after Day 15, 18-09-2008, (2nd region), negligible fluctuation of the MLSS concentration values was observed, (Figure 5.1). Observing Figure 6.3, it can be seen that the TMP values were always in scattered areas. These scattered areas appeared mainly due to the “saw-tooth” phenomenon. The “saw-tooth” phenomenon, as described in Section 4.3.1, can lead to a fictitious increase in the TMP values. The ability to measure the instant pressure values on the feed side of the membranes would have led to less scatter in Figure 6.3. However, scatter cannot be entirely avoided as fluctuations also appear during the time the proportional-integral-derivative (PID) controller is trying to stabilise the real permeate flow rate at the selected set-point. Finally, it can be seen that the scatter appeared to be slightly reduced when longer periods of recording time were applied, that is to say before Day 50, 23-10-2008. This is due to the fact that reduced data filtering was possible at shorter sampling times.

As seen in Figure 6.3 a slight increase in the TMP value, from an initial average TMP value of 0.009 bar to a final one of 0.013 bar, occurred. As the MLSS concentration did not dramatically change throughout this time period, this TMP increase can be attributed to the fact that the temperature of the mixed-liquor decreased from an initial high value of about 39 °C down to a lower value of about 24 °C. This change of the mixed-liquor temperature could be responsible for the increase in the TMP values, as lower mixed-liquor temperatures can affect the membrane performance when viscosity increases, and some membrane fouling may take place. Under these operating conditions, it was concluded that membrane fouling was insignificant and the corresponding net MPF of $9.47 \text{ L m}^{-2} \text{ h}^{-1}$ is sustainable, leading to a reliable long-term membrane performance.

The permeability profile against time is shown Figure 6.4.

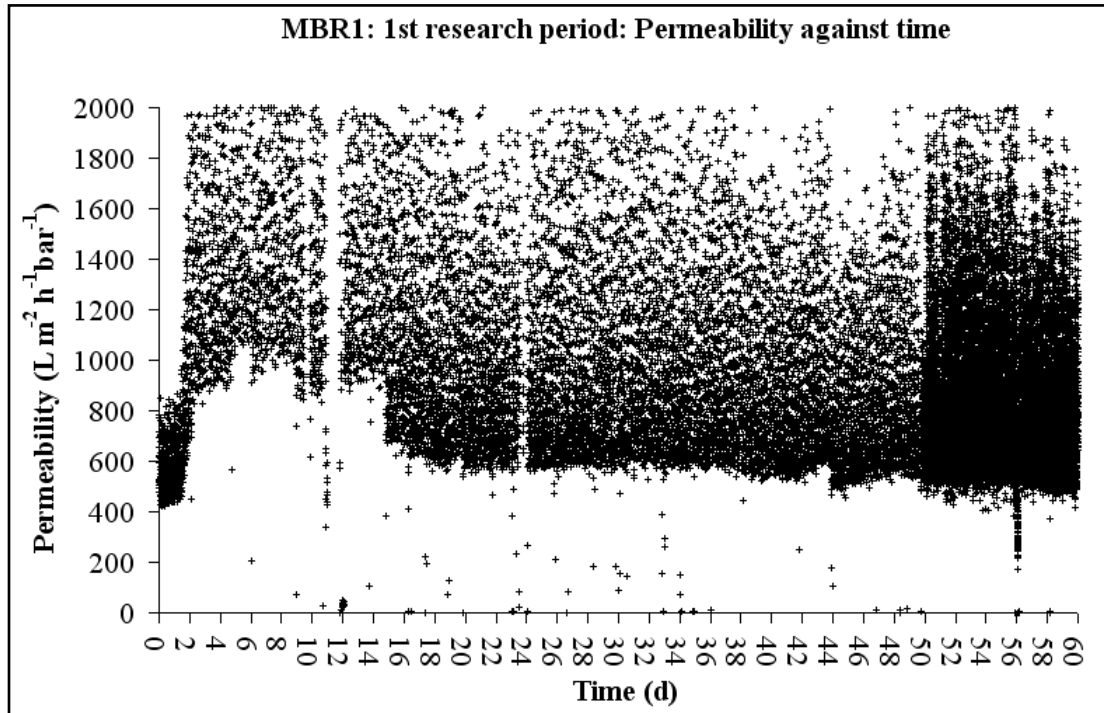


Figure 6.4 MBR1: 1st research period: Permeability against time: Day 1 until Day 60: $\theta_C = 15$ d, $\theta = 1.01$ d, $X_{MLSS} = 4.643$ g L⁻¹, $T_{ML} = 27.5$ °C, $Q_{AIR, MS} = 4,200$ L h⁻¹

The instant permeability values were subject to even larger scatter than the instant real MPFs or the instant TMP values, but this can be expected as the permeability values are the quotient of real MPFs and TMP values. The combination of two parameters, which were both subject to scatter, could lead to even larger scatter. If the first 15 days of start-up will not be taken into account, it can be said that the majority of the permeability values were roughly between $500 \text{ L m}^{-2} \text{ h}^{-1} \text{ bar}^{-1}$ and $800 \text{ L m}^{-2} \text{ h}^{-1} \text{ bar}^{-1}$ leading to an average value of $650 \text{ L m}^{-2} \text{ h}^{-1} \text{ bar}^{-1}$ at 27.5 °C. By temperature-correcting this value at 20 °C, (Equation 4.7), a value equal to $540 \text{ L m}^{-2} \text{ h}^{-1} \text{ bar}^{-1}$ was obtained. As expected, this value was lower compared to the value estimated during the clean water tests, which was found to be $610 \text{ L m}^{-2} \text{ h}^{-1} \text{ bar}^{-1}$ at 20 °C. This is also in line with literature, which indicates permeability values for Kubota membranes at 15 °C to range between $300 - 400 \text{ L m}^{-2} \text{ h}^{-1} \text{ bar}^{-1}$, [Van Bentem *et al.*, 2007], or by temperature correcting at 20 °C between $340 - 453 \text{ L m}^{-2} \text{ h}^{-1} \text{ bar}^{-1}$.

Finally, as the time elapsed, the instant permeability values decreased, so practically the overall resistance relating to the mass transfer through the membranes increased.

This is also in line with the increase in the TMP values. This may be well-connected with the decrease in the temperature of the mixed-liquor that happened during this time period.

To conclude, the net MPF of $9.47 \text{ L m}^{-2} \text{ h}^{-1}$ was a sustainable net MPF under the present operating conditions, namely average MLSS concentration of 4.643 g L^{-1} , average temperature of the mixed-liquor of $27.5 \text{ }^\circ\text{C}$ and air flow rate for membrane scouring of $4,200 \text{ L h}^{-1}$. However, this MLSS concentration did not succeed in producing treated water of the appropriate quality - see Chapter 5. This means that whether this net MPF is sustainable or not, the final objective of producing treated permeate capable of being used for unrestricted irrigation in Tunisia was not achieved. However, this MBR system was not designed to operate at such a low MLSS concentration - see Chapter 5.

• Short-term flux-step tests

During this research period, a short-term flux-step test was also conducted. This experiment aimed to explore the TMP response at different real MPFs indicating whether the applied operating conditions could lead to membrane fouling or not. This is an easy way to predict stable long-term membrane performance under sustainable real MPF conditions. In order to do so, the TMP values that were calculated during this test must not be affected by the “saw-tooth” phenomenon, otherwise accurate information about probable membrane fouling cannot be obtained. One way to avoid the “saw-tooth” phenomenon was to maintain constant pressure on the feed side of the membranes during the short-term flux-step test, *i.e.* to maintain the height of waste water within the MBR tank at a constant level. That was successfully achieved by recycling treated permeate to the MBR tank during the short-term tests.

A flux-step method was applied, [Le-Clech *et al.*, 2003], according to which real MPF was increased in steps and for each step the TMP values were recorded. At the end of the test, the real MPF was reset to its initial value. The time period during which a real MPF was tested was not a crucial parameter, and it was not strictly defined, as TMP values usually respond quite rapidly to a real MPF change, and it

can be easily determined whether the real MPF can lead to the formation of membrane fouling or not.

The whole test was conducted on Day 50, 23-10-2008. The gassing rate for membrane scouring was not altered, the MLSS concentration was equal to about 5.55 g L^{-1} and the average mixed-liquor temperature was equal to about $27.5 \text{ }^\circ\text{C}$. A more accurate mixed-liquor temperature reading was not available as the MBR3 system was not operational on that day.

Real MPFs against time around Day 50, 23-10-2007, are plotted in Figure 6.5. The whole test had a total duration of less than 4 hours.

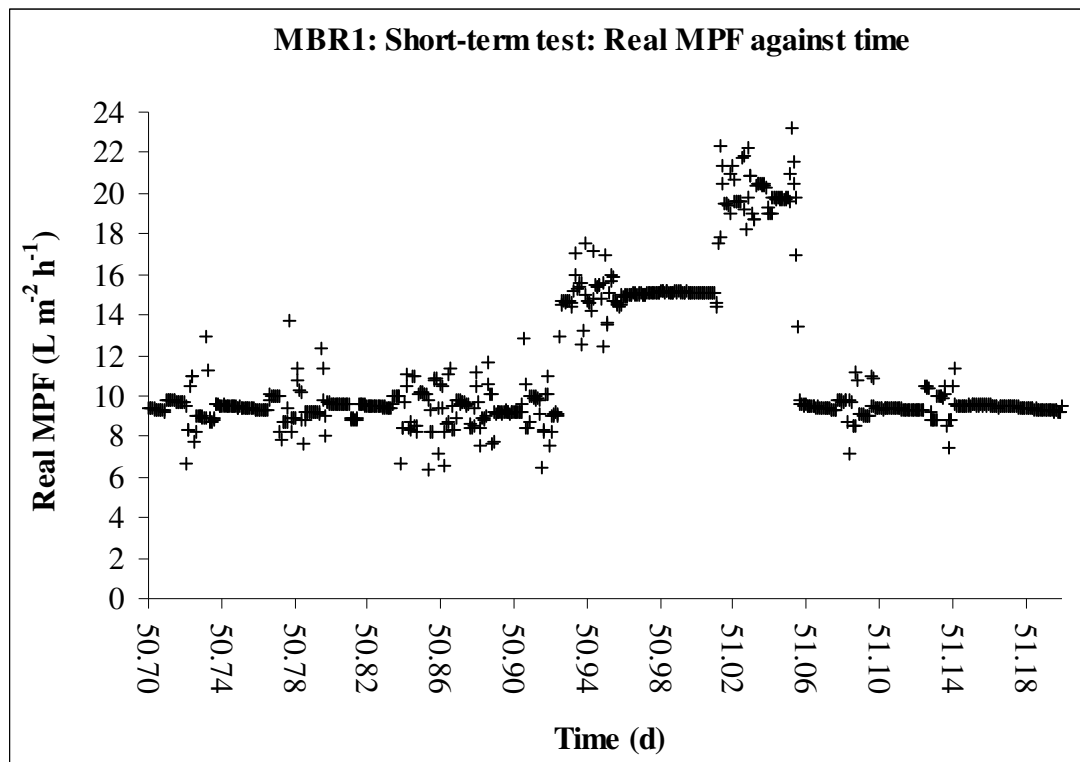


Figure 6.5 MBR1: Short-term flux-step test: Real MPF against time: $X_{\text{MLSS}} = 5.05 \text{ g L}^{-1}$, $T_{\text{ML}} = 27.5 \text{ }^\circ\text{C}$, $Q_{\text{AIR, MS}} = 4,200 \text{ L h}^{-1}$

Three different flux-steps were tested (three different set-points) leading respectively to average real MPFs of $9.47 \text{ L m}^{-2} \text{ h}^{-1}$, $15.05 \text{ L m}^{-2} \text{ h}^{-1}$ and $19.61 \text{ L m}^{-2} \text{ h}^{-1}$. As seen in Figure 6.5, these MPFs were well-controlled, however, it will be the TMP profile against time that will prove whether the higher real MPFs of $15.05 \text{ L m}^{-2} \text{ h}^{-1}$ and

19.61 L m⁻² h⁻¹ can be characterised as sustainable conditions. At the moment, net MPFs were similar to the real MPFs as filtration was continuous. The TMP profile against time is shown in Figure 6.6.

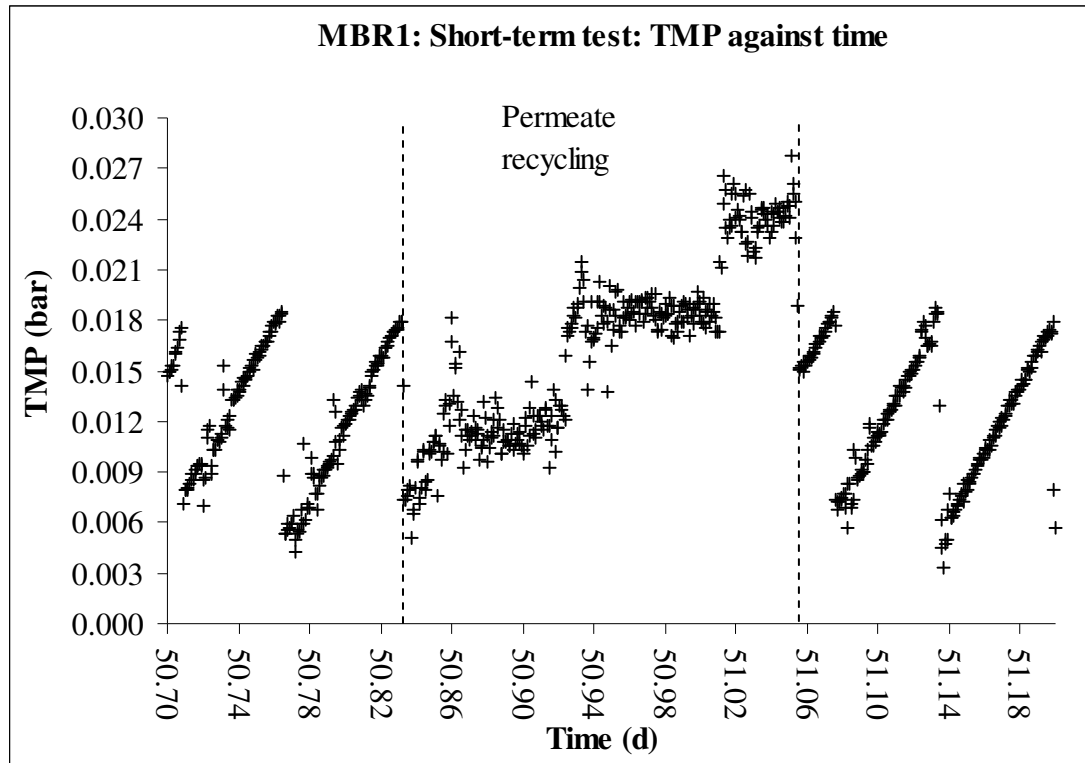


Figure 6.6 MBR1: Short-term flux-step test: TMP against time: $X_{MLSS} = 5.05$ g L⁻¹, $T_{ML} = 27.5$ °C, $Q_{AIR, MS} = 4,200$ L h⁻¹

Figure 6.6 shows that the TMP values remained constant for each real MPF. This means that these real MPFs may lead to successful long-term MBR operation, even though this assumption about successful long-term MBR operations is strictly connected to the situation of the system during the test, and any change, *i.e.* a change of the waste water composition, will affect the TMP values.

The “saw-tooth” effect can now be clearly seen in Figure 6.6. The phenomenon can be easily observed in the region before the start as well as in the region after the end of the short-term flux-step test. During these time periods permeate was collected instead of being recycled to MBR1. The “saw-tooth” effect is not present during the short-term tests.

Figure 6.7 showing the permeability profile against time is plotted.

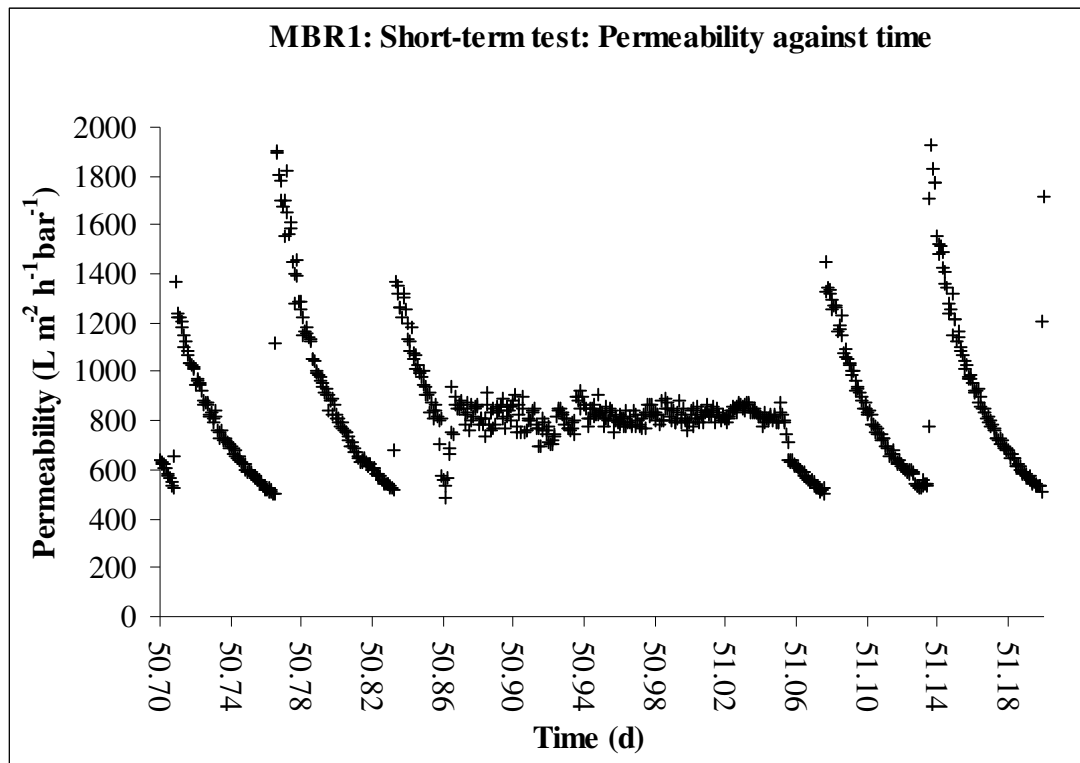


Figure 6.7 MBR1: Short-term flux-step test: Permeability against time: $X_{MLSS} = 5.05 \text{ g L}^{-1}$, $T_{ML} = 27.5 \text{ }^{\circ}\text{C}$, $Q_{AIR, MS} = 4,200 \text{ L h}^{-1}$

All the permeability values appeared to be in the same range of values regardless of the real MPF which was being tested. This can be expected as almost no membrane fouling appeared during this short-term flux-step test - no increase in the TMP values was recorded. With respect to this specific waste water, these permeability values seemed to be the maximum values that could be reached under the present operating conditions. An average permeability value was found to be equal to about $800 \text{ L m}^{-2} \text{ h}^{-2} \text{ bar}^{-1}$ at $27.5 \text{ }^{\circ}\text{C}$. By temperature-correcting at $20 \text{ }^{\circ}\text{C}$ a maximum permeability value of $665 \text{ L m}^{-2} \text{ h}^{-1}$ was estimated. This value, as expected, is lower than the value, which is provided by the manufacturer for reverse osmosis (RO) clean water at $20 \text{ }^{\circ}\text{C}$ - a value of $977 \text{ L m}^{-2} \text{ h}^{-1} \text{ bar}^{-1}$. However, it appeared to be slightly higher than the permeability of clean water as described in Chapter 4. Even though the permeability value at $20 \text{ }^{\circ}\text{C}$ as calculated after performing the clean water seems to be questionable, it is worth mentioning that during the clean water tests the “saw-tooth” phenomenon

had not been removed and the whole test was subject to scatter, which affected the accuracy of the calculations.

6.3.2.2 2nd research period: From 02-11-2008 until 21-01-2009

During this research period severe irreversible membrane fouling occurred due to an operational failure. On Day 64, 06-11-2008, the aeration pipeline cracked. As air escaped through the crack, no air was provided within the MBR tank and membrane fouling occurred rapidly. The crack in the air line was repaired and the air flow rate was reinstated. Filtration was re-started and membrane performance appeared to have been restored by a period of gassing in the absence of filtration. On Day 76, 18-11-2008, an attempt to increase the real MPF was made. This resulted in rapid exponential increase in the TMP values. By plotting the courses of instant real MPFs, TMP values and permeability values against time, a better representation of the data collected is given.

Figure 6.8 shows the course of real MPF against time.

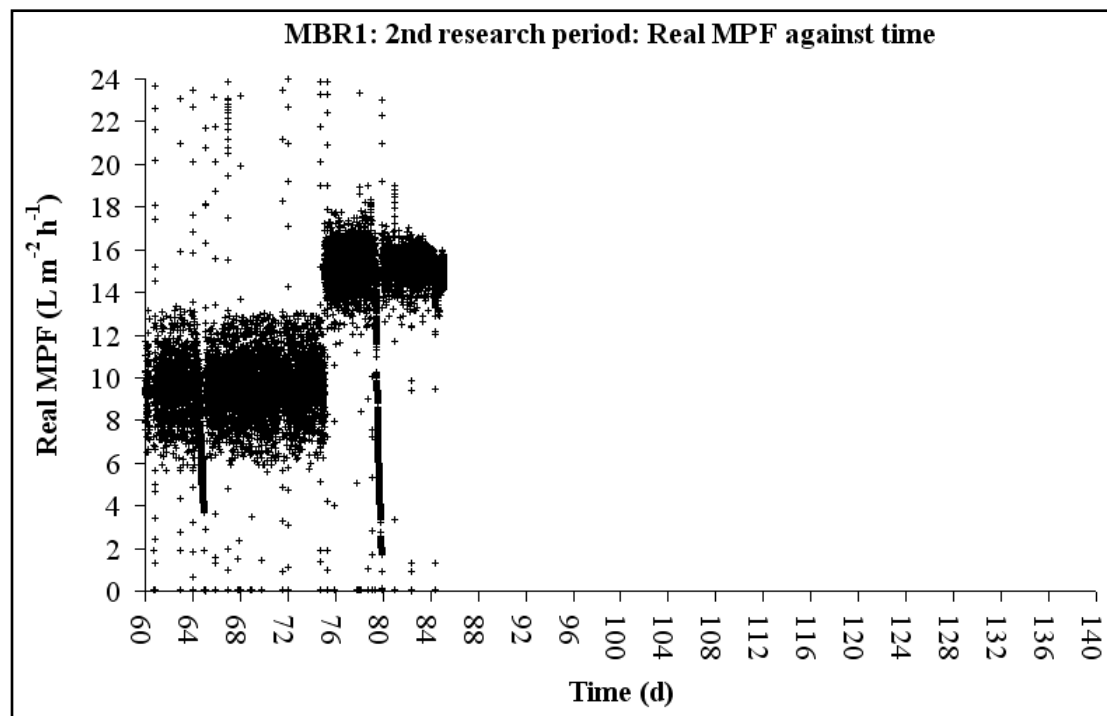


Figure 6.8 MBR1: 2nd research period: Real MPF against time: From Day 60 until Day 75: $\theta_C = 15$ d, $\theta = 1.01$ d, $X_{MLSS} = 4.643$ g L⁻¹, $T_{ML} = 21.2$ °C, $Q_{AIR, MS} = 4,200$ L h⁻¹

As seen in Figure 6.8, the real MPF initially remained at the same value as it was during the previous research period. The net MPF was equal to $9.47 \text{ L m}^{-2} \text{ h}^{-1}$. The average MLSS concentration was 4.643 g L^{-1} and the temperature of the mixed-liquor had decreased to an average value of $21.2 \text{ }^\circ\text{C}$. However, on Day 76, 18-11-2008, an attempt to further increase the real MPF was made. This attempt lasted until Day 86, 28-11-2008, but due to the serious build-up of membrane fouling the filtration was suspended. Figure 6.9 shows the changes of the TMP values against time during this time period. It is also worth mentioning that on Day 83, 25-11-2008, real MPF started to gradually decrease. This will be explained later in this section.

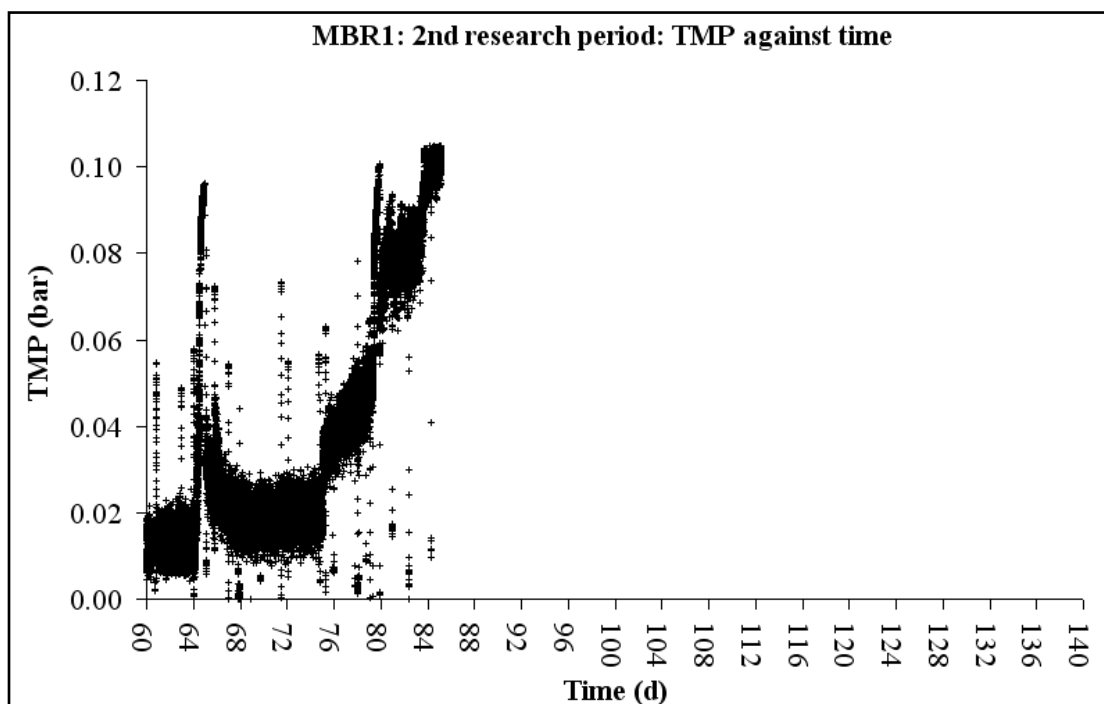


Figure 6.9 MBR1: 2nd research period: TMP against time: From Day 60 until Day 75: $\theta_C = 15 \text{ d}$, $\theta = 1.01 \text{ d}$, $X_{\text{MLSS}} = 4.643 \text{ g L}^{-1}$, $T_{\text{ML}} = 21.2 \text{ }^\circ\text{C}$, $Q_{\text{AIR, MS}} = 4,200 \text{ L h}^{-1}$

By observing Figure 6.9, two important conclusions can be made. Regarding the time period from Day 64, 06-11-2008, until Day 75, 17-11-2008, the net MPF of $9.47 \text{ L m}^{-2} \text{ h}^{-1}$ was successfully maintained even though lower gassing rates than the value proposed by the equipment supplier were applied. This actually means that, for most of the earlier operation, the MBR1 system had been operated under excess air flow conditions with respect to membrane scouring. This practically means that higher than required running energy-relating costs had to be paid. By reducing and

optimising the air flow rates, running costs with respect to the energy consumption of the MBRs can be significantly reduced, however, this analysis is not within the aim of this research but could be able to be explored in the future.

Regarding the time period from Day 76, 18-11-2008, to Day 140, 21-01-2009, the real MPF was increased. Even though both the MLSS concentration and the temperature of the mixed-liquor did not significantly change, immediately after the application of this increased real MPF, severe membrane fouling took place as indicated by a rapid exponential TMP increase. As mentioned in Chapter 2, exponential TMP increase at a constant-flux operation happens when a single membrane panel becomes fouled. The rest of the panels have automatically to do more work, or the selected real MPF cannot be maintained. This additional work makes these panels more likely to become fouled and TMP values start therefore to increase very rapidly. The new selected real MPF was an unsustainable condition.

A physical cleaning was applied on Day 79, 21-11-2008, by interrupting filtration but keeping on scouring the membranes. However, this physical cleaning ended up being unsuccessful. The membrane fouling was residual, or irreversible, so the application of physical cleaning did not succeed in removing it. Physical cleaning can successfully remove any cake material over the membrane but it cannot remove irreversible membrane fouling, [Chua, 2003], which was most likely caused due to the failure of the aeration system. TMP values finally increased beyond a value of 0.104 bar, so the operation was interrupted due to the risk of membranes becoming seriously damaged. A chemical cleaning based on solutions of NaOCl was applied.

Finally, it is worth mentioning that these severe membrane fouling conditions might have affected the instant real MPF as well. As seen in Figure 6.8, up to Day 83, 25-11-2008, the real MPF did not decrease at all, but managed to be maintained. After that day, the real MPF could no longer be maintained at the selected average value and the trend was slightly decreasing downwards. This is another indication that this specific membrane fouling had very seriously affected the membrane performance.

Figure 6.10 shows the course of permeability against time.

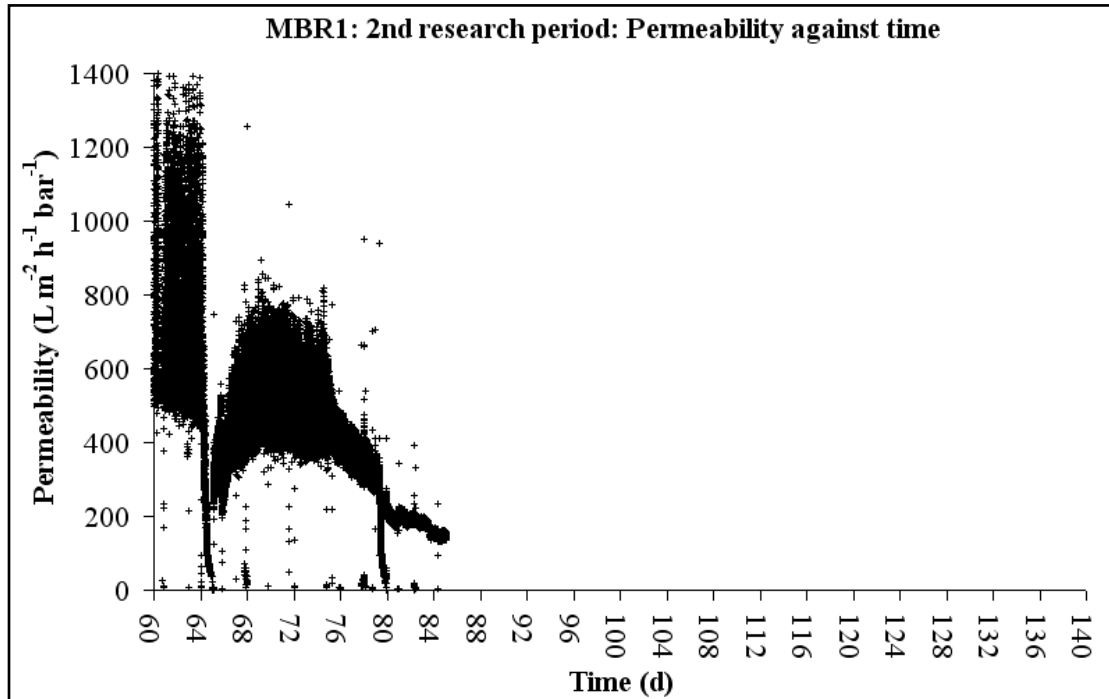


Figure 6.10 MBR1: 2nd research period: Permeability against time: From Day 60 until Day 75: $\theta_C = 15$ d, $\theta = 1.01$ d, $X_{MLSS} = 4.643$ g L⁻¹, $T_{ML} = 21.2$ °C, $Q_{AIR, MS} = 4,200$ L h⁻¹

Figure 6.10 shows that just before the shut-down of the MBR system, permeability values had reduced to 150 L m⁻² h⁻¹ bar⁻¹ at a temperature of 21.2 °C. By correcting this permeability value to 20 °C a temperature-corrected membrane permeability of 145 L m⁻² h⁻¹ bar⁻¹ was calculated. This permeability value is a quite low value compared to other measured permeability values. This reduction in the permeability values is another indication that membrane fouling had been occurred.

6.3.2.3 3rd research period: From 21-01-2009 until 11-04-2009

The MBR1 system was started-up again on Day 142, 23-01-2009. For a better representation of the data, the 3rd research period will be divided into three shorter time periods. During the time period from Day 144, 25-01-2009, to Day 158, 08-02-2009, MLSS concentration was allowed to increase from a value of about $4 - 5$ g L⁻¹ to a new value of about $9 - 10$ g L⁻¹. The SRT was fixed at 30 d and the HRT was fixed at 1.01 d. The mixed-liquor temperature during this time period was around an average of 21.2 °C.

The next time period started on Day 159, 09-02-2009, and finished on Day 168, 18-02-2009. Both SRT and HRT remained the same, however, the MLSS concentration had already been stabilised around the selected value of 9 - 10 g L⁻¹. As MLSS concentration during this time period was properly controlled, an average of 9.528 g L⁻¹ was calculated from the experimental values. Temperature of the mixed-liquor was not significantly affected, and it was still equal to 21.2 °C on average. The corresponding real/net MPF value during this time period was 9.81 L m⁻² h⁻¹.

The last time period started on Day 168, 18-02-2009, and finished on Day 220, 11-04-2009. During this time period, the SRT was set to a value of 29 d and the HRT was set to 0.91 d. An average MLSS concentration of 10.168 g L⁻¹ was calculated, even though, during the first two weeks, high MLSS concentrations up to values equal to 12.71 g L⁻¹ were measured. The mixed-liquor temperature had started increasing and a new average value equal to 24.7 °C was calculated. During this time period, an attempt to operate the membranes intermittently was also made. More details will be given after plotting the courses of instant real MPF values, TMP values and permeability values against time.

The course of real MPF against time is plotted in Figure 6.11.

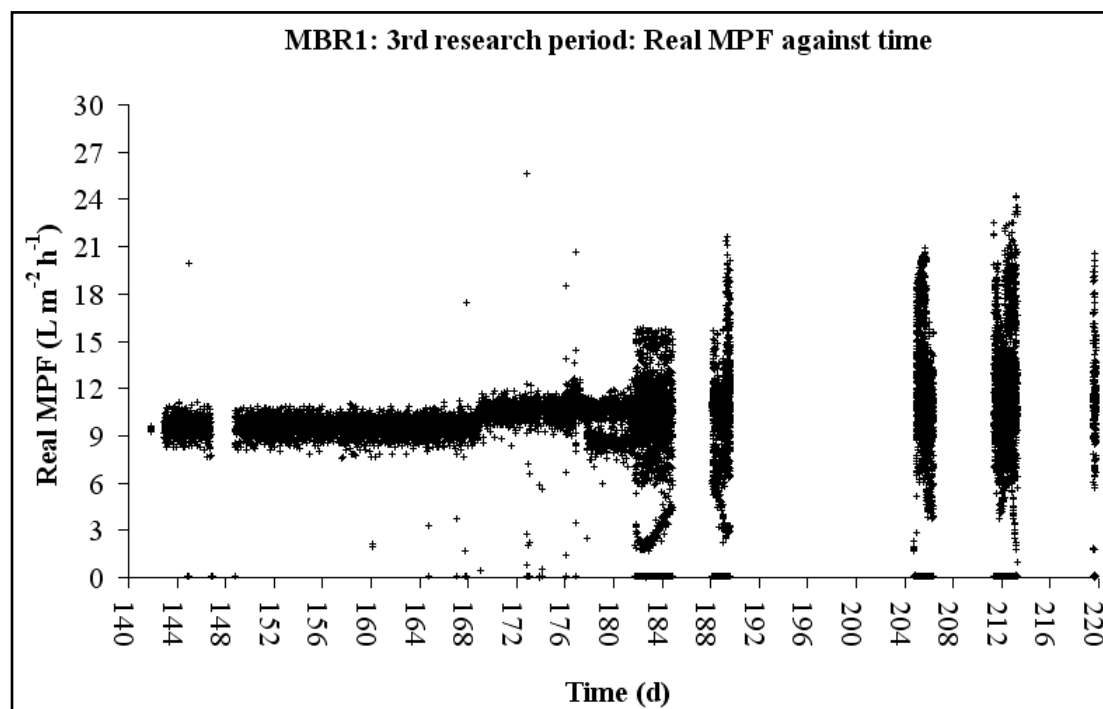


Figure 6.11 MBR1: 3rd research period: Real MPF against time: From Day 159 until Day 168: $\theta_C = 30$ d, $\theta = 1.01$ d, $X_{MLSS} = 9.528$ g L⁻¹, $T_{ML} = 21.2$ °C, $Q_{AIR, MS} = 4,200$ L h⁻¹, From Day 169 until Day 220: $\theta_C = 29$ d, $\theta = 0.91$ d, $X_{MLSS} = 10.168$ g L⁻¹, $T_{ML} = 24.7$ °C, $Q_{AIR, MS} = 4,200$ L h⁻¹, (From Day 144 until Day 158: Transition period)

As seen in Figure 6.11, real MPF was well-controlled until Day 182, 28-02-2009, which was 13 days after setting SRT to 29 d and HRT at 0.91 d. On Day 182, 28-02-2009, it was attempted to turn continuous filtration into intermittent by installing a timer to control the filtration cycle. Intermittent filtration is a technique of mitigating membrane fouling allowing for a better membrane performance at higher real/net MPFs or at lower air flow rates within the MBR tanks. The selected filtration/relaxation cycle was equal to 20 min, out of which 19 min of filtration were followed by 1 min of membrane relaxation.

The MBR1 system, as provided by the manufacturer, is supposed to operate continuous filtration and the application of intermittent filtration would be a challenge. As observed in Figure 6.11, after the application of intermittent filtration and until Day 220, 11-04-2009, real MPFs could not be controlled well. The timer appeared to interfere with the operation of the PID controller, which regulated the permeate actuated valve in order to control permeate flow. Various sampling times were tested

to avoid interferences between the filtration timer and the flow control loop. Additionally, the operation of the data logger was seriously affected and raw data was not recorded for long periods of time, hence gaps with no data appear in Figure 6.11. Intermittent filtration was continued until Day 220, 11-04-2009, making it difficult for reliable conclusions to be made after Day 182, 28-02-2009.

As intermittent filtration affected the stability of the operation, reliable conclusions can be drawn only for the time period between Day 169, 19-02-2009, and Day 181, 27-02-2009. During these days, filtration was still continuous and the corresponding real/net MPF was calculated to be equal to $10.92 \text{ L m}^{-2} \text{ h}^{-1}$.

Figure 6.12 shows the TMP values against time.

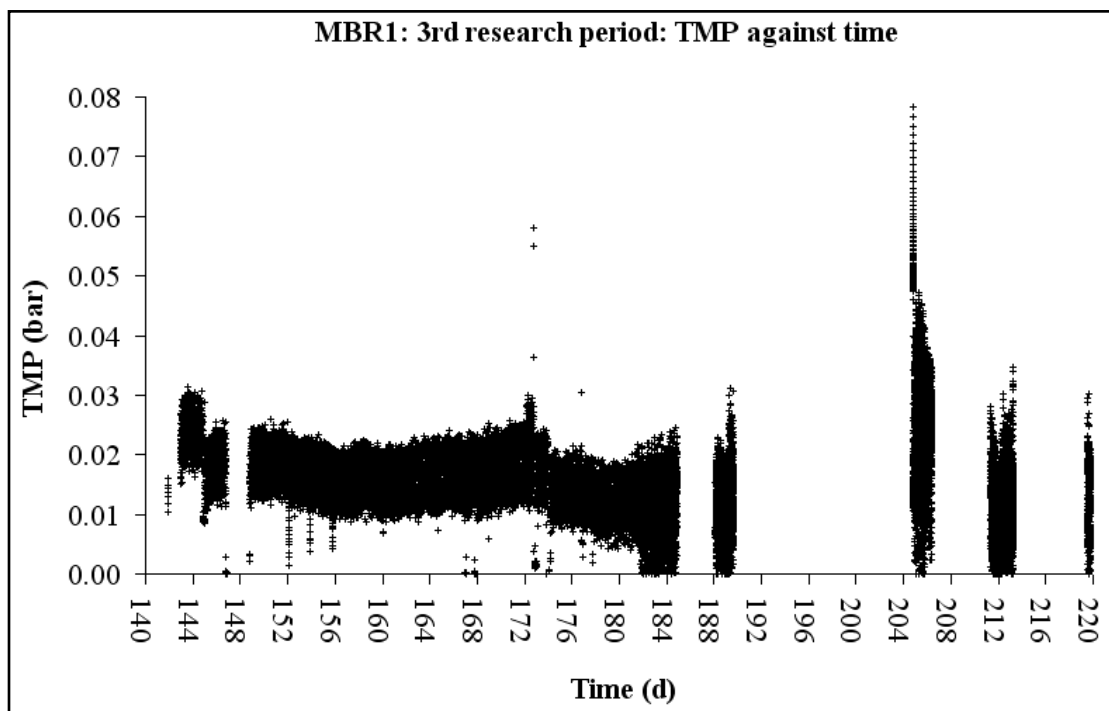


Figure 6.12 MBR1: 3rd research period: TMP against time: From Day 159 until Day 168: $\theta_C = 30 \text{ d}$, $\theta = 1.01 \text{ d}$, $X_{MLSS} = 9.528 \text{ g L}^{-1}$, $T_{ML} = 21.2 \text{ }^\circ\text{C}$, $Q_{AIR, MS} = 4,200 \text{ L h}^{-1}$, From Day 169 until Day 220: $\theta_C = 29 \text{ d}$, $\theta = 0.91 \text{ d}$, $X_{MLSS} = 10.168 \text{ g L}^{-1}$, $T_{ML} = 24.7 \text{ }^\circ\text{C}$, $Q_{AIR, MS} = 4,200 \text{ L h}^{-1}$, (From Day 144 until Day 158: Transition period)

As seen in Figure 6.12, during this time period between Day 144, 08-02-2009, and Day 220, 11-04-2009, only negligible increase in the TMP values took place, even

during the transition MLSS concentration time period, from Day 144, 25-01-2009, until Day 158, 08-02-2009. Both net MPFs of $9.81 \text{ L m}^{-2} \text{ h}^{-1}$ - from Day 159, 09-02-2009, until Day 168, 18-02-2009, - and $10.92 \text{ L m}^{-2} \text{ h}^{-1}$, together with their corresponding operating conditions appeared to be sustainable. At the same time, treated water quality was significantly improved as the measured COD concentration values in the effluent were lower than the target COD concentration value of 90 mg L^{-1} . The net MPFs of $9.81 \text{ L m}^{-2} \text{ h}^{-1}$ and $10.92 \text{ L m}^{-2} \text{ h}^{-1}$ can then both lead to a reliable long-term membrane performance and produce treated permeate of appropriate quality. Later, in Chapter 7, it will also be analysed whether these net MPFs and their corresponding operating conditions can also be combined with reasonable specific energy consumption values.

Figure 6.13 shows the permeability values over this research period.

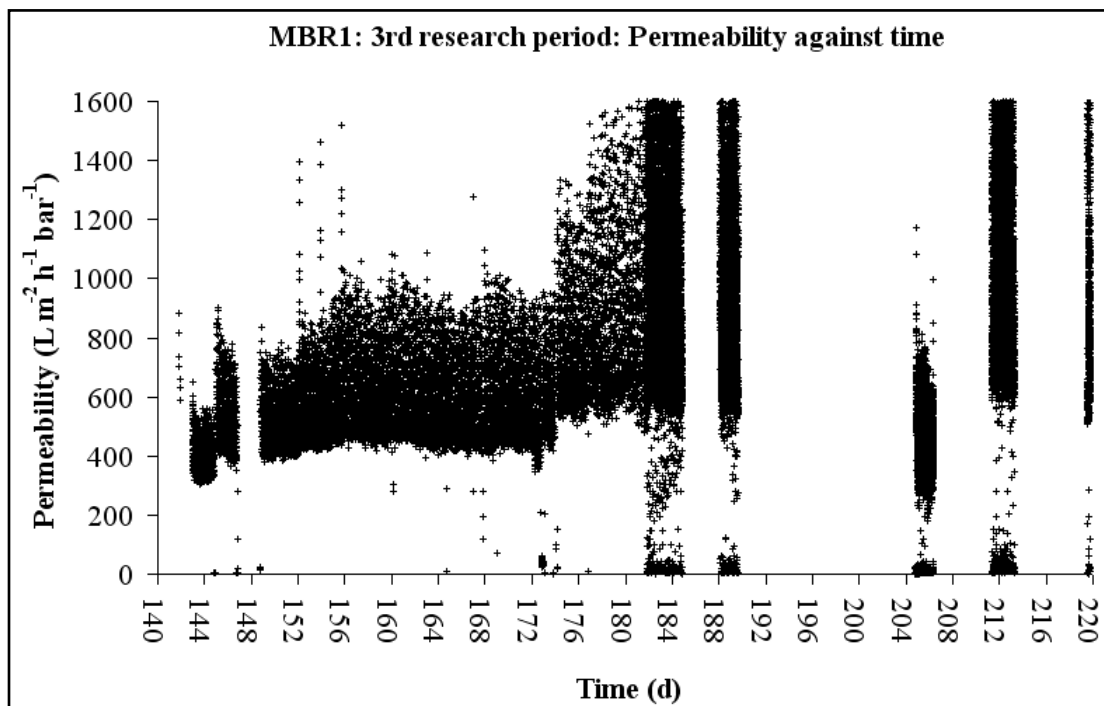


Figure 6.13 MBR1: 3rd research period: Permeability against time: From Day 159 until Day 168: $\theta_C = 30 \text{ d}$, $\theta = 1.01 \text{ d}$, $X_{MLSS} = 9.528 \text{ g L}^{-1}$, $T_{ML} = 21.2 \text{ }^\circ\text{C}$, $Q_{AIR, MS} = 4,200 \text{ L h}^{-1}$, From Day 169 until Day 220: $\theta_C = 29 \text{ d}$, $\theta = 0.91 \text{ d}$, $X_{MLSS} = 10.168 \text{ g L}^{-1}$, $T_{ML} = 24.7 \text{ }^\circ\text{C}$, $Q_{AIR, MS} = 4,200 \text{ L h}^{-1}$, (From Day 144 until Day 158: Transition period)

Even though scatter was increased due to cyclic filtration, it can be said that for the time period between Day 159, 09-02-2009, and Day 168, 18-02-2009, (SRT: 30 d, HRT: 1.01 d), the permeability values mainly fluctuated between 400 and 500 L m⁻² h⁻¹ bar⁻¹ at 21.1 °C, leading to an average permeability value equal to 450 at 21.1 °C. For the time period between Day 169, 19-02-2008, and Day 181, 27-02-2009, (SRT: 29 d, HRT: 0.91 d) the permeability values fluctuated between 500 and 600 L m⁻² h⁻¹ bar⁻¹ at 24.7 °C, leading to an average permeability value equal to 550 L m⁻² h⁻¹ bar⁻¹ at 24.7 °C. By temperature-correcting these values at 20 °C, the value of 450 L m⁻² h⁻¹ bar⁻¹ becomes 436 L m⁻² h⁻¹ bar⁻¹ and the value of 550 L m⁻² h⁻¹ bar⁻¹ becomes 489 L m⁻² h⁻¹ bar⁻¹. Both temperature-corrected permeability values are in line with published values mentioned in Sections 6.3.2.1 and 6.3.2.2.

All details regarding the two sustainable net MPFs and their corresponding operating conditions are summarised in Table 6.3. As the aim of this research was to maximise the daily volume of the treated permeate, it is the higher MPF of 10.92 L m⁻² h⁻¹ that is of interest.

Table 6.3 MBR1: Sustainable net MPFs and their corresponding operating conditions

Parameter	Value		Unit
Time period	Day 159 until Day 168	Day 169 until Day 181	d
Net MPF	9.81	10.92	L m ⁻² h ⁻¹
Maximum TMP	About 0.03	About 0.03	bar
Temperature-corrected permeability at 20 °C	436	489	L m ⁻² h ⁻¹ bar ⁻¹
SRT	30	29	d
HRT	1.01	0.91	d
Average MLSS concentration	4.643	10.168	g L ⁻¹
Average mixed-liquor temperature	21.2	24.7	°C
Air flow rate			
Membrane scouring only	4,200	4,200	L h ⁻¹
Operating cycle	Continuous	Continuous	min on/min off

To conclude with regard to the 3rd time period, the application of intermittent filtration was not successful, so this MBR system is better operated under continuous filtration as originally proposed by the membrane supplier.

6.2.2.4 4th research period: From 11-04-2009 until 14-06-2009

The 4th and final research period started on Day 220, 11-04-2009, and finished on Day 284, 14-06-2009. This 4th time period was characterised by the removal of the intermittent filtration on Day 262, 23-05-2009, and the second rapid membrane fouling of MBR1. During this time period, the real MPF values were increased as much as possible to explore the maximum sustainable net MPF. Initially, the SRT was still equal to 29 d and the SRT was equal to 0.91 d, as the operating conditions remained constant until Day 232, 23-04-2009.

On Day 233, 24-04-2009, the operating times were changed - the SRT was decreased to 25.5 d and the HRT was also decreased to 0.835 d. This set of operating conditions was applied until Day 244, 05-05-2009. Filtration was still intermittent, so the corresponding net and real MPF values were respectively equal to $11.88 \text{ L m}^{-2} \text{ h}^{-1}$ and $12.5 \text{ L m}^{-2} \text{ h}^{-2}$.

From Day 245, 06-05-2009, to Day 277, 07-06-2009, the SRT was set to 23.5 d and the HRT was set to 0.77 d. On Day 262, 23-05-2009, the timer was removed and continuous filtration reinstated. After that day, both real and net MPF values were identical and equal to $12.88 \text{ L m}^{-2} \text{ h}^{-1}$.

Finally, from Day 278, 08-06-2009, up to the end of the experiment, on Day 284, 14-06-2009, the SRT was set to 21.8 d and the HRT was reduced to 0.72 d, leading to a real/net MPF equal to $13.77 \text{ L m}^{-2} \text{ h}^{-1}$.

The profiles of real MPFs, TMP values and permeability values against time are plotted in Figures 6.14, 6.15 and 6.16 respectively, so the effect of the gassing rate for membrane scouring, the temperature of the mixed-liquor and the changes of the MLSS concentration on the membrane performance could be observed.

Figure 6.14 showing the profile of the real MPF against time is as follows:

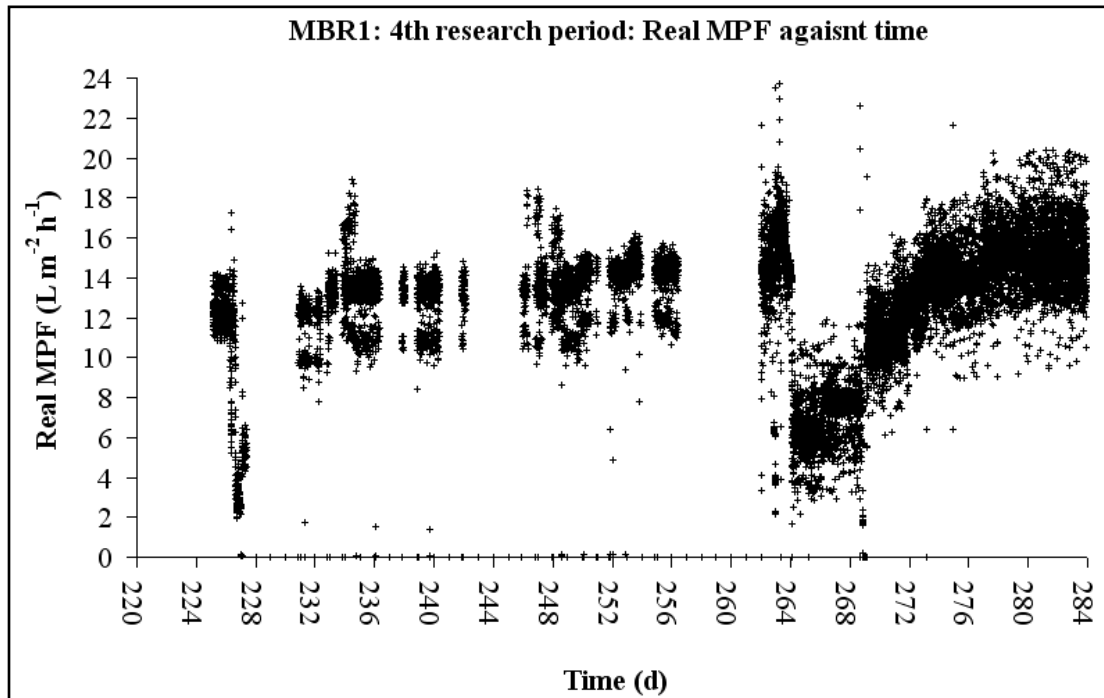


Figure 6.14 MBR1: 4th research period: Real MPF against time: From Day 220 until Day 232: $\theta_C = 29$ d, $\theta = 0.91$ d, $X_{MLSS} = 10.168$ g L⁻¹, $T_{ML} = 24.7$ °C, $Q_{AIR, MS} = 4,200$ L h⁻¹, From Day 233 until Day 244: $\theta_C = 25.5$ d, $\theta = 0.835$ d, $X_{MLSS} = 9.013$ g L⁻¹, $T_{ML} = 25.6$ °C, $Q_{AIR, MS} = 4,200$ L h⁻¹, From Day 245 until Day 277: $\theta_C = 23.5$ d, $\theta = 0.77$ d, $X_{MLSS} = 8.846$ g L⁻¹, $T = 28.9$ °C, $Q_{AIR, MS} = 4,200$ L h⁻¹, From Day 278 until Day 284: $\theta_C = 21.8$ d, $\theta = 0.72$ d, $X_{MLSS} = 9.259$ g L⁻¹, $T_{ML} = 30.2$ °C, $Q_{AIR, MS} = 4,200$ L h⁻¹

Once again the time period during which intermittent filtration was operating has to be neglected as it leads to inaccurate conclusions. However, as seen in Figure 6.14, even after the removal of intermittent filtration the real MPFs were very poorly-controlled around the expected values and large scatter appeared.

Figure 6.15 shows the changes of the TMP values against time.

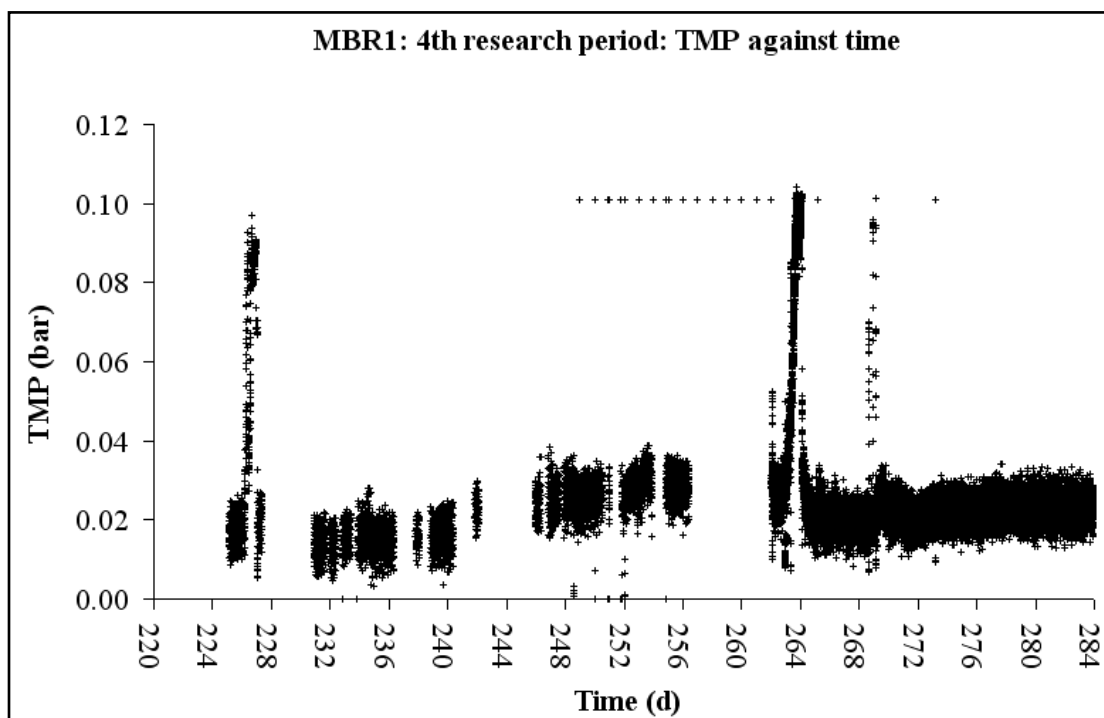


Figure 6.15 MBR1: 4th research period: TMP against time: From Day 220 until Day 232: $\theta_C = 29$ d, $\theta = 0.91$ d, $X_{MLSS} = 10.168$ g L⁻¹, $T_{ML} = 24.7$ °C, $Q_{AIR, MS} = 4,200$ L h⁻¹, From Day 233 until Day 244: $\theta_C = 25.5$ d, $\theta = 0.835$ d, $X_{MLSS} = 9.013$ g L⁻¹, $T_{ML} = 25.6$ °C, $Q_{AIR, MS} = 4,200$ L h⁻¹, From Day 245 until Day 277: $\theta_C = 23.5$ d, $\theta = 0.77$ d, $X_{MLSS} = 8.846$ g L⁻¹, $T_{ML} = 28.9$ °C, $Q_{AIR, MS} = 4,200$ L h⁻¹, From Day 278 until Day 284: $\theta_C = 21.8$ d, $\theta = 0.72$ d, $X_{MLSS} = 9.259$ g L⁻¹, $T_{ML} = 30.2$ °C, $Q_{AIR, MS} = 4,200$ L h⁻¹

On Day 264, 25-05-2009, an attempt to increase the net MPF above the value of 12.88 L m⁻² h⁻² was made, however, rapid severe membrane fouling occurred and after a few hours of continuous increase in the TMP values, the MBR operation was interrupted. At that time, TMP values were higher than 0.1 bar. Membranes were cleaned once again both physically and chemically and the net MPF was gradually restored to its previous 12.88 L m⁻² h⁻¹. Then, a final attempt to increase the net MPF was made - that took place from Day 278, 08-06-2009, up to the end of the experiment, on Day 284, 14-06-2009. The SRT was set to 21.8 d and HRT was set to 0.72 d leading to a net MPF of 13.77 L m⁻² h⁻¹. This time the net MPF was successfully sustained as the TMP profile appeared to be quite stable. However, a few days later, the MBR was shut-down at the end of the project trial period.

There was also a membrane fouling event around Day 225, 16-04-2009. This is likely to have been another side-effect of the operation of intermittent filtration, as neither the MLSS concentration, nor the temperature of the mixed-liquor experienced any serious change during that day. In addition, operation was successfully restored to normal via physical cleaning by gassing in the absence of filtration.

Regarding the MLSS concentrations, it can be said that during this research period they were properly controlled at around 9 - 10 g L⁻¹. The values measured experimentally did not significantly fluctuate so that the average MLSS concentrations, as given in Table 5.4, can be used. Temperature of the mixed-liquor during this period of time had started increasing as summer was approaching. From Day 245, 06-05-2009, to Day 277, 07-06-2009, an average value equal to 28.9 °C was calculated, whereas from Day 278, 08-06-2009, up to the end of the experiment, on Day 284, 14-06-2009, it was found to be equal to 30.2 °C. The increase in this temperature can positively influence the membrane performance, via a reduction in the viscosity of the mixed-liquor, and perhaps higher real MPFs may be able to be sustained.

Figure 6.16 depicts the course of permeability against time.

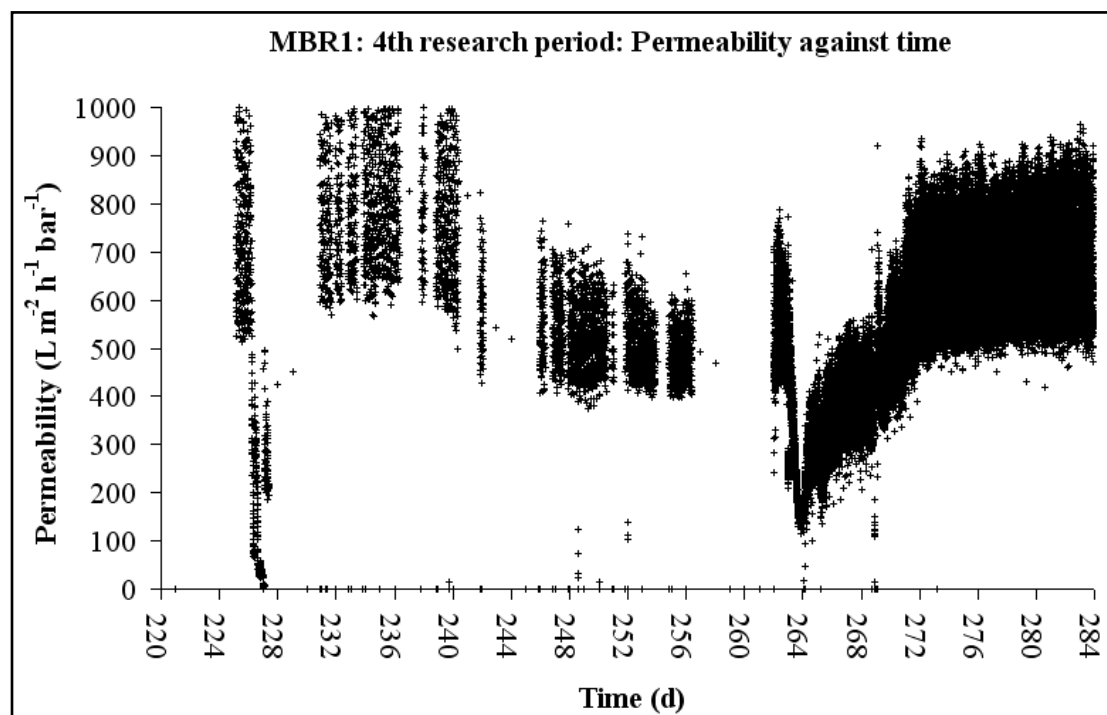


Figure 6.16 MBR1: 4th research period: Permeability against time: From Day 220 until Day 232: $\theta_C = 29$ d, $\theta = 0.91$ d, $X_{MLSS} = 10.168$ g L⁻¹, $T_{ML} = 24.7$ °C, $Q_{AIR, MS} = 4,200$ L h⁻¹, From Day 233 until Day 244: $\theta_C = 25.5$ d, $\theta = 0.835$ d, $X_{MLSS} = 9.013$ g L⁻¹, $T_{ML} = 25.6$ °C, $Q_{AIR, MS} = 4,200$ L h⁻¹, From Day 245 until Day 277: $\theta_C = 23.5$ d, $\theta = 0.77$ d, $X_{MLSS} = 8.846$ g L⁻¹, $T_{ML} = 28.9$ °C, $Q_{AIR, MS} = 4,200$ L h⁻¹, From Day 278 until Day 284: $\theta_C = 21.8$ d, $\theta = 0.72$ d, $X_{MLSS} = 9.259$ g L⁻¹, $T_{ML} = 30.2$ °C, $Q_{AIR, MS} = 4,200$ L h⁻¹

Due to the huge scatter, a clear conclusion regarding the permeability values cannot be made. However, it can be said that, regardless of the operating conditions, the permeability values always remained at values higher than 500 L m⁻² h⁻¹ bar⁻¹ at 30.2 °C. By temperature-correcting this value, it can be concluded that permeability figures remained always higher than 389 L m⁻² h⁻¹ bar⁻¹ at 20 °C, which is within the range of typical values in the literature, [Van-Bentem *et al.*, 2007].

Table 6.4 summarises details regarding the new net sustainable MPFs and their corresponding operating conditions.

Table 6.4 MBR1: Sustainable net membrane MPFs and their corresponding operating conditions

Parameter	Value		Unit
Time period	Day 245 until Day 277	Day 278 until Day 284	d
Net MPF	12.88	13.77	L m ⁻² h ⁻¹
Maximum TMP	About 0.02	About 0.03	bar
Temperature-corrected permeability at 20 °C	Higher than 389	Higher than 389	L m ⁻² h ⁻¹ bar ⁻¹
SRT	23.5	21.8	d
HRT	0.77	0.72	d
Average MLSS concentration	8.846	9.259	g L ⁻¹
Average mixed-liquor temperature	28.9	28.9	°C
Air Flow rate			
Membrane scouring only	4,200	4,200	L h ⁻¹
Operating cycle	Continuous	Continuous	min on/min off

To conclude, the maximum average sustainable net MPF, as estimated during the long-term experiment, was 13.77 L m⁻² h⁻¹ - this value may be further improved, however, the long-term experiment had to be stopped at the end of the project period. As a lot of scatter appeared, it may be worth re-testing this average MPF so as more accurate conclusions are made.

6.4 Membrane performance of MBR2

6.4.1 Introduction

MBR2 was started-up for a first time on 02-09-2008. However, the MBR system experienced some operational problems and was shut down whilst these were addressed. MBR2 was re-started on 07-11-2008, Day 1, and initially, biomass was allowed to increase spontaneously to a value of 4 - 5 g L⁻¹. The SRT was fixed at 15 d and the HRT was fixed at 1.01 d - a combination of operating times that would be able to increase the biomass concentration up to the selected value.

The air flow rate for biomass maintenance/membrane scouring within the MBR tank was set to the manufacturer's standard setting. The value was $12,000 \text{ L h}^{-1}$, that is to say, $6,000 \text{ L h}^{-1}$ per each air blower, and this value was not altered during the long-term experiment. The amount of air that was provided within the biological tank for biomass maintenance was also as suggested by the membrane manufacturer. Regarding MBR2 operation, it can be said that biomass was successfully maintained all the time and the microbial cultures never suffered from lack of oxygen as they were always capable of successfully consuming most of the organic substrate of the influent leading to very low effluent COD concentration values. Cross flow filtration was applied and was operated in a constant-flux mode. Filtration was intermittent - a 10-min long operational filtration/relaxation cycle was applied, with 9 min of filtration being followed by 1 min of membrane relaxation. This filtration/relaxation cycle remained constant during the long-term experiment and was only briefly changed when some short-term flux-step tests were performed. Details about these specific changes of the operational filtration/relaxation cycle will be given later in Section 6.4.2.2, when the flux-step experiments are described.

6.4.2 Data Processing

The experimental time period was divided into three data processing periods so as to allow a clearer presentation of results. These research periods are summarised in Table 6.5.

Table 6.5 MBR2: Data processing periods

Research time periods (dates)	Number of days
07-11-2008 until 11-01-2009	1 to 65
11-01-2009 until 23-03-2009	65 to 136
23-03-2009 until 14-06-2009	136 to 219

Based on the raw data, which was collected during the long-term experiment the instant real MPFs, TMP values and permeability values were estimated through Equations 4.8, 4.13 and 4.14. Figures showing the courses of these three parameters

against time were plotted and even though some scatter was present, reliable average values of these parameters could be calculated. Then for each set of operating conditions the corresponding net/real MPFs were calculated with the aid of the equations shown in Table 6.2, together with Equations 6.1 and 6.2., and it was possible to check whether good control of the instant real MPFs was achieved. Also, directly from the figures, it was possible to calculate average TMP and permeability values. Finally, if necessary, temperature-corrected average permeability values at a reference temperature of 20 °C were calculated through Equation 4.7.

6.4.2.1 1st research period: From 07-11-2008 until 11-01-2009

This research period started on Day 1, 07-11-2008, and finished on Day 65, 11-01-2009. From Day 1, 07-11-2008, to about Day 57, 03-01-2009, average biomass concentration was equal to 4.592 g L⁻¹ - the SRT was set to 15 d and the HRT was set to 1.01 d. On Day 57, 03-01-2009, up to the end of this time period, on Day 65, 11-01-2009, MLSS concentration was under dynamic conditions following the adjustment of the SRT to 30 d and HRT to 1.01 d. This was a deliberate decision as it was necessary to increase the MLSS concentration up to a new value of 9 - 10 g L⁻¹. On Day 65, 11-01-2009, which was the last day during this time period, the MLSS concentration, had reached a new increased value of 6.5 g L⁻¹. More details about the transition period regarding the changes of the MLSS concentrations are given in Section 6.4.2.2.

Figure 6.17 shows the real MPF profile against time.

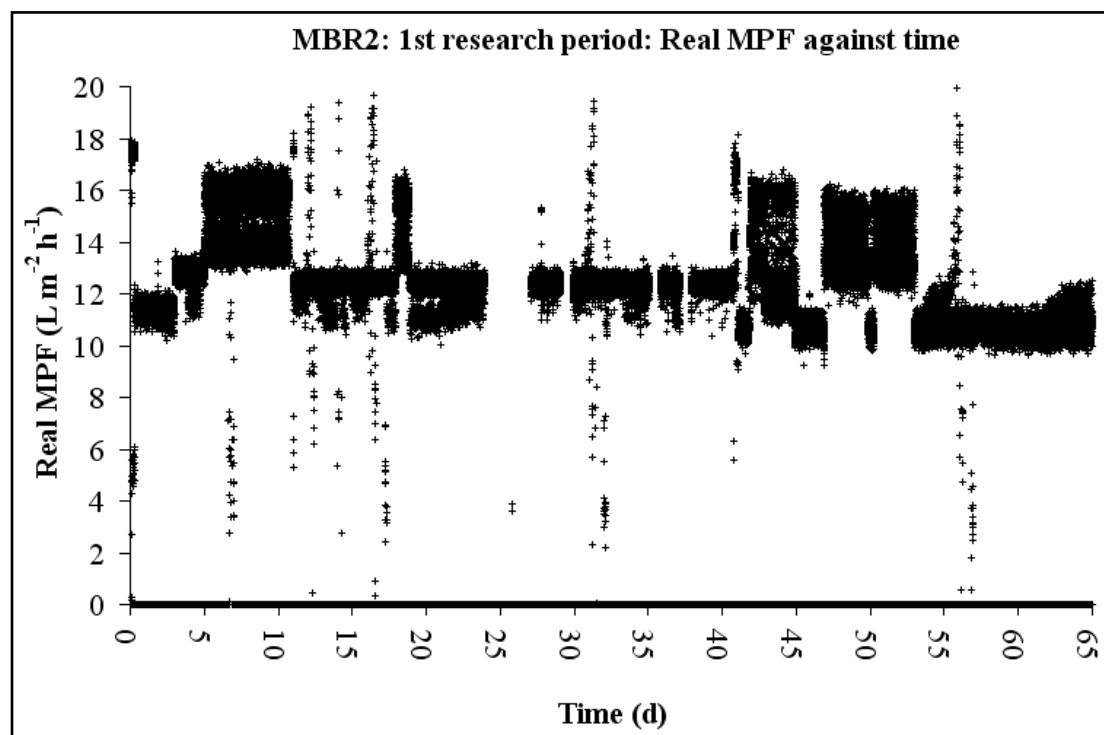


Figure 6.17 MBR2: 1st research period: Real MPF against time: From Day 1 until Day 57: $\theta_C = 15$ d, $\theta = 1.01$ d, $X_{MLSS} = 4.592$ g L⁻¹, $T_{ML} = 21.2$ °C, $Q_{AIR, MS} = 12,000$ L h⁻¹, (From Day 58 until Day 65: Transition period)

The gaps appearing in Figure 6.17 are due to power cuts that took place during the 1st research period. During the time period between Day 1, 07-11-2008, and Day 57, 03-01-2009, the SRT was equal to 15 d, the HRT was equal to 1.01 d and the corresponding net MPF was equal to 11.12 L m⁻² h⁻¹ (corresponding real MPF: 12.35 L m⁻² h⁻¹).

During the time period from Day 12, 19-11-2008, to Day 41, 18-12-2008, the MBR2 system was operated under steady state operating conditions and reliable conclusions can be drawn. As seen in Figure 6.17, the instant real MPFs were properly controlled around the expected real value of 12.35 L m⁻² h⁻¹ - the net MPF was equal to 11.12 L m⁻² h⁻¹. The zero data values represent the instant real MPF values during relaxation. Before concluding whether the net MPF of 11.12 L m⁻² h⁻¹ was a sustainable condition or not, the TMP profile against time has to be observed. Figure 6.18 shows the course of TMP values against time.

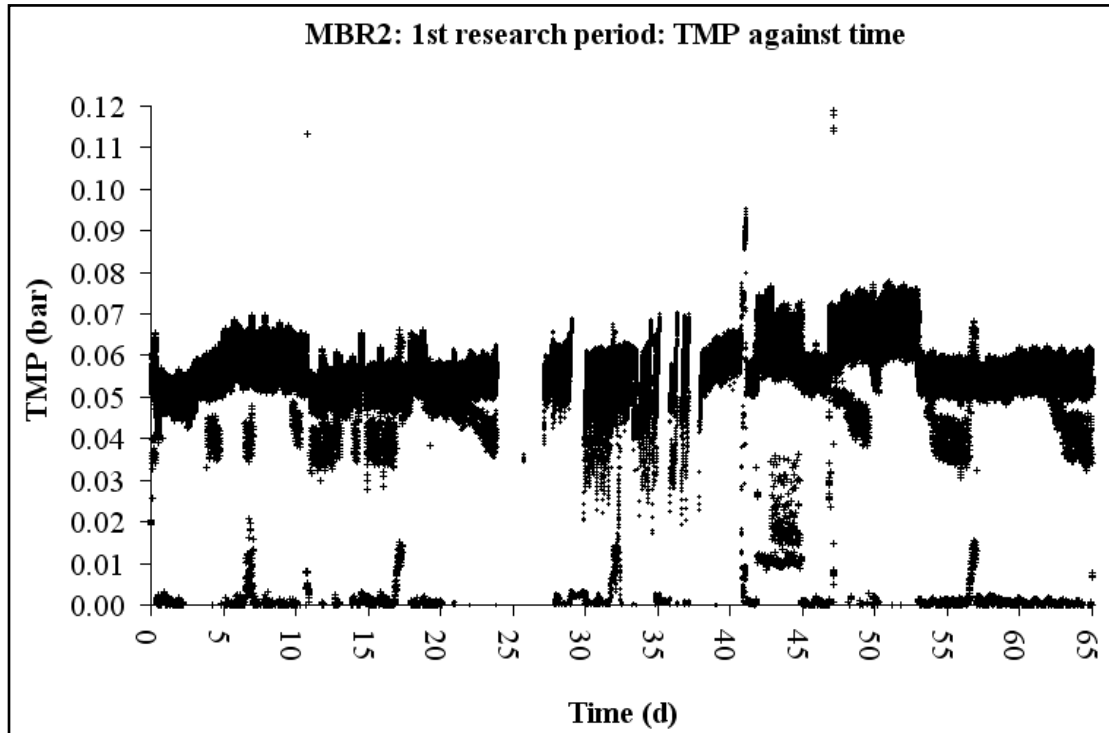


Figure 6.18 MBR2: 1st research period: TMP against time: From Day 1 until Day 65: $\theta_C = 15$ d, $\theta = 1.01$ d, $X_{MLSS} = 4.592$ g L⁻¹, $T_{ML} = 21.2$ °C, $Q_{AIR, MS} = 12,000$ L h⁻¹, (From Day 58 until Day 65: Transition period)

In general, it can be said that during the 1st research period, no membrane fouling occurred as TMP values never increased dramatically. Each time the real MPF increased or decreased, the instant TMP values respectively increased or decreased, meaning that the MBR system reacted as expected each time the set-point of the flow meter was altered.

With regard to the TMP values during the time period from Day 12, 19-11-2008, to Day 41, 18-12-2008, as seen in Figure 6.18, the MBR2 system was operated without having any membrane fouling problems as the TMP values did not increase and an average TMP value of 0.059 bar was achieved. The net MPF of 11.12 L m⁻² h⁻² under these operating conditions was a sustainable condition. However, it is worth checking how the permeability values responded during this time period.

Figure 6.19 shows the permeability values against time.

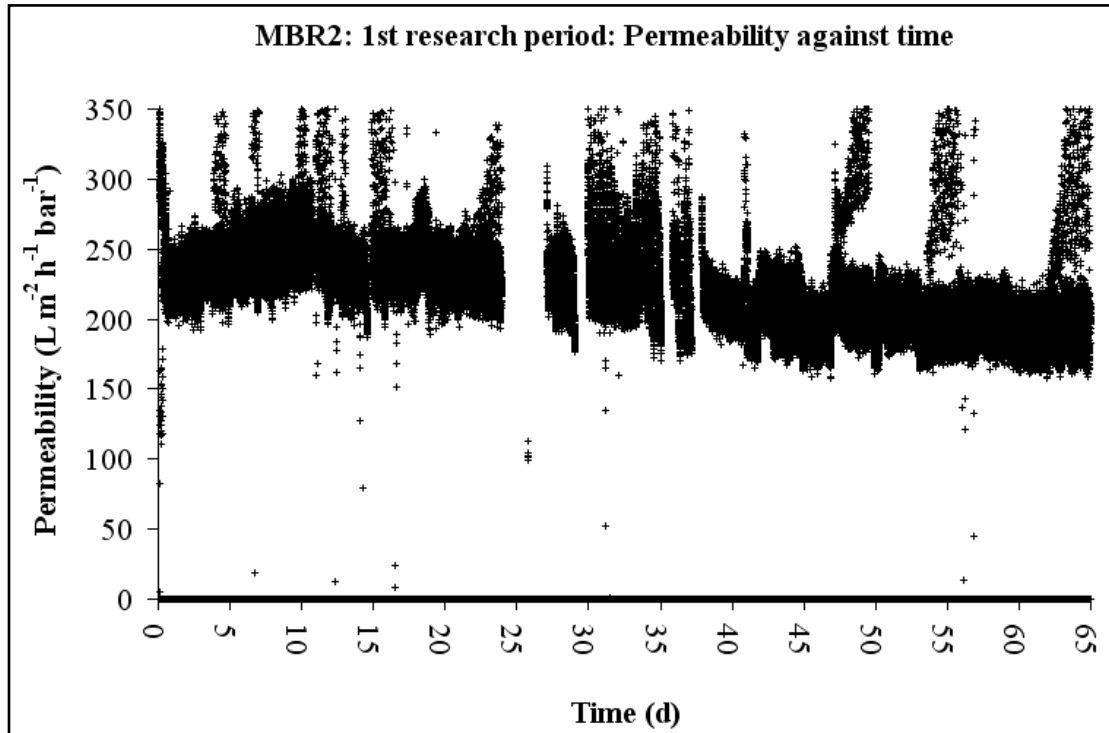


Figure 6.19 MBR2: 1st research period: Permeability against time: From Day 1 until Day 65: $\theta_C = 15$ d, $\theta = 1.01$ d, $X_{MLSS} = 4.592$ g L⁻¹, $T_{ML} = 21.2$ °C, $Q_{AIR, MS} = 12,000$ L h⁻¹, (From Day 58 until Day 65: Transition period)

For the time period between Day 12, 19-11-2008, to Day 41, 18-12-2008, an average permeability value at 21.2 °C was estimated to be 235 L m⁻² h⁻¹ bar⁻¹. By correcting this value to 20 °C, a temperature-corrected permeability value of 228 L m⁻² h⁻¹ bar⁻¹ was obtained. This value makes good sense, as it was found to be lower than the estimated value for clean water at 20 °C, which was 494 L m⁻² h⁻² bar⁻¹.

A promising set of operating conditions that are capable of leading to a stable long-term MBR operation and producing treated water that can be used for unrestricted irrigation in Tunisia have been identified, and these are shown in Table 6.6.

Table 6.6 MBR2: Sustainable MPF and its corresponding operating conditions.

Parameter	Value	Unit
Time period	Day 12 until Day 41	d
Net MPF	11.12	L m ⁻² h ⁻¹
Maximum TMP	0.059	bar
Temperature-corrected permeability at 20 °C	228	L m ⁻² h ⁻¹ bar ⁻¹
SRT	15	d
HRT	1.01	d
Average MLSS concentration	4.592	g L ⁻¹
Average mixed-liquor temperature	21.2	°C
Air Flow rate		
Membrane scouring only	12,000	L h ⁻¹
Operating cycle	9/1	min on/min off

6.4.2.2 2nd research period: From 11-01-2009 until 23-03-2009

The 2nd research period started on Day 65, 11-01-2009, and finished on Day 136, 23-03-2009. During this time period, a short-term flux-step test was also performed and the first serious membrane fouling occurred. Until Day 83, 29-01-2009, the biomass concentration was left to increase to a new value equal to about 9 - 10 g L⁻¹. The SRT value was set to 30 d and the HRT was set to 1.01 d since Day 57, 03-01-2009.

From Day 84, 30-01-2009, to Day 105, 20-02-2009, the MBR2 system continued to be operated under the same conditions, however, the MLSS concentration had already reached steady state and it had stabilised at an average value of 9.687 g L⁻¹. The combination of the SRT/HRT led to a net MPF value equal to 11.52 L m⁻² h⁻¹ (real MPF: 12.8 L m⁻² h⁻¹). Average mixed-liquor temperature was 21.2 °C during this time period. On Day 105, 20-02-2009, and until Day 126, 13-03-2009, an attempt to increase the net MPF was made. However, during this time period, membrane fouling occurred and, on Day 126, 13-03-2009, it was decided to suspend operation - more details will be given later in this section. Chemical cleaning was applied and, on Day

130, 17-03-2009, the MBR was re-started with an SRT re-set to 30 d and an HRT re-set to 1.01 d. The previous real MPF set-point was re-selected and net MPF was reduced to the value of $11.52 \text{ L m}^{-2} \text{ h}^{-1}$. These operating conditions did not change until the end of the 2nd time period, on Day 136, 23-03-2009.

Figure 6.20 shows the course of real MPF against time.

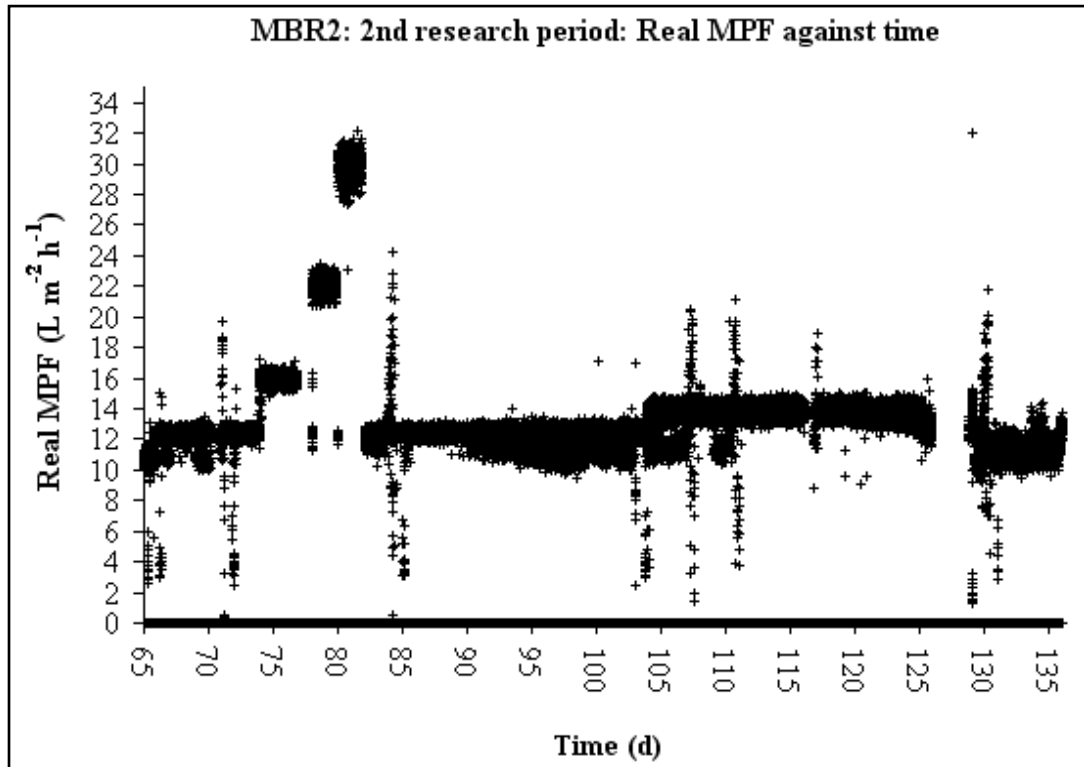


Figure 6.20 MBR2: 2nd research period: Real MPF against time: From Day 84 until Day 136: $\theta_C = 30 \text{ d}$, $\theta = 1.01 \text{ d}$, $X_{\text{MLSS}} = 9.687 \text{ g L}^{-1}$, $T_{\text{ML}} = 21.2 \text{ }^\circ\text{C}$, $Q_{\text{AIR, MS}} = 12,000 \text{ L h}^{-1}$, (From Day 65 until Day 83: Transition period)

As seen in Figure 6.20, the applied real MPF of $12.8 \text{ L m}^{-2} \text{ h}^{-1}$ - from Day 84, 30-01-2009, to Day 105, 20-02-2009, - was properly controlled. During this time period, the STR was adjusted to 30 d and the HRT was adjusted to 1.01 d. The net MPF was $11.52 \text{ L m}^{-2} \text{ h}^{-1}$ (real MPF: $12.8 \text{ L m}^{-2} \text{ h}^{-1}$). The average MLSS concentration was 9.687 g L^{-1} and the average temperature of the mixed-liquor was $21.2 \text{ }^\circ\text{C}$. This time period is the only time period that was able to lead to a sustainable net MPF. However, more details will be given after plotting the TMP values against time, (Figure 6.21).

The course of TMP values against time is shown in Figure 6.21.

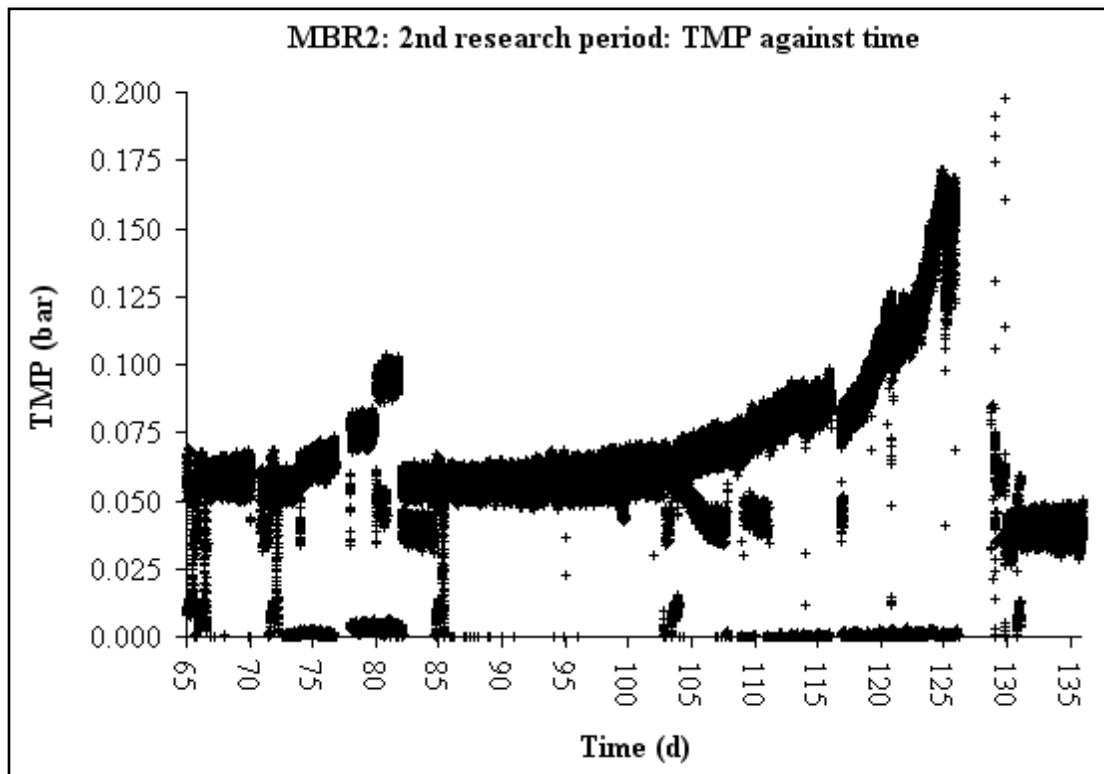


Figure 6.21 MBR2: 2nd research period: TMP against time: From Day 84 until Day 136; $\theta_C = 30$ d, $\theta = 1.01$ d, $X_{MLSS} = 9.687$ g L⁻¹, $T_{ML} = 21.2$ °C, $Q_{AIR, MS} = 12,000$ L h⁻¹, (From Day 65 until Day 83: Transition period)

As seen in Figure 6.21, the net MPF of 11.52 L m⁻² h⁻¹ did lead to a reliable long-term membrane performance - average TMP values were still equal to 0.059 bar. On Day 106, 21-02-2009, an attempt to further increase the real MPF above 12.8 L m⁻² h⁻¹ took place, and as seen in Figure 6.21, severe membrane fouling appeared. Initially it can be accepted that a linear increase in the TMP values took place. This linear increase in the TMP values lasted until Day 116, 03-03-2009. On that day membranes were cleaned physically, which means that filtration was suspended but air was still being provided within the MBR tank so that membrane scouring was taking place. When filtration was re-started, initial TMP values seemed to have been significantly reduced indicating removal of membrane fouling, however, the TMP started increasing immediately after reinstating filtration and this time the increase appeared to be exponential. The physical cleaning was not effective as residual membrane fouling had already been formed. As suggested by the membrane supplier, the MBR2

system should not be operated at MLSS concentrations higher than 12 g L^{-1} and the MLSS concentration values around these days was higher than 10 g L^{-1} , which might well have affected the membrane performance. On Day 126, 13-03-2009, the operation was interrupted so that chemical membrane cleaning based on NaOCl solutions was applied. This attempt to increase the net MPF under the present operating conditions was unsuccessful and that net MPF value was not a sustainable condition. After the application of the chemical cleaning the real MPF value was reduced to its previous value of $12.8 \text{ L m}^{-2} \text{ h}^{-1}$.

The course of permeability against time is plotted - this is shown in Figure 6.22.

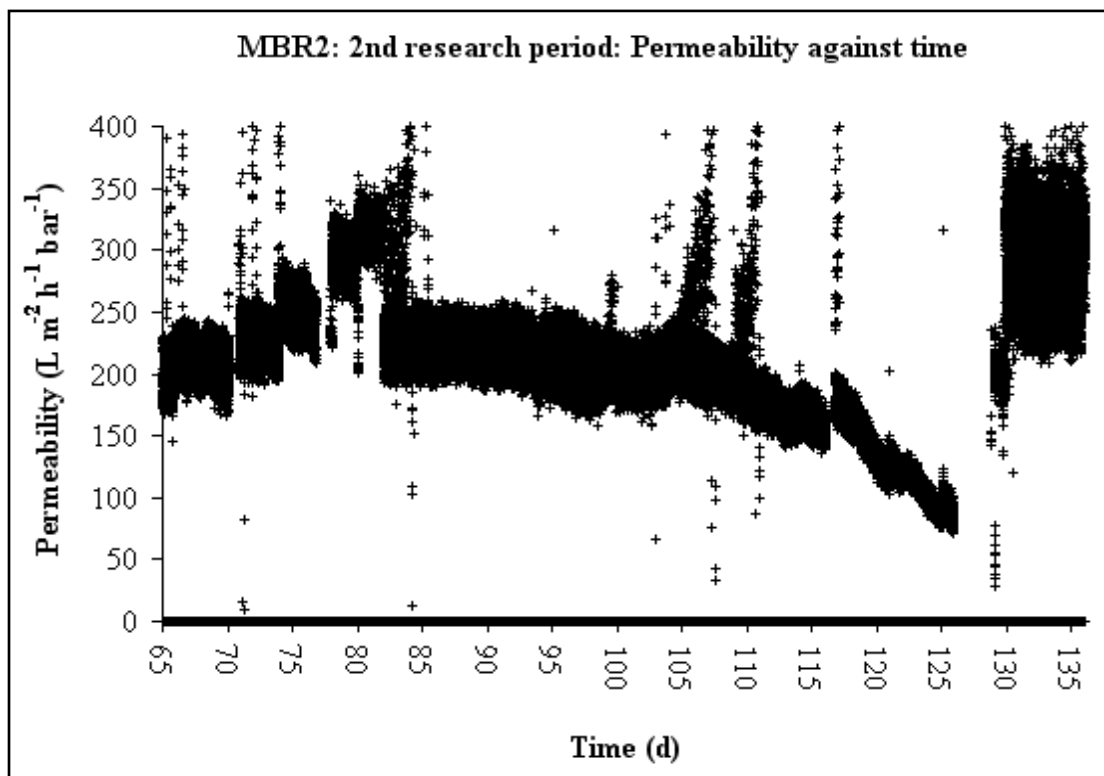


Figure 6.22 MBR2: 2nd research period: Permeability against time: From Day 84 until Day 136: $\theta_C = 30 \text{ d}$, $\theta = 1.01 \text{ d}$, $X_{MLSS} = 9.687 \text{ g L}^{-1}$, $T_{ML} = 21.2 \text{ }^\circ\text{C}$, $Q_{AIR, MS} = 12,000 \text{ L h}^{-1}$, (From Day 65 until Day 83: Transition period)

As seen in Figure 6.22, after the exponential TMP increase, the permeability values started to decrease rapidly, reaching very low values of about $75 \text{ L m}^{-2} \text{ h}^{-1} \text{ bar}^{-1}$ at $21.2 \text{ }^\circ\text{C}$ on Day 126, 13-03-2009. By correcting this value to $20 \text{ }^\circ\text{C}$ a very low

permeability value of $72 \text{ L m}^{-2} \text{ h}^{-1} \text{ bar}^{-1}$ is arrived at and operation was interrupted to allow for chemical cleaning of the membranes.

However, an average permeability value of $216 \text{ L m}^{-2} \text{ h}^{-1} \text{ bar}^{-1}$ at $21.2 \text{ }^\circ\text{C}$ can be calculated for the set of operating conditions, which led to a net MPF equal to $11.52 \text{ L m}^{-2} \text{ h}^{-1}$ - MBR operation between Day 84, 30-01-2009, and Day 105, 20-02-2009. By correcting this permeability value, a value of $210 \text{ L m}^{-2} \text{ h}^{-1} \text{ bar}^{-1}$ at $20 \text{ }^\circ\text{C}$ can be estimated, which is in line with manufacturers data quoted in Section 6.4.2.1. A promising set of operating conditions capable of leading to a constant long-term MBR operation, which is also able to produce treated water of the appropriate quality, is shown in Table 6.7.

Table 6.7 MBR2: Sustainable net membrane MPF and its corresponding operating conditions

Parameter	Value	Unit
Net MPF	11.52	$\text{L m}^{-2} \text{ h}^{-1}$
Average TMP	0.059	bar
Temperature-corrected permeability at $20 \text{ }^\circ\text{C}$	210	$\text{L m}^{-2} \text{ h}^{-1} \text{ bar}^{-1}$
SRT	30	d
HRT	1.01	d
Average MLSS concentration	9.687	g L^{-1}
Average mixed-liquor temperature	21.2	$^\circ\text{C}$
Air Flow rate		
Membrane scouring only	12,000	L h^{-1}
Operating cycle	9/1	min on/min off

• Short-term flux-step tests

A short-term flux-step test was performed during the 2nd research time period. During this test, both real MPFs during filtration, and the relaxation time of a 10 min-long filtration/relaxation cycle, were adjusted so that the net MPF value remained constant. This practically means that each time a higher real MPF was tested, a longer relaxation time, so consequently a shorter filtration time, was applied. The

combinations that were tested are shown in Table 6.8. This test was conducted so as the beneficial effect of the relaxation time on the mitigation of membrane fouling could be explored.

The short-term flux-step test started on Day 74, 20-01-2009, and finished on Day 82, 28-01-2009. Throughout this time period, the MLSS concentration was essentially stable, with an initial value of 8.97 g L^{-1} and final value of 9.9 g L^{-1} . Table 6.8 includes information with regard to the operating conditions applied during this test. During this test, the net MPF was controlled to around the value of $11.52 \text{ L m}^{-2} \text{ h}^{-1}$.

Table 6.8 MBR2: Operating conditions during the short-term flux-step test: X_{MLSS} : Between 8.97 g L^{-1} and 9.9 g L^{-1} , $T_{\text{ML}} = 21.2 \text{ }^{\circ}\text{C}$, $Q_{\text{AIR, MS}} = 12,000 \text{ L h}^{-1}$

Real MPF during the filtration time ($\text{L m}^{-2} \text{ h}^{-1}$)	Filtration/Relaxation cycle		Net MPF ($\text{L m}^{-2} \text{ h}^{-1}$)
	Filtration time (min)	Relaxation time (min)	
16.06	7	3	11.23
22.11	5	5	11.01
29.67	4	6	11.88

From Table 6.8, it can be seen that the net MPFs remained around the same value, as expected - real MPFs as shown in Table 6.8 are average values estimated by making use of the instant real MPFs that were recorded during the test. Figure 6.23 shows the profiles of the real MPFs during against time.

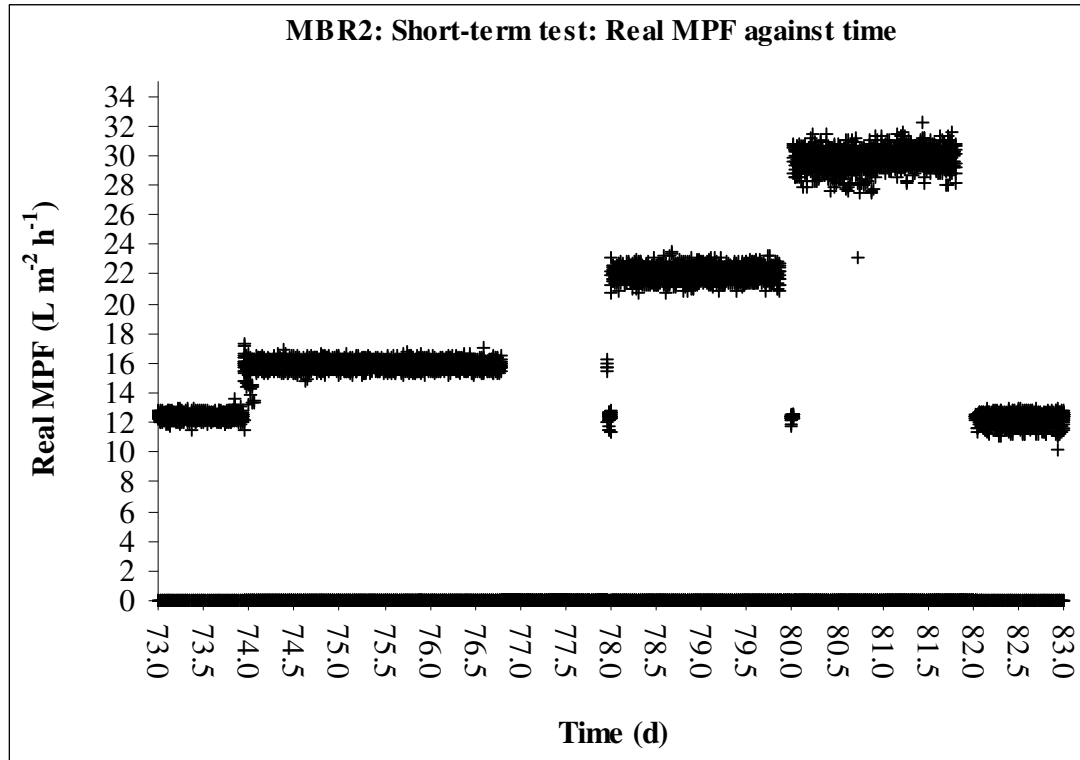


Figure 6.23 MBR2: Short-term flux-step test: Real MPF against time: X_{MLSS} :
Between 8.97 g L^{-1} and 9.9 g L^{-1} , $T_{ML} = 21.2 \text{ }^{\circ}\text{C}$, $Q_{AIR} = 12,000 \text{ L h}^{-1}$

Figure 6.23 shows that the real MPFs that were tested were well-controlled, even though the higher real MPF values gave more scatter around the selected set-points. The scatter at higher real MPFs is due to the influence of the PID control system on the permeate pump. Thus, more scatter was expected when shorter filtration time periods at higher MPFs were tested.

Figure 6.24 shows the TMP changes against time.

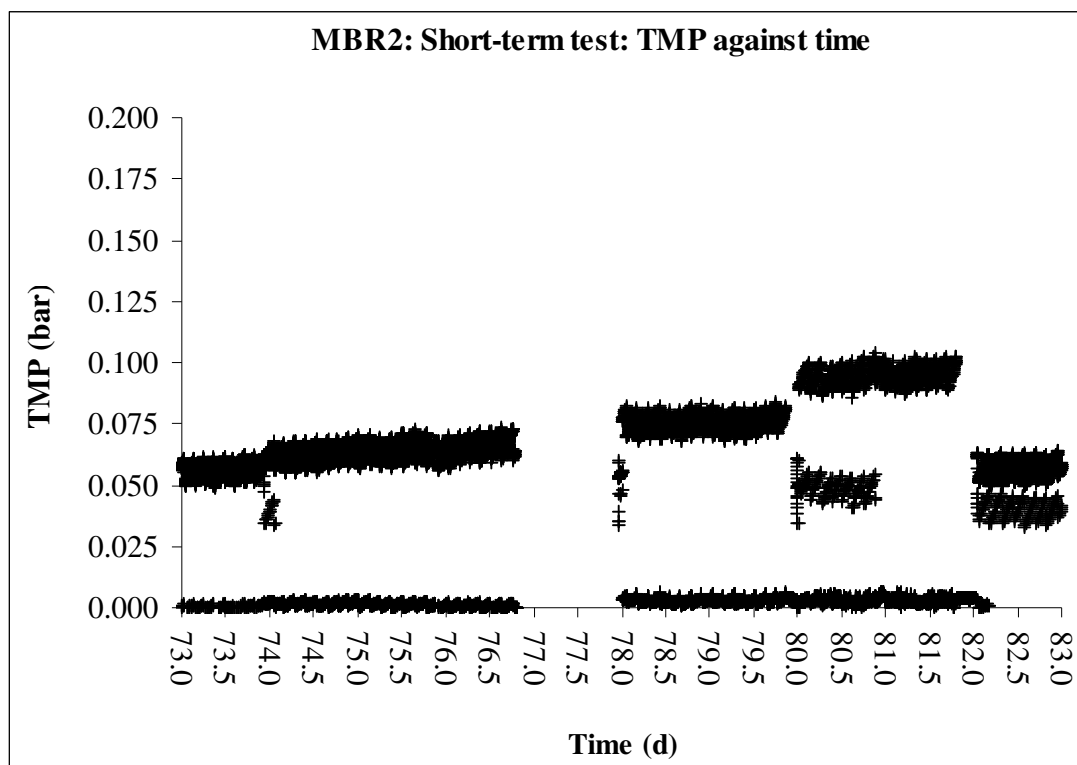


Figure 6.24 MBR2: Short-term flux-step test: TMP against time: X_{MLSS} : Between 8.97 g L^{-1} and 9.9 g L^{-1} , $T_{ML} = 21.2 \text{ }^{\circ}\text{C}$, $Q_{AIR} = 12,000 \text{ L h}^{-1}$

As seen in Figure 6.24, the “saw-tooth” effect took place again, as the instant TMP values on the feed side of the membranes could not be measured. However, the “saw-tooth” effect for the MBR2 system is obviously less serious than for the MBR1 system, so it was not removed.

As already known, when the filtration/relaxation cycle is set to 9/1 min/min on/off, the average net MRF of $11.52 \text{ L m}^{-2} \text{ h}^{-1}$ is sustainable at an average MLSS concentration of 9.687 g L^{-1} and a mixed-liquor temperature of $21.2 \text{ }^{\circ}\text{C}$.

For the time period between Day 74, 20-01-2009, and Day 77, 23-01-2009, the relaxation time was adjusted to a new value of 3 min. During this time period, the average TMP values increased from about 0.064 bar, on Day 74, 20-01-2009, to about 0.067 bar, on Day 77, 23-01-2009. For the time period between Day 80, 26-01-2009, and Day 82, 28-01-2009, the relaxation time was adjusted again to 6 min. During these two days, the average TMP values did not change at all but remained on average at 0.097 bar. The fact that the instant TMP values were higher during this

time period was due to the fact that a higher real MPF had been selected, or otherwise the selected net MPF would not be able to be maintained. The fact that the average TMP remained at a constant value proves that longer relaxation times can positively influence the membrane performance and delay, or even prohibit, any formation of membrane fouling.

Practically, even though all the operating conditions tested can lead to a reliable long-term membrane performance, the longer relaxation time of 6 min can possibly lead to an improved membrane performance capable of lasting for an even longer time period before the application of a chemical cleaning becomes obligatory. This can reduce possible running costs with regard to the purchase of chemicals, as well as to extend the life time of the membranes as chemical cleaning can deteriorate the quality of the membrane material. The fact that longer relaxation times can improve the operation of MBRs is also reported in the MBR literature - see, [Howell *et al.*, 2004].

The permeability course against time is shown in Figure 6.25.

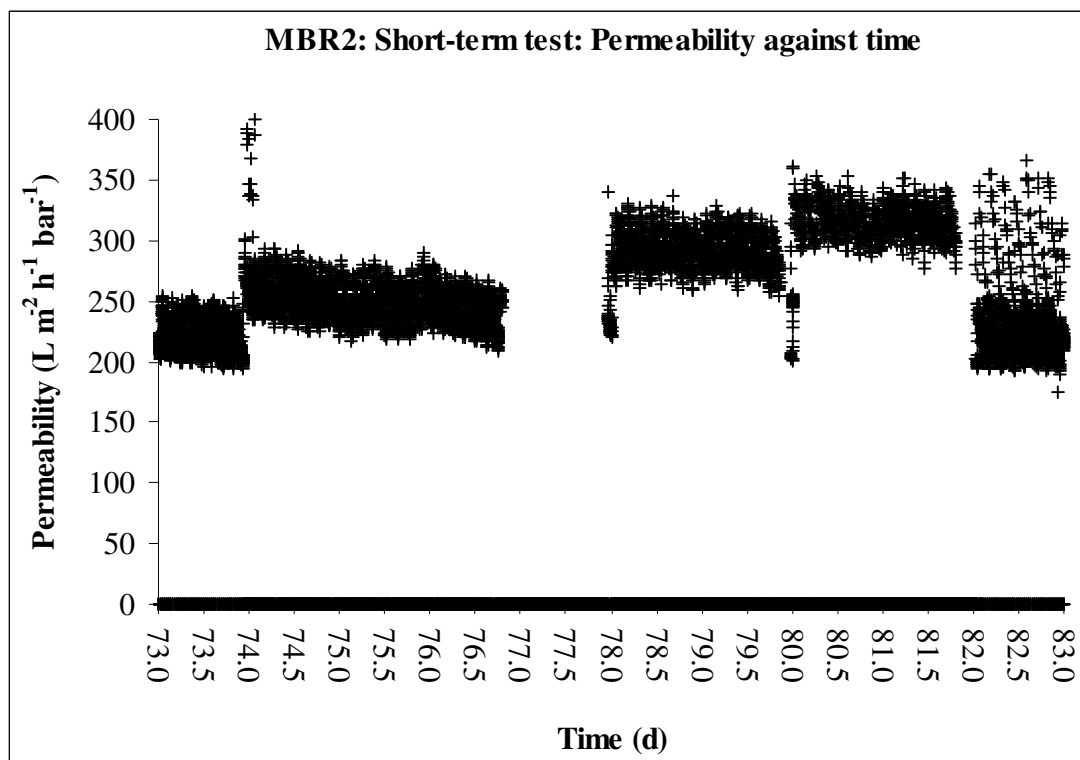


Figure 6.25 MBR2: Short-term flux-step test: Permeability against time: X_{MLSS} : Between 8.97 g L^{-1} and 9.9 g L^{-1} , $T_{ML} = 21.2 \text{ }^\circ\text{C}$, $Q_{AIR} = 12,000 \text{ L h}^{-1}$

Similar comments can be made regarding the permeability profile against time. For similar net MPFs, longer relaxation times resulted in higher permeability values. The overall resistance against filtration when longer relaxation times were applied was smaller, indicating that the application of a higher real MPF and a longer relaxation time led to a better membrane performance compared to a lower real MPF and a shorter relaxation time. However, there may be a trade-off between these two contradictory conditions as the application of very high real MPFs will not be able to be controlled by the use of a long relaxation time at high MLSS values, and the formation of membrane fouling will become inevitable.

6.4.3.3 3rd research period: From 23-03-2009 until 14-06-2009

This is the 3rd and final research period before the shut-down of the MBR2 system during which a further attempt to increase the sustainable net MPFs above the value of $11.52 \text{ L m}^{-2} \text{ h}^{-1}$ was made. This time period started on Day 136, 23-03-2009, and ended on Day 219, 14-06-2009. From Day 136, 23-03-2009, to Day 152, 08-04-2009, the SRT remained at 30 d and the HRT remained at 1.01 d, as after the application of the chemical cleaning the real MPF had to be reduced to value prior to membrane fouling.

On Day 152, 08-04-2009, another attempt to increase the net MPF was made. The SRT was set to 29 d and the HRT was set to 0.91 d. These operating conditions were applied until Day 168, 24-04-2009, and a net MPF was estimated at $12.81 \text{ L m}^{-2} \text{ h}^{-1}$ (real MPF: $14.24 \text{ L m}^{-2} \text{ h}^{-1}$).

Finally, from around Day 169, 25-04-2009, up to the end of the long-term experiment, on Day 219, 16-04-2009, the SRT followed the adjustment of 25.5 d and the HRT that one of 0.835 d corresponding to a new net MPF value equal to $13.94 \text{ L m}^{-2} \text{ h}^{-1}$ (real MPF: $15.49 \text{ L m}^{-2} \text{ h}^{-1}$). Details about the MLSS concentrations during the 3rd research period and the mixed-liquor temperatures are given later in this section.

Figure 6.26 shows the average net MPF against time.

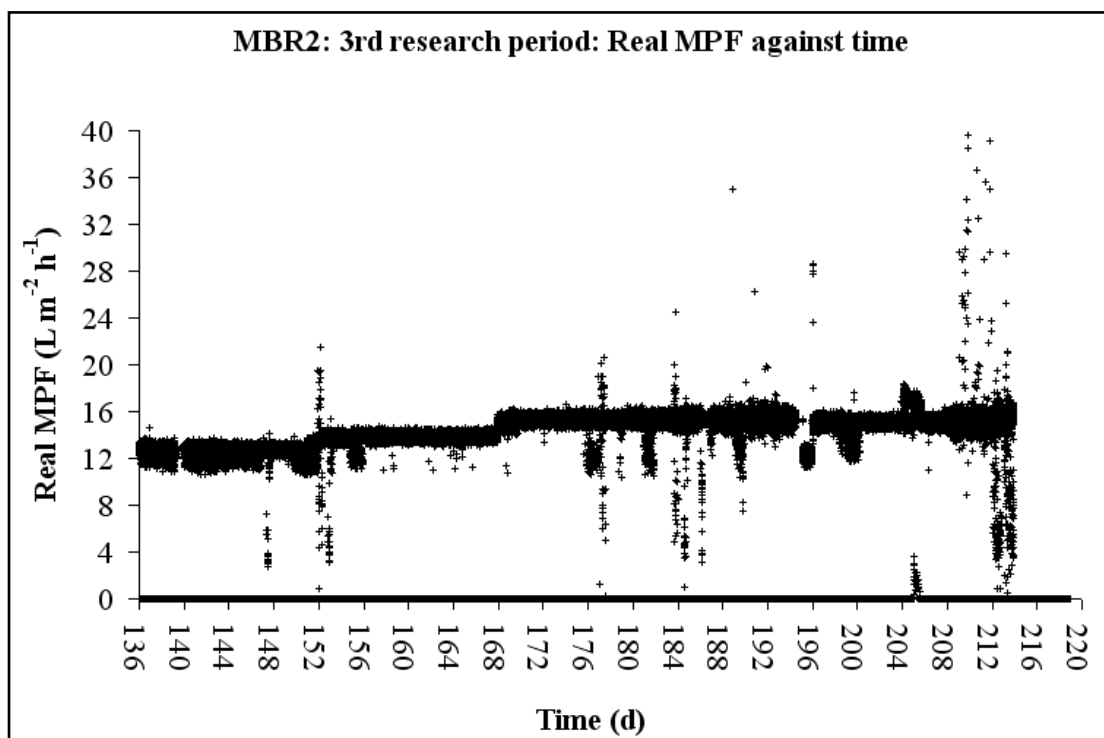


Figure 6.26 MBR2: 3rd research period: Real MPF against time: From Day 136 until Day 152: $\theta_C = 30 \text{ d}$, $\theta = 1.01 \text{ d}$, $X_{MLSS} = 9.687 \text{ g L}^{-1}$, $T_{ML} = 21.2 \text{ }^\circ\text{C}$, $Q_{AIR, MS} = 12,000 \text{ L h}^{-1}$, From Day 153 until Day 168: $\theta_C = 29 \text{ d}$, $\theta = 0.91 \text{ d}$, $X_{MLSS} = 9.206 \text{ g L}^{-1}$, $T_{ML} = 21.2 \text{ }^\circ\text{C}$, $Q_{AIR, MS} = 12,000 \text{ L h}^{-1}$, From Day 169 until Day 219: $\theta_C = 25.5 \text{ d}$, $\theta = 0.835 \text{ d}$, $X_{MLSS} = 9.379 \text{ g L}^{-1}$, $T_{ML} = 28.8 \text{ }^\circ\text{C}$, $Q_{AIR, MS} = 12,000 \text{ L h}^{-1}$

Figure 6.26 shows that all real MPFs were properly controlled and little scatter appeared - even the highest real MPF of $15.49 \text{ L m}^{-2} \text{h}^{-1}$ that was tested during this long-term experiment was well-controlled. However, it is TMP values which will show whether average net MPFs higher than $11.52 \text{ L m}^{-2} \text{h}^{-1}$ were finally sustainable or not.

Figure 6.27 shows the profile of the TMP against time.

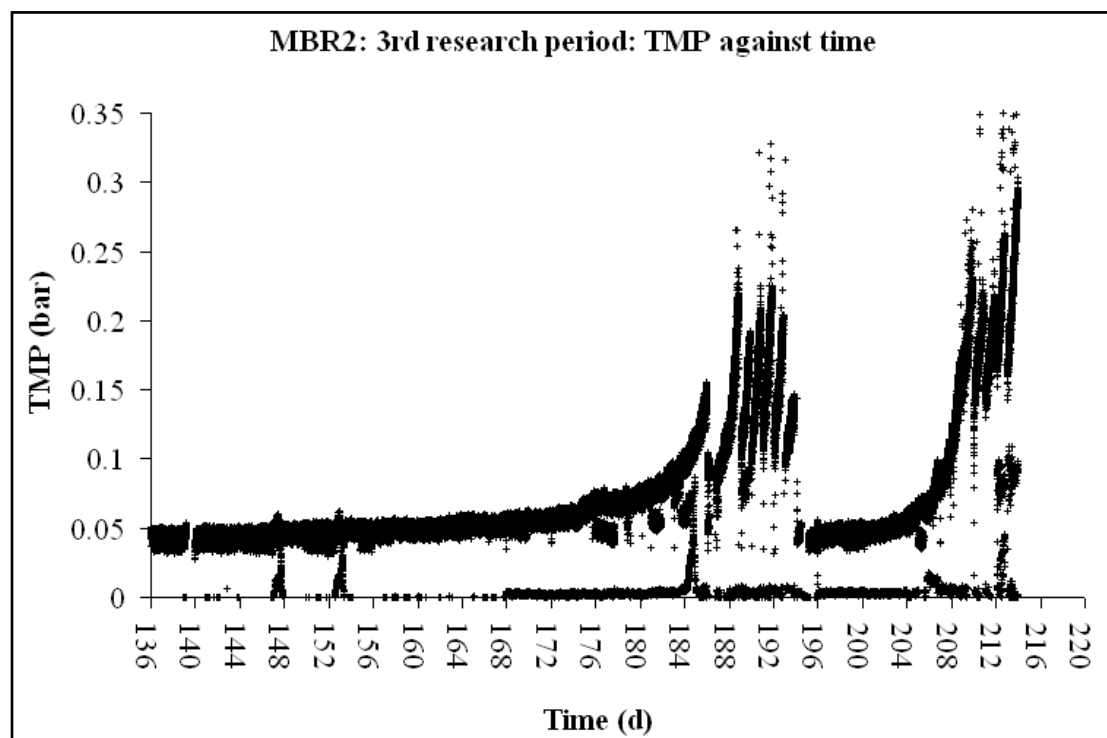


Figure 6.27 MBR2: 3rd research period: TMP against time: From Day 136 until Day 152: $\theta_C = 30$ d, $\theta = 1.01$ d, $X_{MLSS} = 9.687$ g L⁻¹, $T_{ML} = 21.2$ °C g L⁻¹, $Q_{AIR, MS} = 12,000$ L h⁻¹, From Day 153 until Day 168: $\theta_C = 29$ d, $\theta = 0.91$ d, $X_{MLSS} = 9.206$ g L⁻¹, $T_{ML} = 21.2$ °C, $Q_{AIR, MS} = 12,000$ L h⁻¹, From Day 169 until Day 219: $\theta_C = 25.5$ d, $\theta = 0.835$ d, $X_{MLSS} = 9.379$ g L⁻¹, $T_{ML} = 28.8$ °C, $Q_{AIR, MS} = 12,000$ L h⁻¹

As seen in Figure 6.27, the net MPF of 12.81 L m⁻² h⁻¹ was sustainable as TMP values never exceeded a maximum value of 0.059 bar. The fact that this time a net MPF higher than 11.52 L m⁻² h⁻¹ ended up being sustainable can be attributed to a number of reasons. The membranes were quite clean as chemical cleaning had been applied a few days earlier. MLSS concentrations had been significantly reduced - MLSS concentrations values as low as 8.09 g L⁻¹ had been measured and an average MLSS concentration equal to 9.206 g L⁻¹ was calculated. In addition, the mixed-liquor temperature had increased from an average value of 21.2 °C to a new average value of 23.9 °C. As all these changes can have a positive effect on the membrane performance, the net MPF of 12.81 L m⁻² h⁻¹, together with the corresponding operating conditions, was now found to be sustainable.

On Day 169, 25-05-2009, the SRT was decreased to a new value of 25.5 d and the HRT was also decreased to a new value of 0.835 d. These operating conditions

remained constant until the end of the long-term experiment, on Day 219, 16-04-2009. Their corresponding net MPF of $13.94 \text{ L m}^{-2} \text{ h}^{-1}$ was then applied - that was the highest net MPF that was tested during the long-term experiment -, and, as seen in Figure 6.27, it led to a quite rapid exponential increase in the TMP values. Membrane fouling had occurred again. On Day 186, 12-05-2009, until Day 196, 22-05-2009, the membrane fouling was mitigated after the application of a series of successive physical cleanings, but this was only a temporary solution as residual membrane fouling had already been formed. On Day 196, 22-05-2009, filtration was suspended due to severe membrane fouling. The membranes were taken out from the MBR tank and were cleaned chemically. Filtration started again on the same day - initially, rational average TMP values in the range of 0.043 bar were recorded. A few days later, on Day 203, 29-05-2009, TMP values started increasing exponentially once again, and on Day 219, 14-06-2009, the operation of MBR2 system was ceased. In the mean time, a series of successive physical cleanings had also been applied in order to extend the MBR2 operation.

MLSS concentrations during the time period between Day 169, 25-05-2009, and Day 219, 16-04-2009, did not significantly change leading to an average value equal to 9.379 g L^{-1} . Regarding the mixed-liquor temperature, a new increased average value equal to $28.8 \text{ }^{\circ}\text{C}$ was measured. This means that neither the good control of the MLSS concentration, nor the increase in the mixed-liquor temperature succeeded in sustaining this high net MPF. During that long-term experiment, a maximum average sustainable net MPF of $12.81 \text{ L m}^{-2} \text{ h}^{-1}$ was found to be possible. Higher sustainable net MPFs may now reached only by increasing the air flow rate within the MBR tank, even though higher running costs will arise.

Figure 6.28 shows the course of permeability against time.

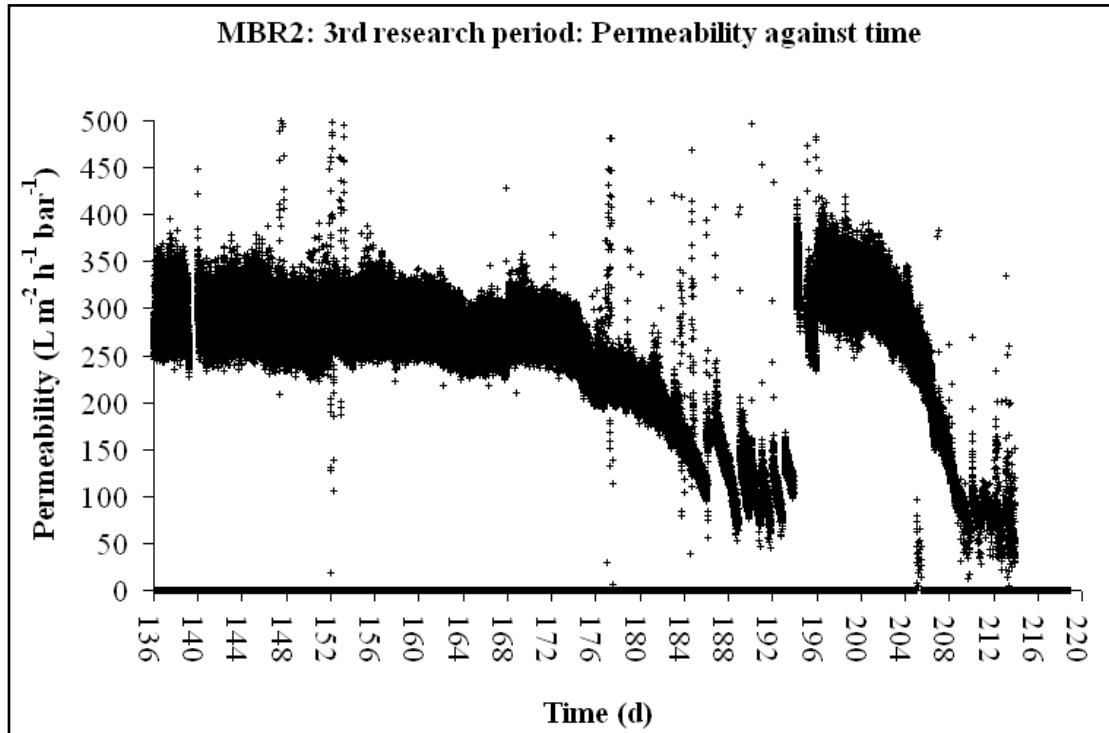


Figure 6.28 MBR2: 3rd research period: Permeability against time: From Day 136 until Day 152: $\theta_C = 30$ d, $\theta = 1.01$ d, $X_{MLSS} = 9.687$ g L⁻¹, $T_{ML} = 21.2$ °C g L⁻¹, $Q_{AIR, MS} = 12,000$ L h⁻¹, From Day 153 until Day 168: $\theta_C = 29$ d, $\theta = 0.91$ d, $X_{MLSS} = 9.206$ g L⁻¹, $T_{ML} = 21.2$ °C, $Q_{AIR, MS} = 12,000$ L h⁻¹, From Day 169 until Day 219: $\theta_C = 25.5$ d, $\theta = 0.835$ d, $X_{MLSS} = 9.379$ g L⁻¹, $T_{ML} = 28.8$ °C, $Q_{AIR, MS} = 12,000$ L h⁻¹

Figure 6.28 shows that average membrane permeability between Day 152, 08-04-2009, and Day 168, 24-04-2009, was equal to 300 L m⁻² h⁻¹ bar⁻¹ at 23.9 °C. By correcting to 20 °C, a temperature-corrected permeability value of 272 L m⁻² h⁻¹ bar⁻¹ is obtained, which is a rational value after being compared with the permeability values resulting from the clean water tests.

Table 6.9 shows the operating conditions of the maximum average sustainable MPF as estimated through the long-term experiment.

Table 6.9 MBR2: Sustainable net membrane MPF and its corresponding operating conditions

Parameter	Value	Unit
Net MPF	12.81	L m ⁻² h ⁻¹
Average TMP	0.059	bar
Temperature-corrected permeability at 20 °C	272	L m ⁻² h ⁻¹ bar ⁻¹
SRT	29	d
HRT	0.91	d
Average MLSS concentration	9.206	g L ⁻¹
Average mixed-liquor-temperature	23.9	°C
Air Flow rate		
Membrane scouring only	12,000	L h ⁻¹
Operating cycle	9/1	min on/min off

6.5 Membrane performance of MBR3

6.5.1 Introduction

MBR3 started-up on 02-09-2008 but data collection started a few days later on Day 1, 12-09-2008. Raw data was then continuously recorded until Day 275, 14-06-2009. The air flow rate for both biomass maintenance and membrane scouring in the filtration tank was set to the standard setting of 7,300 L h⁻¹ taking into consideration the manufacturer's guidelines. This value was never altered during the experiment. Similarly, the aeration within the aeration tank for biomass maintenance was chosen after taking into account the manufacturer's guidelines. Also it is worth mentioning that the bacteria never suffered from lack of oxygen during the long-term experiment as measured COD concentrations in the effluent were always lower than the target COD value. On Day 29, 11-10-2008, after experiencing some technical problems, together with the formation of severe irreversible membrane fouling, the MBR3 system had to be shut-down.

Another start-up of the MBR3 system took place on Day 68, 19-11-2008. The SRT was initially adjusted to 15 d and HRT was adjusted to 1.01 d. Cross flow filtration

was applied and that filtration was intermittent - a 20-min long operational filtration/relaxation cycle was applied, with 17 min of filtration followed by 3 min of relaxation. This operational cycle remained constant during the long-term experiment and it was only briefly changed when some short-term flux-step tests were performed. Details about these specific short-term changes of the operational filtration/relaxation cycle will be given later, in Section 6.4.2.1, when the short-term flux-step tests are analysed.

6.5.2 Data processing

With regard to membrane performance of the MBR3 system, three data processing research periods were selected to allow a clearer representation of the data, and these are presented in Table 6.10.

Table 6.10 MBR3: Data processing periods

Research time periods (dates)	Number of days
12-09-2008 until 11-02-2009	1 to 152
11-02-2009 until 10-05-2009	152 to 240
10-05-2009 until 14-06-2009	240 to 275

Based on the raw data, the instant real MRFs, the TMP values and the permeability values were estimated with the aid of Equations 4.16, 4.19 and 4.20 and were plotted against time. Based on Table 6.2 and Equations 6.1 and 6.2, real/net MPFs were calculated for each set of the applied operating conditions. By comparing the calculated real MPFs with their corresponding instant values, it could be concluded whether or not real MPFs were properly controlled during the long-term experiment. Then, based on the figures, average TMP values and permeability values were estimated. Finally, if necessary, average temperature-corrected permeability values at 20 °C were estimated with the aid of Equation 4.21.

6.5.2.1 1st research period: From 12-09-2008 to 11-02-2009

• Long-term experiment

This research period can be divided into two shorter time periods. The first time period is from Day 1, 12-09-2008, until Day 67, 18-11-2008, and the second time period is from Day 68, 19-11-2008, until Day 152, 11-02-2009. MBR3 was started-up on Day 1, 12-09-2008. During the first time period, a technical problem relating to the membrane module itself appeared and had to be resolved. The membrane module as designed to be sitting at the bottom of the aeration tank to take advantage of the hydraulic pressure on the feed side of the membranes. But, during the first time period, the module was tending to float near the surface. As the pressure transducer had been calibrated to measure directly TMP values providing that the membrane module was sitting at the bottom of the aeration tank, the TMP values that were recorded during this time period were questionable - the default calibration was not valid.

In addition, during this period, severe membrane fouling appeared. The increase in the TMP values was exponential, completely out of control. On Day 20, 02-10-2008, physical cleaning was applied. The operation was stopped and the membrane module was cleaned both by agitating the waste water around the membrane module and by interrupting filtration whilst maintaining aeration. The physical cleaning proved to be inefficient. TMP did not remain at low values and it increased again rapidly. On Day 27, 09-10-2008, a second physical cleaning was performed, but again it was not successful. As TMP had already reached very high values in the range of 0.18 bar, the operation was interrupted so as to apply chemical cleaning.

The MBR3 system was re-started on Day 68, 19-11-2008 - this is the second time period, which lasted up to Day 152, 11-02-2009. The membrane module had been cleaned chemically and it was fixed at the bottom of the aeration tank. All TMP values recorded after that day can be assumed as reliable TMP values. During this time, period a short-term flux-step test was also performed.

On Day 68, 19-11-2008, the SRT was adjusted to 15 d and the HRT was adjusted to 1.01 d. The operating conditions remained to these values until Day 113, 03-01-2008. Based on the MLSS concentration measurements, an average MLSS concentration equal to 4.033 g L^{-1} was calculated during this period of time. Average temperature of the mixed-liquor was $21.2 \text{ }^\circ\text{C}$. Based on equations as given in Table 6.2, together with Equation 6.1, net MPF was found to be equal to $13.58 \text{ L m}^{-2} \text{ h}^{-1}$ (real MPF: $15.98 \text{ L m}^{-2} \text{ h}^{-1}$). This initial net MPF value for the MBR3 system appeared to be higher than the initial net MBFs for the MBR1 system and the MBR2 system, however, the set of the initial operating conditions was the same for all MBR systems. Also, this specific initial real MPF was suggested directly by the supplier of the MBR3 system.

From Day 114, 04-01-2009, to Day 146, 05-02-2009, biomass was allowed to increase. The new SRT was set to 30 d and the HRT remained at the same value of 1.01 d. During this time period, MLSS concentration was dynamic, and the MLSS concentration increase was the dominant phenomenon with respect to any changes with regard to membrane performance.

From Day 146, 05-02-2009, to the end of the 1st research period, on Day 152, 11-02-2009, the operating conditions did not alter. However, the MLSS concentration had already stabilised at a constant value of about $9 - 10 \text{ g L}^{-1}$, as steady state had been reached. More details about this set of operating conditions and their corresponding net MPF are given in the next Section 6.4.2.2.

Figure 6.29 shows the real MPF against time. This figure includes only the values after the second start-up of the MBR3, as no clear comments based on the unsuccessful start-up period from Day 1, 12-09-2008, to Day 68, 19-11-2008, can be made.

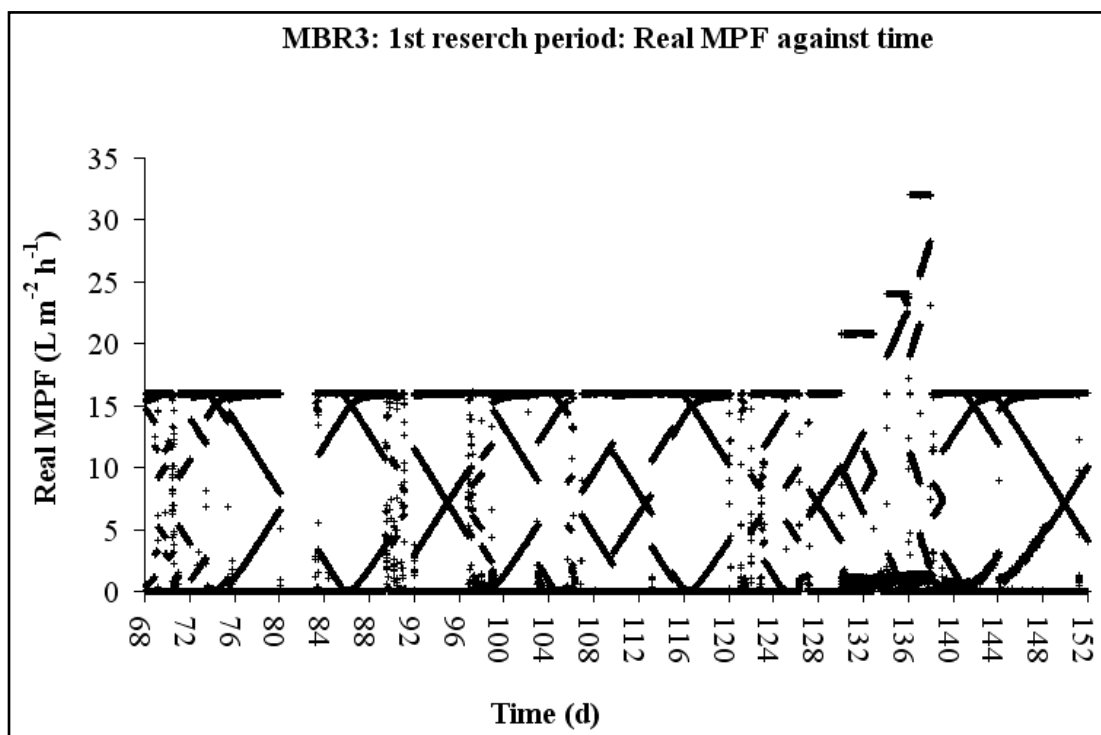


Figure 6.29 MBR3: 1st research period: Real MPF against time: From Day 68 until 113: $\theta_C = 15$ d, $\theta = 1.01$ d, $X_{MLSS} = 4.033$ g L⁻¹, $T_{ML} = 21.2$ °C, $Q_{AIR, MS} = 7,300$ L h⁻¹, From Day 147 until Day 152: $\theta_C = 30$ d, $\theta = 1.01$ d, $X_{MLSS} = 9.151$ g L⁻¹, $T_{ML} = 21.2$ °C, $Q_{AIR, MS} = 7,300$ L h⁻¹, (From Day 114 until Day 146: Transition period)

The most important time period is between Day 68, 19-11-2008, and Day 113, 03-01-2009. During this time period, the SRT was set to 15 d and the HRT was set to 1.01 d leading to an average MLSS concentration of 4.033 g L⁻¹. The net MPF was 13.58 L m⁻² h⁻¹ (real MPF: 15.98 L m⁻² h⁻¹). As seen in Figure 6.29, instant real MPFs were very well-controlled around the expected real MPF value. The zero points in Figure 6.29 indicate real MPFs during relaxation. As for the short-term flux-step test, it has not been taken into account yet. The scatter appeared in Figure 6.29 came from the fact that the short sampling times that were applied during the long-term experiment led to reduced data filtering.

Figure 6.30 shows the TMP values against time.

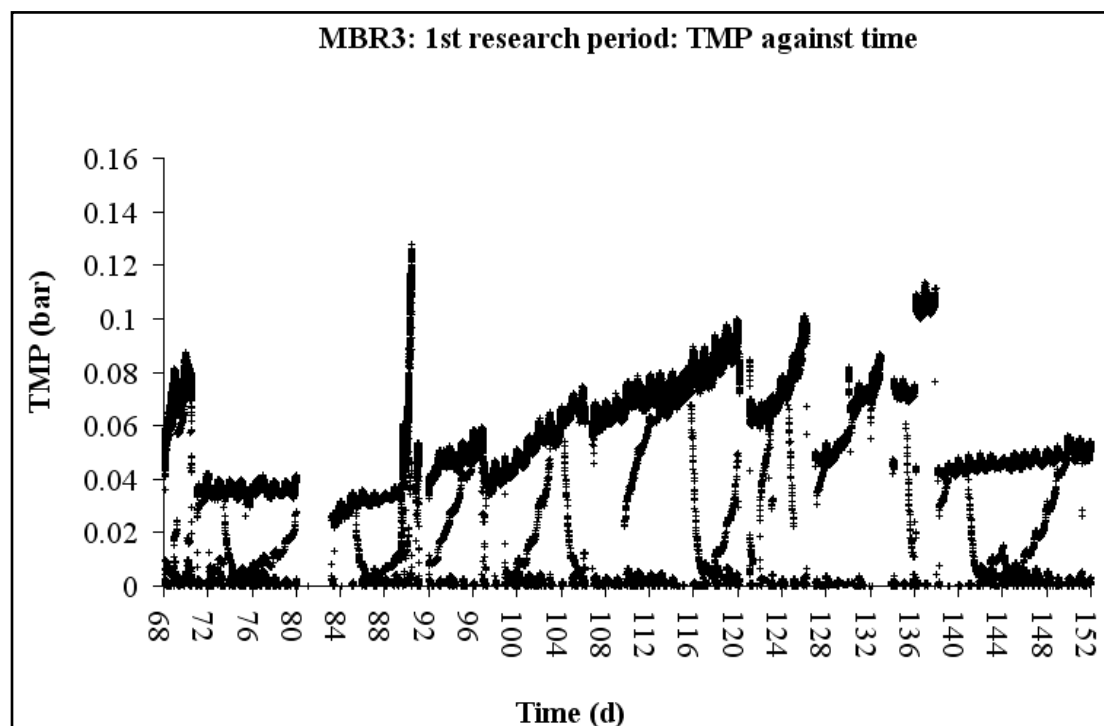


Figure 6.30 MBR3: 1st research period: TMP against time: From Day 68 until 113: $\theta_C = 15$ d, $\theta = 1.01$ d, $X_{MLSS} = 4.033$ g L⁻¹, $T_{ML} = 21.2$ °C, $Q_{AIR, MS} = 7,300$ L h⁻¹, From Day 147 until Day 152: $\theta_C = 30$ d, $\theta = 1.01$ d, $X_{MLSS} = 9.151$ g L⁻¹, $T_{ML} = 21.2$ °C, $Q_{AIR, MS} = 7,300$ L h⁻¹, (From Day 114 until Day 146: Transition period)

Figure 6.30 shows that membrane performance during the 1st research period was very unstable. The fact that TMP values remained at low values was a direct consequence of the application of a series of successive physical cleanings. Any time a TMP decrease is observed in Figure 6.30, a physical cleaning had just been applied by interrupting the filtration and allowing air scouring the membrane panels to help remove some of the fouling material which had been deposited on their surface. Although the application of successive physical cleaning seemed to work, it is rather demanding on the operators. Also, whenever a physical cleaning is applied, filtration must be suspended and treated permeate is not available, hence the daily production of treated permeate is reduced. As seen from Figure 6.30, the initial TMP values after a physical cleaning are higher than the initial TMP values of the previous physical cleanings. This is an indication that irreversible membrane fouling becomes worse with the time. Application of successive physical cleanings can only extend the MBR operation before the application of a chemical cleaning is necessitated.

Regarding the most important time period so far, or the time period between Day 68, 19-11-2008, and Day 113, 03-01-2009, it can be said that the average net MPF of $13.58 \text{ L m}^{-2} \text{ h}^{-1}$, together with its corresponding set of operating conditions, was not a sustainable condition.

The permeability profile against time is shown in Figure 6.31.

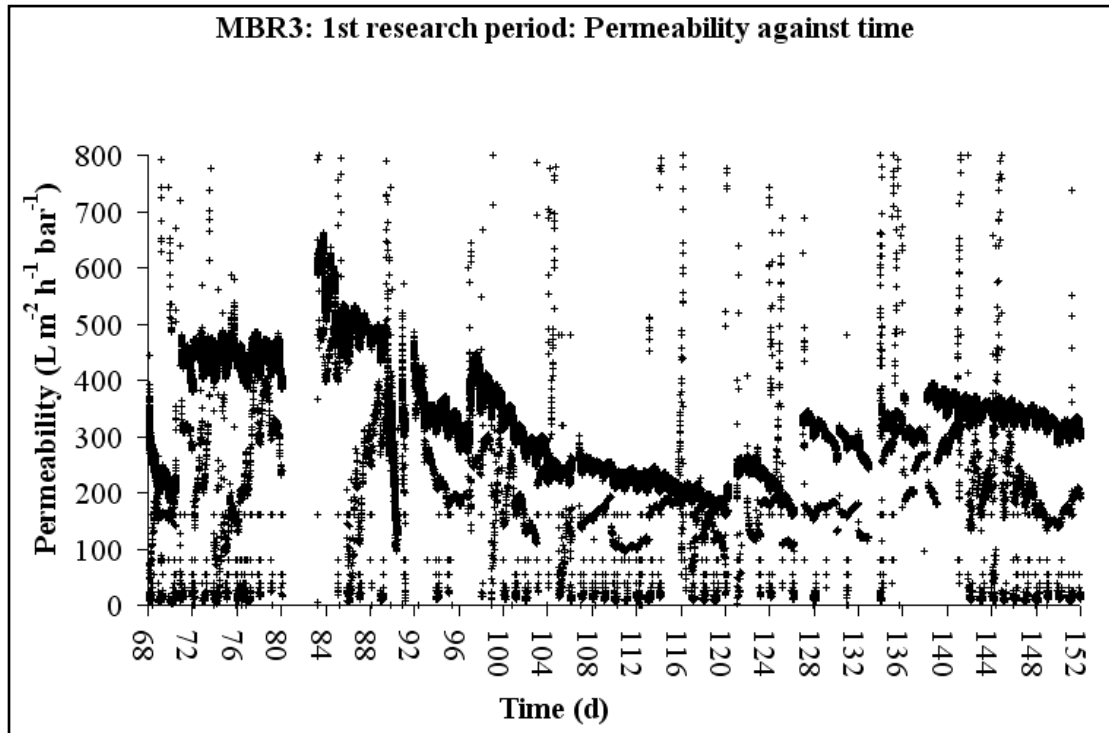


Figure 6.31 MBR3: 1st research period: Permeability against time: From Day 68 until 113: $\theta_C = 15 \text{ d}$, $\theta = 1.01 \text{ d}$, $X_{MLSS} = 4.033 \text{ g L}^{-1}$, $T_{ML} = 21.2 \text{ }^\circ\text{C}$, $Q_{AIR, MS} = 7,300 \text{ L h}^{-1}$, From Day 147 until Day 152: $\theta_C = 30 \text{ d}$, $\theta = 1.01 \text{ d}$, $X_{MLSS} = 9.151 \text{ g L}^{-1}$, $T_{ML} = 21.2 \text{ }^\circ\text{C}$, $Q_{AIR, MS} = 7,300 \text{ L h}^{-1}$, (From Day 114 until Day 146: Transition period)

Even though the scatter with respect to the permeability figures appeared to increase, (Figure 6.31), it is still possible to conclude that during the 1st research period membrane fouling seriously affected the membrane performance, as the trend of the permeability values was always decreasing downwards.

• Short-term flux-step tests

A short-term flux-step test was conducted during the 1st research period. This test was similar to the short-term flux-step test for the MBR2 system. During the test, both real MPFs and the filtration/relaxation times of a 20-min long operational filtration/relaxation cycle were adjusted so that the net MPF remained at around the same value. Thus, each time the real MPF increased, a longer relaxation time and consequently a shorter filtration time were applied, as their sum had to be always equal to 20 min. As the MBR operation had been suffering from continuous membrane fouling, it was decided to test whether another combination of filtration/relaxation cycle could turn the selected net MPF of $13.58 \text{ L m}^{-2} \text{ h}^{-1}$ into a sustainable condition. The short-term flux-step test was started on Day 127, 17-01-2009, and finished on Day 138, 28-01-2009. Although gassing rate for membrane scouring remained constant during the short-term flux-steps, the temperature of the mixed-liquor ranged from a minimum of $16 \text{ }^{\circ}\text{C}$ to a maximum of $23 \text{ }^{\circ}\text{C}$ leading to an average value of $20.3 \text{ }^{\circ}\text{C}$. The MLSS concentration was continuously increasing, as the test was being performed during the dynamic transition time period. However, as only a small increase in the MLSS concentration values from 6.91 g L^{-1} to 7.55 g L^{-1} took place during the test, it is unlikely for the MLSS concentrations to have affected the membrane performance.

The combinations of real MPFs - this time the real MPFs were estimated as average values out of the recorded instant real MPF values - and filtration/relaxation times of a 20-min long operational cycle, which were tested during the short-term flux-step test, are shown in Table 6.11.

Table 6.11 MBR3: Operating conditions during the short-term flux-step test: X_{MLSS} : Between 6.91 g L^{-1} and 7.55 g L^{-1} , $T_{\text{ML}} = 20.3 \text{ }^{\circ}\text{C}$, $Q_{\text{AIR, MS}} = 7,300 \text{ L h}^{-1}$

Real MPF during the filtration time ($\text{L m}^{-2} \text{ h}^{-1}$)	Filtration/Relaxation cycle		Net MPF ($\text{L m}^{-2} \text{ h}^{-1}$)
	Filtration time (min)	Relaxation time (min)	
20.82	13	7	13.58
24.02	11	9	13.58
32.05	8	12	12.83

Figure 6.32 shows the course of the real MPF against time during the short-term flux-step test.

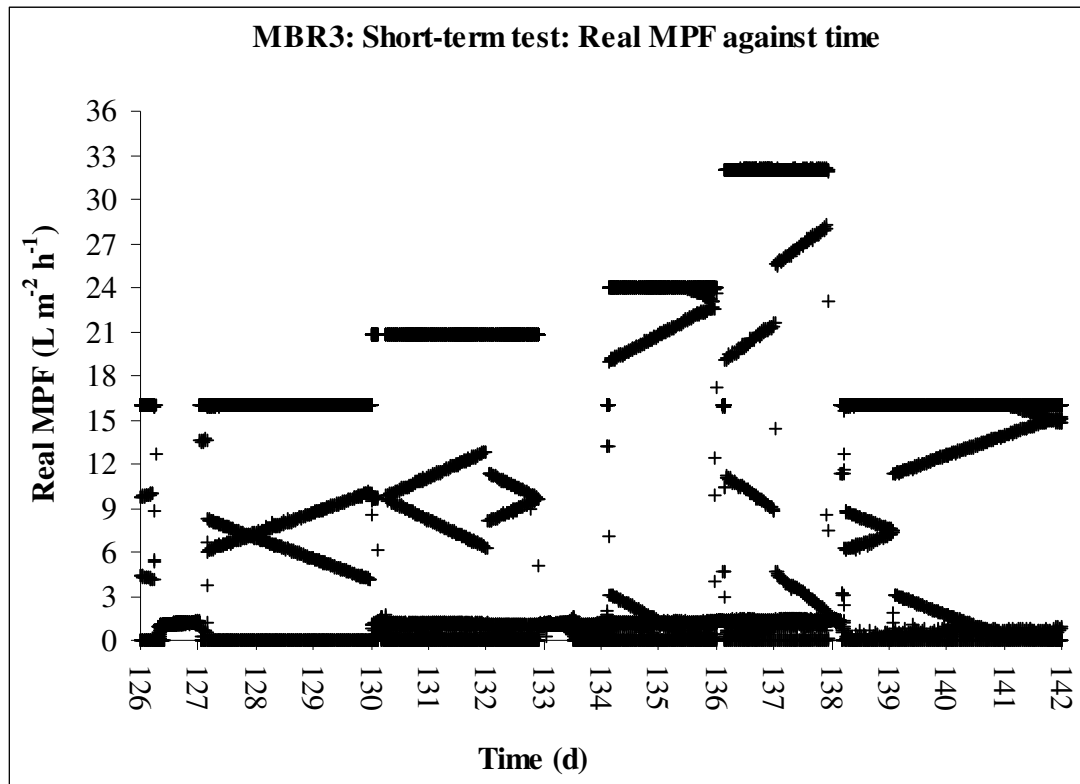


Figure 6.32 MBR3: Short-term flux-step test: Real MPF against time: X_{MLSS} : Between 6.91 g L^{-1} and 7.55 g L^{-1} , $T_{ML} = 20.3 \text{ }^{\circ}\text{C}$, $Q_{AIR, MS} = 7,300 \text{ L h}^{-1}$

The real MPFs, as shown Figure 6.32, were well-controlled during the short-term test.

Figure 6.33 shows the course of TMP against time.

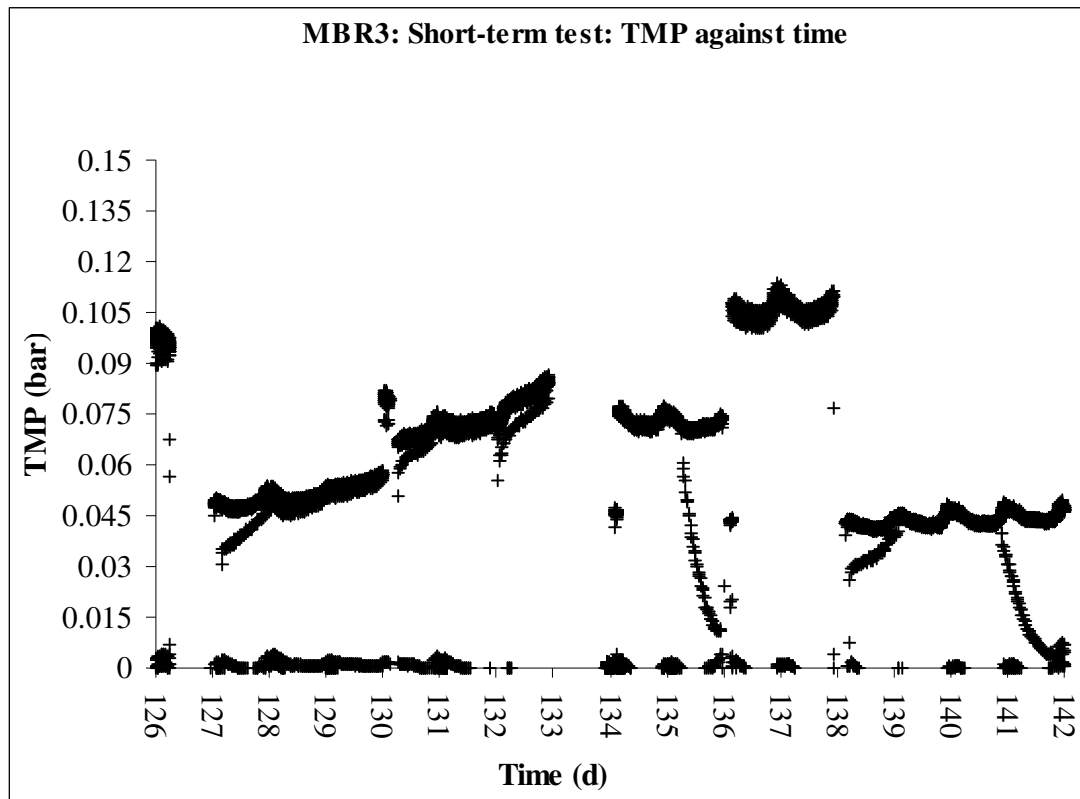


Figure 6.33 MBR3: Short-term flux-step test: TMP against time: X_{MLSS} : Between 6.91 g L^{-1} and 7.55 g L^{-1} , $T_{ML} = 20.3 \text{ }^{\circ}\text{C}$, $Q_{AIR, MS} = 7,300 \text{ L h}^{-1}$

Regarding the TMP values, as shown in Figure 6.33, the following comments can be made. As expected the TMP increased each time a new higher real MPF was tested. In addition, longer relaxation time periods appeared to improve MBR operation as TMP values seemed to stabilise, and significant increase in TMP values was no longer recorded.

Figure 6.34 shows the profile of permeability against time.

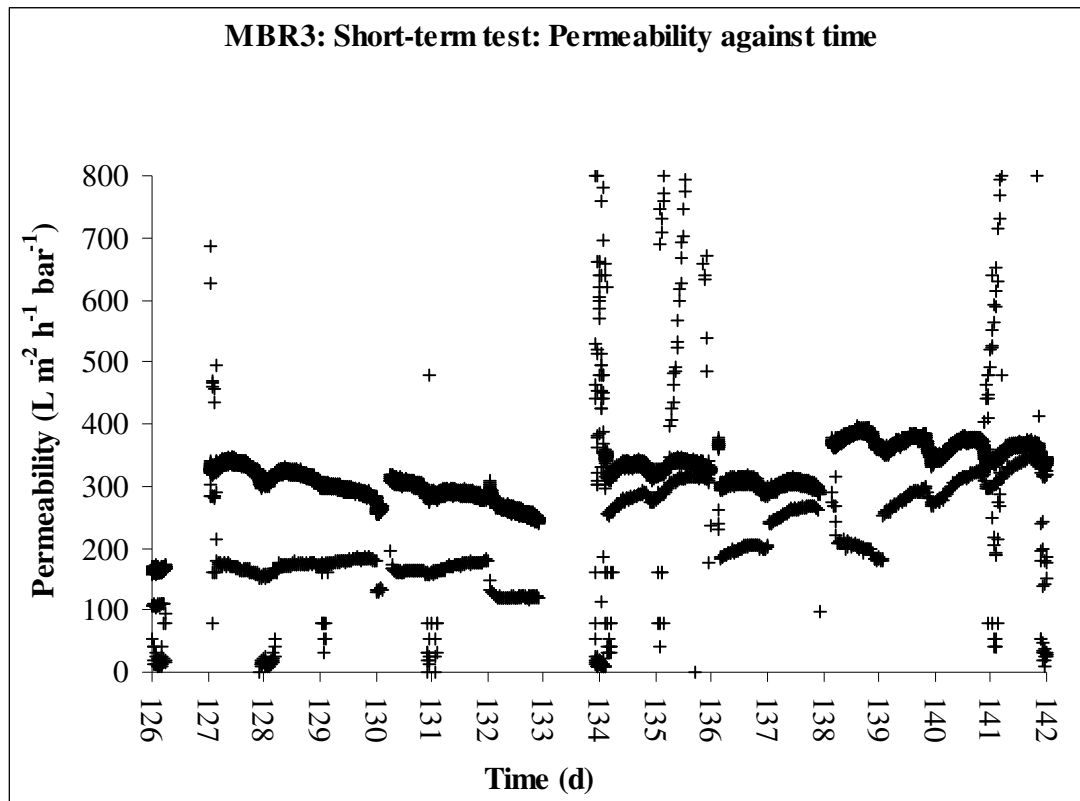


Figure 6.34 MBR3: Short-term flux-step test: Permeability against time: X_{MLSS} Between 6.91 g L^{-1} and 7.55 g L^{-1} , $T_{ML} = 20.3 \text{ }^{\circ}\text{C}$, $Q_{AIR, MS} = 7,300 \text{ L h}^{-1}$

Observing Figure 6.34, similar comments can be made. Regarding membrane fouling, it is better-controlled when both the real MPF and the relaxation time increase. This practically means that the relaxation time appears to be the influential parameter with respect to the formation of a cake layer on the membranes. In general, the longer the relaxation time was, the more reliable the membrane performance appeared to be, which is also in line with literature, [Howell *et al.*, 2004]. However, for the majority of this research the filtration/relaxation cycle remained constant, that is to say 17 min of filtration - 3 min of membrane relaxation, as it was decided to operate the MBR system according to the manufacturer's guidelines.

6.5.2.2 2nd research period: From 11-02-2009 until 10-05-2009

During the 2nd time period, the real MPF was increased step by step. MLSS concentration had increased to values of about $9 - 10 \text{ g L}^{-1}$ and steady state had been reached. This increase in the real MPFs had to be performed as one of the objectives

of this work was to increase as much as possible the daily production of the treated permeate, hence to reduce the SED values of the MBR systems. However, these real MPFs must be sustainable, or there is no point in applying them, as stable membrane performance cannot be achieved. Also, it is necessary that treated water of the appropriate quality should always be produced.

Details about the real/net MPFs that were tested during this time period, together with their corresponding operating conditions, will be given after plotting the profile of the real MPF against time for this research period, (Figure 6.35).

Figure 6.35 shows the real MPFs against time.

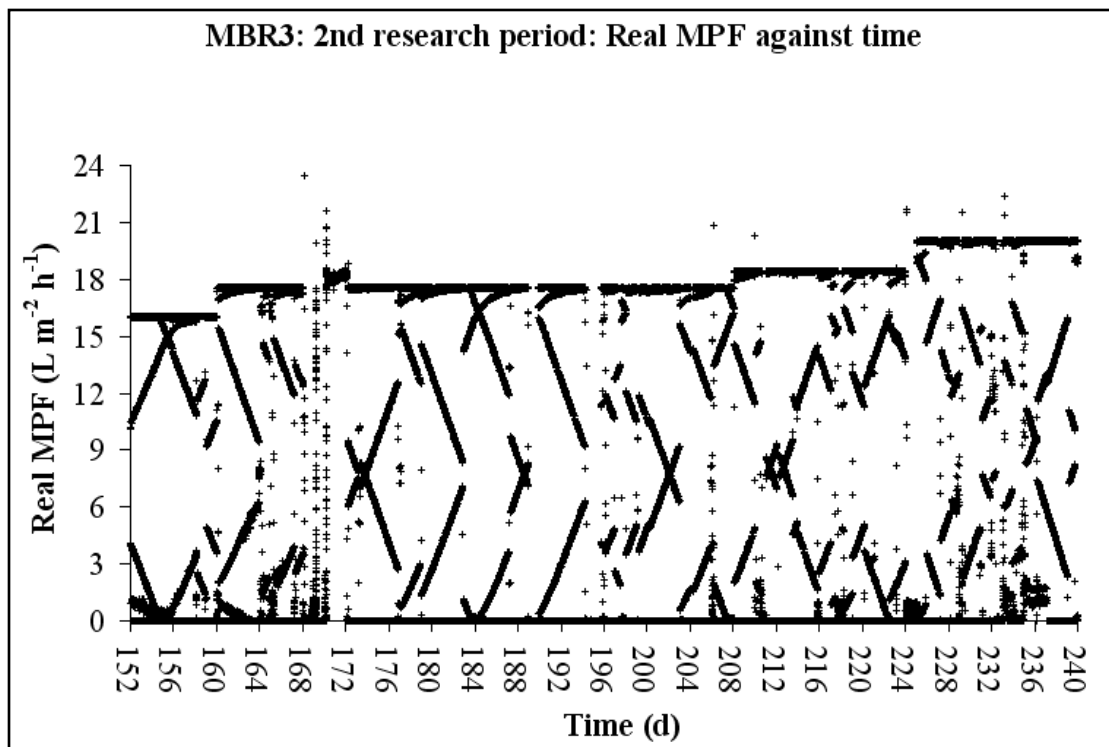


Figure 6.35 MBR3: 2nd research period: Real MPF against time: Day 152 until Day 207: $\theta_C = 30$ d, $\theta = 1.01$ d, $X_{MLSS} = 9.151$ g L⁻¹, $T_{ML} = 21.2$ °C, $Q_{AIR, MS} = 7,300$ L h⁻¹, Day 208 until Day 225: $\theta_C = 29$ d, $\theta = 0.91$ d, $X_{MLSS} = 8.793$ g L⁻¹, $T_{ML} = 24$ °C, $Q_{AIR, MS} = 7,300$ L h⁻¹, From Day 226 until Day 240: $\theta_C = 25.5$ d, $\theta = 0.835$ d, $X_{MLSS} = 8.53$ g L⁻¹, $T_{ML} = 25.5$ °C, $Q_{AIR, MS} = 7,300$ L h⁻¹

Based on Figure 6.35, the following comments can be made. Regarding the time period during which the SRT was set to 30 d and the HRT was set to 1.01 d, a good

conclusion can be drawn after Day 160, 19-02-2009, and up to Day 207, 07-04-2009, - it would be better not to take into account the MLSS concentration transition period. The net MPF was found to be equal to $14.07 \text{ L m}^{-2} \text{ h}^{-1}$ (average real MPF: $16.55 \text{ L m}^{-2} \text{ h}^{-1}$), and, as seen in Figure 6.35, the real MPF was satisfactorily controlled. The average MLSS concentration was 9.151 g L^{-1} and the mixed-liquor temperature was $21.2 \text{ }^\circ\text{C}$.

From Day 208, 08-04-2009, to Day 225, 25-04-2009, the SRT was set to 29 d and the HRT was set to 9.91 d. The net MPF was increased to $15.65 \text{ L m}^{-2} \text{ h}^{-1}$ (real MPF: $18.42 \text{ L m}^{-2} \text{ h}^{-1}$), and once again it was successfully controlled. The MLSS concentration during this time period was successfully controlled with an average value of 8.793 g L^{-1} . Temperature of the mixed-liquor was equal to $24 \text{ }^\circ\text{C}$. The instant real MPFs were again well-controlled around their expected corresponding real MPF value of $18.42 \text{ L m}^{-2} \text{ h}^{-1}$.

Finally, it is the time period, which started on Day 226, 26-04-2009, and ended on Day 240, 10-05-2009, that has to be analysed. During this time period, the SRT was set to 25.5 d and the HRT was set to 0.835 d. Average MLSS concentration was found to be equal to 8.53 g L^{-1} , and the mixed-liquor temperature had slightly increased to a new average value of $25.5 \text{ }^\circ\text{C}$. At the end of this research period, some attempts to reduce the MLSS concentration to the initial values of about $4 - 5 \text{ g L}^{-1}$ were made but more details will be given in Section 6.5.2.3. The new net MPF was found to be $17.04 \text{ L m}^{-2} \text{ h}^{-1}$ (real MPF: $20.04 \text{ L m}^{-2} \text{ h}^{-1}$). As seen from Figure 6.35, the real MPF was very well-controlled.

It is worth mentioning that the real MPFs that were tested during this research period are highly unlikely to be sustainable, as the lower net MPF of $13.58 \text{ L m}^{-2} \text{ h}^{-1}$ at a lower MLSS concentration of 4.033 g L^{-1} has already been found to be an unsustainable condition. As the same sets of solids residence times (SRTs)/hydraulic residence times (HRTs) had to be tested for all three MBR systems, the long-term experiment had to be continued as planned in the experimental protocol.

The profile of TMP against time is shown in Figure 6.36.

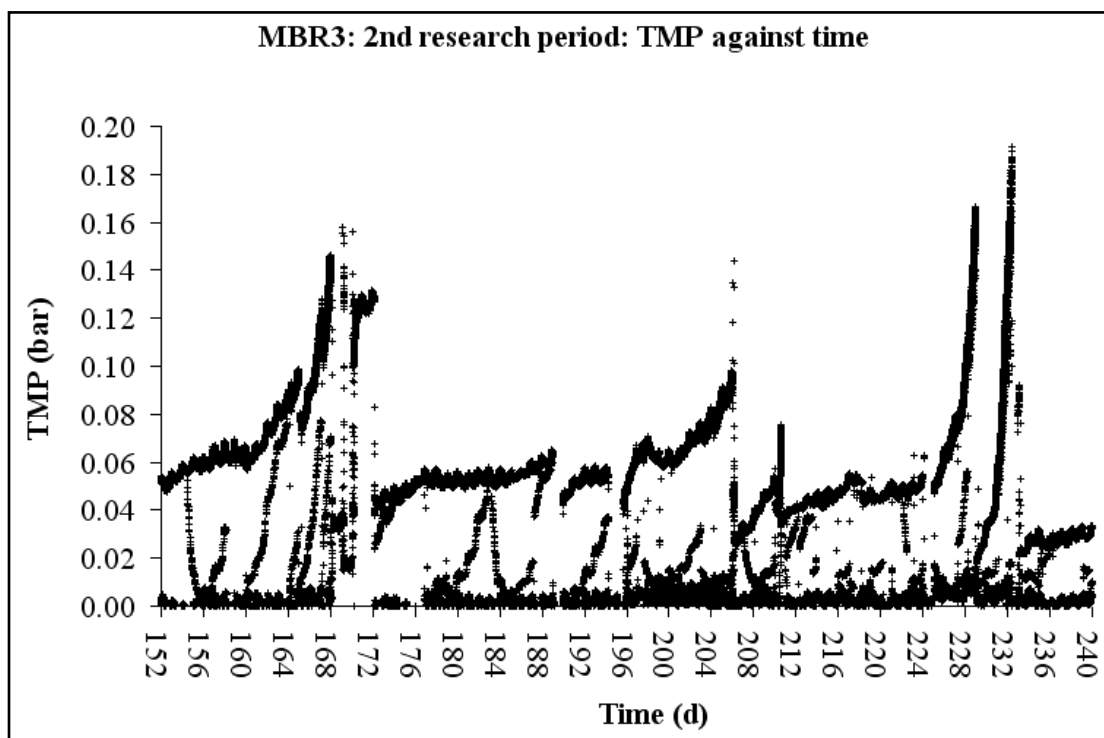


Figure 6.36 MBR3: 2nd research period: TMP against time: Day 152 until Day 207: $\theta_C = 30$ d, $\theta = 1.01$ d, $X_{MLSS} = 9.151$ g L⁻¹, $T_{ML} = 21.2$ °C, $Q_{AIR, MS} = 7,300$ L h⁻¹, Day 208 until Day 225: $\theta_C = 29$ d, $\theta = 0.91$ d, $X_{MLSS} = 8.793$ g L⁻¹, $T_{ML} = 24$ °C, $Q_{AIR, MS} = 7,300$ L h⁻¹, From Day 226 until Day 240: $\theta_C = 25.5$ d, $\theta = 0.835$ d, $X_{MLSS} = 8.53$ g L⁻¹, $T_{ML} = 25.5$ °C, $Q_{AIR, MS} = 7,300$ L h⁻¹

As expected and seen in Figure 6.36, the net MPFs that were tested during this research period were not sustainable, as they were resulted in TMP values that were continuously increasing. On Day 168, 27-02-2009, operation was interrupted as TMP had already reached the high value of 0.15 bar. The membrane module was removed from the filtration tank and it was cleaned chemically, then filtration was re-started. Until Day 224, 24-04-2009, filtration was maintained with the application of successive physical cleanings applied any time the TMP seemed to increase fast.

From Day 225, 25-04-2009, onwards membrane fouling took place rapidly and it appeared to be completely out of control - rapid exponential TMP increase occurred. The MBR operation was stopped and membranes were cleaned chemically again. Membranes were placed back into the filtration tank and filtration re-started. However, exponential TMP increase occurred again. The application of the high net

MPF of $17.035 \text{ L m}^{-2} \text{ h}^{-1}$ was followed by rapid exponential increase in the TMP, making this net MPF unsustainable, even for a short period of time.

Figure 6.37 shows the permeability against time.

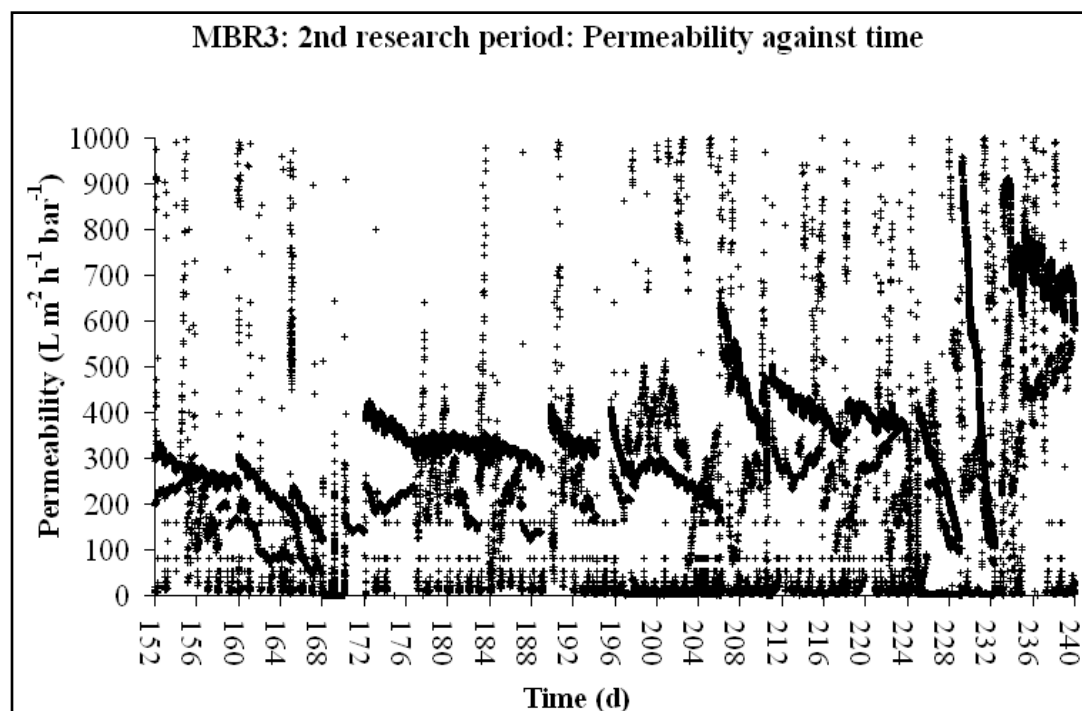


Figure 6.37 MBR3: 2nd research period: Permeability against time: Day 152 until Day 207: $\theta_C = 30 \text{ d}$, $\theta = 1.01 \text{ d}$, $X_{MLSS} = 9.151 \text{ g L}^{-1}$, $T_{ML} = 21.2 \text{ }^\circ\text{C}$, $Q_{AIR, MS} = 7,300 \text{ L h}^{-1}$, Day 208 until Day 225: $\theta_C = 29 \text{ d}$, $\theta = 0.91 \text{ d}$, $X_{MLSS} = 8.793 \text{ g L}^{-1}$, $T_{ML} = 24 \text{ }^\circ\text{C}$, $Q_{AIR, MS} = 7,300 \text{ L h}^{-1}$, From Day 226 until Day 240: $\theta_C = 25.5 \text{ d}$, $\theta = 0.835 \text{ d}$, $X_{MLSS} = 8.53 \text{ g L}^{-1}$, $T_{ML} = 25.5 \text{ }^\circ\text{C}$, $Q_{AIR, MS} = 7,300 \text{ L h}^{-1}$

Figure 6.36 shows that membrane permeate values, when the high net MPF of $17.04 \text{ L m}^{-2} \text{ h}^{-1}$ was applied, reached values below $100 \text{ L m}^{-2} \text{ h}^{-1} \text{ bar}^{-1}$ at $25.5 \text{ }^\circ\text{C}$. By correcting to $20 \text{ }^\circ\text{C}$ a corresponding temperature-corrected permeability values lower than $87 \text{ L m}^{-2} \text{ h}^{-1} \text{ bar}^{-1}$, indicating that filtration could no longer be continued.

6.5.2.3 3rd research period: From 10-05-2009 until 14-06-2009

This is the 3rd and final research period before shutting-down the MBR3 system. During this time period the MLSS concentration was decreased to the initial low

value of about 4 - 5 g L⁻¹. At around Day 241, 11-05-2009, to the shut-down of the MBR3 system, on Day 275, 14-06-2009, the MBR3 system was operated at an SRT of 12 d and at an HRT of 0.77 d. The selected set of operating conditions reduced the MLSS concentrations to values around 4 - 5 g L⁻¹, just like the initial set of [SRT, HRT]: [15 d, 1.01 d]. Even though both sets of operating conditions successfully controlled the MLSS concentration around the same value of about 4 - 5 g L⁻¹, the set that includes the shorter SRT and the shorter HRT led as expected to a higher net MPF, which was calculated to be 17.87 L m⁻² h⁻¹ (real MPF: 21.03 L m⁻² h⁻¹). The average MLSS concentration during this time period was 5.043 g L⁻¹ and the average temperature of the mixed-liquor was 28.8 °C. The net MPF was expected to be an unsustainable condition, however, it will be the course of TMP against time, (Figure 6.39), - that will show whether or not this is the case.

Figure 6.38 shows the course of real MPF against time.

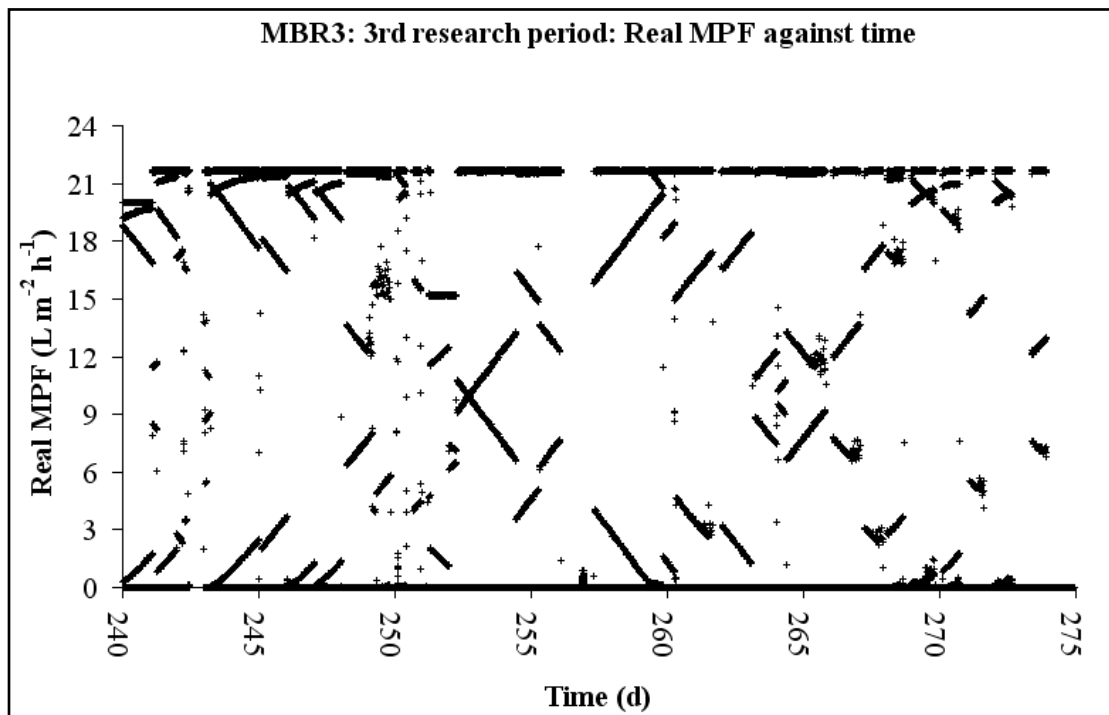


Figure 6.38 MBR3: 3rd research period: Real MPF against time: Day 240: $\theta_C = 25.5$ d, $\theta = 0.835$ d, $X_{MLSS} = 8.53$ g L⁻¹, $T_{ML} = 25.5$ °C, $Q_{AIR, MS} = 7,300$ L h⁻¹, Day 241 until Day 275: $\theta_C = 12$ d, $\theta = 0.77$ d, $X_{MLSS} = 5.043$ g L⁻¹, $T_{ML} = 28.8$ °C, $Q_{AIR, MS} = 7,300$ L h⁻¹

Figure 6.38 shows that the net MPF of $17.87 \text{ L m}^{-2} \text{ h}^{-1}$ was well-controlled. The scatter appearing indicates reduced filtering of the collected data due to the application of short sampling times.

Figure 6.39 shows the course of TMP values against time.

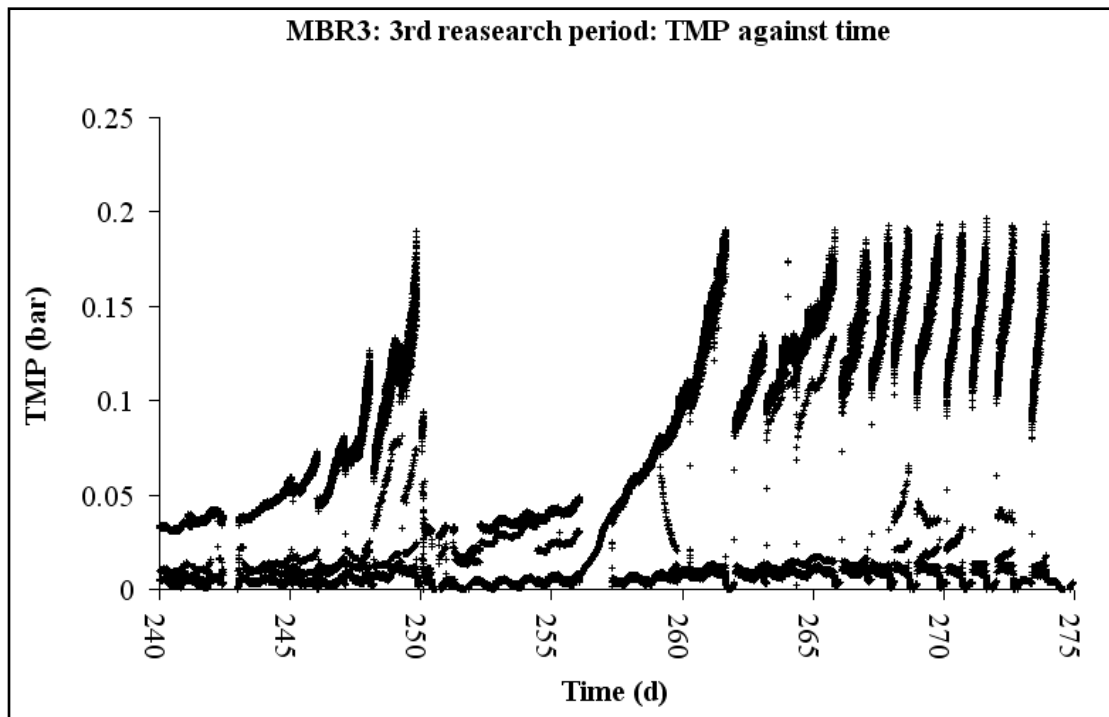


Figure 6.39 MBR3: 3rd research period: TMP against time: Day 240: $\theta_C = 25.5 \text{ d}$, $\theta = 0.835 \text{ d}$, $X_{\text{MLSS}} = 8.53 \text{ g L}^{-1}$, $T_{\text{ML}} = 25.5 \text{ }^\circ\text{C}$, $Q_{\text{AIR, MS}} = 7,300 \text{ L h}^{-1}$, Day 241 until Day 275: $\theta_C = 12 \text{ d}$, $\theta = 0.77 \text{ d}$, $X_{\text{MLSS}} = 5.043 \text{ g L}^{-1}$, $T_{\text{ML}} = 28.8 \text{ }^\circ\text{C}$, $Q_{\text{AIR, MS}} = 7,300 \text{ L h}^{-1}$

Based on Figure 6.39, it can be seen the membrane performance was very unstable due to frequent increase in the TMP values. On Day 250, 20-05-2009, the MBR operation was interrupted and the membranes were cleaned chemically. TMP initially reached low values of about 0.032 bar, but the trend was increasing upwards very rapidly indicating that the applied operating conditions would lead to unstable membrane performance soon. On Day 261, 31-05-2009, chemical cleaning was carried out successfully. From that day onwards, a series of successive physical cleanings were performed around the same time every day, however, it was impossible to maintain filtration. As expected, the average net MPF of $17.87 \text{ L m}^{-2} \text{ h}^{-1}$ was an unsustainable condition.

Figure 6.40 shows the course of permeability against time.

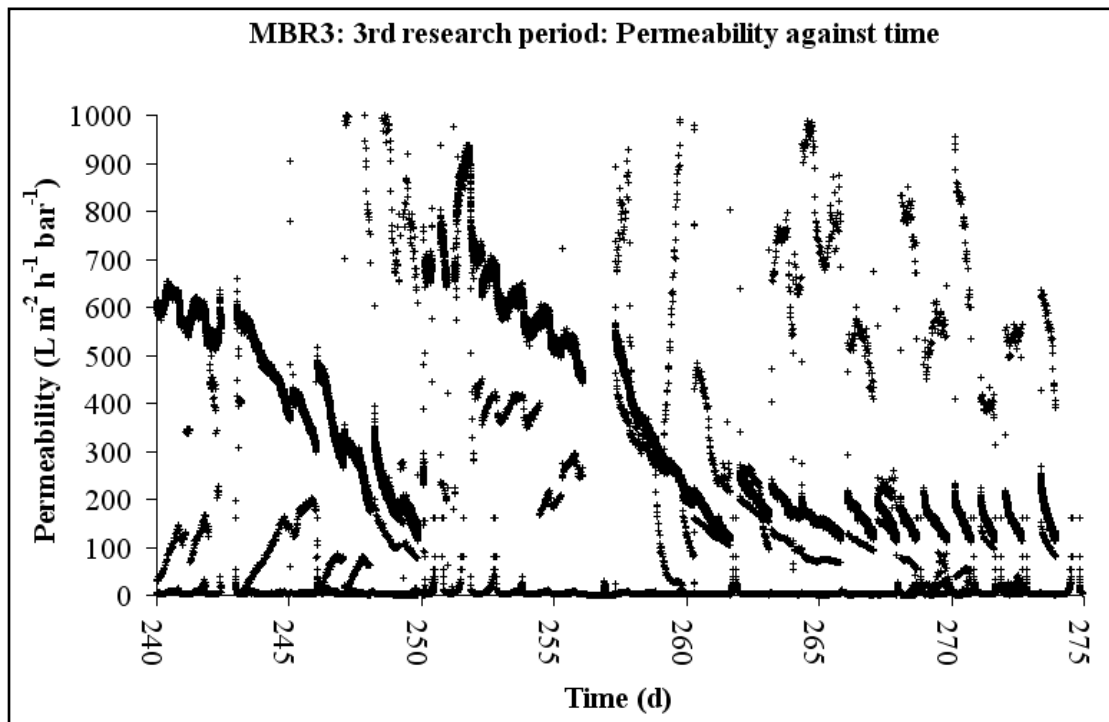


Figure 6.40 MBR3: 3rd research period: Permeability against time: Day 240: $\theta_C = 25.5$ d, $\theta = 0.835$ d, $X_{MLSS} = 8.53$ g L⁻¹, $T_{ML} = 25.5$ °C, $Q_{AIR, MS} = 7,300$ L h⁻¹, Day 241 until Day 275: $\theta_C = 12$ d, $\theta = 0.77$ d, $X_{MLSS} = 5.043$ g L⁻¹, $T_{ML} = 28.8$ °C, $Q_{AIR, MS} = 7,300$ L h⁻¹

Figure 6.40 shows that permeability values rapidly decreased to values of 115 L m⁻² h⁻¹ bar⁻¹ at 28.8 °C - by correcting to 20 °C a temperature-corrected permeability value of 92.5 L m⁻² h⁻¹ bar⁻¹ is found. The MBR was still suffering from serious membrane fouling problems, which could not be resolved, so the operation of the MBR3 system was decided to be ceased.

Even though the net MPFs that were tested during the long-term experiment were unsustainable, it was worth conducting the trials, as all MBR systems were operated under similar operating conditions and direct comparisons regarding their operations can be made.

6.6 Membrane fouling

Photographs showing irreversible membrane fouling of all three MBR systems are as follows:

- **MBR1**



Figure 6.41 MBR1: Irreversible membrane fouling



Figure 6.42 MBR2: Irreversible membrane fouling



Figure 6.43 MBR3: Irreversible membrane fouling

6.7 Conclusions

This chapter analysed the membrane performance of the three MBR systems. Even though two different MLSS concentrations were tested, that is to say $4 - 5 \text{ g L}^{-1}$ and $9 - 10 \text{ g L}^{-1}$, an attempt to maximise the daily production of permeate of the MBR systems was mainly made only when the MBR systems were operated at the high MLSS concentration of $9 - 10 \text{ g L}^{-1}$. Real MPFs were increased up to values that were no longer sustainable so that the maximum average sustainable net MPF per MBR system could be predicted. By predicting these MPFs, the daily production of treated permeate would be maximised, leading at the same time to reduced specific energy consumption values.

Each MBR system was operated under different combinations of SRTs/HRTs. Each combination could lead to a different corresponding net (or real) MPF value, however, all these combinations could successfully control the MLSS concentration at about $9 - 10 \text{ g L}^{-1}$. Final conclusions with respect to each MBR system and the net MPFs that were tested are as follows:

• MBR1

When the high MLSS concentration of $9 - 10 \text{ g L}^{-1}$ was applied, the following net MPFs were tested: $9.81 \text{ L m}^{-2} \text{ h}^{-1}$ (SRT: 30 d, HRT: 1.01 d), $10.92 \text{ L m}^{-2} \text{ h}^{-1}$ (SRT: 29 d, HRT: 0.91 d), $11.88 \text{ L m}^{-2} \text{ h}^{-1}$ (SRT: 25.5 d, HRT: 0.835 d), $12.88 \text{ L m}^{-2} \text{ h}^{-1}$ (SRT:

23.5 d, HRT: 0.77 d) and $13.77 \text{ L m}^{-2} \text{ h}^{-1}$ (SRT: 21.8 d, HRT: 0.72 d). Even though the MBR1 system occasionally suffered from membrane fouling, it was concluded that all the net MPFs were sustainable, hence the maximum average sustainable net MPF was equal to $13.77 \text{ L m}^{-2} \text{ h}^{-1}$. The operating conditions of the MBR1 system that corresponded with the net MPF of $13.77 \text{ L m}^{-2} \text{ h}^{-1}$ were as follows: Average MLSS concentration: 9.26 g L^{-1} , average mixed-liquor temperature: $28.9 \text{ }^\circ\text{C}$, membrane scouring air flow rate: $4,200 \text{ L h}^{-1}$. Filtration was continuous without any membrane relaxation. As the long-term experiment had to come to an end, average net MPFs higher than the value of $13.77 \text{ L m}^{-2} \text{ h}^{-1}$ were not tested, hence it may be possible to further increase the daily production of treated permeate in the future.

• MBR2

At the same high MLSS concentration of $9 - 10 \text{ g L}^{-1}$, the following net MPFs were applied with respect to operation of MBR2: $11.52 \text{ L m}^{-2} \text{ h}^{-1}$ (SRT: 30 d, HRT: 1.01 d), $12.81 \text{ L m}^{-2} \text{ h}^{-1}$ (SRT: 29 d, HRT: 0.91 d) and $13.94 \text{ L m}^{-2} \text{ h}^{-1}$ (SRT: 25.5 d, HRT: 0.835 d). As the highest net MBF of $13.94 \text{ L m}^{-2} \text{ h}^{-1}$ was found to be unsustainable, it was the net MPF of $12.81 \text{ L m}^{-2} \text{ h}^{-1}$ that was found to be the maximum average net sustainable MPF. The corresponding operating conditions were as follows: Average MLSS concentration: 9.379 g L^{-1} , average mixed-liquor temperature: $23.9 \text{ }^\circ\text{C}$, membrane scouring air flow rate: $12,000 \text{ L h}^{-1}$. Filtration was intermittent with a filtration/relaxation cycle equal to 9/1 min/min on/off - membranes were filtering for 9 min and then membrane relaxation was applied for 1 min.

• MBR3

Regarding operation of the MBR3 system at the high MLSS concentration of $9 - 10 \text{ g L}^{-1}$, the maximum average net sustainable MPFs could not be predicted, as all the tested real MPFs ended up being unsustainable, even though the same sets of SRTs/HRTs were applied for all three MBR systems. Despite applying intermittent filtration with a filtration/relaxation cycle equal to 17/3 min/min on/off, membrane fouling could not be avoided. MBR3 should be operated at longer HRTs so as to reduce the corresponding net MPFs to values lower than the value of $13.58 \text{ L m}^{-2} \text{ h}^{-1}$, which was the lowest net MPF that was tested during the long-term experiment. At

the same time, longer SRTs should be applied so as to maintain the MLSS concentration around the value of 9 - 10 g L⁻¹.

Finally, with respect to both MBR2 and MBR3, it may be worth checking different operating cycles, as longer relaxation times may be able to improve the maximum average sustainable net MPF of the MBR2 system, or improve in general the membrane performance of the MBR3 system.

Chapter 7, which follows, will analyse the performance of the MBR systems in terms of their energy demand. Also, in the same chapter, an attempt to model the MBR performances, and predict SED values will be made.

CHAPTER 7 ENERGY CONSUMPTION AND MBR MODELLING

7.1 Introduction

Conventional waste water treatment (WWT) processes may not be able to treat waste waters efficiently, which can then cause water pollution, if directly discharged into water bodies. The use of membrane bioreactors (MBRs) can resolve this problem as one of their most important advantages is their capability of producing treated water of exceptional quality, free of pathogens - see Chapter 2. Their application in the WWT market would then be a very promising alternative. However, MBRs currently have high operating costs as they consume quite a lot more energy than the conventional activated sludge (AS) plants, [Liao *et al.*, 2006], [Water Environmental Federation, 2006]. This happens because submerged membrane bioreactor (MBR) configurations require air blowers for biomass maintenance within the MBR tanks and additionally have to operate air scour blowers to protect the membranes against their fouling. In addition, apart from recycle pumps, they have also to operate suction pumps as occasionally negative pressures have to be applied, or permeate cannot be collected.

These high energy-related costs can make the installation and the operation of MBRs to be questionable, especially in regions where expenditure in public services is a critical factor, *i.e.* Tunisia, which is the country under study in this research. In this “sustainable membrane bioreactor (MBR)” research - see Chapter 1, three MBR systems were trialled and their energy consumption rates were measured. The MBRs systems were located at the North Sfax “Office National de l' Assainissement” (ONAS) site and they treated local municipal waste water. The ideal MBR would be capable of producing treated waste water at low specific energy demand (SED) values. In this work, the target is for SED values equal to or lower than 3 kW m^{-3} of treated permeate, which is the current SED value of the full-scale conventional AS plant operated by ONAS in Tunisia.

Experiments were conducted to obtain measurements of the energy consumption rates for the MBRs in both short-term power-analysis and longer-term energy-analysis trials. During power-analysis experiments, the average power consumption for all

MBR components was recorded with the aid of in-line electricity meters. As the operating times of all MBR components over a day were known, the energy that was consumed by each individual MBR component throughout a day could be calculated. By adding all these values, the overall energy over a day for each MBR system was also calculated. Dividing this energy consumption rate by the net permeate flow rate provides an estimate of the SED value for each MBR system. The SED value is a useful parameter regarding WWT plant operations, which indicates the amount of energy that is consumed per unit volume of treated water, [Judd, 2007], and it allows direct comparisons to be made between different WWT plants, including the pilot MBR systems in this work.

During the energy-analysis experiments, both the amount of energy that was consumed by the MBR systems, and the time during which these energy consumption measurements took place, were recorded by in-line electricity meters. By dividing the energy consumption reading by the time and normalising this figure over a day, the energy that was consumed by each MBR system throughout a day could be calculated, together with the SED value for each MBR system. These SED values can then be compared with the SED values provided by the power-analysis experiments so that the data, which was recorded during the short-term power-analysis experiment, could be validated.

Short-term power-analysis and longer-term energy-analysis experiments were conducted for both membrane bioreactor 1 (MBR1) and membrane bioreactor 2 (MBR2), but for membrane bioreactor 3 (MBR3) only longer-term energy-analysis experiments could be performed. The MBR3 system was powered by a three-phase electric system, which made direct connections of in-line electricity meters more difficult. As all MBR systems also incorporated electricity meters with rotating counters in the main electrical power cable, an additional estimation of the overall energy consumed by all MBRs could be made.

The data collected during the short-term component-analysis experiments was used to build an Excel-based model for the MBR1 and the MBR2 system. This MBR model could predict SED values of the MBR systems under different sets of operating conditions, namely solids residence times (SRTs), hydraulic residence times (HRTs),

mixed-liquor suspended solids (MLSS) concentrations and net membrane permeate fluxes (MPFs). Thus, it could be predicted which combinations of operating conditions could achieve SED values equal to or lower than the desired 3 kWh m^{-3} . This Excel-based model will be described later in Section 7.6.

7.2 Energy consumption analysis for MBR1

7.2.1 MBR1: Operating conditions during the experiments

The operating conditions of membrane bioreactor 1 (MBR1) when both power-analysis and energy-analysis experiments were conducted are shown in Table 7.1.

Table 7.1 MBR1: Operating conditions during the power-analysis and energy-analysis experiments

Parameter	Average value	Unit
Solids residence time (SRT)	23.5	d
Sludge wasting flow rate	0.059	$\text{m}^3 \text{ d}^{-1}$
Hydraulic residence time (HRT)	0.77	d
Feed flow rate	1.79	$\text{m}^3 \text{ d}^{-1}$
Net permeate flow rate	1.731	$\text{m}^3 \text{ d}^{-1}$
Net membrane permeate flux (MPF)	12.88	$\text{L m}^{-2} \text{ h}^{-1}$
MLSS concentration	8.846	g L^{-1}
Air flow rate		
Biology maintenance + Membrane scouring	4.2	$\text{m}^3 \text{ h}^{-1}$
Filtration	Continuous	–

7.2.2 Energy-consuming components

The energy-consuming components of the MBR1 system were:

- The control panel, which was always switched on providing a baseline with respect to energy consumed.

- An air compressor, which provided air both for membrane scouring and for the biomass maintenance inside the MBR tank.
- Feed Pump 1, which delivered waste water from the FS/AN tank into the MBR tank.

When all the energy-consuming components are switched off, a small amount of electricity is still consumed due to the fact that the control panel, which is shown in Figure 3.7, is always switched on providing a baseline with respect to energy consumption rates. In a fully-automated process, a sludge pump is also installed so that sludge wasting takes place automatically. However, MBR1 was operated without a sludge pump and sludge wasting took place manually.

These power-consuming components, along with a hypothetical sludge pump, are shown in Figure 7.1 - the control panel is not included in this figure.

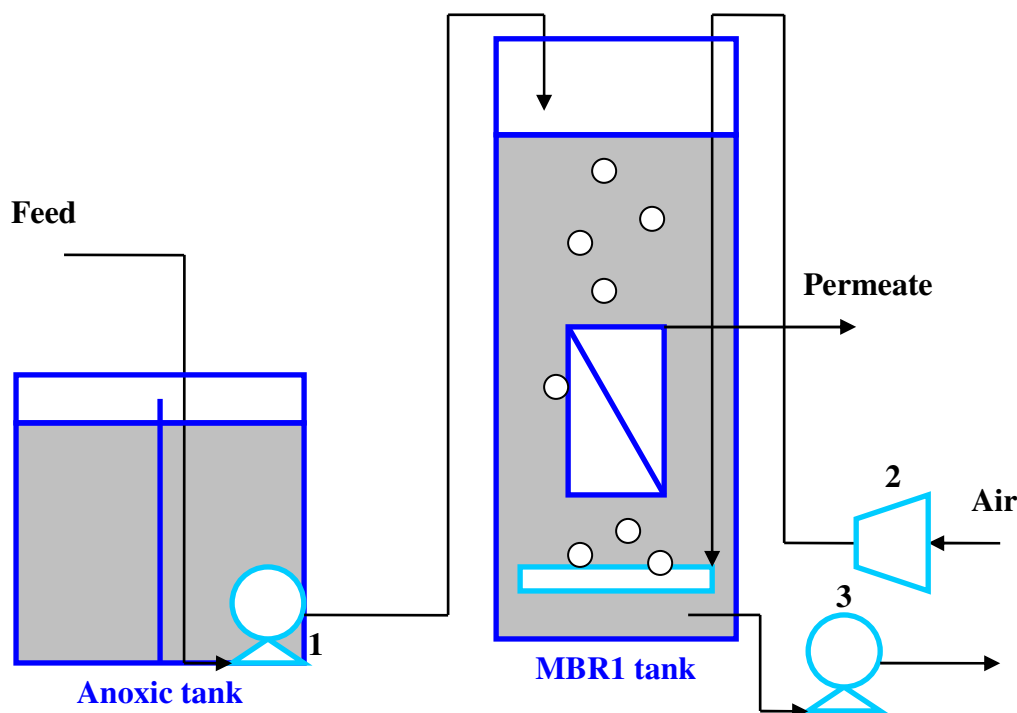


Figure 7.1 MBR1: Energy-consuming components: 1: Feed Pump 1, 2: Air blower, 3: Hypothetical sludge pump - The control panel is not shown in this figure

7.2.3 MBR1: Power-analysis experiments

The power values of the components of the MBR1 system are shown in Table 7.2. Measurements were taken with the aid of the control panel and in-line electricity meters - all components were switched off except for the one which was under study, and then power values for that component were recorded. Out of the recorded power figures, an average power value was calculated. All average power values per component are presented in Table 7.2.

Table 7.2 MBR1: Power values per component during the power-analysis experiments

Component	Power (W)
Baseline	32.8
Baseline + Feed Pump 1	1007.5
Baseline + Air blower (MBR tank) Biology maintenance + Membrane scouring	370.6

Some comments about the data provided in Table 7.2 are as follows:

- **Baseline**

Two different baseline power values were measured depending on whether the permeate protection valve was switched on (32.8 W) or off (28.9 W), but there is little difference between these two figures. As the protection valve had to be switched on all the time during the pilot trials, the higher power value was selected as it represents the real case during operation.

- **Baseline + Feed Pump 1**

The power value shown in Table 7.2 is an average value between a minimum recorded value of 1005 W and a maximum of 1010 W. As Feed Pump 1 was a constant speed pump, it could deliver only a certain amount of waste water, which means that the flow rate of Feed Pump 1 was of a fixed value - it was equal to $5 \text{ m}^3 \text{ h}^{-1}$.

As a fixed flow rate could be provided by this pump, it can be assumed that the average power, as shown in Table 7.2, remained constant. The parameter responsible for any change of the overall energy consumed by Feed Pump 1 was the runtime of this pump. Variation in the feed flow rate of the MBR1 system caused Feed pump 1 to run for different periods of time, and hence influenced the energy that was consumed.

To make it clear, an example calculation of the energy consumed by Feed Pump 1 is as follows:

The pump feed flow, $Q_{fp,1}$, is equal to $5 \text{ m}^3 \text{ hr}^{-1}$, or $120 \text{ m}^3 \text{ d}^{-1}$. The runtime of Feed Pump 1 (over a 24-hour time period), $t_{run,1}$, corresponding to a particular feed flow rate of the MBR1 system, $Q_{f,1}$, can be estimated as follows:

$$t_{run,1} = \frac{Q_{f,1}}{Q_{fp,1}} \cdot 24 \quad \text{Equation 7.1}$$

where:

$t_{run,1}$	=	Runtime of Feed Pump 1	h d^{-1}
$Q_{f,1}$	=	Feed flow rate of MBR1 during the experiment	$\text{m}^3 \text{ d}^{-1}$
$Q_{fp,1}$	=	Designed feed flow rate of Feed Pump 1	$120 \text{ m}^3 \text{ d}^{-1}$

By applying Equation 7.1, Table 7.3, which shows random example estimations of the runtime for different feed flow rates of the MBR1 system, is constructed. The MBR feed flow rate of $2.027 \text{ m}^3 \text{ d}^{-1}$, which was the feed flow rate during the power-analysis experiment, is also shown in Table 7.3.

Table 7.3 MBR1: Estimation of the runtime of Feed Pump 1 for a range of feed flow rates of the MBR1 system

MBR1 feed flow rate ($\text{m}^3 \text{d}^{-1}$)	Runtime (h d^{-1})
1.498	0.3
1.997	0.4
2.027	0.41
2.506	0.51
2.999	0.6

• **Baseline + Air blower**

Power values were recorded for three different air flow rates, as shown in Table 7.4. During the power-analysis experiment, negligible changes of the liquid height within the MBR tank occurred due to filtration, so it can be successfully assumed that the hydraulic pressure head over the diffuser was constant when the measurements were taken.

Table 7.4 MBR1: Power values of the air blower at different air flow rates

Air flow rate ($\text{m}^3 \text{h}^{-1}$)	Power rate (W)
5.2	370.8
4.2	370.6
3.2	370.4

As seen in Table 7.4, the power of the air blower was hardly affected by the air flow rates, at least for the range of the air flow rates that were tested. The fact that the power did not change during the power-analysis experiment indicates that this air compressor may not be a very cost-effective solution with respect to the application of lower air flow rates. This practically means that another air compressor would be able to reduce the current energy consumption rates and it could be interesting to further investigate this option in the future. At the moment, the power rate of 370.6 W was

selected to be the average power value for the MBR1 air compressor as that was the value recorded when the normal air flow rate of $4.2 \text{ m}^3 \text{ h}^{-1}$ was applied.

As the runtime for each component over a day was also known, the energy that was consumed throughout a day by each component could be calculated. By adding these individual energy consumption rates, the overall energy that was consumed by the MBR1 system throughout a day was also estimated, and it is shown in Table 7.5.

Table 7.5 MBR1: Power-analysis experiments: Estimation of the overall energy consumed throughout a day

Component	Runtime (h d ⁻¹)	Energy consumption rate (kWh d ⁻¹)
Baseline	24	0.787
Feed Pump 1	0.36	0.349
Air blower	24	8.107
All components	–	9.243

Then, the SED value for this series of measurements was estimated, and is shown in Table 7.6.

Table 7.6 MBR1: Power-analysis experiments: Estimation of the SED value

Parameter	Value	Unit
Total energy consumed throughout a day	9.243	kWh d ⁻¹
Net permeate flow rate	1.731	m ³ d ⁻¹
SED	5.339	kWh m ⁻³

The SED value is 78 % higher than the target SED value of 3 kWh m^{-3} , however, it is known that MBRs usually consume more energy when compared to conventional AS processes. Finally, SED values are usually system-specific, and pilot WWT systems may easily consume relatively more energy than full-scale WWT plants.

7.2.4 MBR1: Energy-analysis experiments

7.2.4.1 MBR1: Energy-analysis experiments conducted with the aid of in-line electricity meters

Both the energy consumed by the MBR1 system and the time period during which this amount of energy was consumed were recorded. Assuming that there is a linear relationship between the time elapsed and the energy consumed by MBR1, the energy consumption rate was normalised over a 24-hour time period. The SED value for this series of experiments was also calculated. The data, both recorded and calculated, is shown in Table 7.7.

Table 7.7 MBR1: Energy-analysis experiments conducted with the aid of in-line electricity meters: Estimation of the SED value

Parameter	Value	Unit
Total energy consumed throughout a day	9.225	kWh d ⁻¹
Net permeate flow rate	1.731	m ³ d ⁻¹
SED	5.329	kWh m ⁻³

The two different series of experiments provided slightly different SED values. The SED value of 5.329 kWh m⁻³ provided by the longer-term energy-analysis experiment is likely to be more accurate as it was measured over a longer period of time. However, the component-based analysis, described in Section 7.2.3, is also a valid methodology and, as can be seen, the difference between the two different values is negligible. The accuracy of these values is therefore confirmed.

7.2.4.2 MBR1: Energy-analysis experiments conducted with the aid of electricity meters with rotating counters

The principle with respect to this SED measurement was exactly the same as the one mentioned in Section 7.2.4.1., but, instead of using in-line electricity meters, the energy measurements were taken with the aid of electricity meters with rotating counters connected to the main electrical power cable. These energy values were also

normalised over a 24-hour time period. The SED value was calculated, and is shown in Table 7.8.

Table 7.8 MBR1: Energy-analysis experiments conducted with the aid of electricity meters with rotating counters: Estimation of the SED value

Parameter	Value	Unit
Total energy consumed throughout a day	9.477	kWh d ⁻¹
Net permeate flow rate	1.731	m ³ d ⁻¹
SED	5.475	kWh m ⁻³

As seen in Table 7.8, this experiment provided a SED value slightly higher than the previous two SED values. This is due to the fact that the readings as provided by the electricity meters with the rotating counters, are less accurate than the readings provided by the in-line electricity meters. However, this SED figure is still similar in value.

The three SED values were higher than the target value of 3 kWh m⁻³ of the full-scale conventional AS plant at the ONAS site. The fact that all three SED estimates were nearly similar in value indicates that correct SED values have been calculated and that the SED value, as provided by short-term component-based experiment, has been successfully validated by the SED values as provided by the longer-term energy-analysis experiment.

7.3 Energy consumption analysis for MBR2

7.3.1 MBR2: Operating conditions during the experiments

The operating conditions of the membrane bioreactor 2 (MBR2) system, when both power-analysis and energy-analysis experiments were conducted are shown in Table 7.1. Filtration was intermittent based on a filtration/relaxation operational cycle equal to 9/1 min/min on/off.

Table 7.9 MBR2: Operating conditions during the power-analysis and energy-analysis experiments

Parameter	Average value	Unit
SRT	25.5	d
Sludge wasting flow rate	0.079	m ³ d ⁻¹
HRT	0.835	d
Feed flow rate	2.422	m ³ d ⁻¹
Net permeate flow rate	2.343	m ³ d ⁻¹
Net MPF	13.94	L m ⁻² h ⁻¹
MLSS concentration	9.379	g L ⁻¹
Air flow rate (BT tank) Biology maintenance	6	m ³ h ⁻¹
Air flow rate (MBR tank) Biology maintenance + Membrane scouring	12	m ³ h ⁻¹
Filtration	Intermittent: 9/1	min on/min off

7.3.2 Energy-consuming components

The energy-consuming components of the MBR2 system were:

- The control panel of the MBR system, which was always switched on providing a baseline with respect to the energy consumed.
- An air compressor, which provided air within the biological tank for biomass maintenance.
- Two air compressors that provided air inside the MBR tank both for membrane scouring and for biomass maintenance, as two membrane modules had also been located within the MBR tank. Also, underneath each membrane module, an air diffuser was located and was connected with an air compressor - see Chapter 3. These air blowers were of the same specification, and they were provided directly from the equipment supplier. As only slight changes of the liquid height both within the

biological and MBR tanks occurred during the power-analysis and the energy-analysis experiments, it can be assumed that the hydraulic pressure head over the diffusers was effectively constant.

- Feed Pump 2, which delivered waste water from the FS/AN tank to the MBR tank.
- A recirculation pump, which delivered waste water from the MBR tank to the biological tank.
- A suction pump, which provided the required negative pressures in order to collect permeate.

It is worth mentioning that when all the energy-consuming components are switched off, a small amount of electricity is still consumed due to the fact that the control panel, which is shown in Figure 3.7, was always switched on providing a baseline with respect to energy consumption rates.

Finally, in a fully-automated process, a sludge pump is usually installed to waste excess sludge automatically. Regarding the MBR2 system, sludge was initially wasted manually but later, in March 2009, a sludge pump was installed and operated. Energy consumed by the sludge pump will be ignored when the SED values of the MBR2 system are calculated otherwise a direct comparison with the SED values of the MBR1 system cannot be made.

The energy-consuming components of the MBR2 system, except for the control panel, are shown in Figure 7.2.

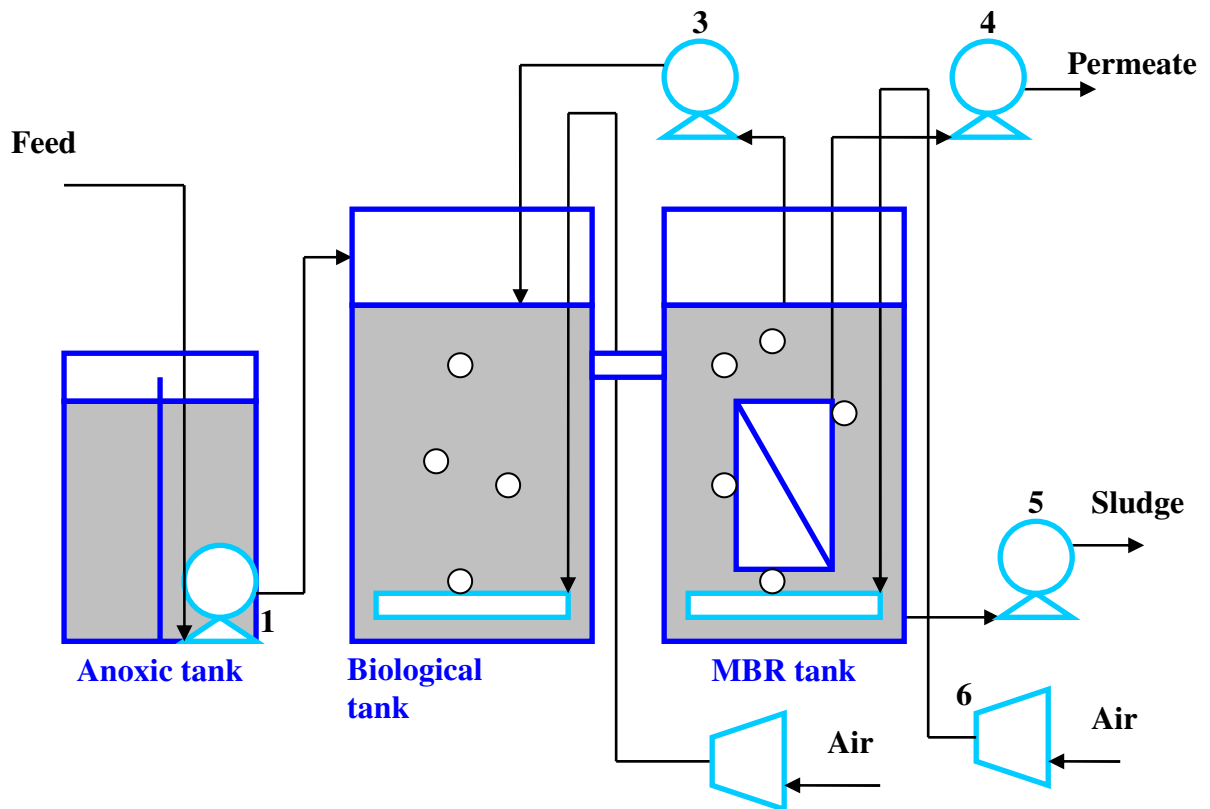


Figure 7.2 MBR2: Energy-consuming components: 1: Feed Pump 2, 2: Air blower (biological tank), 3: Recirculation pump, 4: Suction pump, 5: Sludge pump, 6: Air blowers (MBR tank) - The control panel is not shown in this figure. Also, only one membrane module and only one air blower providing air within the MBR tank are shown in this figure

7.3.3 MBR2: Power-analysis experiments

A breakdown regarding the power values of the different components of the MBR2 system was performed. Measurements were taken with the aid of the control panel and in-line electricity meters - all components were switched off, except for the one that was under study. Then, power values for that component were recorded - out of these power values an average power value was calculated. In addition, the suction pump was operated at different net permeate flow rates and the relationship between the permeate flow rates and the pump's average power values was investigated. Feed Pump 2 and the sludge pump could not be operated by the MBR2 control panel. These

two devices were powered directly from the main electric box of the plant. The power measurements are as follows:

• **All components excluding Feed Pump 2 and the sludge pump**

Table 7.10 shows the power values of all the components that were regulated by the control panel. The power values of the suction pump are not presented in Table 7.10 because they will be analysed separately.

Table 7.10 MBR2: Power values per component during the power-analysis experiments - Feed pump 2, the sludge pump and the suction pump are not shown in this table

Component	Power (W)
Baseline	16.7
Baseline + Air compressor Biology maintenance	105.3
Baseline + 2 Air compressors Biology Maintenance + Membrane scouring	191.9
Baseline + Recirculation pump	183.5

Regarding the suction pump, power values were recorded for a range of different real permeate flow rates, and they are presented in Table 7.11. The values shown in Table 7.11 are average values between a minimum power value and a maximum power value both recorded during the component-based experiment, but the difference between the minimum and the maximum power value was always very small, between 1 W and 3 W.

Table 7.11 MBR2: Baseline + Suction pump: Power values under different real permeate flow rates - Corresponding net permeate flow rates are also provided

Selected real permeate flow rate (L min ⁻¹)	Corresponding net permeate flow rate (m ³ d ⁻¹)	Power (W)
1.45	1.789	124.5
1.83	2.376	125.5
2.21	3.182	128
2.8	4.032	131
3.4	4.896	135.5

By taking into account the power values shown in Table 7.11, it can be said that only small changes of the average power occurred each time a new real permeate flow rate was applied - at least for the range of the real permeate flow rates that were tested. Also, each time the real permeate flow rate was increased, the pump power was also increased, although these changes were not significant.

Both the real permeate flow rate values (in L min⁻¹) and the pump power values were modelled, and a best-fit straight line was obtained. The function describing this line was found to be as follows:

$$P_{sp,2} = 5.710Q_{p,r,2} + 115.55 \quad \text{Equation 7.2}$$

where:

$$P_{sp,2} = \text{Power of suction pump of MBR2} \quad \text{W}$$

Based on Equation 7.2, the pump power for a net permeate flow of 2.343 m³ d⁻¹, which was the net permeate flow rate when the power-analysis experiment was conducted, was found to be equal to 125.8 W. This is acceptably close to the value measured directly during the test.

• Feed pump 2

Feed Pump 2 was not powered from the control panel, so individual measurements were taken. Feed Pump 2 was a constant speed pump providing a fixed flow rate value of $8 \text{ m}^3 \text{ h}^{-1}$. As it was a constant-speed pump, the power value was assumed to remain constant, and the only parameter that was changed, each time the feed flow value of the MBR2 system was adjusted, was the pump runtime. The power of Feed Pump 2 was recorded with the aid of an in-line electricity meter and it was found to be 231.5 W. This was an average value between a minimum value of 231 and a maximum value of 232 W. It can also be seen that Feed Pump 2 was less energy-consuming compared to the Feed Pump 1 as a lower power value was recorded.

The runtime of Feed Pump 2 is calculated as follows:

$$t_{run,2} = \frac{Q_{f,2}}{Q_{fp,2}} \cdot 24 \quad \text{Equation 7.3}$$

where:

$t_{run,2}$	=	Runtime of Feed Pump 2	h d^{-1}
$Q_{f,2}$	=	Feed flow rate of MBR2 during the experiment	$\text{m}^3 \text{ d}^{-1}$
$Q_{fp,2}$	=	Designed feed flow rate of Feed Pump 2	$192 \text{ m}^3 \text{ d}^{-1}$

Based on Equation 7.3, Table 7.12 shows random example calculations of the runtime for different feed flow rates of the MBR2 system. The feed flow rate of $2.393 \text{ m}^3 \text{ d}^{-1}$, which was the feed flow rate value of the MBR2 system during the component-based experiment, is also shown in Table 7.12.

Table 7.12 MBR2: Estimation of the runtime of Feed Pump 1 for a range of feed flow rates of the MBR2 system

MBR2 feed flow rate ($\text{m}^3 \text{d}^{-1}$)	Runtime (h d^{-1})
1.498	0.19
2.002	0.25
2.393	0.3
2.497	0.31
2.996	0.37

By taking into account measurements/calculations as provided both in Table 7.10 and in Table 7.12, it can be said that, in terms of energy demand, the MBR2 system was designed more carefully than the MBR1 system, as both the air blowers and Feed Pump 2 were less energy-consuming devices than those operated by the MBR1 system. However, the MBR2 system had to operate with more devices than the MBR1 system.

• Sludge pump

Sludge was initially wasted manually. In March 2009, a sludge pump was installed, so MBR2 operation became fully-automated. The power of the sludge pump was 0.396 kW and the runtime for maintaining the MLSS concentration at the average value of 9.379 g L^{-1} , as given in Table 7.9, was about 2.18 h d^{-1} . By multiplying the power rate with the runtime, the energy consumed throughout a day was found to be 0.863 kWh d^{-1} .

As the power values and runtimes of all components are known, the energy consumed over a day by each component, together with the overall energy consumption rate, can be estimated, and the results are shown in Table 7.13. The sludge pump has been deliberately excluded from these calculations, or otherwise a comparison among the MBR systems could not be made - the MBR1 system did not operate a sludge pump.

Table 7.13 MBR2: Power-analysis experiments: Estimation of the overall energy consumed throughout a day - Sludge pump is excluded

Component	Runtime (h d ⁻¹)	Energy consumption rate (kWh d ⁻¹)
Baseline	24	0.401
Feed pump 2	0.3	0.071
Recirculation pump	4	0.667
Filtration pump	21.6	2.35
Air blower (BT tank)	12	1.063
2 air blowers (MBR tank)	24	4.205
All components	–	8.757

Based on the information provided both in Table 7.9 and in Table 7.13, a composite table can be produced and the SED value of the MBR2 system is estimated, (Table 7.14).

Table 7.14 MBR2: Power-analysis experiments: Estimation of the SED value - Sludge pump is excluded

Parameter	Value	Unit
Total energy consumed throughout a day	8.757	kWh d ⁻¹
Net permeate flow rate	2.343	m ³ d ⁻¹
SED	3.738	kWh m ⁻³

The SED value is higher than the target SED value of 3 kWh m⁻³, however it is a promising SED value, taking into account that MBRs, in general, need more energy to operate compared to the conventional WWT processes.

The SED value would have been higher if the energy consumption rate of the sludge pump had been taken into consideration. Table 7.15 shows the overall energy consumption rate when the sludge pump energy consumption is taken into account.

Table 7.15 MBR2: Power-analysis experiments: Estimation of the overall energy consumed throughout a day - Sludge pump is included

Parameter	Value	Unit
All components except for the sludge pump	8.757	kWh d ⁻¹
Sludge pump	0.863	kWh d ⁻¹
All components	9.62	kWh d ⁻¹

Based on the information provided both in Table 7.9 and in Table 7.15, a composite table is produced and the SED of the MBR2 system is re-calculated, (Table 7.16).

Table 7.16 MBR2: Power-analysis experiments: Estimation of the SED value - Sludge pump is included

Parameter	Value	Unit
Total energy consumed throughout a day	9.62	kWh d ⁻¹
Net permeate flow rate	2.343	m ³ d ⁻¹
SED	4.105	kWh m ⁻³

Comparing the SED values given in Table 7.14 and in Table 7.16, it can be concluded that the operation of a sludge pump increased the SED value by a small percentage, equal to about 9.9 %, but in fully-automated MBR operations sludge pumps must be operated.

7.3.4 MBR2: Energy-analysis experiments

7.3.4.1 MBR2: Energy-analysis experiments conducted with the aid of in-line electricity meters

Both the energy consumed by the MBR2 system and the time period, during which this amount of energy was consumed, were recorded. However, it was not possible to directly record the overall energy consumption rate because Feed Pump 2 was not powered from the control panel. Two individual measurements were made, one for all the MBR2 components except for Feed Pump 2, and another one for Feed Pump 2

itself. Both energy consumption rates were normalised over a 24-hour time period and added together. Table 7.17 presents the results.

Table 7.17 MBR2: Energy-analysis experiments conducted with the aid of in-line electricity meters: Estimation of the total energy consumption rate

Component	Energy consumption rate (kWh d ⁻¹)
All components except for Feed Pump 2	8.98
Feed Pump 2	0.154
All MBR2 components	9.134

The SED value resulting from these measurements is presented in Table 7.18.

Table 7.18 MBR2: Energy-analysis experiments conducted with the aid of in-line electricity meters: Estimation of the SED value

Parameter	Value	Unit
Total energy consumed throughout a day	9.134	kWh d ⁻¹
Net permeate flow rate	2.343	m ³ d ⁻¹
SED	3.899	kWh m ⁻³

This time the SED value is higher than the SED value estimated by the component-based experiment described in Section 7.3.3, although the difference between the two different SED values is negligible. The SED value calculated here is likely to be more accurate as it relies on energy measurements over longer periods of time, but this does not mean that the SED value estimated during the short-term power-analysis experiment is less valid.

7.3.4.2 MBR2: Energy-analysis experiments conducted with the aid of electricity meters with rotating counters

Additional energy measurements were taken with the aid of electricity meters with rotating counters connected with the main electrical power cable. The energy that was

consumed by the MBR2 system was measured over a period of time and it was then normalised over a 24-hour basis. To this was added the energy consumption rate of Feed Pump 2, which was assumed to be equal to the energy consumption rate as measured by the in-line electricity meter. The overall energy consumption rate of the MBR2 system was calculated and is shown in Table 7.19.

Table 7.19 MBR2: Energy-analysis experiments conducted with the aid of electricity meters with rotating counters: Estimation of the total energy consumption rate

Component	Energy consumption rate (kWh d ⁻¹)
All components except for Feed Pump 2	8.928
Feed Pump 2	0.154
All MBR2 components	9.082

Based on Table 7.8 and Table 7.19, a composite table providing the SED value is produced.

Table 7.20 MBR2: Energy-analysis experiments conducted with the aid of electricity meters with rotating counters: Estimation of the SED value

Parameter	Value	Unit
Total energy consumed throughout a day	9.082	kWh d ⁻¹
Net permeate flow rate	2.343	m ³ d ⁻¹
SED	3.877	kWh m ⁻³

This SED value is very similar to the SED value estimated in Section 7.3.4.1, which means that the SED values provided by the energy-analysis experiments matched, either in-line electricity meters or electricity meters with rotating counters were used.

7.4 Energy consumption analysis for MBR3

In-line electricity meters could not be connected due to the fact that the membrane bioreactor 3 (MBR3) system was powered by a three-phase power supply so the control panel could not be powered via a main cable. On the other hand, energy-analysis experiments with the aid of electricity meters with rotating counters were performed as usual.

7.4.1 Operating conditions during the experiments

The operating conditions of the MBR3 system, during the energy-analysis experiments are shown in Table 7.21. Filtration was intermittent, based on a filtration/relaxation operational cycle equal to 17/3 min/min on/off.

Table 7.21 MBR3: Operating conditions during the energy-analysis experiments conducted with the aid of electricity meters with rotating counters

Parameter	Value	Unit
SRT	12	d
Sludge wasting flow rate	0.184	m ³ d ⁻¹
HRT	0.77	d
Feed flow rate	2.865	m ³ d ⁻¹
Net permeate flow rate	2.681	m ³ d ⁻¹
Net MPF	17.87	L m ⁻² h ⁻¹
MLSS concentration	5.043	g L ⁻¹
Air flow rate (Aeration tank)		
Biology maintenance	N/A	-
Air flow rate (Filtration tank)		
Biology maintenance + Membrane scouring	7.3	m ³ h ⁻¹
Filtration	Intermittent	
	17/3	min on/min off

7.4.2 Energy-consuming components

The energy-consuming components of the MBR3 system were:

- The control panel, which controlled the MBR operation.
- A submersible aerator-mixer inside the aeration tank, which provided air for the biomass maintenance.
- An air compressor, which provided air both for membrane scouring and for biomass maintenance inside the filtration tank. The liquid level in this tank was constant due to an overflow, which was delivering waste water to the aeration tank at all times, hence the hydraulic pressure head above the diffuser was also constant.
- Feed Pump 3, which delivered waste water from the FS/AN tank to the aeration tank.
- A recirculation pump, which delivered waste water from the aeration tank into the filtration tank.
- A suction pump, which delivered permeate out of the membranes by applying a slight negative pressure.

Excess sludge produced by the MBR3 system was initially wasted manually but later, in March 2009, a sludge pump was installed and operated. These energy-consuming components of the MBR3 system, excluding the control panel, are now shown in Figure 7.3. However, it has to be mentioned that, as no component-based experiments were carried out, the power values per component could not be measured.

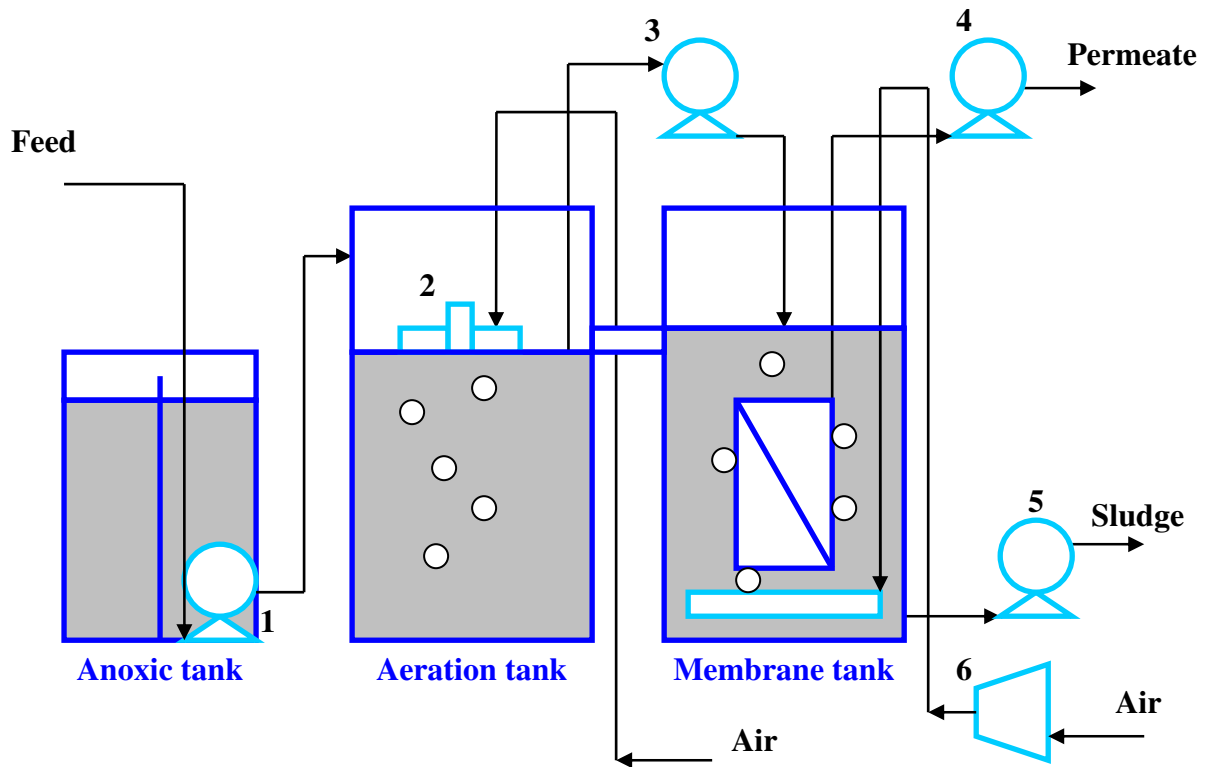


Figure 7.3 MBR3: Energy-consuming components: 1: Feed pump 3, 2: Aerator-mixer inside the aeration tank, 3: Recirculation pump, 4: Suction pump, 5: Sludge pump, 6: Air compressor - The control panel is not shown in this figure

7.4.3 MBR3: Energy-analysis experiments conducted with the aid of electricity meters with rotating counters

During these experiments, only one energy consumption rate was measured, as the electricity meter with rotating counters was able to measure all the energy that was consumed by all components of the MBR3 system, except for Feed Pump 3. The figure was recorded and it was normalised over a 24-hour basis. The sludge pump was once again neglected. The energy consumed by Feed Pump 3 was calculated indirectly as this pump was exactly the same as Feed Pump 2. As the feed flow rate was known and equal to $2.81 \text{ m}^3 \text{ d}^{-1}$, the runtime was estimated through Equation 7.3, and was found to be 0.35 h d^{-1} . The power value for Feed Pump 3 was 231.5 W. By multiplying the power value with the runtime, the energy consumed by Feed Pump 3 over a day was calculated and was found to be equal to 0.081 kWh d^{-1} . Table 7.22 includes the energy consumption rates that were estimated.

Table 7.22 MBR3: Energy-analysis experiments conducted with the aid of electricity meters with rotating counters: Estimation of the total energy consumption rate

Component	Energy consumption rate (kWh d ⁻¹)
All components except for Feed Pump 3	12.391
Feed Pump 3	0.081
All MBR3 components	12.472

Table 7.23 provides the SED value for the MBR3 system.

Table 7.23 MBR3: Energy-analysis experiments conducted with the aid of electricity meters with rotating counters: Estimation of the SED value

Parameter	Value	Unit
Total energy consumed throughout a day	12.472	kWh d ⁻¹
Net permeate flow rate	2.681	m ³ d ⁻¹
SED	4.652	kWh m ⁻³

The estimated SED value is in the same range as the SED values of the MBR1 and the MBR2 systems, and between the 5.5 kWh m⁻³ and the 3.9 kWh m⁻³ for MBR1 and MBR2 respectively.

7.5 Analysis of the results

7.5.1 MBR energy consumption breakdown

This section will provide further commentary and analysis of the MBR energy consumption data. First, the MBR1/MBR2 power-analysis experiments will be analysed. MBR3 will not be included in the following analysis of the data, as such experiments could not be performed due to its three-phase power supply. Initially, the data collected during these component-based experiments are converted into percentages, so an easier comparison between the MBR1 system and the MBR2 system is made.

These percentages express the contribution of each component to the overall energy consumption value, which is represented by the maximum percentage of 100 %. The calculations were done through an Excel 2003 spreadsheet, which could also model mass balances across the MBR systems, the biological kinetics and stoichiometry of the MBR operation, and issues relating to MBR energy demand. The model was calibrated and validated by using raw data collected during the trials and it will be described in detail in Section 7.6.

The estimated percentages are presented in Table 7.24. All MBR components, excluding the baselines due to control panels, are related either to liquid pumping or to aeration. Overall percentages for energy consumption were also calculated. These percentages are also shown in Table 7.24.

Table 7.24 MBR1/MBR2: Energy consumption percentages

Activity	Components	Energy consumption percentage (%)	
		MBR1	MBR2
Stand-by conditions	Control panels		
	All equipment is switched off	8.5	4.6
Liquid pumping	Feed pumps	3.8	0.8
	Recirculation pumps	0	7.6
	Filtration pumps	0	26.8
	All the pumps	3.8	35.3
Aeration	Biological maintenance	N/A	12.1
	Biological maintenance and membrane scouring	87.7	48
	Overall aeration	87.7	60.2
All activities	All components	100	100

In addition, Figure 7.4 shows the energy percentage for each activity.

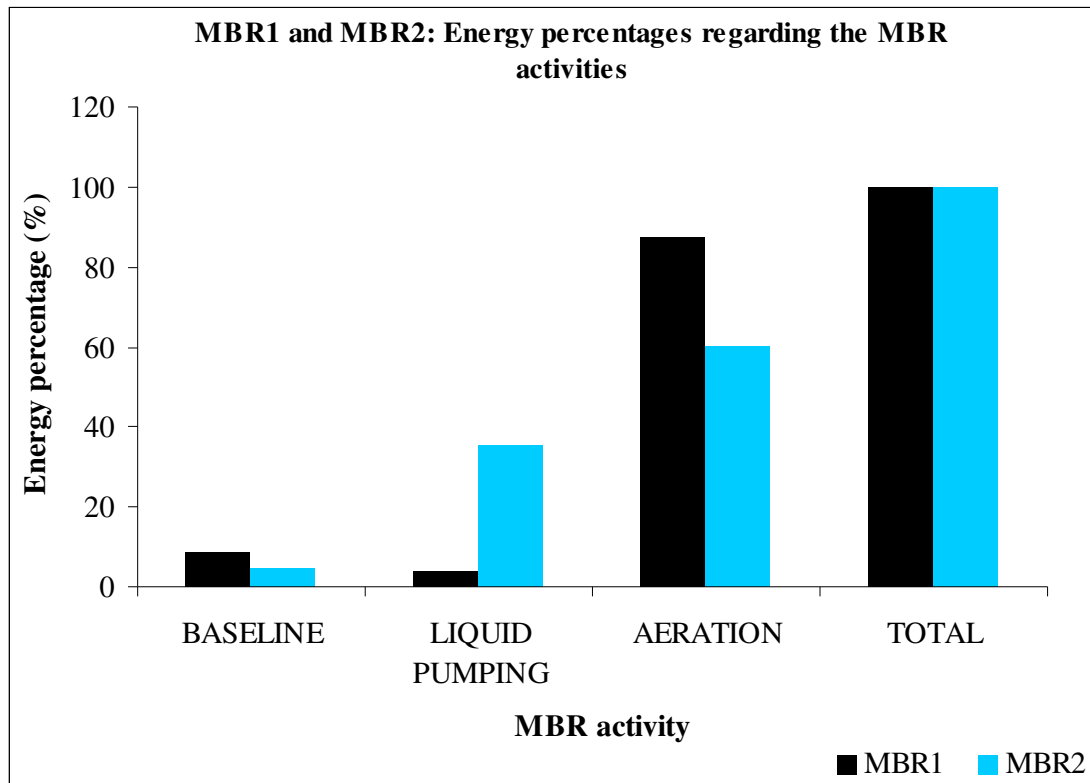


Figure 7.4 MBR1/MBR2: Energy consumption percentages with respect to MBR activities, namely baseline required by the control panels, pumping waste/treated water and MBR aeration

The baseline in Figure 7.4 represents the energy required by the control panels - all other equipment is switched off. MBR1 employs only one pump for liquid pumping, *i.e.* Feed Pump 1. MBR2 employed three pumps, namely Feed Pump 2, a recirculation pump and a suction pump. With regard to aeration, MBR1 operated with one air blower, whereas MBR2 operated with three air blowers.

This was because the two MBR systems had different tank configurations. MBR1 consisted of only one tank, hence both the biological treatment and filtration took place within the same tank. This means that the air provided was both for biomass maintenance and membrane scouring. MBR2, on the other hand, comprised two tanks, the biological tank and the MBR tank. MBR1, as seen in Table 7.24, had only one aeration percentage, which represents the total aeration energy demand, whereas MBR2 had two different aeration percentages, one for each tank.

The energy consumption percentages of each individual component generate Figure 7.5.

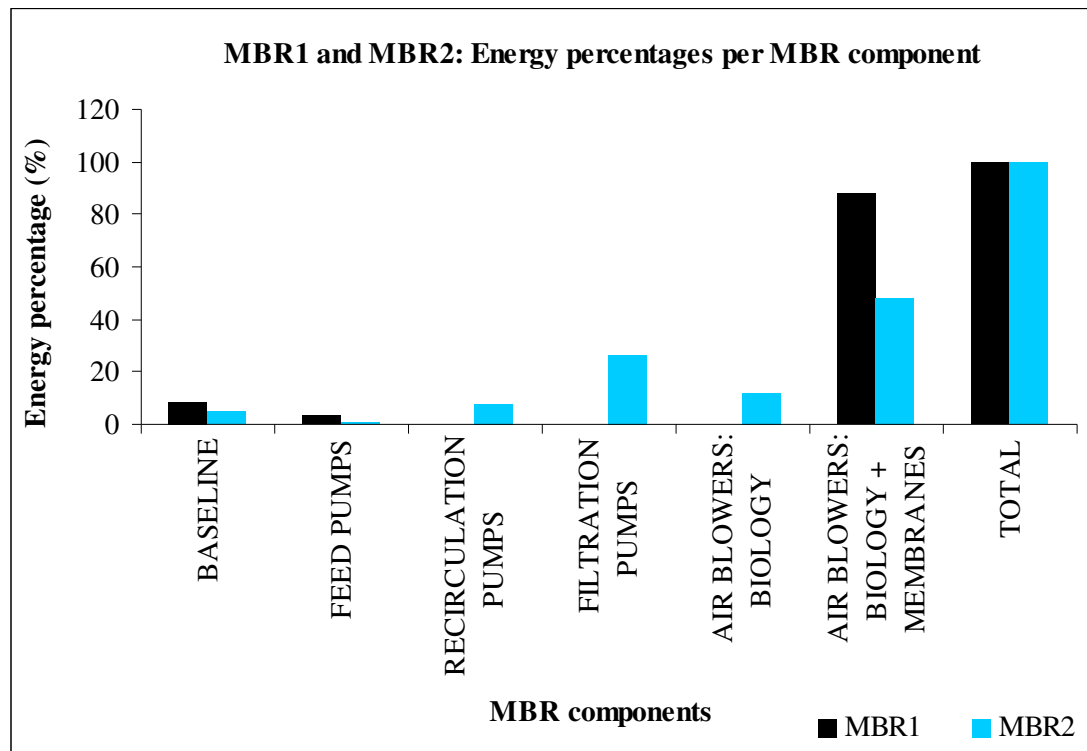


Figure 7.5 MBR1/MBR2: Energy consumption percentages per MBR component

Comments based on Figure 7.4 and Figure 7.5 are as follows:

- **Baseline**

Due to the fact that pilot plants and not full-scale plants were operated, baseline percentages appeared to be quite high. At the moment, these percentages could not be assumed as negligible. As control panels consume a constant amount of electricity, a full-scale plant is likely to have a smaller energy consumption percentage with respect to baseline energy demand than a pilot plant. It is therefore appropriate to ignore the baseline energy consumption figures of the pilot units when comparing their performance to full-scale MBR plants.

• Liquid Pumping

Energy consumed by liquid pumping counted only for about 3.8 % - a quite negligible value - of the total energy that was consumed. This small percentage can be attributed to the fact that Feed Pump 1 was operational only for a very short period of time over a day. Due to the fact that the MBR2 system had to operate three pumps in total, the energy percentage regarding liquid pumping appeared to be much higher than the percentage for the MBR1 system. This increase in the energy percentage is related to the fact that both the recirculation pump and the filtration pump were operational for quite long time periods. The filtration suction pump on its own consumed 26.7 % of the total energy. To conclude, the energy consumption rates of the feed pumps will increase any time the feed flow of the MBR systems increases as they have to be operational for longer periods of time. Also, the MBR2 suction pump will consume more energy at higher real/net MPFs.

Feed Pump 2 consumed very little energy as with Feed Pump 1. In addition, it is worth mentioning that Feed Pump 2 was a better choice as it appeared to be more efficient than Feed Pump 1 due to its higher fixed feed flow rate and its lower power value. This practically means that by replacing the current Feed Pump 1 with a pump similar to Feed Pump 2, improved SED values with regard to the MBR1 system will be obtained. This will be further explored in Section 7.6.3.3.

• Aeration

The air blower of the MBR1 system consumed the highest amount of the overall energy, at a percentage slightly less than 90 %, which is very similar with literature values for submerged gravity-driven MBRs, [Gander *et al.*, 2000]. With respect to MBR2, the air blowers also consumed the highest amount of energy but the estimated percentage was lower, in the range of 60 %. This happened because MBR2 was not a gravity-driven MBR but treated permeate had to be collected by operating a suction pump. Also, a recirculation pump was operated. The operation of these pumps increased the energy percentage of liquid pumping decreasing at the same time the energy percentage of aeration.

However, it is worth mentioning that the air compressor operated by the MBR1 system seemed not to have been optimised. Based on the power-analysis data, it was found that the energy consumption rate for aeration of the MBR1 system was 4.683 kWh m^{-3} , whereas it was 2.249 kWh m^{-3} for MBR2. It is true that MBR1 needed a more powerful air blower as it had to work against a higher hydraulic pressure than MBR2, however, a more cost-effective solution has yet to be found as a proper replacement the MBR1 air blower could further reduce the SED values of the MBR1 system - more details will be given in Section 7.6.3.3.

7.5.2 Presentation of the SED values

SED values based either on power-analysis or energy-analysis experiments are summarised in Table 7.25. These values were estimated with the aid of a spreadsheet constructed by using Excel 2003, details of which will be given later in Section 7.6.

Table 7.25 SED values

MBR system	S.E.D. Values (kWh m^{-3})		
	Power-analysis experiments	Energy-analysis experiments	
		In-line electricity meters	Electricity meters with rotating counters
MBR1	5.339	5.329	5.475
MBR2	3.738	3.889	3.887
MBR3	-	-	4.652

Based on Table 7.25, some comments are as follows:

As long as similar SED values were estimated by both the short-term component-based experiments and the longer-term energy-analysis experiments, the short-term experiment is successfully validated by the longer-term experiment. As seen in Table 7.25, the SED values so far are higher than the target value of 3 kWh m^{-3} , which is the SED value for the full-scale conventional AS plant.

From Table 7.25, it can be seen that the MBR2 system provided the lowest SED values, followed by the MBR3 system and finally by the MBR1 system. Despite the fact that MBR1 appeared to have the highest SED value, it was the only MBR system that was being operated under a stable membrane performance when the power-analysis/energy-analysis experiments were conducted. The SED values of the MBR2 system and the MBR3 system are questionable as these MBRs were operated under unsustainable net MPFs. It will then be the predicted SED values under sustainable net MPFs that will finally help conclude about the least energy-consuming MBR system.

The application of the MBR model, as described later in Section 7.6, will help predict the SED values under sustainable MPFs so that a fair comparison between the different SED values will be possible. It will then be possible to predict which set of operating conditions can lead to a stable long-term MBR operation, without serious membrane fouling problems, with the lowest SED values. MBR3 will be excluded as this MBR was never operated under sustainable net MPFs during the long-term experiment. Finally, it will also be checked whether these SED values are equal to or lower than the target value of 3 kWh m^{-3} .

7.6 MBR modelling

7.6.1 General information on the MBR modelling

Operation of the MBR systems was modelled with the aid of an Excel-based spreadsheet. This model was able to successfully calculate, combine, compare and finally predict each MBR system response with respect to the three following issues.

- **Mass balancing**

A mass balance around each MBR system was developed. The operating conditions, namely the HRTs and SRTs, together with the operating MBR volumes and the membrane areas were known. With the aid of the model, the sludge wasting rate, the feed flow rate, the corresponding real/net permeate flow rate and the real/net MPF could be estimated.

- **Kinetics/Stoichiometry of the aerobic biological oxidation**

The model was able to predict the best combinations of the three most important kinetic parameters, namely k (or μ_{\max}), k_d and K_S , as well as the stoichiometric parameter $Y_{X/S}$ value, all defined in Chapter 2. By estimating these values the model was calibrated and validated against the experimental data. Further calculations of MLSS/MLVSS concentrations and COD concentrations can be made. More details about the model calibration and validation are provided in Section 7.6.2.

- **Energy consumption rates and SED values**

The model can predict SED values over a range of HRTs, SRTs, MLSS concentrations, net permeate flow rates and their corresponding net MPFs. It was then used to see which sets of operating conditions led to SED values equal to or lower than 3 kWh m^{-3} . Also, to check whether these sets of operating conditions could lead to the production of treated permeate of the appropriate quality, and to ensure a stable long-term membrane performance.

7.6.2 Calibration/Validation of the MBR model

Before applying the MBR model to predict different SED values under different biological/membrane conditions, it has to be shown that the model is capable of providing reliable estimations. During the calibration of the model, the kinetic/stoichiometric parameters, whose values must also be in accordance with literature, *i.e.* [Tchobanoglous *et al.*, 2004], have to be estimated, as these values were not measured experimentally. During the validation of the model, the estimates of the kinetic/stoichiometric parameters were adjusted so that the model predictions correlated with the experimentally-measured MLSS and COD concentrations. Both calibration and validation happened at the same time and the process is as follows:

The HRT and the SRT values were known as both values were pre-selected operational parameters which were controlled during the long-term experiments. The biomass concentration, *i.e.* MLSS concentration and the influent/effluent COD concentration were also measured during the long-term experiments and average

values were calculated. Regarding the COD concentration in the feed, one average value representing the influent COD concentration for all MBR systems was estimated and was found to be 624 mg L^{-1} .

First, the kinetic/stoichiometric parameters were assumed from the literature, and the biomass concentration and the COD concentration both in the feed and in the permeate were calculated from the model. The parameters were then adjusted until the difference between the measured MLSS/Effluent COD concentration values and their corresponding estimated values was as small as possible. These kinetic/stoichiometric parameter values were selected to be the best-fit set with respect to the model calibration.

7.6.2.1 Calibration/Validation of the model for MBR1

Several combinations of kinetic/stoichiometric parameters were tested, until the difference between the measured and the predicted MLSS/Effluent COD concentration values was as small as possible. This process was based on a trial-and-error method until the best-fit kinetic/stoichiometric parameters were achieved. These parameters are shown in Table 7.26.

Table 7.26 MBR1: Estimation of best-fit kinetic/stoichiometric parameters

Parameter	Value	Unit
μ_{\max}	1.289	d^{-1}
k_d	0.15	d^{-1}
K_S	400	mg L^{-1}
$Y_{X/S}$	0.41	–

As seen in Table 7.26, the $Y_{X/S}$ -value was found to be of about 0.4, a value which is typical of extended SRT bioreactor designs like the pilot MBRs of this research.

Table 7.27 shows the selected operating times, the measured MLSS/Effluent COD concentration values, and their corresponding values as calculated with the aid of the model.

Table 7.27 MBR1: Validation of the model

a/a	Selected parameter		Measured parameter		Estimated Parameter	
	HRT (d)	SRT (d)	MLSS concentration (g L ⁻¹)	Effluent COD concentration (mg L ⁻¹)	MLSS concentration (g L ⁻¹)	Effluent COD concentration (mg L ⁻¹)
1	1.01	15	4.643	131.5	4.706	80.8
2	1.01	30	9.528	71.8	9.663	66.3
3	0.91	29	10.168	59.3	10.358	66.8
4	0.835	25.5	9.013	51.8	9.891	68.8
5	0.77	23.5	8.846	52.8	9.859	70.2
6	0.72	21.8	9.259	65	9.756	71.8

Figure 7.6 shows the measured and the estimated MLSS concentrations. In addition, Figure 7.7 shows the measured and the estimated COD concentrations, however, this time the first measurement of 131.5 mg L⁻¹ has not been into consideration, as it is already known that MBR1 at low MLSS concentrations failed to produce treated permeate of appropriate quality.

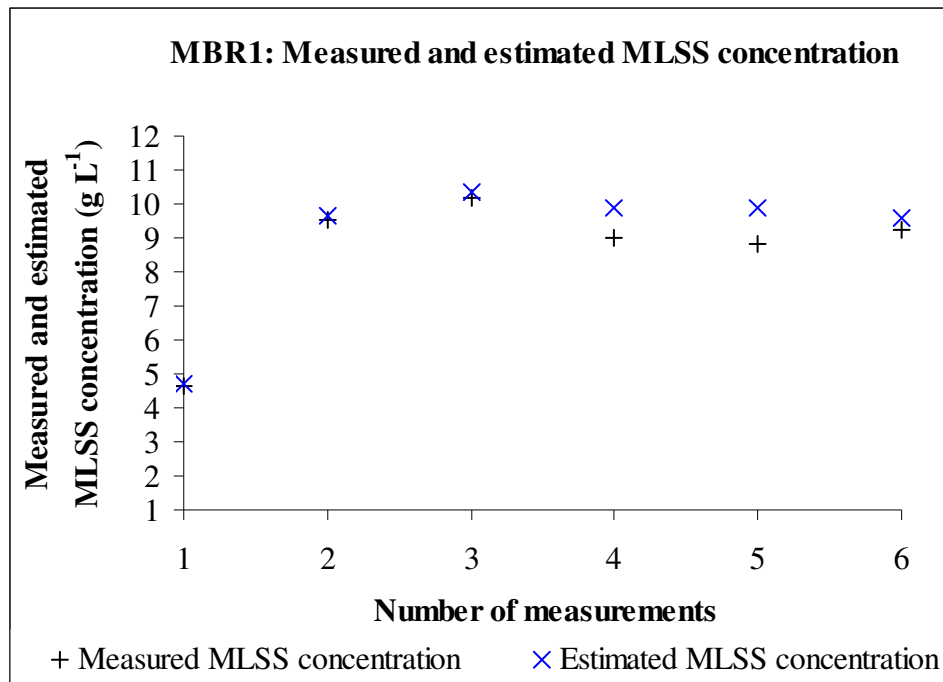


Figure 7.6 MBR1: Comparison between measured and estimated MLSS concentrations

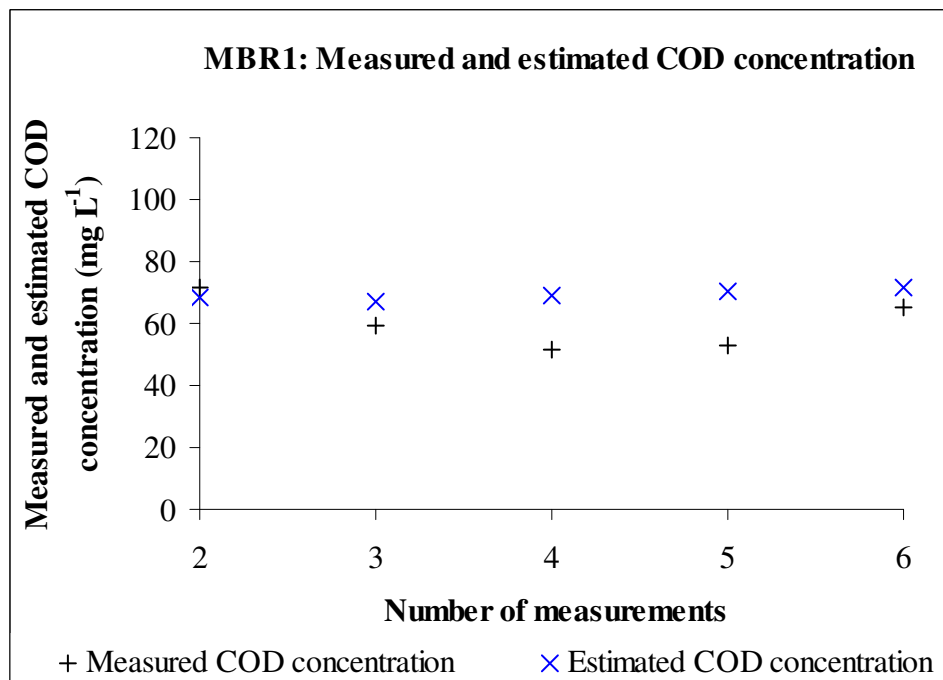


Figure 7.7 MBR1: Comparison between measured and estimated COD concentrations

Observing Table 7.26 and Figures 7.6 and 7.7, it can be said that the model was well-calibrated especially if it is taken into account that for WWT plants it is very typical

there to be fluctuation in the real influent COD concentration values making generic prediction difficult with a mathematical model.

7.6.2.2 Calibration/Validation of the model for MBR2

The following best-fit kinetic/stoichiometric parameters were found for MBR2 in the same way as for MBR1, and these are shown in Table 7.28. The values of the parameters were quite similar to those of MBR1.

Table 7.28 MBR2: Estimation of best-fit kinetic/stoichiometric parameters

Parameter	Value	Unit
μ_{\max}	1.289	d^{-1}
k_d	0.15	d^{-1}
K_s	350	mg L^{-1}
$Y_{X/S}$	0.41	–

Table 7.29 shows the selected operating conditions, the measured MLSS/Effluent COD concentrations, and the estimated MLSS/COD concentrations from the model.

Table 7.29 MBR2: Validation of the model

a/a	Selected parameter		Measured parameter		Estimated Parameter	
	HRT (d)	SRT (d)	MLSS concentration (g L^{-1})	Effluent COD concentration (mg L^{-1})	MLSS concentration (g L^{-1})	Effluent COD concentration (mg L^{-1})
1	1.01	15	4.592	65.7	4.794	70.7
2	1.01	30	9.687	61.5	9.807	58.2
3	0.91	29	9.206	55.2	10.514	58.4
4	0.835	25.5	9.379	52.5	10.044	60.2

Figure 7.8 shows the measured and the estimated MLSS concentrations and Figure 7.9 shows the measured and the estimated COD concentration values in the effluent.

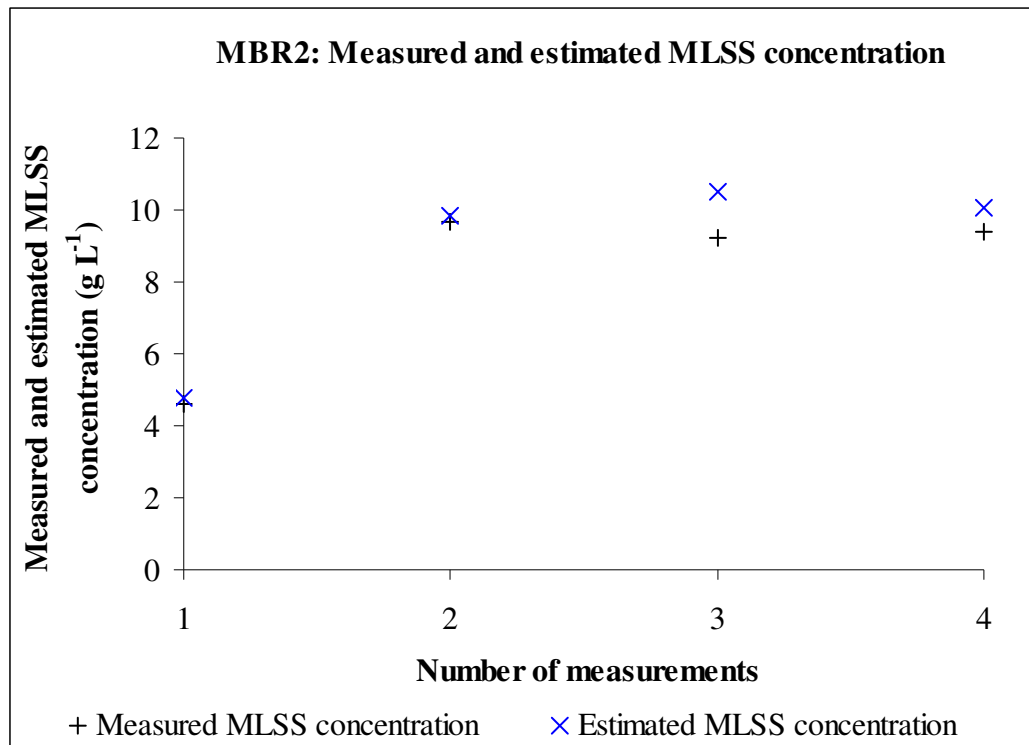


Figure 7.8 MBR2: Comparison between measured and estimated MLSS concentrations

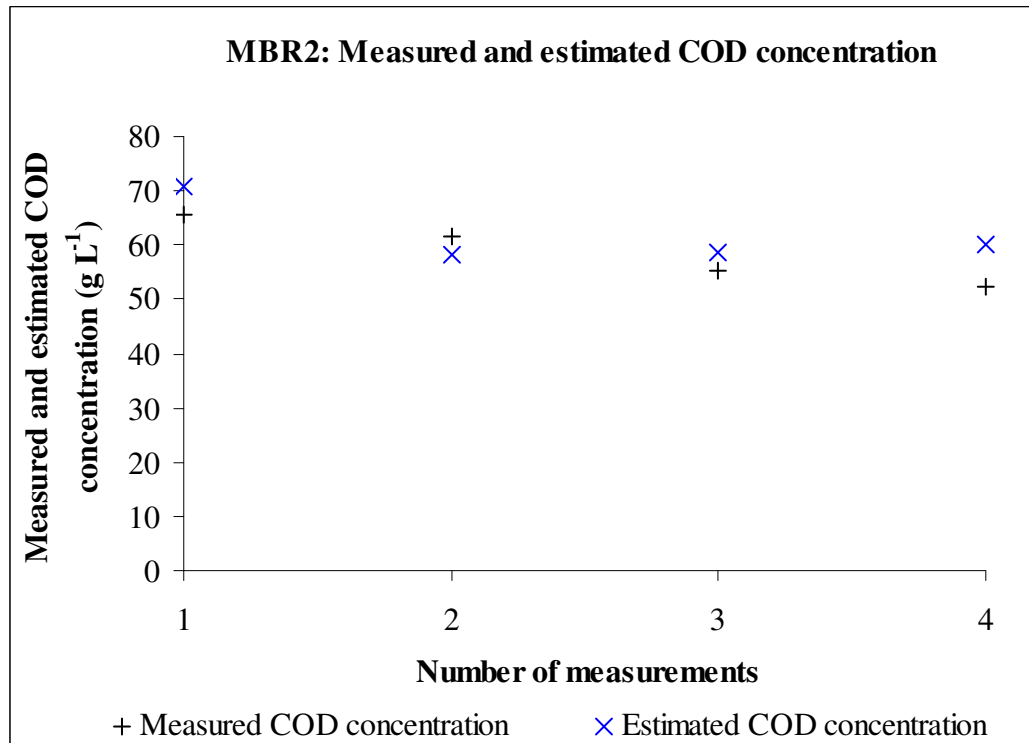


Figure 7.9 MBR2: Comparison between measured and estimated COD concentrations

Even though there is some small deviation between the measured and calculated MLSS/Effluent COD concentrations, it can be said that the model managed to predict reliable values.

7.6.2.3 Calibration/Validation of the model for MBR3

With respect to the MBR3 system, the following set of best-fit kinetic/stoichiometric parameters was estimated.

Table 7.30 MBR3: Estimation of best-fit kinetic/stoichiometric parameters

Parameter	Value	Unit
μ_{\max}	1.289	d^{-1}
k_d	0.15	d^{-1}
K_s	300	mg L^{-1}
$Y_{X/S}$	0.41	–

Table 7.31 provides a comparison between the measured and the calculated MLSS/Effluent COD concentrations.

Table 7.31 MBR3: Validation of the model

a/a	Selected parameter		Measured parameter		Estimated Parameter	
	HRT (d)	SRT (d)	MLSS concentration (g L^{-1})	Effluent COD concentration (mg L^{-1})	MLSS concentration (g L^{-1})	Effluent COD concentration (mg L^{-1})
1	1.01	15	4.033	83.8	4.881	60.6
2	1.01	30	9.151	69.3	9.95	49.7
3	0.91	29	8.793	44.4	10.669	50.1
4	0.835	25.5	8.53	60.4	10.197	51.6
5	0.77	12	5.043	49.9	5.070	66.3

Figure 7.10 shows the measured and estimated MLSS concentrations and Figure 7.11 shows the measured and estimated COD concentrations.

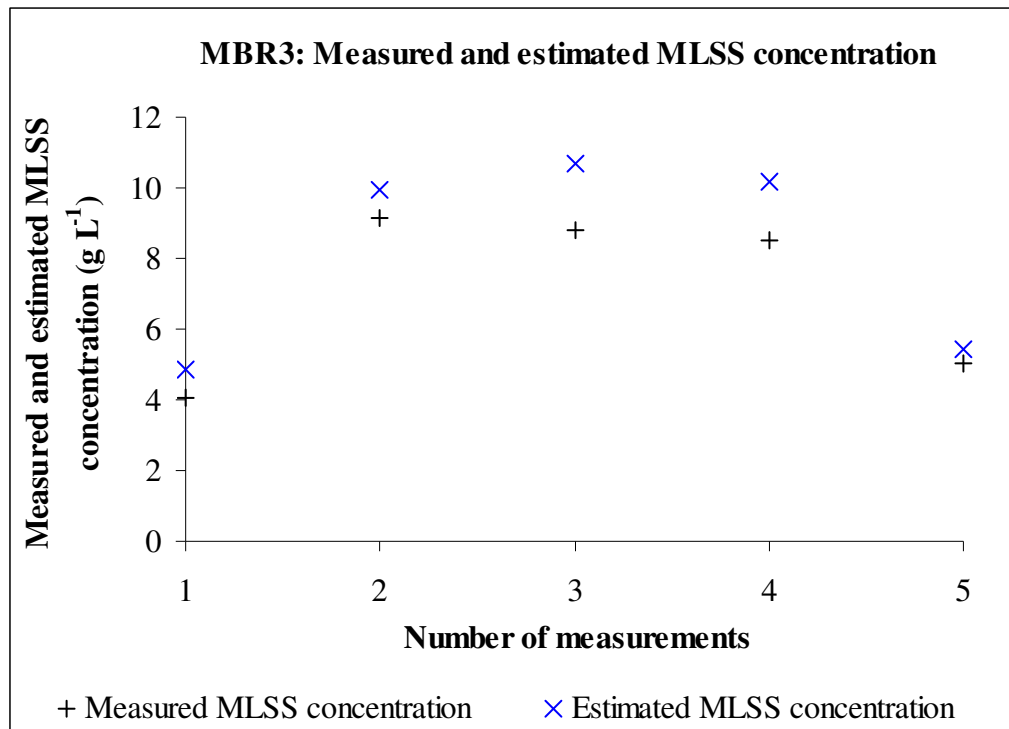


Figure 7.10 MBR3: Comparison between measured and estimated MLSS concentrations

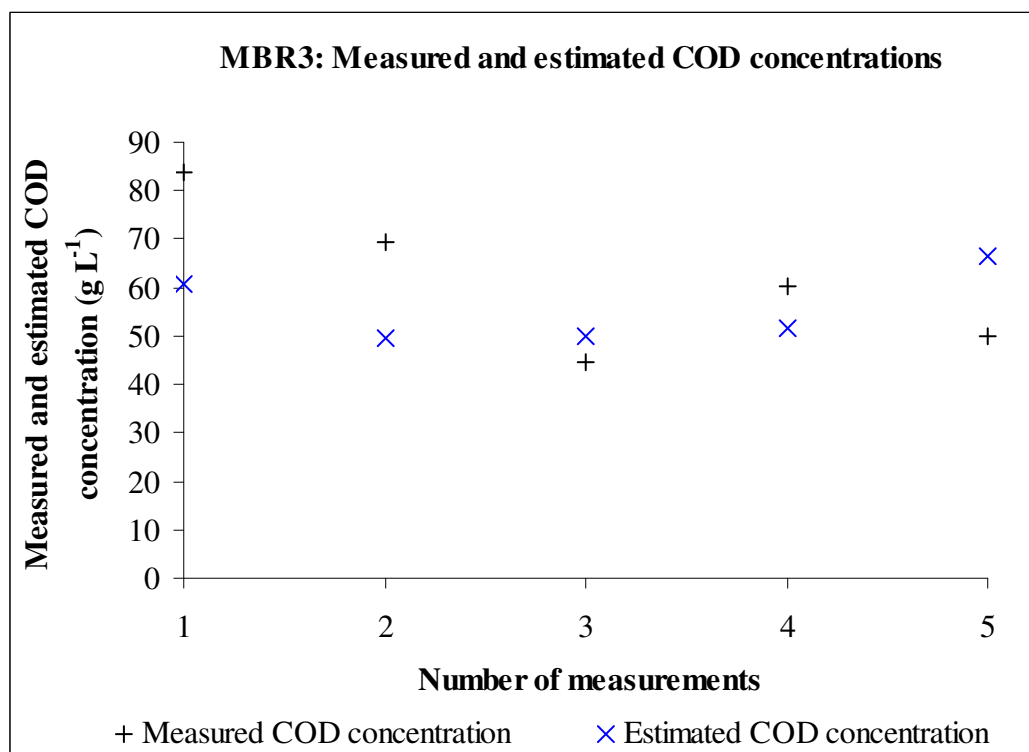


Figure 7.11 MBR3: Comparison between measured and estimated COD concentrations

The calibration/validation of the model with respect to the MBR3 system seems to be less accurate than for MBR1 and MBR2, however, a reasonable correlation between model and real data is achieved. Part of the reason for poorer model performance could be that MBR3 suffered frequent interruptions in operation in order to apply chemical cleaning. This could have had a knock-on effect with regard to the biological performance of this MBR system. Consequently, the remaining modelling effort will focus on MBR1 and MBR2.

7.6.2.4 Sample of the MBR model

A sample of the MBR model is shown in Table 7.32. Random operating conditions were chosen to be presented in this example as the model can be used under any set of SRTs/HRTs.

Table 7.32 MBR modelling sample

MBR MODELLING					
	SYMBOL	MBR1 VALUE	MBR2 VALUE	MBR3 VALUE	UNITS
1. PROCESS CALCULATIONS					
1.A. DIMENSIONS					
MBR1: AVERAGE LIQUID HEIGHT	L_{AVE-1}	2.43			m
MBR2-3: BIOLOGICAL TANK AVERAGE LIQUID HEIGHT	$L_{AVE-BIOL-2-3}$		1.07	1.36	m
MBR2-3: MEMBRANE TANK AVERAGE LIQUID HEIGHT	$L_{AVE-MEMB-2-3}$		1.07	1.45	m
CROSS-SECTIONAL AREA	A_{CS}	0.57	0.95	0.79	m ²
MBR2-3: BIOLOGICAL TANK VOLUME	V_{BT}		1.01	1.07	m ³
MBR2-3: MEMBRANE TANK VOLUME	V_{MT}		1.01	1.14	m ³
OVERALL OPERATIONAL VOLUME	V_{TOTAL}	1.38	2.02	2.21	m ³
1.B. FILTRATION					
FILTRATION	t_F	10.00	9.00	17.00	min
RELAXATION	t_R	0.00	1.00	3.00	min
UPTIME/(UPTIME+DOWNTIME)	a	1.00	0.90	0.85	–
1.C. MASS BALANCES					
SOLIDS RETENTION TIME (SRT)	θ_c	23.50	25.50	12.00	d
		564.00	612.00	288.00	h
SLUDGE WASTING RATE	Q_W	0.059	0.079	0.184	m ³ d ⁻¹
		2.44	3.30	7.66	L h ⁻¹
HYDRAULIC RESIDENCE TIME (HRT)	θ	0.770	0.835	0.770	d
		18.48	20.04	18.48	h
FEED FLOW RATE	Q_F	1.790	2.422	2.865	m ³ d ⁻¹
		74.58	100.91	119.36	L h ⁻¹
NET PERMEATE FLOW RATE	$Q_{P,NET}$	1.731	2.343	2.681	m ³ d ⁻¹
		72.13	97.61	111.70	L h ⁻¹
REAL PERMEATE FLOW RATE (SET-POINTS)	$Q_{P,REAL}$	1.20	1.63	1.86	L min ⁻¹
		1.73	2.60	3.15	m ³ d ⁻¹

		72.13	108.45	131.42	L h ⁻¹
		1.20	1.81	2.19	L min ⁻¹
MEMBRANE AREA	A _{MEMBRANE}	5.60	7.00	6.25	m ²
NET PERMEATE FLUX	J _{P,NET}	12.881	13.944	17.873	L m ⁻² h ⁻¹
REAL PERMEATE FLUX	J _{P,REAL}	12.881	15.493	21.027	L m ⁻² h ⁻¹
FEED TO PERMEATE CONVERSION	Q _{P,NET} /Q _F	0.967	0.967	0.936	–

1.D. AIR REQUIREMENT (MEMBRANE SCOURING ONLY)

AIR FLOW RATE	Q _{AIR}	4200	12000	7300	L h ⁻¹
		100.80	288.00	175.20	m ³ d ⁻¹
AERATION INTENSITY	Q _{AIR} /A	750	1714	1168	L m ⁻² h ⁻¹
AIR FLOW RATE/TREATED WATER FLOW RATE	Q _{AIR} /Q _{P, NET}	58.22	122.94	65.35	–

2. BIOLOGICAL CALCULATIONS**2.A. KINETIC/STOICHIOMETRY**

MAXIMUM SPECIFIC SUBSTRATE UTILISATION RATE (20 °C)	k ₂₀	3	3	3	d ⁻¹
		0.125	0.125	0.125	h ⁻¹
TEMPERATURE-ACTIVITY COEFFICIENT	C _θ	1.04	1.04	1.04	–
REFERENCE TEMPERATURE	T	20	20	20	°C
TEMPERATURE	T ₀	21.2	21.2	21.2	°C
MAXIMUM SPECIFIC SUBSTRATE UTILISATION RATE (T °C)	k _T	3.145	3.145	3.145	d ⁻¹
		0.1310	0.1310	0.1310	h ⁻¹
BIOMASS TO SUBSTRATE SYNTHESIS YIELD COEFFICIENT	Y _(X/S)	0.410	0.410	0.410	–
MAXIMUM SPECIFIC BACTERIAL GROWTH RATE	μ _{MAX}	1.289	1.289	1.289	d ⁻¹
		0.0537	0.0537	0.0537	h ⁻¹
SPECIFIC GROWTH RATE	μ	0.043	0.039	0.083	d ⁻¹
		0.0018	0.0016	0.0035	h ⁻¹
ENDOGENOUS DECAY COEFFICIENT	k _d	0.150	0.150	0.150	d ⁻¹
		0.0063	0.0063	0.0063	h ⁻¹
HALF-VELOCITY COEFFICIENT	K _S	400	350	300	mg L ⁻¹

2.B. OXYGEN TRANSFER

SATURATED DISSOLVED OXYGEN CONCENTRATION	O _{SAT}	9.8	9.8	9.8	mg L ⁻¹
LIQUID-PHASE MASS TRANSFER (O ₂ -to-WASTE H ₂ O) COEFFICIENT	k _L a	20	20	20	h ⁻¹
BIOMASS TO DISSOLVED OXYGEN YIELD COEFFICIENT	Y _(X/O)	0.5	0.5	0.5	–

3.C. BIOLOGICAL CHARACTERISTICS

FEED CHEMICAL OXYGEN DEMAND CONCENTRATION	S _F - COD _{IN}	624	624	624	mg L ⁻¹
PERMEATE CHEMICAL OXYGEN DEMAND CONCENTRATION	S - COD _{OUT}	70.23	60.20	66.29	mg L ⁻¹
MIXED LIQUOR VOLITILE SUSPENDED SOLIDS CONCENTRATION	X	6931	7061	3564	mg L ⁻¹
AVERAGE MLVSS OVER MLSS RATIO	(X/X _{MLSS}) _{AVE}	0.703	0.703	0.703	mg L ⁻¹
MIXED LIQUOR SUSPENDED SOLIDS CONCENTRATION	X _{MLSS}	9859	10044	5070	mg L ⁻¹
DISSOLVED OXYGEN CONCENTRATION	O	9.17	9.20	9.16	mg L ⁻¹
WASTE SLUDGE PRODUCTION	m _w	0.406	0.560	0.655	kg d ⁻¹
FOOD TO MICROORGANISM RATIO	F/M	0.0900	0.0884	0.1751	–
MASS FLOW RATE OF CHEMICAL OXYGEN DEAMAND REMOVAL	m _s	0.959	1.321	1.495	kg d ⁻¹
5-DAY BIOLOGICAL OXYGEN DEMAND REMOVAL	S _{REMOVED}	88.7	90.4	89.4	%

3. ENERGY CALCULATIONS**3.A. POWER-RELATED MEASUREMENTS****DISPLAY ELECTRICITY METERS****MAIN FEED PUMP**

POWER RATE	R_{MFP}	–	–	–	kW
OPERATING TIME	t_{MFP}	–	–	–	$h\ d^{-1}$
POWER CONSUMED	P_{MFP}	–	–	–	$kWh\ d^{-1}$
BASELINE					
POWER RATE	R_{BL}	0.0328	0.0167	–	kW
OPERATING TIME	t_{BL}	24	24	–	$h\ d^{-1}$
POWER CONSUMED	P_{BL}	0.787	0.401	–	$kWh\ d^{-1}$
FEED PUMPS					
POWER RATE	R_{FP}	0.9747	0.2315	–	kW
OPERATING TIME	t_{FP}	0.36	0.30	–	$h\ d^{-1}$
POWER CONSUMED	P_{FP}	0.349	0.070	–	$kWh\ d^{-1}$
AIR BLOWERS FOR BIOLOGICAL MAINTENANCE					
POWER RATE	R_{BM}	0.0000	0.0886	–	kW
OPERATING TIME	t_{BM}	24	12	–	$h\ d^{-1}$
POWER CONSUMED	P_{BM}	0.0000	1.063	–	$kWh\ d^{-1}$
AIR BLOWERS FOR MEMBRANE CLEANING					
POWER RATE	R_{MC}	0.3378	0.1752	–	kW
OPERATING TIME	t_{MC}	24	24	–	$h\ d^{-1}$
POWER CONSUMED	P_{MC}	8.107	4.205	–	$kWh\ d^{-1}$
FILTRATION PUMPS					
POWER RATE	R_{PSP}	–	0.1088	–	kW
OPERATING TIME	t_{PSP}	–	21.6	–	$h\ d^{-1}$
POWER CONSUMED	P_{PSP}	–	2.350	–	$kWh\ d^{-1}$
RECIRCULATION PUMPS					
POWER RATE	R_{PSP}	–	0.1668	–	kW
OPERATING TIME	t_{PSP}	–	4	–	$h\ d^{-1}$
POWER CONSUMED	P_{PSP}	–	0.667	–	$kWh\ d^{-1}$
ALL COMPONENTS					
POWER CONSUMED	P_{AC}	9.243	8.756	–	$kWh\ d^{-1}$
SPECIFIC ENERGY DEMAND	$W_{B,V}$	5.339	3.738	–	$kWh\ m^{-3}$
3.B. ENERGY-RELATED MEASUREMENTS					
3.B.1. DISPLAY ELECTRICITY METERS					
POWER CONSUMED	P_{AC}	9.225	9.134	–	$kWh\ d^{-1}$
SPECIFIC ENERGY DEMAND	$W_{B,V}$	5.329	3.899	–	$kWh\ m^{-3}$
3.B. METERS WITH ROTATING COUNTERS					
POWER CONSUMED	P_{AC}	9.477	9.082	–	$kWh\ d^{-1}$
SPECIFIC ENERGY DEMAND	$W_{B,V}$	5.474	3.877	–	$kWh\ m^{-3}$
3.C. PERCENTAGES					
BASELINE		8.5	4.6	–	%
FEED PUMPS		3.8	0.8	–	%
RECIRCULATION PUMPS		0.0	7.6	–	%
FILTRATION PUMPS		0.0	26.8	–	%
AIR BLOWERS: BIOLOGY		0.0	12.1	–	%
AIR BLOWERS: BIOLOGY + MEMBRANES		87.7	48.0	–	%
TOTAL		100.0	100.0	–	%
BASELINE		8.5	4.6	–	%
LIQUID PUMPING		3.8	35.3	–	%
AERATION		87.7	60.2	–	%
TOTAL		100.0	100.0	–	%

7.6.3 Application of MBR model: SED predictions

The aim of this section is to predict the SED values under different sets of operating conditions, and to show how the measured SED values alter when a new set of operating conditions is applied. Initially, the effect of SRTs/HRTs on the SED values will be explored, and then the linkage between MLSS concentrations and SED values will be investigated. Data relating to SRTs, HRTs, MLSS concentrations and net MPFs will be combined and SED values will be calculated to check whether the target SED value can be achieved. At the same time, it will be checked whether these SED values can lead to a stable long-term membrane performance and whether they are capable of producing treated permeate of the appropriate quality. Finally, an attempt to improve the SED values of MBR1 system will be made as it is known that the components of this MBR system can be successfully replaced by less energy-consuming devices - more details are available in Section 7.6.3.3. The MBR3 system will not be taken into account as it was never operated under sustainable net MPFs during the long-term experiments. A mixed-liquor temperature was selected as 21.2 °C and the gassing rates that were applied were those that were suggested by the membrane suppliers. This operating temperature is conservative as for most of the time the MBRs were operating at higher temperatures, and hence the mixed-liquor in the MBRs would be at a lower viscosity. The lower viscosity would lead to lower potential for membrane fouling, and thence to higher values of sustainable MPFs.

7.6.3.1 Prediction of SED values for MBR1

A range of HRTs - from 0.4 d to 1.1 d - were tested, coupled with two different SRTs, 15 d and 30 d. Table 7.33, which shows the effect of the different MPFs on the SED values is constructed, and then Figure 7.12 is plotted.

Table 7.33 MBR1: A combination of SRTs, HRTs, net MPFs and their corresponding SED values

HRT (d)	SRT: 15 d		SRT: 30 d	
	Net MPF (L m ⁻² h ⁻¹)	SED value (kWh m ⁻³)	Net MPF (L m ⁻² h ⁻¹)	SED value (kWh m ⁻³)
0.4	24.95	2.852	25.29	2.814
0.5	19.83	3.54	20.17	3.48
0.6	16.41	4.237	16.75	4.15
0.7	13.97	4.943	14.31	4.825
0.8	12.13	5.66	12.48	5.505
0.9	10.71	6.386	11.05	6.189
1	9.57	7.123	9.91	6.878
1.1	8.37	7.871	8.98	7.572

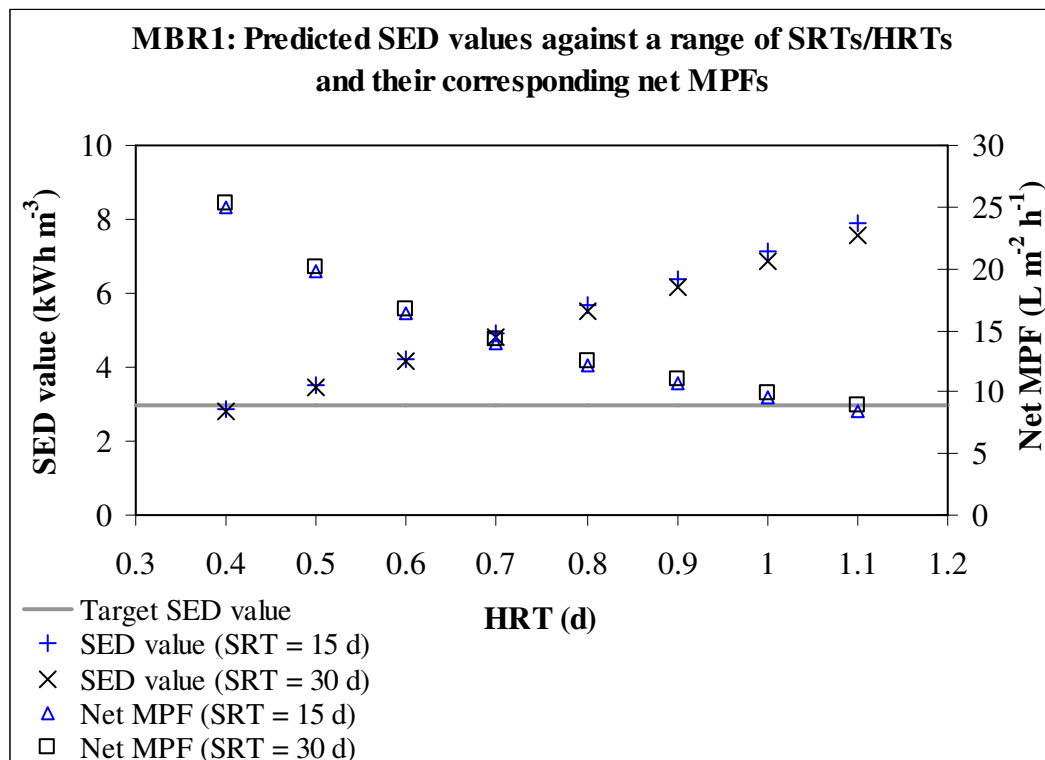


Figure 7.12 MBR1: Effect of net MPFs on the SED values

As can be seen from Figure 7.12, the change of the SRTs did not significantly affect the SED values as similar values were predicted when the SRT was equal to 15 d and

30 d. As the quality of the treated permeate improves at longer SRTs, these are more preferable. Longer SRTs lead to higher MLSS concentrations, which can generally provide treated water of better quality. However, the increase in the SRTs is limited by the membrane performance as the higher MLSS concentrations within the MBRs can lead to membrane fouling formation.

On the other hand, variation in HRTs can significantly and more seriously affect the SED values. For a fixed SRT, an increase in the HRT is followed by a significant increase in the SED values. This is due to the fact that if an increase in the HRT occurs, a decrease in the net MPF takes place. Consequently, less treated water is produced and the SED values will increase. SED values and net MPFs are inversely proportional variables.

The effect of the MLSS concentrations on the SED values is shown both in Table 7.34 and in Figure 7.13.

Table 7.34 MBR1: A combination of SRTs, HRTs, MLSS concentrations and their corresponding SED values

HRT (d)	SRT: 15 d		SRT: 30 d	
	MLSS concentration (g L ⁻¹)	SED value (kWh m ⁻³)	MLSS concentration (g L ⁻¹)	SED value (kWh m ⁻³)
0.4	11.883	2.852	24.399	2.814
0.5	9.506	3.54	19.519	3.48
0.6	7.922	4.237	16.266	4.15
0.7	6.79	4.943	13.942	4.825
0.8	5.941	5.66	12.2	5.505
0.9	5.281	6.386	10.844	6.189
1	4.753	7.123	9.76	6.878
1.1	4.321	7.871	8.872	7.572

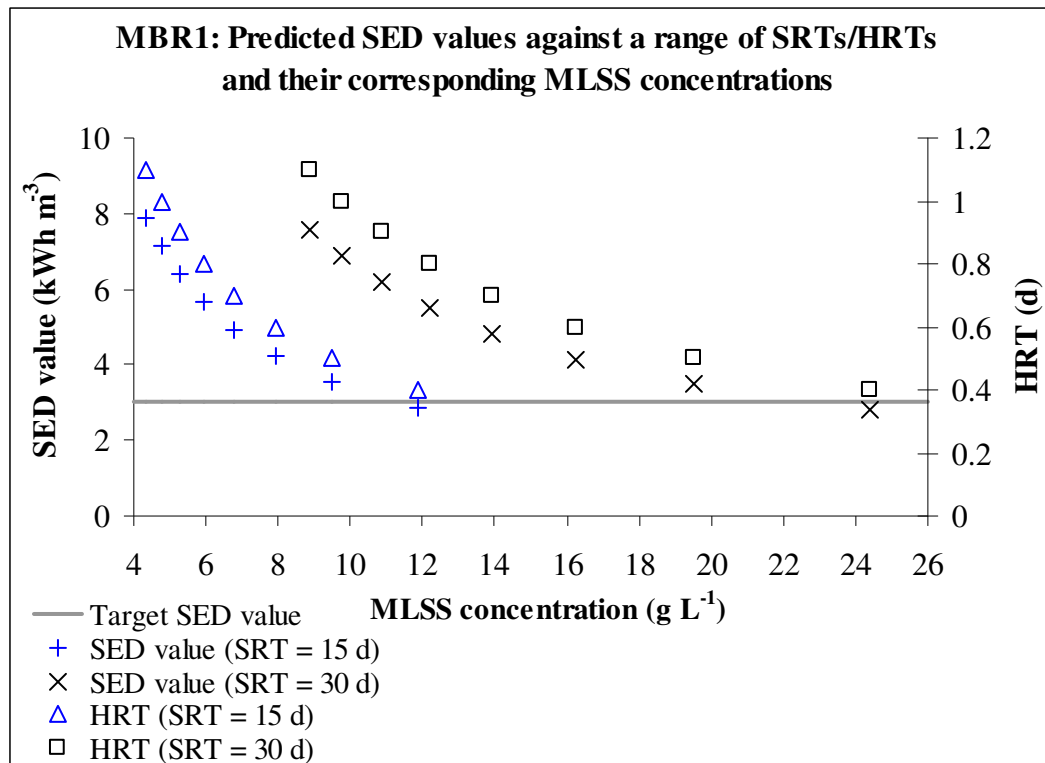


Figure 7.13 MBR1: Effect of MLSS concentrations on the SED values

As seen in Figure 7.13, when the MLSS concentrations increase the SED values decrease. This makes sense as higher MLSS concentrations correspond to shorter HRTs, and shorter HRTs provide lower SED values.

Figure 7.14 shows the combined effect of the net MPFs and the MLSS concentrations on the SED values.

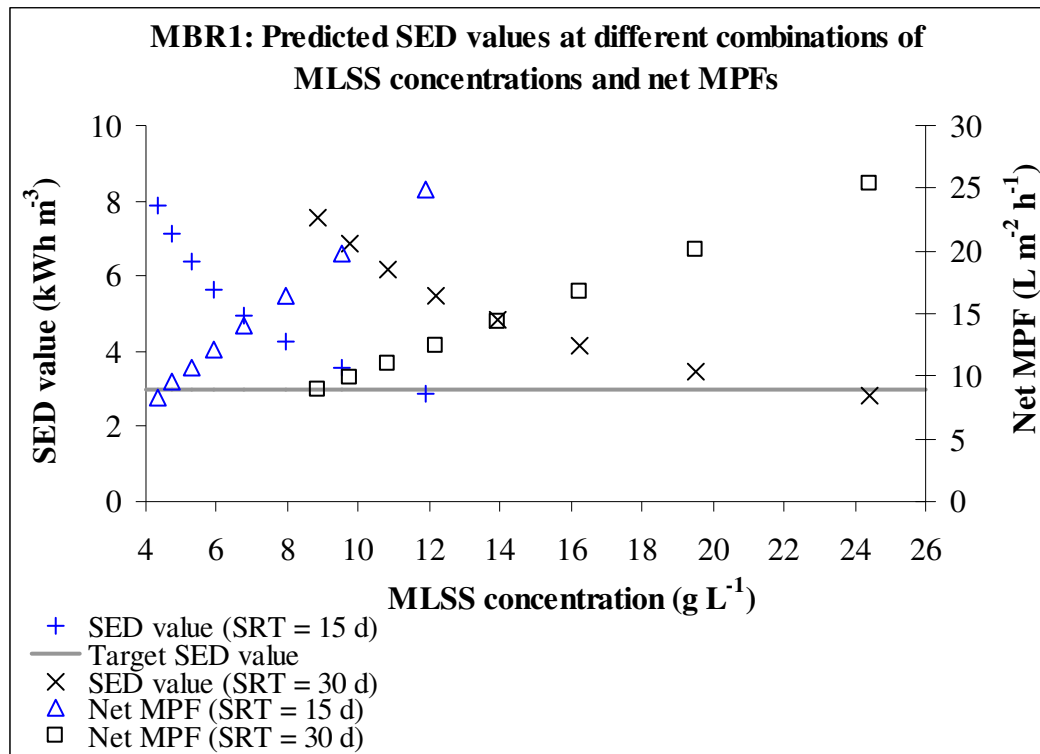


Figure 7.14 MBR1: Effect of MLSS concentrations and net MPFs on the SED values

From Figure 7.14 it can be seen that for both of the SRTs tested, only a very short HRT (0.4 d) provided SED values lower than 3 kWh m⁻³. For an SRT equal to 15 d MBR1 failed to produce treated water of appropriate quality during the pilot trials. In this case the model predicts that treated permeate of the appropriate quality can be produced as the estimated effluent COD value was found to be equal to 80.8 mg L⁻¹. This simply reflects the fact that the model is not perfect.

On the other hand, for an SRT of 30 d, treated permeate of the appropriate quality could be produced. However, for a SED value equal to or lower than 3 kWh m⁻³, the corresponding net MPF has to be 25.29 L m⁻² h⁻¹ or higher at an MLSS concentration of 24.399 g L⁻¹. This combination leads to membrane fouling and an unstable membrane performance as explained in Chapter 5, where it was concluded that combinations of even lower MLSS concentrations and even longer HRTs did finally lead to exponential TMP increase.

Finally, by taking into account the membrane performance as described in Section 6.3, the maximum average sustainable net MPF that was predicted for the MBR1 system was $13.77 \text{ L m}^{-2} \text{ h}^{-1}$ at an average MLSS concentration of 9.26 g L^{-1} . For this net MPF, the model predicted an MLSS concentration of 9.756 g L^{-1} and a SED value of 5.007 kWh m^{-3} , which is higher than the target SED value. To conclude, the model predicts that MBR1 was not able to produce treated permeate of the appropriate quality, at a stable membrane performance, and at SED values around 5.007 kWh m^{-3} or lower. This means that the target SED value was not achieved under the conditions tested.

7.6.3.2 Prediction of SED values for MBR2

A range of HRTs ranging from 0.4 d to 1.1 d were tested, coupled with SRTs of 15 d and 45 d. Table 7.35 shows the effect of the net MPFs on the SED values and Figure 7.15 is plotted. Treated permeate of the appropriate quality was always produced regardless of the SRT that was applied.

Table 7.35 MBR2: A combination of SRTs, HRTs, net MPFs and their corresponding SED values

HRT (d)	SRT: 15 d		SRT: 30 d	
	Net MPF ($\text{L m}^{-2} \text{ h}^{-1}$)	SED value (kWh m^{-3})	Net MPF ($\text{L m}^{-2} \text{ h}^{-1}$)	SED value (kWh m^{-3})
0.4	29.29	1.846	29.69	1.823
0.5	23.27	2.292	23.67	2.255
0.6	19.26	2.743	19.66	2.689
0.7	16.39	3.201	16.8	3.127
0.8	14.24	3.666	14.65	3.568
0.9	12.57	4.137	12.97	4.012
1	11.24	4.614	11.64	4.458
1.1	10.47	5.099	10.54	4.908

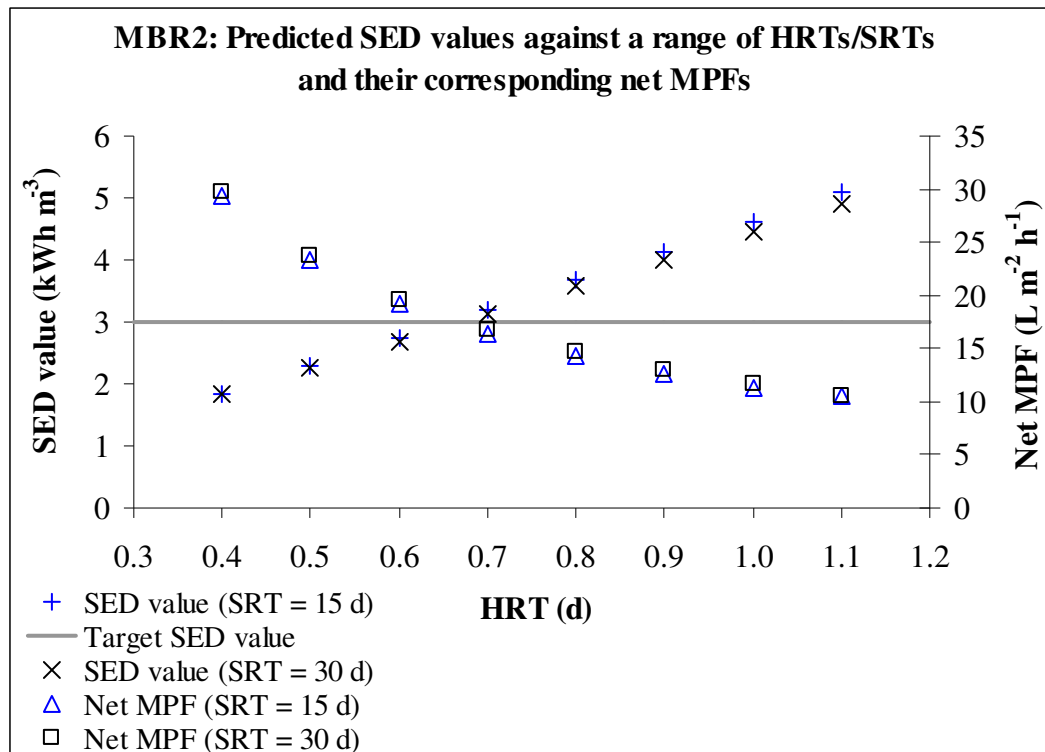


Figure 7.15 MBR2: Effect of net MPFs on the SED values

As expected, the SRT changes did not affect the SED values significantly - also the shorter the HRT, the lower the SED value. As seen in Figure 7.15, for both SRTs, the less HRT of 0.6 d reduced the SED value to below the target value of 3 kWh m⁻³. However, it can be seen that the corresponding net MPFs, namely 19.26 L m⁻² h⁻¹ for an SRT of 15 d and 19.66 L m⁻² h⁻¹ for an SRT of 30d, were quite high, so they may well not be sustainable conditions. However, it is the combined effect of the net MPFs and the MLSS concentrations that will show whether it is possible to operate at these net MPFs or not.

The effect of the MLSS concentrations on the SED values is shown in Table 7.36 and in Figure 7.16.

Table 7.36 MBR2: A combination of SRTs, HRTs, MLSS concentrations and their corresponding SED values

HRT (d)	SRT: 15 d		SRT: 30 d	
	MLSS concentration (g L ⁻¹)	SED value (kWh m ⁻³)	MLSS concentration (g L ⁻¹)	SED value (kWh m ⁻³)
0.4	12.224	1.846	25.077	1.823
0.5	9.799	2.292	20.061	2.255
0.6	8.149	2.743	16.718	2.689
0.7	6.985	3.201	14.329	3.127
0.8	6.112	3.666	12.538	3.568
0.9	5.433	4.137	11.145	4.012
1	4.89	4.614	10.031	4.458
1.1	4.445	5.099	9.119	4.908

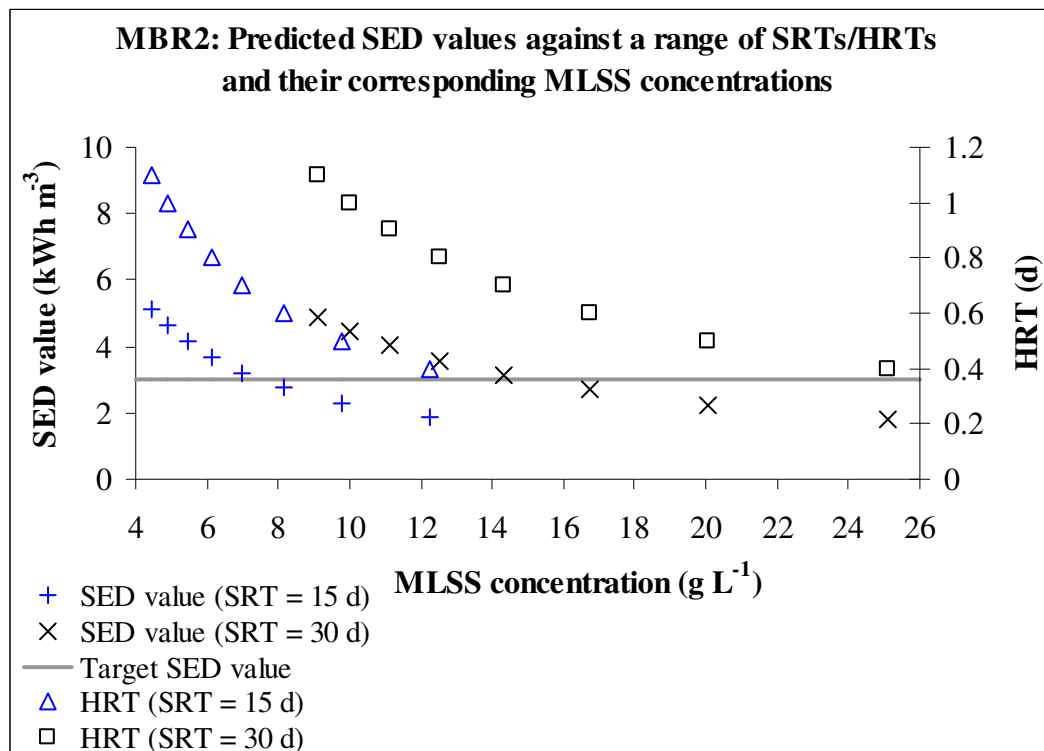


Figure 7.16 MBR2: Effect of MLSS concentrations on the SED values

The model predicts that for an SRT of 15 d and a HRT of 0.6 d, the estimated MLSS concentration was 8.149 g L⁻¹. On the other hand, for an SRT of 30 d and a HRT of

0.6 d, it predicts an MLSS concentration of 16.718 g L^{-1} . As explained in Chapter 5, both MLSS concentration values can produce treated permeate of the appropriate quality, so it is the lower MLSS concentration that is preferable as lower MLSS concentrations are more likely to lead to stable long-term membrane performance. However, as already mentioned, it is the combined effect of the net MPFs and the MLSS concentrations that indicates whether it is possible to operate at these MLSS concentrations or not.

Figure 7.17 shows the combined effect of the net MPFs and the MLSS concentrations.

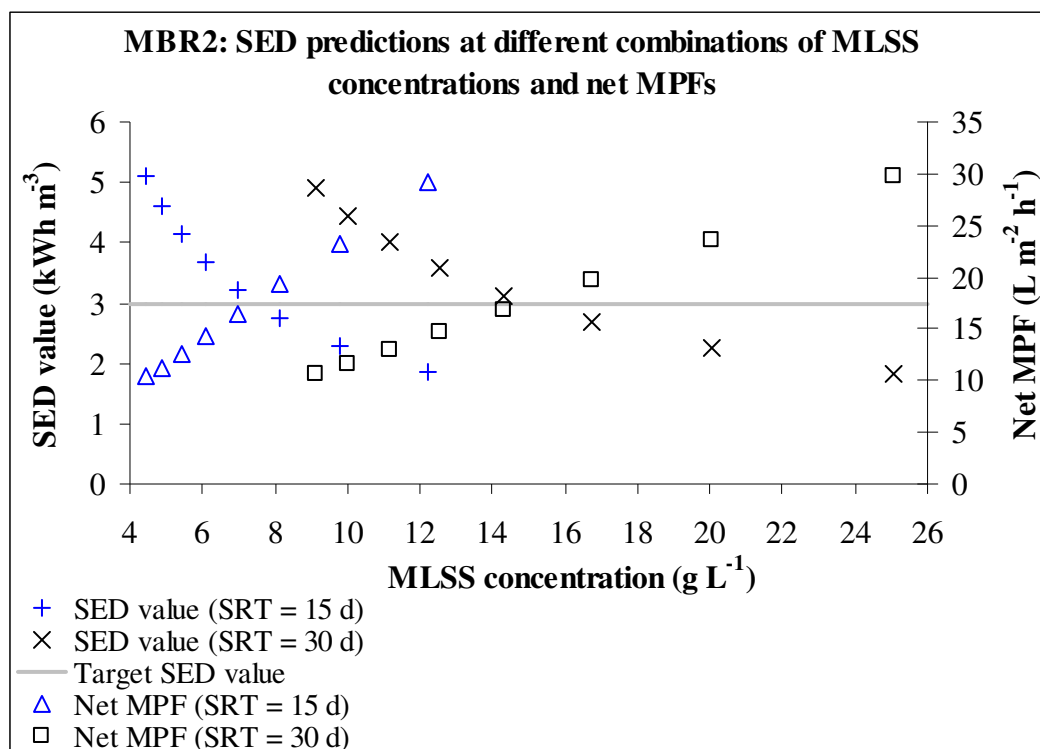


Figure 7.17 MBR2: Effect of MLSS concentrations and net MPFs on the SED values

As seen in Figure 7.17, when the SRT was set to 15 d and the HRT was set to 0.6 d, a SED value lower than 3 kWh m^{-3} was achieved. This set of operating conditions simultaneously led to a net MPF of $19.26 \text{ L m}^{-2} \text{ h}^{-1}$, and an MLSS concentration of 8.149 g L^{-1} . As the MLSS concentration is in the range of $9 - 10 \text{ g L}^{-1}$, it has already been known that this net MPF is unable to lead to a stable long-term membrane performance. During the pilot trials, the maximum average sustainable net MPF was

equal to $12.81 \text{ L m}^{-2} \text{ h}^{-1}$ at an MLSS concentration equal to 9.379 g L^{-1} - see Section 6.4.

When the SRT was set to 30 d and the HRT was set to 0.6 d, the SED value was again below 3 kWh m^{-3} . The corresponding net MPF was $19.66 \text{ L m}^{-2} \text{ h}^{-1}$ at an elevated MLSS concentration of 16.718 g L^{-1} . This combination can lead to quick exponential TMP increase and severe membrane fouling, and is therefore not feasible.

Finally, by taking into account the membrane performance, the maximum average sustainable net MPF that was predicted for the MBR2 system was $12.81 \text{ L m}^{-2} \text{ h}^{-1}$ at an average MLSS concentration of 9.206 g L^{-1} . For this net MPF, the model predicted a SED value of 4.06 kWh m^{-3} , which is higher than the target SED value, but it is lower than the value predicted for the MBR1 system.

To conclude, MBR2 did not succeed in producing treated permeate of the appropriate quality, at a stable membrane performance, at SED values lower than 4.06 kWh m^{-3} , which means that the target SED value was not achieved. However, as treated permeate could be produced at both low and high MLSS concentrations, it is better to operate this MBR at low MLSS concentrations ($4 - 5 \text{ g L}^{-1}$). This is consistent with the supplier of MBR2 who indicated that this system should not be operated at MLSS concentrations higher than 12 g L^{-1} .

7.6.3.3 Prediction of SED values for a modified MBR1

A theoretical attempt to modify MBR1 by replacing the oversized Feed Pump 1 and the oversized air compressor with less energy-consuming devices is made. Feed Pump 1 could be successfully replaced by Feed Pump 2. Feed Pump 2 had a fixed flow rate equal to $8 \text{ m}^3 \text{ h}^{-1}$, whereas Feed Pump 1 had a fixed flow rate equal to $5 \text{ m}^3 \text{ h}^{-1}$. Additionally, the average consumption of Feed Pump 2 was found to be 231.5 W , whereas the average consumption rate of Feed Pump 1 was found to be 1007.5 W . This is a significant difference, so, by making this replacement, the amount of energy consumed by the MBR1 system will be significantly reduced. In addition, the fact that Feed Pump 2 had a higher fixed flow rate means that after the replacement the

runtime of the device will also be reduced, hence energy demand will be further reduced.

It is also known that the air compressor of the MBR1 system was not a cost-effective device. Air blowers operated by the MBR2 system were less energy-consuming than the MBR1 air blower, however, this time a direct replacement could not be made. During the long-term experiment, the MBR1 air blower was replaced by one of the MBR2 air blowers, but it could not maintain the required air flow rate of 4,200 L h⁻¹. This was due to the fact that the liquid level above the diffuser within the MBR1 tank was higher than that within the MBR2, and the MBR2 blower could not work against the additional hydraulic head. However, the supplier of the MBR2 blower can provide a slightly more powerful model: Model No DBMX100, which can provide the required air flow rate of 4,200 L h⁻¹ under these conditions, [www.airmac.com.tw, 2010]. The average energy rate if the new blower would be 188.6 W, significantly lower than for the original MBR1 blower.

By using the model, SED values can now be predicted for the modified version of MBR1. Table 7.37 shows the effect of the MPFs on the SED values and Table 7.38 shows the effect of the MLSS concentrations on the SED values.

Table 7.37 Modified MBR1: A combination of SRTs, HRTs, net MPFs and their corresponding SED values

HRT (d)	SRT: 15 d		SRT: 30 d	
	Net MPF (L m ⁻² h ⁻¹)	SED value (kWh m ⁻³)	Net MPF (L m ⁻² h ⁻¹)	SED value (kWh m ⁻³)
0.4	24.95	1.379	25.29	1.361
0.5	19.83	1.729	20.17	1.699
0.6	16.41	2.083	16.75	2.04
0.7	13.97	2.442	14.31	2.384
0.8	12.13	2.806	12.48	2.729
0.9	10.71	3.175	11.05	3.077
1	9.57	3.55	9.91	3.427
1.1	8.64	3.93	8.98	3.78

Table 7.38 Modified MBR1:A combination of SRTs, HRTs, MLSS concentrations and their corresponding SED values

HRT (d)	SRT: 15 d		SRT: 30 d	
	MLSS concentration (g L ⁻¹)	SED value (kWh m ⁻³)	MLSS concentration (g L ⁻¹)	SED value (kWh m ⁻³)
0.4	11.883	1.379	24.399	1.361
0.5	9.506	1.729	19.519	1.699
0.6	7.922	2.083	16.266	2.04
0.7	6.79	2.442	13.942	2.384
0.8	5.941	2.806	12.2	2.729
0.9	5.281	3.175	10.844	3.077
1	4.753	3.55	9.76	3.427
1.1	4.321	3.93	8.972	3.78

Based on Tables 7.35 and 7.36, Figure 7.18 shows the effect of the net MPFs on the SED values and Figure 7.19 shows the effect of the MLSS concentrations on the SED values. Figure 7.20 shows the combined effect of the net MPFs and the MLSS concentrations.

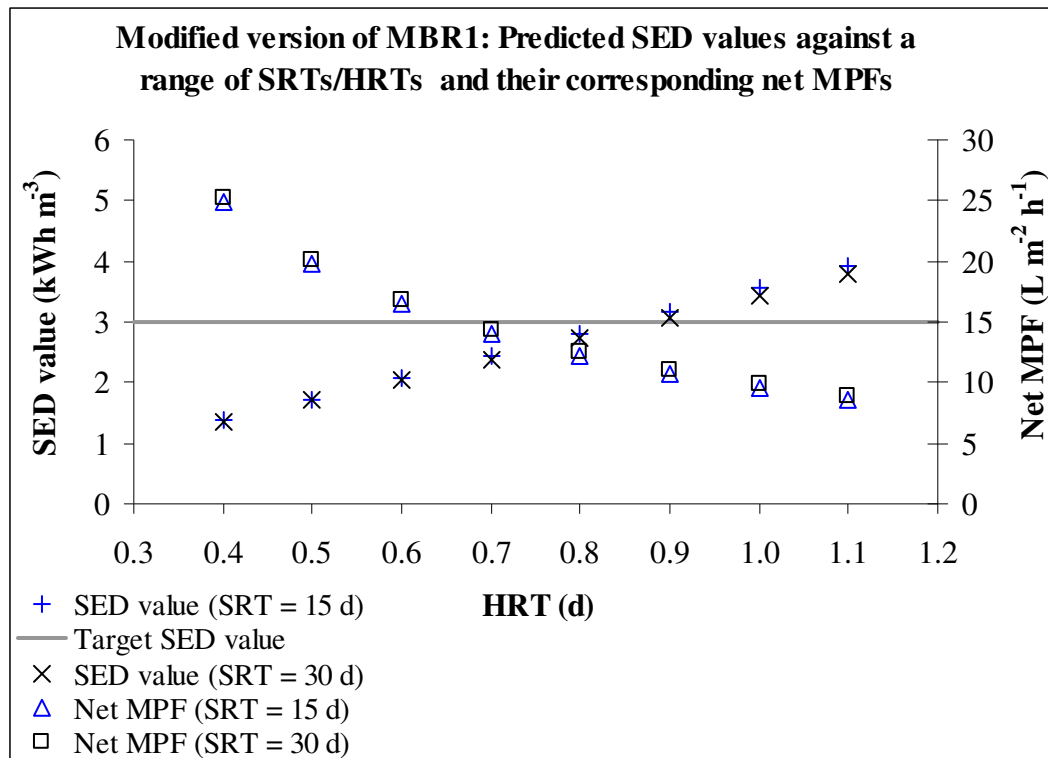


Figure 7.18 Modified MBR1: Effect of net MPFs on the SED values

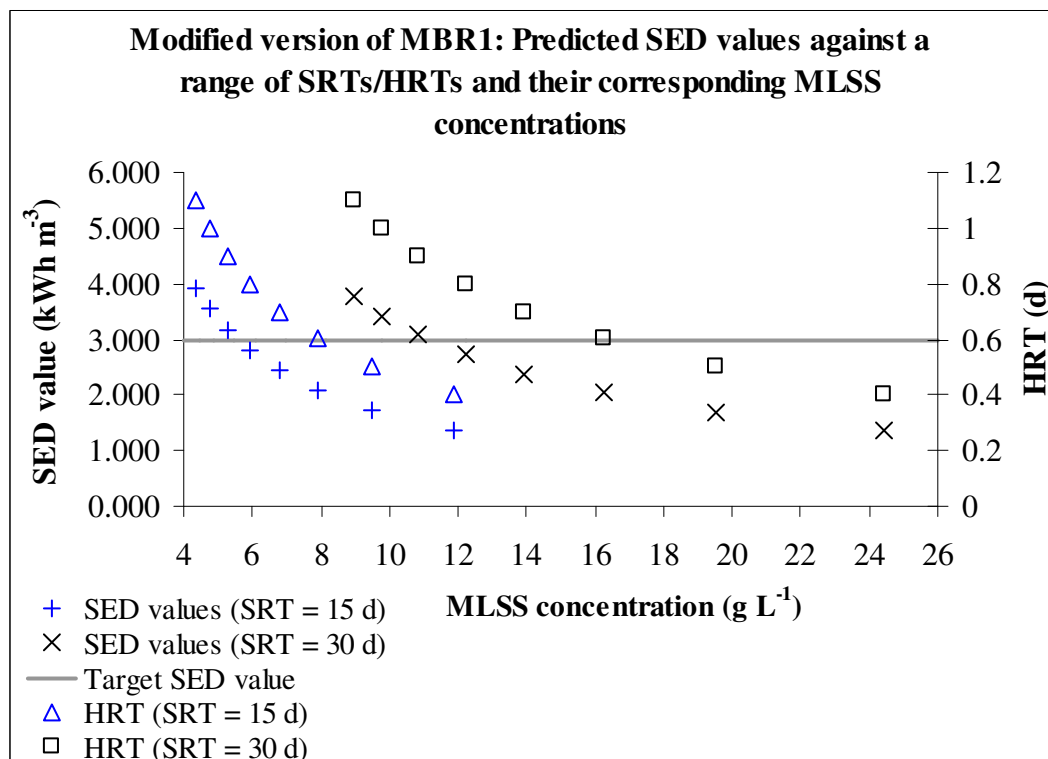


Figure 7.19 Modified MBR1: Effect of MLSS concentrations on the SED values

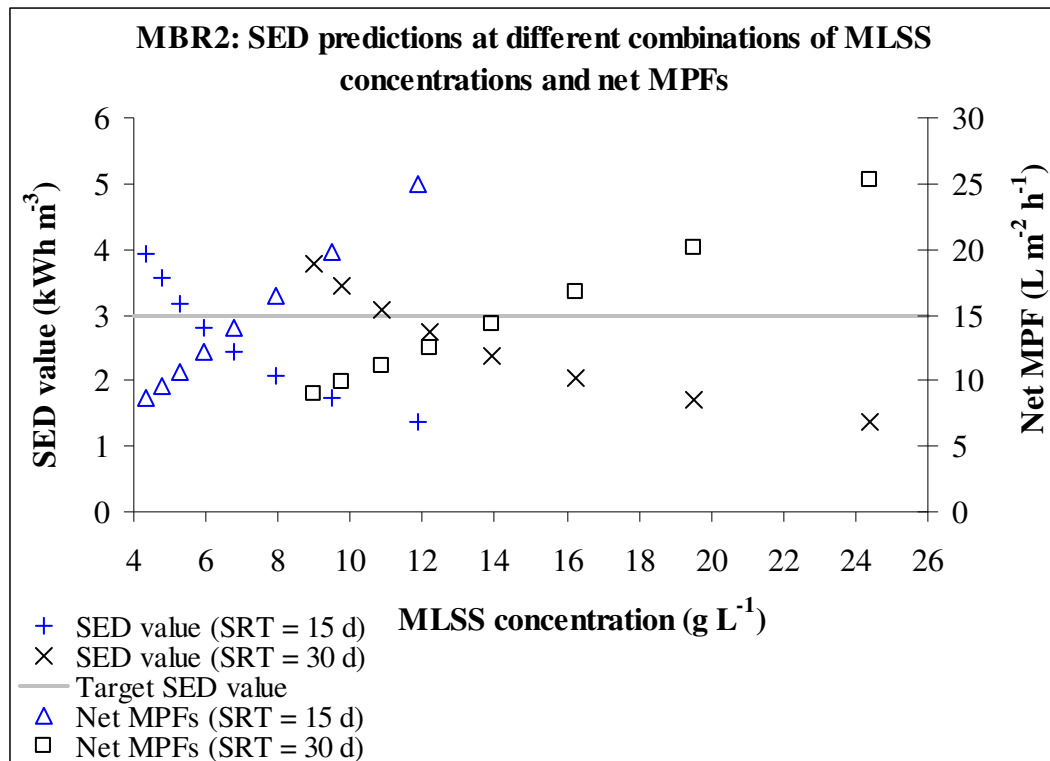


Figure 7.20 Modified MBR1: Effect of MLSS concentrations and net MPFs on the SED values

As seen in Figures 7.18, 7.19 and 7.20, when the SRT was set to 15 d, all HRTs lower than 0.9 d succeeded in reducing the SED values to below the target value. However, we know from the pilot trials that as long as the MLSS concentrations are in the range of 4 - 5 g L^{-1} , treated permeate cannot be produced. For very short HRTs, *i.e.* 0.5 d, the MLSS concentration increased to a value of 9.506 g L^{-1} , which can produce treated permeate of the appropriate quality. However, the corresponding net MPF of 19.83 $\text{L m}^{-2} \text{h}^{-1}$ is an unsustainable condition, which means that membrane performance is likely to be unstable. In general, sets of operating conditions consisting of an SRT equal to 15 d and HRTs, which range from 0.4 d to 1.1 d, did not succeed in achieving the objectives of this research.

When the SRT was set to 30 d and the HRT was set to 0.8 d, the model predicts a SED value of 2.729 kWh m^{-3} , which is below the target value. The corresponding net MPF was 12.48 $\text{L m}^{-2} \text{h}^{-1}$ and the MLSS concentration was 12.2 g, (mixed-liquor temperature: 21.2 $^{\circ}\text{C}$ and gassing rate within the MBR tank: 4,200 L h^{-1}). Based on the pilot trial data described in Section 6.3, this set of operating conditions is able to

produce treated permeate of the appropriate quality as well as being very likely to lead to a stable long-term MBR operation.

Finally, it is worth using the model to predict the exact HRT that provides a SED value equal to 3 kWh m^{-3} assuming that the SRT is set to 30 d. This set of operating conditions may provide the best combination with respect to net MPF and MLSS concentration. These parameters, as predicted by the model, are summarised in Table 7.39.

Table 7.39 Modified MBR1: Best-fit operating conditions regarding the objectives of this work

Parameter	Value	Unit
SRT	30	d
HRT	0.878	d
Net MPF	11.34	$\text{L m}^{-2} \text{ h}^{-1}$
Average MLSS concentration	11.116	g L^{-1}
COD concentration in the effluent	66.31	mg L^{-1}
Average mixed-liquor temperature	21.2	$^{\circ}\text{C}$
Air Flow rate Membrane scouring only	4,200	L h^{-1}
Operating cycle	Continuous	–
SED	3	kWh m^{-3}

Taking into account the information provided in Table 6.4, it can be concluded that the set of operating conditions as shown in Table 7.39 can lead to a reliable long-term membrane performance, as well as producing treated permeate of the appropriate quality. At the same time, the target SED value was successfully achieved.

To conclude, the model predicts that a modified version of MBR1 can operate successfully at SED values equal to those of the full-scale conventional AS plant. Also, it can produce treated permeate of appropriate quality, whereas the full-scale

conventional AS plant can not. This modified version of MBR1 makes it a very promising solution in terms of the objectives of this research.

7.7 Conclusions

This chapter explored the issues that are related to the total energy that was consumed by the three MBR systems. Both short-term power-analysis and longer-term energy-analysis experiments were conducted and initial SED values of the MBR systems were calculated. Both short-term power-analysis and longer-term energy-analysis experiments managed to provide similar SED values. These preliminary SED values showed that MBR1 was the most-energy consuming MBR system followed by MBR3 and finally by MBR2. However, it has to be clarified that when the power-analysis/energy-analysis experiments were performed, only the MBR1 system was being operated under a sustainable net MPF, whereas the other two MBR systems were operating under continual membrane fouling conditions.

The short-term component-based power-analysis experiments were successfully validated by the longer-term energy-analysis experiments. The power-analysis experiments were very useful as energy consumption rates for each MBR component were measured, even though that was possible only for the MBR1 and the MBR2 system. With respect to the MBR3 system, component-based analysis experiments could not be conducted due to the three-phase power supply.

An Excel-based model was built, calibrated and validated. By taking into account the energy consumption rates per MBR component, the model was able to predict SED values of the MBR1 system and the MBR2 system under different operating conditions.

The model predicted that both MBR1 and MBR2 were unable to combine SED values equal to or lower than lower than 3 kWh m^{-3} with sustainable net MPFs. However, a slightly modified version of the MBR1 system succeeded in reducing the SED values. The modified version of the MBR1 system seems to be a very promising solution, as it is predicted to produce treated permeate of the appropriate quality at SED values equal to or lower than 3 kWh m^{-3} , whilst also ensuring a stable long-term membrane

performance. Overall conclusions, together with some ideas regarding possible future work, will be given in Chapter 8.

CHAPTER 8 CONCLUSIONS & FUTURE WORK

8.1 Conclusions

This work focused on the operation of low energy membrane bioreactors (MBRs) for decentralised waste water treatment (WWT) in the Middle East and North Africa (MENA) region. Final conclusions with respect to the objectives of this research as defined in Section 1.3 are as follows:

• Objective 1

In order to investigate whether or not treated permeate of the appropriate quality was produced, the membrane bioreactor (MBR) systems were operated at two different mixed-liquor suspend solids (MLSS) concentrations, which were successfully controlled by applying suitable sets of solids residence times (SRTs) and hydraulic residence times (HRTs). These MLSS concentrations were equal to about 4 - 5 g L⁻¹ and about 9 - 10 g L⁻¹. The treated water should be suitable for re-use in unrestricted irrigation in Tunisia, *i.e.* the chemical oxygen demand (COD) concentration in the permeate stream should be equal to or lower than 90 mg L⁻¹.

The low MLSS concentration of 4 - 5 g L⁻¹ was chosen because it was similar to the value of the full-scale conventional activated sludge (AS) plant, so a comparison could be made. At this MLSS concentration, only membrane bioreactor 2 (MBR2) and membrane bioreactor 3 (MBR3) managed to produce treated permeate of the appropriate quality, whereas membrane bioreactor 1 (MBR1) was not successful in doing so. At low MLSS concentrations, the COD concentration removal efficiencies were calculated to be equal to 71.4 % for MBR1, 88 % for MBR2 and 87.7 % for MBR3.

On the other hand, the high MLSS concentration of 9 - 10 g L⁻¹ was chosen because, according to the membrane manufactures, all MBR systems could be operated at this MLSS concentration value without experiencing any serious membrane fouling problems. During the trials at this MLSS concentration, all three MBR systems

produced treated permeate of the appropriate quality. The COD concentration removal efficiencies were higher this time, namely 89.4 % for MBR1, 89.7 % for MBR2 and 90.9 % for MBR3.

MBR1 was designed to operate at MLSS concentrations at about 9 - 10 g L⁻¹ or even higher, whereas MBR2 at MLSS concentrations up to about 12 g L⁻¹ and MBR3 at MLSS concentrations between 3 and 14 g L⁻¹. This explains why MBR1 failed to produce treated permeate of the appropriate quality at low MLSS concentrations, whereas MBR2 and MBR3 were both successful. MBR2 and MBR3 contain ultrafiltration (UF) membranes, whereas MBR1 was equipped with microfiltration (MF) membranes. UF membranes are technically able to reject more organic material than MF membranes, [Kim *et al.*, 2008], regardless of the applied MLSS concentration values, so this also explains why MBR2 and MBR3 produced treated permeate of better quality than MBR1.

Finally, the full-scale activated sludge (AS) plant did not manage to produce treated water of the appropriate quality. In general, higher MLSS concentrations can easily produce treated water of better quality, [Stamou and Vogiatzis, 1994], however, only MBRs are successful in operating at elevated MLSS concentrations - see Section 2.1.3.

• Objective 2

Even though detailed measurements of dissolved oxygen (DO) concentration within the MBR tanks was not part of this work, it can be said that the aerobic bacterial cultures never suffered from lack of oxygen during the long-term experiments. Typically, oxygen has to be maintained at a level of 1 to 3 mg L⁻¹, [Tchobanoglous *et al.*, 2004]. In this research, the air flow rates that were applied during the long-term experiments were directly suggested by the membrane equipment suppliers. Even though direct DO concentration measurements were not made in this work, the COD concentration measurements in the influent and effluent show that bacteria were active. The organic matter in the effluent was always below or at the COD concentration expected in a completely treated effluent (< 100 mg L⁻¹).

• Objective 3

In order to maximise the daily production of the treated permeate, several net membrane permeate fluxes (MPFs) were applied so that the maximum average sustainable net membrane permeate flux (MPF) for each MBR system could be determined. Each MBR's maximum average sustainable net MPF value was predicted at the high MLSS concentration of 9 - 10 g L⁻¹, as that was a reasonable operating value proposed by the membrane manufactures. Also, at this MLSS concentration, all three MBR systems produced treated permeate of the appropriate quality. Operation at the maximum average sustainable net MPF values leads to maximisation of the daily production of treated water, together with stable long-term membrane performance. However, it is worth mentioning that sustainable net MPFs are a function of the MBR operating conditions, mainly MLSS concentrations, mixed-liquor temperatures and gassing rates for membrane scouring. This practically means that there are not sustainable net MPFs specifically, but there actually are sustainable sets of operating conditions.

With respect to MBR1 operation at the high MLSS concentration of 9 - 10 g L⁻¹, the net MPFs applied during the long-term experiment are as follows: 9.81 L m⁻² h⁻¹ (solids residence time (SRT): 30 d, hydraulic residence time (HRT): 1.01 d), 10.92 L m⁻² h⁻¹ (SRT: 29 d, HRT: 0.91 d), 11.88 L m⁻² h⁻¹ (SRT: 25.5 d, HRT: 0.835 d), 12.88 L m⁻² h⁻¹ (SRT: 23.5 d, HRT: 0.77 d) and 13.77 L m⁻² h⁻¹ (SRT: 21.8 d, HRT: 0.72 d). Despite the fact that some membrane fouling was formed during the long-term experiment, it was concluded that these net MPFs were sustainable. The maximum average sustainable net MPF that was predicted was 13.77 L m⁻² h⁻¹. The average MLSS concentration was equal to 9.26 g L⁻¹, the average mixed-liquor temperature was 28.9 °C and the gassing rate for membrane scouring was 4,200 L h⁻¹. Filtration was continuous without any membrane relaxation. By applying this net MPF, the daily production of treated permeate is maximised and the membranes operate without significant membrane fouling problems.

Regarding MBR2 operation at the high MLSS concentration of 9 - 10 g L⁻¹, the net MPFs applied during the long-term experiment are as follows: 11.52 L m⁻² h⁻¹ (SRT: 30 d, HRT: 1.01 d), 12.81 L m⁻² h⁻¹ (SRT: 29 d, HRT: 0.91 d) and 13.94 L m⁻² h⁻¹

(SRT: 25.5 d, HRT: 0.835 d). It was then concluded that the highest net MPF of $13.94 \text{ L m}^{-2} \text{ h}^{-1}$ and its corresponding operating conditions was an unsustainable condition. The maximum average sustainable net MPF, as provided by the long-term experiment, was $12.81 \text{ L m}^{-2} \text{ h}^{-1}$. The average MLSS concentration was 9.379 g L^{-1} , the average mixed-liquor temperature was $23.9 \text{ }^{\circ}\text{C}$ and the gassing rate regarding membrane scouring was $12,000 \text{ L h}^{-1}$. Filtration was intermittent with a filtration/relaxation cycle equal to 9/1 min/min on/off - membranes were filtering for 9 min before membrane relaxation was applied for 1 min.

With regard to MBR3 operation at the high MLSS concentration of $9 - 10 \text{ g L}^{-1}$, the maximum average sustainable net MPF could not be predicted. Despite the fact that all three MBR systems were operated under the same sets of SRTs/HRTs, the corresponding net MPFs of the MBR3 system were found to be equal to or higher than $13.58 \text{ L m}^{-2} \text{ h}^{-1}$ (SRT: 30 d, HRT: 1.01 d), and all MBR3 MPFs tested end up being unsustainable. This practically means that both the SRTs and the HRTs have to increase simultaneously in order to maintain the MLSS concentration at the selected value and reduce the corresponding net MPFs. However, this was not tested during this research, as, in order to provide a fair comparison, the same sets of operating conditions were tested for all three MBRs. Intermittent filtration was with a filtration/relaxation cycle equal to 17/3 min/min on/off or 17 minutes of filtration were followed by 3 minutes of membrane relaxation. Membrane fouling could not be avoided under any of the conditions tested during the pilot trial.

• Objective 4

Energy consumption rates and initial specific energy demand (SED) values were calculated after conducting both short-term component-based power-analysis experiments and longer-term energy-analysis experiments. Based on these experiments, an initial evaluation of the total amount of energy that was consumed by all three MBR systems can be made. According to the estimated SED values, MBR1 appeared to be the most-energy consuming MBR system - SED values were between 5.329 kWh m^{-3} and 5.475 kWh m^{-3} , and MBR2 appeared to be the least-energy consuming MBR system - SED values were between 3.738 kWh m^{-3} and 3.889 kWh m^{-3} . However, it must be clarified that when the short-term power-analysis

experiments and longer-term energy-analysis experiments were carried out, only MBR1 was being operated under a clear sustainable net MPF, whereas operations of MBR2 and MBR3 were subject to serious membrane fouling.

As long as similar SED values were recorded by both short-term power-analysis experiments and the longer-term energy-analysis experiments, it can be said that the short-term power-analysis experiments were successfully validated by the longer-term energy-analysis experiments. However, power-analysis experiments could be conducted only for the MBR1 system and the MBR2 system. Based on the short-term power-analysis experiments, the following final comments can be made.

Out of the total amount of energy that was consumed by the MBR1 system, 87.7 % of the total energy was consumed to supply air within the MBR tank. Despite being quite high, it is a reasonable percentage for submerged gravity-driven MBRs, [Gander *et al.*, 2000]. On the other hand, only 3.5 % of the total amount of energy was consumed to pump liquids - only Feed Pump 1 was operated -, together with 8.5 % consumed by the control panel.

Out of the total amount of energy that was consumed by the MBR2 system, 60.2 % of the total energy was consumed in order to supply air within the biological and membrane tanks. Even though aeration was still the activity that consumed most of the total energy that was consumed by the MBR2 system, this percentage is lower than that for MBR1. This is because MBR2 operated with more pumps, namely a recirculation pump and a membrane suction pump, together with Feed Pump 2. 35.5 % of the total energy, which was consumed by MBR2, was then due to the operation of these pumps, together with the energy consumed by the control panel, which accounted for 4.6 % of the total.

• Objective 5

An Excel-based MBR model capable of predicting SED values under different combinations of SRTs/HRTs was constructed, calibrated/validated and finally explored. The $Y_{X/S}$ -value of about 0.4, as predicted by the MBR model, is a typical value of extended SRT bioreactor designs like the three pilot MBRs of this research.

Application of the model showed that neither the MBR1 system nor the MBR2 system succeeded in producing treated permeate of the appropriate quality at a stable long-term membrane performance and at SED values equal to or lower than the target value of 3 kWh m^{-3} .

However, the model predicted that a modified version of the MBR1 system could succeed in doing so. The modified version of the MBR1 system was based on the replacement of the current components with less energy-consuming devices.

There may be many combinations of operating conditions that can combine production of treated permeate of the appropriate quality, stable long-term membrane performance and SED values equal to or lower than 3 kWh m^{-3} . The set of operating conditions shown in Table 7.37 can successfully do so, as predicted by the MBR model and as validated by the experimental data from the long-term pilot experiments. An SRT of 30 d and a HRT of 0.878 d are proposed. This combination leads to an MLSS concentration of 11.116 g L^{-1} , an average net MPF of $11.34 \text{ L m}^{-2} \text{ h}^{-1}$ and predicts a borderline SED value of 3 kWh m^{-3} . The mixed-liquor temperature is assumed to be $21.2 \text{ }^\circ\text{C}$ and gassing flow rate for membrane scouring is $4,200 \text{ L h}^{-1}$.

To conclude, it is worth mentioning that the objective SED standard of 3 kWh m^{-3} , which represents the SED value of the full-scale AS plant at the ONAS site, appears to be much higher than the SED values of conventional AS processes provided in Section 2.4.1. Thus, it is recommended that further analysis regarding the power requirements of the full-scale AS plant at the ONAS site may have to be carried out, and power requirements measurements may have to be repeated.

8.2 Future work

8.2.1 Improvement of MBR operation

In this research, the three MBR systems were operated under similar sets of SRTs and HRTs. This was a sensible initial approach, taken in order to determine the performance of the MBR systems under similar operating conditions so that a direct comparison could be made. However, the long-term experiments indicated that each

MBR system can be operated more efficiently under different specific operating conditions and optimisation around these operating conditions would be preferable.

- **MBR1**

MBR1 has to be operated at MLSS concentrations in the range of 9 - 10 g L⁻¹, as MLSS concentrations at about 4 - 5 g L⁻¹ failed to produce treated permeate of the appropriate quality. Assuming operation at MLSS concentrations equal to 9 - 10 g L⁻¹, net MPFs higher than the value of 13.77 L m⁻² h⁻¹ are worth testing to see whether the maximum average sustainable net MPF can be further increased. In this case, the current minimum SED value of 5.007 kWh m⁻³ will further decrease.

Also, even if MLSS concentrations have to be equal to or higher than 9 - 10 g L⁻¹ according to the manufacturer, it may be worth trying to determine the lowest MLSS concentration that can produce treated permeate of the appropriate quality. This has by definition to be between 4 - 5 g L⁻¹ and 9 - 10 g L⁻¹. As lower MLSS concentrations tend to affect the membrane performance less seriously, operating the MBR under this reduced MLSS concentration may lead to a further increase in the maximum average sustainable net MPF, hence to a further decrease of the SED value.

- **MBR2**

MBR2 could be successfully operated both at low (4 - 5 g L⁻¹) and high MLSS concentrations (9 - 10 g L⁻¹), as in both cases treated permeate of the appropriate quality was produced. In the future, MBR2 should be run at the low MLSS concentration and the long-term experiment should be repeated. By applying lower MLSS concentrations, it is expected that the maximum average sustainable net MPF will increase to a value higher than 12.81 L m⁻² h⁻¹, as lower MLSS concentrations are less prone to generate membrane fouling. Higher maximum average sustainable net MPFs will be able to reduce the current SED value of 4.06 kWh m⁻³ estimated during the long-term experiment.

- **MBR3**

As MBR3 was suffering from continuous membrane fouling, the long-term experiment must be repeated by running the MBR at the low MLSS concentration. Then, the net MPFs must be reduced below 13.58 L m⁻² h⁻¹ by applying suitable sets

of SRTs/HRTs. It will then be concluded whether there may be net MPFs that can lead to a stable membrane performance, and which of them appears to be the highest sustainable value. Also, it may be worth trying to optimise the filtration/relaxation cycle, by retaining the filtration time constant and gradually increasing the relaxation time. However, although this may stabilise MPFs, it will also reduce the amount of permeate produced per day.

8.2.2 Improvement of MBR designs

After conducting the long-term experiments, it was found that some MBR components could be replaced with a better alternative, *i.e.* with respect to MBR1, it was concluded that both Feed Pump 1 and the air compressor can be successfully replaced by less energy-consuming devices as described in Section 7.6.3.3. Careful selection of the MBR components when MBR pilot plants are designed can then reduce the SED values, leading consequently to quite promising MBR WWT processes.

8.2.3 Improvement of aeration

In this research, all air flow rates that were applied were those suggested by the manufacturers, and they always remained constant during the long-term experiment. All membranes were then tested at maximum air conditions, so net MPFs lower than the predicted maximum average sustainable net MPF per MBR system were automatically tested under excess air operating conditions. An attempt to optimise aeration with respect to these lower MPF values may then worth a try.

On the other hand, once a maximum average sustainable net MPF has been estimated at a constant MLSS concentration and a constant mixed-liquor temperature, it is only an increase in the gassing rate that could possibly increase this MPF to an even higher value - details are available in Section 2.3.4.4. If the combination of the new energy consumption rate with the improved maximum average sustainable net MPF value is able to reduce the current SED values, it would be worth increasing the air flow rates.

By improving or, if possible, by optimising the air flow rate for a specific set of operating conditions, operational energy-related costs are due to decrease. Even

though operation of the MBR systems will become more complicated, as an additional parameter has to be taken into account, the new SED values of MBRs may be able to successfully combat the SED values of conventional AS WWT processes.

REFERENCES

- Ahmed Z., Cho J., Lim B. R., Song K. G. Ahn K. H., "Effects of sludge retention time on membrane fouling and microbial community structure in a membrane bioreactor", *Journal of Membrane Science*, 287, (2007), 211-218
- Aquino S. F. and Stuckey D. C., "Integrated model of the production of soluble microbial products (SMP) and extracellular polymeric substances (EPS) in anaerobic chemostats during transient conditions", *Biochemical Engineering Journal*, 38, (2008), 138-146
- Arnot T. C., "Lecture 4: Biological reactions and microorganisms in water pollution control", Notes for the Undergraduate Course Unit: CE30145: Environmental Management, Department of Chemical Engineering, University of Bath, (2004)
- Arnot T. C., "Lecture 6: Membrane bioreactors: Water treatment for the future", Notes for the Undergraduate Course Unit: CE30145: Environmental Management, Department of Chemical Engineering, University of Bath, (2004)
- Arnot T. C., Field R. W., Koltuniewicz A. B., "Cross-flow and dead-end microfiltration for oily-water emulsions - Part II: Mechanisms and modelling of flux decline", *Journal of Membrane Science*, 169, (2000), 1-15
- Arnot T. C., Personal communication, (2006-2009)
- Bacchin P., Aimar P., Field R. W., "Critical and sustainable fluxes: Theory, experiments and applications", *Journal of Membrane Science*, 281, (2006), 42-69
- Belfort G. T., Davis R. H., Zydney A. L., "The behaviour of suspensions and macromolecular solutions in cross flow microfiltration: A review", *Journal of Membrane Science*, 96, (1994), 1-58
- Brodkey R. S., Hershey H. C., Translated by Bleris G. L., "Φαινόμενα Μεταφοράς", (1990), ISBN: 960-7219-14-7
- Busch J., Cruse A., Marquardt W., "Modelling submerged hollow fibre membrane filtration for waste water treatment", *Journal of Membrane Science*, 288, (2007), 94-111
- Chang I. S. and Kim S. N., "Waste water treatment using membrane filtration-effect of biosolids concentration on cake resistance", *Process Biochemistry*, 40, (2005), 1307-1314
- Cho B. D. and Fane A. G., "Fouling transients in nominally sub-critical flux operation of a membrane bioreactor", *Journal of Membrane Science*, 209, (2002), 391-403
- Chua H. C., "Turn-up/Turn-down of throughput in membrane bioreactors", PhD Thesis, Department of Chemical Engineering, University of Bath, (2002)
- Chua H. C., Arnot T. C., Howell J. A., "Controlling fouling in membrane bioreactors operated with variable throughput", *Desalination*, 149, (2002), 225-229
- Churchouse S. and Wildgoose D., "Membrane bioreactors progress from the laboratory to full-scale use", *Membrane Technology*, 111, (1999), 4-8
- Churchouse S., "Membrane bioreactors for waste water treatment - Operating experiences with the KUBOTA submerged membrane activated sludge process", *Membrane Technology*, 83, (1997), 5-9

- Comte S., Guibaud G., Baudu M., “Biosorption properties of extracellular polymeric substances (EPS) resulting from activated sludge according to their type: Soluble or bound”, *Process Biochemistry*, 41, (2006), 815-823
- Côté P., Buisson H., Pound C., Arakaki G., “Immersed membrane activated sludge for the reuse of municipal waste water”, *Desalination*, 113, (1997), 189-196
- Coulson J. M. and Richardson J. F., “Coulson and Richardson’s Chemical Engineering - Volume 2: Particle Technology and Separation Processes”, 4th Edition, (1991), ISBN: 0 08 037956 7
- Cui Z. F., Chang S., Fane A. G., “The use of gas bubbling to enhance membrane processes”, *Journal of Membrane Science*, 221, (2003), 1-35
- Delgado S., Villarroel R., González E., “Effect of the shear intensity on fouling in submerged membrane bioreactor for waste water treatment”, *Journal of Membrane Science*, 311, (2008), 173-181
- Doran M. P., “Bioprocess engineering principles”, Academic Press, Elsevier Ltd, (2006), ISBN: 0-12-220855-2
- Durante F., Di-Bella G., Terragrossa M., Viviani G., “Particle size distribution and biomass growth in a submerged membrane bioreactor”, *Desalination*, 199, (2006), 493-495
- Espinasse B., Bacchin P., Aimar P., “Filtration method characterizing the reversibility of colloidal fouling layers at a membrane surface: Analysis through critical flux and osmotic pressure”, *Journal of Colloid and Interface Science*, 320, (2008), 483-490
- Fan Y., Li G., Wu L., Yang W., Dong C., Xu H., Fan W., “Treatment and reuse of toilet waste water by an airlift external circulation membrane bioreactor”, *Process Biochemistry*, 41, (2006), 1364–1370
- Gander M., Jefferson B., Judd S., “Aerobic membrane bioreactors for domestic waste water treatment: A review with cost considerations”, *Separation and Purification Technology*, 18, (2000), 119-130
- Gerardi M., “Waste water bacteria”, (2006), ISBN: 0-471-20691-1
- Germain E., Nelles F., Drews A., Pearce P., Kraume M., Reid E., Judd S. J., Stephenson T., “Biomass effects on oxygen transfer in membrane bioreactors”, *Water Research*, 41, (2007), 1038-1044
- Guglielmi G., Chiarani D., Judd S. J., Andreottola G., “Flux criticality and sustainability in a hollow fibre submerged membrane bioreactor for municipal waste water treatment”, *Journal of Membrane Science*, 289, (2007), 241-248
- Han S. S., Bae T. H., Jang G. G., Tak T. M., “Influence of sludge retention time on membrane fouling and bioactivities in membrane bioreactor system”, *Process Biochemistry*, 40, (2005), 2393-2400
- Hasar H., Kinaci C., Ünlü A., Toğrul H., Ipek U., “Rheological properties of activated sludge in a SBR”, *Biochemical Engineering Journal*, 20, (2004), 1-6
- Henkel J., Lemac M., Wagner M., Cornel P., “Oxygen transfer in membrane bioreactors treating synthetic greywater”, *Water Research*, 43, (2009), 1711-1719

- Hong S. P., Bae T. H., Tak T. M., Hong S., Randall A., "Fouling control in activated sludge submerged hollow fibre membrane bioreactors", *Desalination*, 143, (2002), 219-228
- Howell J. A., Chua H. C., Arnot T. C., "In-situ manipulation of critical flux in a submerged membrane bioreactor using variable aeration rates and effects of membrane history", *Journal of Membrane Science*, 242, (2004), 13-19
- Howell J. A., Sanchez V., Field R. W., "Membranes in bioprocessing: Theory and application", (1993), ISBN: 0-7514-0149-8
- Hwang K. J. and Wu Y. J., "Flux enhancement and cake formation in air-sparged cross-flow microfiltration", *Chemical Engineering Journal*, 139, (2008), 296-303
- Industrial news, COPA acquires MBR company's assets, *Filtration and Separation*, 41, (2004), 8
- Industry focus, "MBR focus: Is submerged best?", Van't-Oever R., *Filtration and Separation*, 42, (2005), 24-27
- Jang N., Ren X., Cho J., Kim S. I., "Steady-state modelling of bio-fouling potentials with respect to the biological kinetics in the submerged membrane bioreactor (SMBR)", *Journal of Membrane Science*, 284, (2006), 352-360
- Jang N., Ren X., Kim G., Ahn C., Cho J., Kim I. S., "Characteristics of soluble microbial products and extracellular polymeric substances in the membrane bioreactor for water reuse", *Desalination*, 202, (2007), 90-98
- Jarusutthirak C. and Amy G., "Understanding soluble microbial products (SMP) as a component of effluent organic matter (E_fOM)", *Water Research*, 41, (2007), 2787-2793
- Judd S., "The MBR book: Principles and application of membrane bioreactors in water and waste water treatment", Elsevier Ltd., (2007), ISBN: 978-1-85617-481-7
- Kennedy S. and Churchouse S., "Progress in membrane bioreactors: New advances", *Proceedings of Water and Waste Water, European Conference, Milan*, (2005)
- Kim J., Di Giano F. A., Reardon R. D., "Autopsy of high-pressure membranes to compare effectiveness of MF and UF pre-treatment in water reclamation, *Water Research*, 42, (2008), 697 – 706
- Kouakou E., Salmon T., Toye D., Marchot P., Crine M., "Gas-liquid mass transfer in a circulating jet-loop nitrifying MBR", *Chemical Engineering Science*, 60, (2005), 6346-6353
- Kyparissidis K., "Ανάλυση και σχεδιασμός των ομογενών χημικών αντιδραστήρων", Notes for the Undergraduate Courses: "Chemical Reactor Design and Analysis I and II", Department of Chemical Engineering, Aristotle University of Thessaloniki, (1994)
- Laspidou C. S. and Rittman B. E., "A unified theory for extracellular polymeric substances, soluble microbial products, and active and inert biomass", *Water Research*, 36, (2002), 2711-2720
- Le-Clech P., Chen V., Fane T. A. G., "Review: Fouling in membrane bioreactors used in waste water treatment", *Journal of Membrane Science*, 284, (2006), 17-53
- Le-Clech P., Jefferson B., Judd S. J., "Impact of aeration, solids concentration and membrane characteristics on the hydraulic performance of a membrane bioreactor", *Journal of Membrane Science*, 218, (2003), 117-129

- Lee W., Kang S., Shin H., "Sludge characteristics and their contribution to microfiltration in submerged membrane bioreactors", *Journal of Membrane Science*, 216, (2003), 217-227
- Lesjean B. and Huisjes E. H., "Survey of the European MBR market: trends and perspectives", *Desalination*, 231, (2008), 71–81
- Liao B. Q., Kraemer J. T., Bagley D. M., "Anaerobic membrane bioreactors: Applications and research directions", *Critical Reviews in Environmental Science and Technology*, 36, (2006), 489-530
- Liu R., Huang X., Sun Y. F., Qian Y., "Hydrodynamic effect on sludge accumulation over membrane surfaces in a submerged membrane bioreactor", *Process Biochemistry*, 39, (2003), 157-163
- Liu R., Huang X., Wang C., Chen L., Qian Y., "Study of hydraulic characteristics in a submerged membrane bioreactor process", *Process Biochemistry*, 36, (2000), 249-254
- Martin Systems: Instructions for installation and operation of PURATREAT siClaro sewage treatment plant, (2008)
- Maximova N. and Dahl O., "Environmental implications of aggregation phenomena: Current understanding", *Current Opinion in Colloid and Interface Science*, 11, (2006), 246-266
- Meng F., Yang F., Shi B., Zhang H., "A comprehensive study on membrane fouling in submerged membrane bioreactors operated under different aeration intensities", *Separation and Purification Technology*, 59, (2008), 91-100
- Metzger U., Le-Clech P., Stuetz M. R., Frimmel F. H., Chen V., "Characterisation of polymeric fouling in membrane bioreactors and the effect of different filtration modes", *Journal of Membrane Science*, 301, (2007), 180-189
- Mohammed A. T., Birima A. H., Noor M. J. M. M., Muyibi A. S., Idris A., "Evaluation of using membrane bioreactor for treating municipal waste water at different operating conditions", *Desalination*, 221, (2008), 502-510
- Ndinisa N. V., Fane A. G., Wiley D. E., "Fouling control in a submerged flat sheet membrane system: Part I: Bubbling and hydrodynamic effect", *Separation Science and Technology*, 41, (2006), 1383-1409, (A)
- Ndinisa N. V., Fane A. G., Wiley D. E., Fletcher D. E., "Fouling control in a submerged flat sheet membrane system: Part II: Two-phase flow characterisation and CDF simulations", *Separation Science and Technology*, 41, (2006), 1411-1445, (B)
- North Sfax ONAS archives: Tunisian standards: Water re-use for irrigation, (2009).
- Nuengjamnong C., Kweon J. H., Cho J., Polprasert C., Ahn K. H., "Membrane fouling caused by extracellular polymeric substances during microfiltration processes", *Desalination*, 179, (2005), 117-124
- Nywening J. P. and Zhou H., "Influence of filtration conditions on membrane fouling and scouring aeration effectiveness in submerged membrane bioreactors to treat municipal waste water", *Water Research*, 43, (2009), 3548-3558
- Ognier S., Wisniewski C., Grasmick A., "Membrane bioreactor fouling in sub-critical filtration conditions: A local critical flux concept", *Journal of Membrane Science*, 229, (2004), 171-177

Okamura D., Mori Y., Hashimoto T., Hori K., “Identification of biofoulant of membrane bioreactors in soluble microbial products”, *Water Research*, 17, (2009), 4356-4362

ONAS, North Sfax archives, (2006)

Personal communication with KUBOTA Membranes Europe, (2009)

Pollice A., Brookes A., Jefferson B., Judd S., “Sub-critical flux fouling in membrane bioreactors a review of recent literature”, *Desalination*, 174, (2005), 221-230

Psoch C. and Schiewer S., “Long-term study of an intermittent air sparged MBR for synthetic waste water treatment”, *Journal of Membrane Science*, 260, (2005), 56-65

PURATREAT project: Deliverable 16: “Proposed best technology and running costs”, (2009)

PURATREAT project: Deliverable 3: “Bioreactor design (MBR1, MBR2, MBR3)”, (2007)

PURATREAT project: Deliverable 5: “MBR control system programmed and installed (MBR1, MBR2, MBR3)”, (2007)

PURATREAT project: Deliverable 6: “Clean water tests and membrane characterisation”, (2009)

Reid E., “Salinity shocking and fouling amelioration in membrane bioreactors”, EngD Thesis, Cranfield University, School of Industrial and Manufacturing Science, School of Water Sciences, (2005)

Ren N., Chen Z., Wang A., Hu D. “Removal of organic pollutants and analysis of MLSS-COD removal relationship at different HRTs in a submerged membrane bioreactor”, *International Biodeterioration and Biodegradation*, 55, (2005), 279-284

Research trends, “Macromolecule adsorption in an MBR mixed liquor suspension”, *Membrane Technology*, 2002, (2002), 16

Rosenberger S., Laabs C., Lesjean B., Gnirss R., Amy G., Jekel M., Schrotter J. C., “Impact of colloidal and soluble organic material on membrane performance in membrane bioreactors for municipal waste water treatment”, *Water Research*, 40, (2006), 710-720

Schoeberl P., Brik M., Bertoni M., Braun R., Fuchs W., “Optimization of operational parameters for a submerged membrane bioreactor treating dyehouse waste water”, *Separation and Purification Technology*, 44, (2005), 61-68

Sheng G. P., Zhang M. L., Yu H. Q., “Characterization of adsorption properties of extracellular polymeric substances (EPS) extracted from sludge” *Colloids and Surfaces B: Biointerfaces*, 62, (2008), 83-90

Sim M. C., “Two-stage MBR to reduce sludge production and total aeration volume”, PhD Thesis, Department of Chemical Engineering, University of Bath, (2003)

Sponza D. T., “Investigation of extracellular polymer substances (EPS) and physicochemical properties of different activated sludge flocs under steady-state conditions”, *Enzyme and Microbial Technology*, 32, (2003), 375-385

Stamou A. I. and Vogiatzis Z. S., “Βασικές αρχές και σχεδιασμός επεξεργασίας αποβλήτων”, 2nd Edition, Technical Chamber of Greece, (1994), ISBN: 960-701849-4

- Stephenson T., Judd S., Jefferson B., Brindle K., "Membrane bioreactors for waste water treatment", (2000), ISBN: 1-900222-07-8
- Tansel B., Sager J., Garland J., Xu S., Levine L., Bisbee P., "Deposition of extracellular polymeric substances (EPS) and microtopographical changes on membrane surfaces during intermittent filtration conditions", *Journal of Membrane Science*, 285, (2006), 225-231
- Tardieu E., Grasmick A., Geaugey V., Manem J., "Hydrodynamic control of bioparticle deposition in an MBR applied to waste water treatment", *Journal of Membrane Science*, 147, (1998), 1-12
- Tchobanoglous G., Burton F. L., Stensel D. H., "Waste water engineering, treatment and reuse", Metcalf and Eddy, Inc., Fourth edition - revised, (2004), ISBN: 007-124140-X
- Ueda T. and Hata K., "Domestic waste water treatment by a submerged membrane bioreactor with gravitational filtration", *Water Research*, 33, (1999), 2888-2892
- Van-Bentem A. G. N., Petri C. P., Schyns P. F.T, Van-Der-Roest H. F., "Membrane bioreactors: Operation and results of an MBR waste water treatment plant", ISBN: 1843391732
- Van-Der-Roest H. F., Lawrence D. P., Van-Bentem A. G. N., "Membrane bioreactors for municipal waste water treatment", (2006), ISBN: 1-843390-11-6
- Van-Kaam R., Archard D. A., Alliet M., Lopez S., Albasi C., "Aeration mode, shear stress and sludge rheology in a submerged membrane bioreactor: Some keys of energy saving", *Desalination*, 199, (2006), 482-484
- Vyas H. K., Bennett R. J., Marshall A. D., "Performance of cross flow microfiltration during constant transmembrane pressure and constant flux operations", *International Dairy Journal*, 12, (2002), 473-479
- Wang F. and Tarabara V. V., "Pore blocking mechanisms during early stages of membrane fouling by colloids", *Journal of Colloid and Interface Science*, 328, (2008), 464-469
- Wang X. M. and Waite D. T., "Impact of gel layer formation on colloid retention in membrane filtration processes", *Journal of Membrane Science*, 325, (2008), 486-494
- Wang Z., Wu Z., Tang S., "Extracellular polymeric substance (EPS) properties and their effects on membrane fouling in a submerged membrane bioreactor", *Water Research*, 43, (2009), 2504-2512
- Water Environment Federation, "Membrane systems for waste water treatment", (2006)
- Weise Water offer: MicroClear AquaCell sewage treatment unit, (2007)
- Weise Water Systems: Main brochure, (2009)
- Weise Water Systems: Operating and maintenance manual, (2008)
- Weise Water Systems: Product catalogue, (2009)
- Wu G., Cui L., Xu Y., "A novel submerged rotating membrane bioreactor and reversible membrane fouling control", *Desalination*, 228, (2008), 255-262
- www.airmac.com.tw - (Model No. DBMX100), 2010

www.bbc.co.uk/weather/world/city_guides, 2010

www.copa.co.uk, 2010

www.eimcotechnologies.com, 2010

www.eimcowatertechnologies.com, 2010

www.hach.com, 2010

www.jung-pumpen.de, 2010

www.kubota-mbr.com, 2010

www.puratreat.com, 2010

www.siclaro.ch, 2010

www.standrardmethods.org, 2010

www.weise-water-systems.com, 2010

www.wessexwater.co.uk, 2010

www.worldbank.org, 2010

www.wtw.com, 2010

Yamamoto K., Hiasa M., Mahmood T., Matsuo T., “Direct solid-liquid separation using hollow fibre membrane in an activated sludge aeration tank”, *Water Science and Technology*, 21, (1989), 43-54

Yamato N., Kimura K., Miyoshi T., Watanabe Y., “Difference in membrane fouling in membrane bioreactors (MBRs) caused by membrane polymer materials”, *Journal of Membrane Science*, 280, (2006), 911-919

Yang S. F. and Li X. Y. , “Influences of extracellular polymeric substances (EPS) on the characteristics of activated sludge under non-steady-state conditions”, *Process Biochemistry*, 44, (2009), 91-96

Yang W., Cicek N., Ilg J., “State-of-the-art of membrane bioreactors: Worldwide research and commercial applications in North America”, *Journal of Membrane Science*, 270, (2006), 201-211

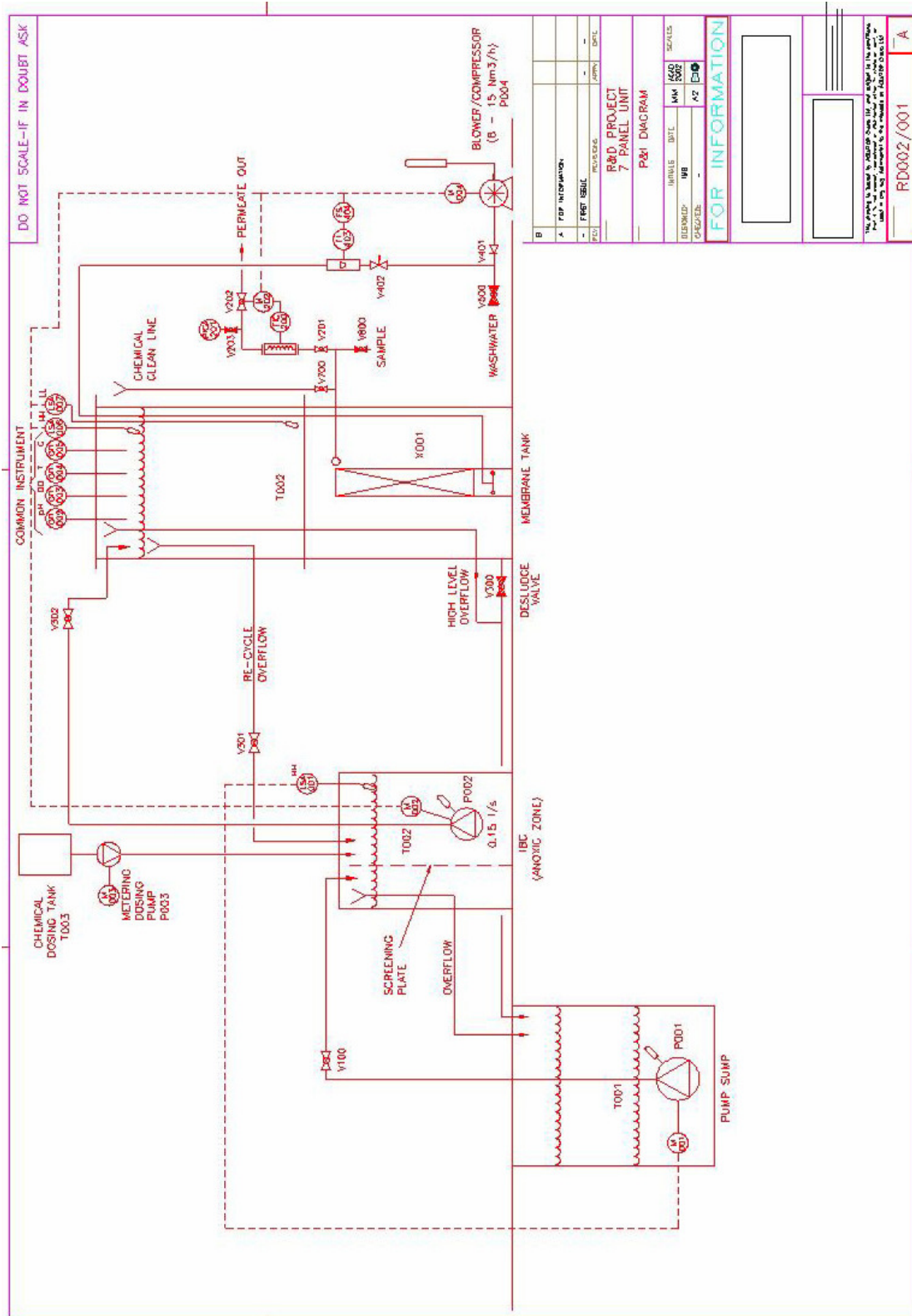
Yun M. A., Yeon K. M., Park J. S., Lee C. H., Chun J., Lim D. J., “Characterization of biofilm structure and its effect on membrane permeability in MBR for dye waste water treatment”, *Water Research*, 40, (2006), 45-52

Zhang J., Chua H. C., Zhou J., Fane A. G., “Factors affecting the membrane performance in submerged membrane bioreactors”, *Journal of Membrane Science*, 284, (2006), 54-66

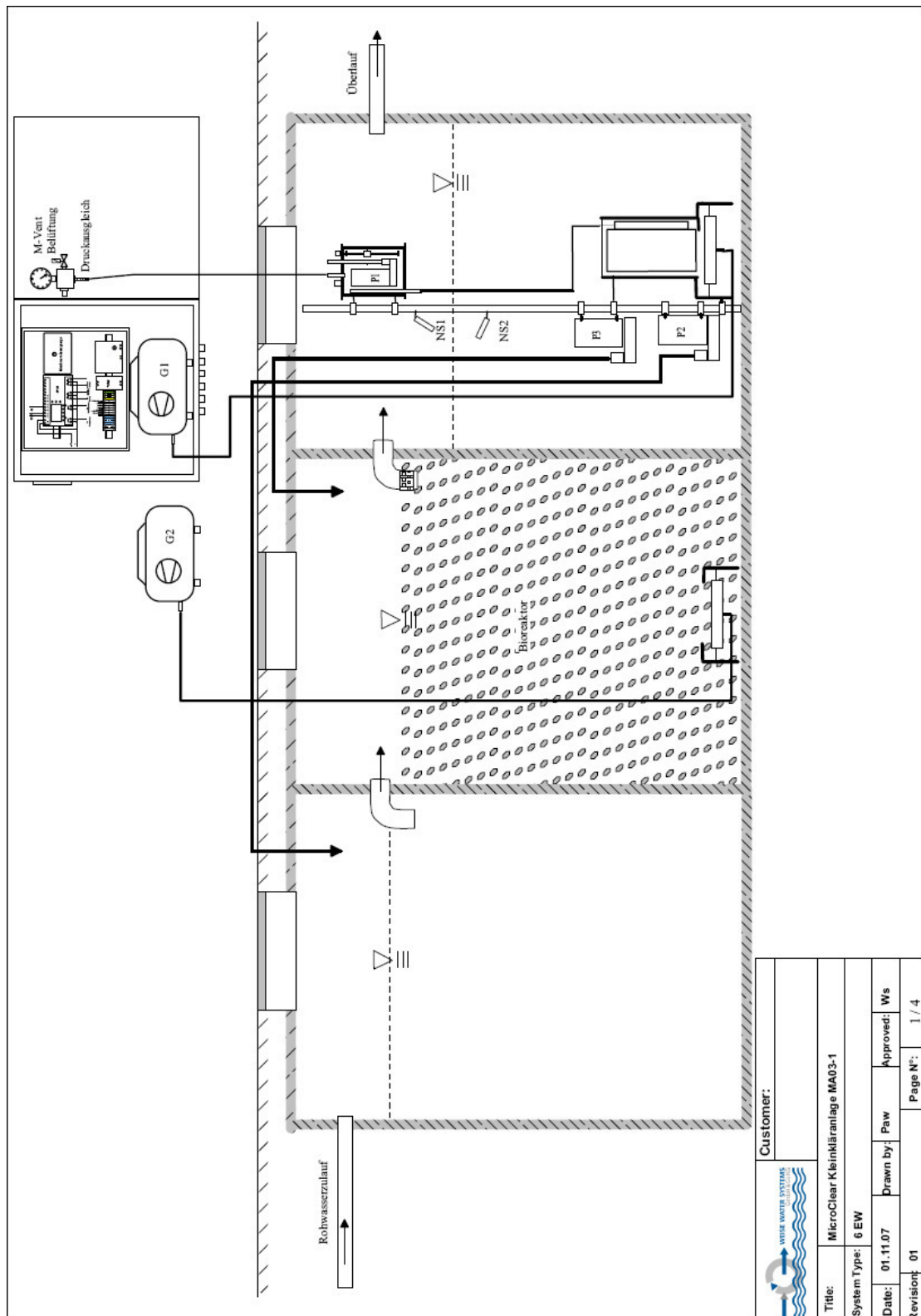
Zhang S., Van Houten R., Eikelboom D. H., Doddema H., Jiang Z., Fan Y., Wang J., “Sewage treatment by a low energy bioreactor”, *Bioresource Technology*, 90, (2003), 185-192


APPENDIX A: P&ID DIAGRAMS FOR THE MBR SYSTEMS.

• MBR1



• MBR2



Customer:			
			
Title: MicroClear Kleinkläranlage MA03-1			
System Type: 6 EW			
Date: 01.11.07	Drawn by: Paw	Approved: Ws	
Revision: 01		Page N°:	1 / 4

• MBR3

